Water Science and Technology Library

THE RÍO CHAGRES, PANAMA

A Multidisciplinary Profile of a Tropical Watershed

edited by

Russell S. Harmon

THE RÍO CHAGRES, PANAMA

Water Science and Technology Library

VOLUME 52

The titles published in this series are listed at the end of this volume.

THE RÍO CHAGRES, PANAMA

A Multidisciplinary Profile of a Tropical Watershed

edited by

RUSSELL S. HARMON

Army Research Office,
Research Triangle Park, NC, U.S.A.

Springer

A C.I.P. Catalogue record for this book is available from the Library of Congress.

ISBN-10 1-4020-3298-6 (HB)
ISBN-13 978-1-4020-3298-1 (HB)
ISBN-10 1-4020-3297-8 (e-book)
ISBN-13 978-1-4020-3297-4 (e-book)

Published by Springer,
P.O. Box 17, 3300 AA Dordrecht, The Netherlands.

www.springeronline.com

Cover illustration: Dry season flow in the upper Rio Chagres above the reach known as 'Three Falls', taken at a point (9:17:26N, 79:27:02W) looking downstream towards the first fall, which is about 2m in height. A scale is provided by the person on the right bank of the river with a surveying instrument. A mixed lithology boulder bar extends into the river from the right side of the picture. The bedrock outcrops are altered andesite. The river valley is typically bank full during the wet season. Annual high water marks are indicated by the location of significant bankside vegetation above the current water level. Photograph by Fred Ogden (U. Connecticut).

Printed on acid-free paper

Printed in the Netherlands.

Dedication

This book is dedicated to Lance Vander Zyl, Eric Nicoliasen, and Thomas Exenberger - colleagues and friends without whose dedicated support the upper Río Chagres basin fieldwork of 2002, which provided the foundation for much of the research described in this volume, would not have been possible.

Contents

Part II: The Upper Río Chagres Basin

Contributing Authors

Salomón Aguilar
Smithsonian Tropical Research Institute
Center for Tropical Forest Science
P.O. 2072, Balboa, Ancón
Panama City, Panama

Wim G.M. Bastiaanssen
WaterWatch
Generaal Foulkesweg 28
Wageningen 6703 BS
The Netherlands

Eldredge Bermingham
Smithsonian Tropical Research Institute
Center for Tropical Forest Science
P.O. 2072, Balboa, Ancón
Panama City, Panama

Paul R. Bierman
Department of Geology
University of Vermont
Burlington, VT 05405 USA

Stephanie Bohlman
W. M. Keck Remote Sensing Laboratory
University of Washington
Seattle, WA 98195 USA
current affiliation:
Smithsonian Tropical Research Institute
Unit 0948, APO AA-34002-0948 USA
Panama City, Panama

Sandra Brown
Winrock International
Ecosystem Services Unit
1621 N. Kent Street, Suite 1200
Arlington, VA 22207

Magnolia O. Calderón
Engineering Division
Autoridad del Canal de Panama
Panama City, Panama

Lucas E. Calvo Gobbetti
Universidad Tecnológica de Panama
Centro de Inv. Hidraulicas e Hidrotecnicas
Universidad Tecnologica de Panama, Ext. Tocumen
Panama City, Panama

Clara Camargo
Smithsonian Tropical Research Institute
Center for Tropical Forest Science
P.O. 2072, Balboa, Ancón
Panama City, Panama

Richard Condit
Smithsonian Tropical Research Institute
Center for Tropical Forest Science
P.O. 2072, Balboa, Ancón
Panama City, Panama

Virginia H. Dale
Oak Ridge National Laboratory
P.O. Box 2008
Oak Ridge, TN 37831-6036, USA

Christopher W. Dick
Smithsonian Tropical Research Institute
Center for Tropical Forest Science
P.O. 2072, Balboa, Ancón
Panama City, Panama

Tufa Dinku
Department of Civil and Environmental Engineering
University of Connecticut
Storrs, CT 06269 USA

Robert C. Faucett
Burke Museum
Box 353010
University of Washington
Seattle, WA 98195-3010 USA

Robert Finkel
Center for Accelerator Mass Spectrometry
Lawrence Livermore National Laboratory
Livermore, CA 94405 USA

Konstantine P. Georgakakos
Hydrologic Research Center
12780 High Bluff Drive, Suite 250
San Diego, CA 92130 USA

Russell S. Harmon
Army Research Office
US Army Research Laboratory
PO Box 12211,
Research Triangle Park, NC 27709-2211 USA

J. Bruce J. Harrison
Department of Earth and Environmental Sciences
New Mexico Institute of Technology
Socorro, NM 87801 USA

Gerald Hartmann
Geoscience Center, Division of Geochemistry
University of Göttingen
37077 Göttingen, Germany

Stanley Heckadon-Moreno
Smithsonian Tropical Research Institute
Box 2072, Balboa
Panama City, Panama

Jan M.H. Hendrickx
Department Earth and Environmental Sciences
New Mexico Institute of Technology
Socorro, NM 87801 USA

Sung-Ho Hong
Department of Earth and Environmental Sciences
New Mexico Institute of Technology
Socorro, NM 87801 USA

Roberto Ibáñez D.
Smithsonian Tropical Research Institute
Center for Tropical Forest Science
P.O. 2072, Balboa, Ancón
Panama City, Panama

David Kinner
INSTAAR, University of Colorado
Boulder CO, USA
and
Water Resources Division
U. S. Geological Survey
3215 Marine Street
Boulder, CO 80302 USA

Ryan Knox
Department of Civil and Environmental Engineering
University of Connecticut
Storrs, CT 06269 USA

Suzanne Lao
Smithsonian Tropical Research Institute
Center for Tropical Forest Science
P.O. 2072, Balboa, Ancón
Panama City, Panama

Jennifer Larsen
Department of Geology
University of Vermont
Burlington, VT 05405 USA

David Lashlee
U.S. Army Yuma Proving Ground
Yuma, AZ 85365 USA

Raúl E. Martínez
Engineering Division
Autoridad del Canal de Panama
Panama City, Panama

Timothy W. Miller
Department of Earth and Environmental Sciences
New Mexico Institute of Technology
Socorro, NM 87801 USA

Helena Mitasova
Department of Marine, Earth, and Atmospheric Sciences
North Carolina State University
Raleigh, NC 27695 USA

Arizmendis S. Montoya
Engineering Division
Autoridad del Canal de Panama
Panama City, Panama

Kyle K. Nichols
Department of Geosciences
Skidmore College
Saratoga Springs, NY 12866 USA

Justin Niedzialek
Department of Civil and Environmental Engineering
University of Connecticut
Storrs, CT 06269 USA

Edwin J.M. Noordman
WaterWatch
Generaal Foulkesweg 28
Wageningen 6703 BS
The Netherlands

Fred L. Ogden
Department of Civil and Environmental Engineering
University of Connecticut
Storrs, CT 06269 USA

Eugene J. Palka
Department of Geography and Environmental Engineering
United States Military Academy
West Point, NY, USA 10996-1695

Rolando Pérez
Smithsonian Tropical Research Institute
Center for Tropical Forest Science
P.O. 2072, Balboa, Ancón
Panama City, Panama

Sievert Rohwer
Burke Museum
Box 353010
University of Washington
Seattle, WA 98195-3010 USA

Pedro Rojas
Autoridad Nacional del Ambiente
Deptartmento Conservación de la Biodiversidad Dirección Nacional de Patrimonio Natural
P.O. Box 0843, Zoná C , Balboa, Ancón.
Panama City, Panama

Augustín Somoza
Departamento Conservación de la Biodiversidad
Autoridad Nacional del Ambiente
P.O. Box 0843, Zoná C , Balboa, Ancón
Panama City, Panama

Klaus Simon
Geoscience Center, Division of Geochemistry
University of Göttingen
37077 Göttingen, Germany

Jason A. Sperfslage
Hydrologic Research Center
12780 High Bluff Drive, Suite 250
San Diego, CA 92130 USA

Gregory Springer
Department of Geological Sciences
Ohio University
Athens, OH, USA 45701

Robert Stallard
Water Resources Division
U. S. Geological Survey
3215 Marine Street
Boulder, CO 80302 USA

Israel Tejada
Autoridad Nacional del Ambiente
Deptartmento Conservación de la Biodiversidad
P.O. Box 0843, Zoná C , Balboa, Ancón
Panama City, Panama

Laura Toma
Department of Computer Science
Duke University
Durham, NC 27707 USA
current affiliation:
Department of Computer Science
Bowdoin College
Brunswick, ME, USA 04011

David Vega
Centro de Inv. Hidraulicas e Hidrotecnicas
Universitá Tecnologica de Panama, Ext. Tocumen
Panama City, Panama

Ellen Wohl
Department of Earth Resources
Colorado State University
Fort Collins, CO 80523 USA

Gerhard Wörner
Geoscience Center, Division of Geochemistry
University of Göttingen
37077 Göttingen, Germany

Preface

This book calls the attention of the scientific community, government organizations and non-government agencies, and the general public, to arguably one of the most important and complex of the world's tropical rainforest regions – the greater Panama Canal Watershed. The Río Chagres basin is the primary source for water to operate the Panama Canal, and also supplies water for electricity generation and potable water for municipal use, but this important national resource is largely unstudied from a scientific standpoint. The broad objective of the book is to characterize and understand the physical and ecological components of an isolated and largely pristine tropical rainforest and describe how the different natural components of a tropical rainforest interact with one another. The majority of the 23 papers contained in the volume are based upon presentations made at an international scientific symposium of the same title held at the Gamboá Rainforest Resort and Conference Center in Gamboá, Panama on 24-26 February 2003. In turn, most of the symposium presentations arose form research undertaken during a multidisciplinary field study conducted in the upper Río Chagres watershed in 2001 by an international group of scientists. Convened under sponsorship of the Autoridad del Canal de Panama, Smithsonian Tropical Research Institute, Universidad Tecnológica de Panama and US Army Yuma Proving Ground Tropic Regions Test Center, this conference brought together some 50 scientists, engineers, and government officials from the international community. The papers in this book follow two perspectives, regional-scale studies of the greater Panama Canal Watershed and more focused papers that consider specific aspects of the upper Río Chagres basin. The book begins with regional geographic overviews of Panama (Ch. 1) and the Panama Canal Watershed (Ch. 2-3). This is followed by two geological papers (Ch. 3-4), the first which describes the geological developmental history of Panama and the second of which presents the geological framework of the upper Río Chagres basin. The next ten papers (Ch. 6-15), forming the central portion of the volume, address the geomorphology, hydrology, and hydrometeorology, and biology of this largely pristine tropical rainforest. The final eight papers (Ch. 16-23) return to the broader perspective, considering similar issues from a regional perspective. A large amount of supplemental material, including a digital elevation model for Panama, species lists from the biological studies, the hydrologic rating curve report for the Rió Piedras, geological field notes and pictures, and other information are available to the interested reader on the web site: http://skagit.meas.ncsu.edu/~helena/riochagres/. A special thanks is due to Brendan Harmon, without whose useful proofreading and editorial assistance the timely preparation of this volume would not have been possible.

RSH

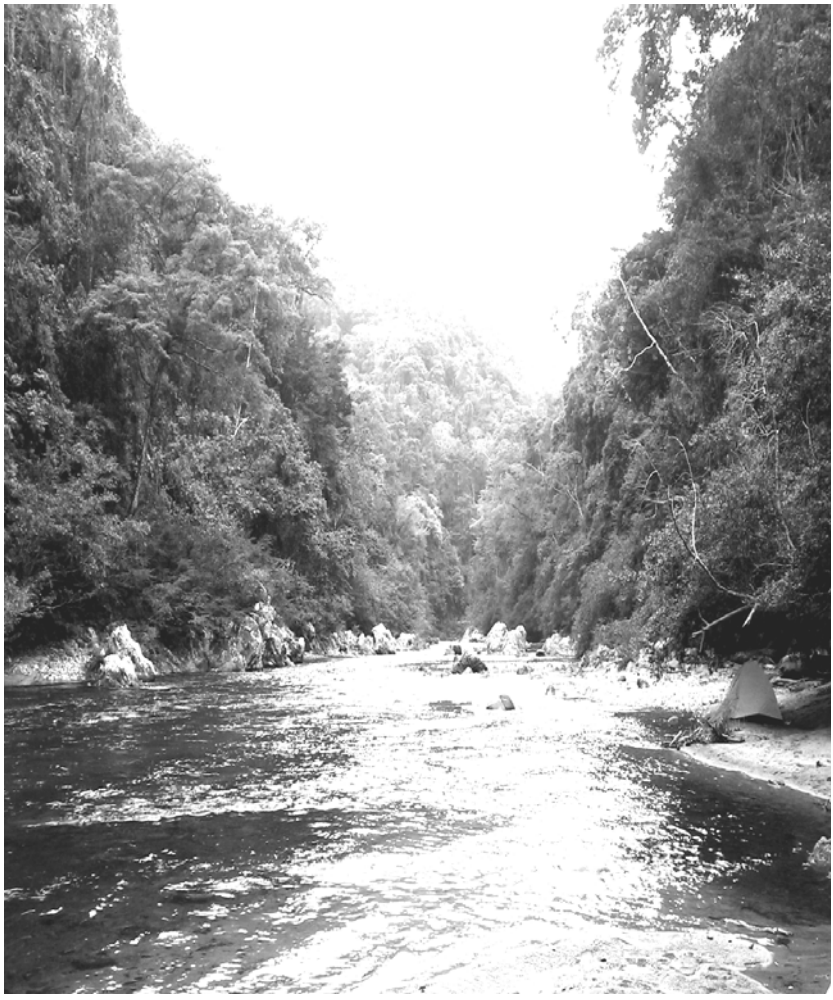

The Upper Río Chagres, Panama

Part I: Setting the Scene

Chapter 1

A GEOGRAPHIC OVERVIEW OF PANAMA:
Pathway to the Continents and Link between the Seas

Eugene J. Palka
United States Military Academy

Abstract: The Republic of Panama occupies about 77,382 km² and, despite its relatively small size, displays a remarkable degree of physical and cultural diversity. Part of the country's physical and biological variety can be attributed to its absolute location within the tropics. Panama's relative location, however, is equally responsible for both the physical and cultural complexity of the country. As the land bridge between the Americas and the major link between the world's two largest oceans, Panama is the crossroads of the western hemisphere. The country's position relative to the continents and oceans constitutes its most important situational advantage. This geographic analysis focuses on the physical geography of Panama, with the goal of providing an overview and larger context for the other papers of this volume. It considers the implications of its relative location and summarizes the physical geography of Panama in general terms drawing from geomorphology, climatology, and biogeography. Although the climate is tropical, Panama experiences significant climate diversity over relatively short distances. Panama also has considerable relief within its comparatively small territorial extent. Elevation differences and associated temperature and precipitation patterns produce distinct vegetative regimes and contribute further to the country's biodiversity. The country's most celebrated resource, however, is its unique location at the intersection of the western hemisphere's continents and oceans.

Key words: Panama; physical geography; geomorphology; climatology; biogeography

1. INTRODUCTION

As an integral part of the land bridge between the continents of North and South America, and as the major connecting link between the world's two largest oceans, the Republic of Panama has proven to be the crossroads of the western hemisphere. The country occupies a territorial extent of about 77,400 km², or an area slightly smaller than the US state of South Carolina (US DOD, 1999). Despite its relatively small size, Panama displays a

R. S. Harmon (ed.), The Río Chagres, Panama, 3-18.

remarkable degree of physical and cultural diversity. Part of the country's physical and biological complexity stems from its position within the tropics, a function of its absolute location. Panama's relative location, however, contributes even further to both the physical and cultural diversity of the country.

This chapter provides a general overview of the country's physical geography in order to provide a larger context for the more comprehensive multidisciplinary analysis of Panama's upper Río Chagres basin, which comprises the majority of this volume. To begin, the country's location is discussed, highlighting the implications of Panama's position relative to the continents and oceans. Then, the physical geography of Panama is examined within the context of three geographic subfields: geomorphology, climatology, and biogeography. The geomorphologic perspective describes the physical relief, principal landforms, and predominant drainage patterns. The climate is addressed in both local terms and within a regional context. Vegetative regimes are discussed in general terms and are connected to physiographic and climatic patterns.

2. THE GEOGRAPHIC PERSPECTIVE

Geography is an extremely broad academic discipline that offers a unique spatial perspective for examining a wide-range of problems, at various geospatial scales, at different points in time, and across disciplinary boundaries. Where geography overlaps with other disciplines, distinct geographic subfields emerge. While each of these subfields can be studied individually, they are also routinely applied in a collective fashion to particular places or regions.

To provide a larger context for the multidisciplinary study of the upper Río Chagres basin, this chapter draws from three distinct geographic subfields - geomorphology, climatology, and biogeography - and generalizes information about Panama using the regional method. As an approach to doing geography, the regional method is best described as a synthesis of the pertinent subfields applied to a specific place. Thus, by definition, most regional geography is both interdisciplinary and multidisciplinary. In this case, a regional geography of Panama introduces some of the distinguishing characteristics of the country and provides a point of departure for the more detailed analyses that comprise the remainder of this volume.

3. LOCATION

One of the keys to understanding the historical development, complexity, and importance of Panama, is derived from an examination of its location. The geographic center of the country lies at approximately 9 °N latitude and 80 °W longitude (Fig. 1). The N-S extent of Panama's borders run approximately from 7-10 °N latitude, and the country extends east to west from 77-83 °W longitude. This E-W extent of about 840 km is equivalent to the approximate distance from Washington, D.C. to Boston in the United States. The country's N-S distance varies between 60-180 km. The most important aspect of Panama's location, which is located entirely within the -5:00 hr GMT time zone, stems from its position on the Isthmus of Panama and its position within the tropics.

Panama is a Central American Republic that is bordered by Costa Rica in the west and Columbia in the east. The country is uniquely located at the crossroads of the western hemisphere. Although Panama has been a sovereign state since gaining its independence from Columbia just over a century ago in 1903, its geographic contiguity with the latter and its position astride the land bridge between continents of North America and South American has left an enduring imprint on its landscape and people.

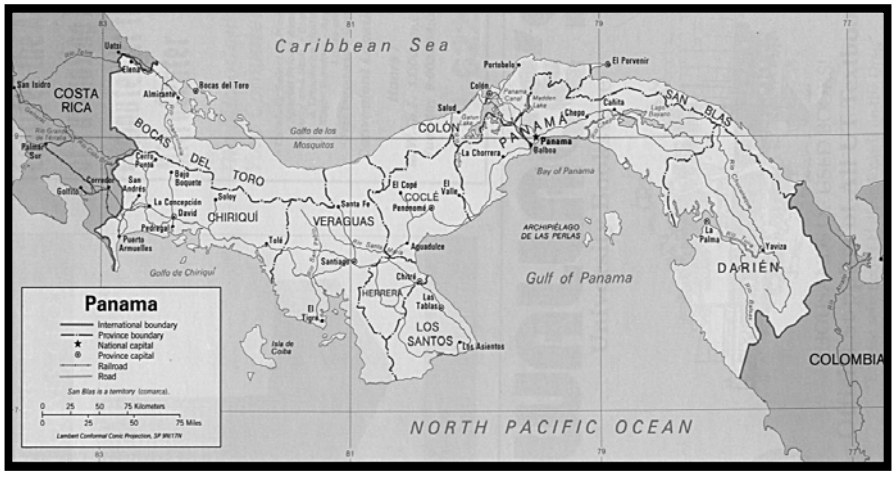

Figure 1. The Republic of Panama (after CIA, 1995).

Panama's location relative to other distinct cultures in the region is apparent in the many different ethnic groups and languages found within its current political borders, where traces of human presence date back more than 11,000 years (Labrut, 19). Located on the narrowest part of the Isthmus of Panama, the territory of the present-day Republic of Panama long

has experienced the flow and interaction of flora, fauna, and people between the continents. Since the completion of the Panama Canal in 1913, the country also has served as the conduit between the Atlantic and Pacific Oceans, contributing further to its biodiversity and re-establishing a connection that previously existed up to about 3 million years ago when the current land bridge formed (Coates and Obando, 1996).

4. GEOMORPHOLOGY

Geomorphology involves the study of landforms and the underlying processes that shape them. It entails understanding the physical relief, or the 'lay of the land', and how it evolved. Coates (1997) provides a comprehensive discussion of the formation of Central American land bridge. He specifically notes that the 'Darién Bridge' of eastern Panama surfaced above sea level only 3 million years ago (Coates, 1997). In the western half of the country, the spine that forms the continental divide is the combined expression of earlier episodes of magmatism and tectonic uplift during which mountains were formed by sub-volcanic intrusions (Weil *et al.,* 1972).

The other more routine geomorphic processes that have continued to shape Panama's surface since the quiescence of magmatic activity include weathering and erosion. The former breaks down surface materials, either by physical or chemical means; the latter refers to the movement of weathered surface material by blowing wind, running water, or wave action. The result of these processes is a dynamic physical landscape that is continually reshaped by the forces of nature and one that is reflective of both the dominant geomorphic forces at work and the pervasive influence of climate and weather.

The territory of present-day Panama has been created over the past 140 million years by the interaction of five major tectonic plates: the South American, Caribbean, North American, Cocos, and Nazca plates (see Harmon, 2005, this volume). The Pacific margin of the country is active tectonically, as compared with the Caribbean (*i.e.,* Atlantic) side, which is passive and characterized by a wide continental shelf. This disparity in tectonic activity establishes the conditions for two distinct coastal zones.

One estimate approximates the total length of coastline in Panama to be about 3,000 km (US DOS, 2000). The Caribbean coastline extends for about 815 km and includes several good natural harbors, whereas the Pacific coast stretches for about 1450 km (Weil *et al.,* 1972). The Caribbean coast features extensive coral reefs and includes the 350 or so San Blas Islands that are arrayed along the coastline for more than 170 km (Meditz and Hanratty, 1987). Strung out along the Pacific coast are more than 1,000

islands (Meditz and Hanratty, 1987), including the Las Perlas Archipelago, the Coiba Island in the Gulf of Chiriquí, and the tourist island of Taboga. The country experiences two distinct tidal regimes, with a microtidal range of less than 2 m along the Caribbean coast, and a macrotidal variation between 4-6 m along the Pacific coast (US DOD, 1999).

The dominant inland terrain feature is a discontinuous spine of mountains running through the middle of southern Central America (Fig. 2), that has several regional names - the Cordillera de Talamanca in Costa Rica, the Serranía de Tabasará as it crosses the border into Panama, and then the Sierra de Veraguns as it straddles the former Canal Zone (Weil *et al*., 1972; Miditz and Hanratty, 1987). Most sources generally use the term 'Cordillera Central' to refer to the range that extends from the border with Costa Rica to the Panama Canal. Other mountainous areas include the San Blas Mountains 'which attain elevations >900 m, the Sapo Mountains which attains heights of >1,100 m, and the Darien Mountains which reach 1,876 m. Thus, the combination of volcanism and tectonic uplift, weathering and erosion, and the pervasive influence of climate has established pronounced physiographic features on the landscape: volcanoes, drainage basins, rivers, and a complex coastline.

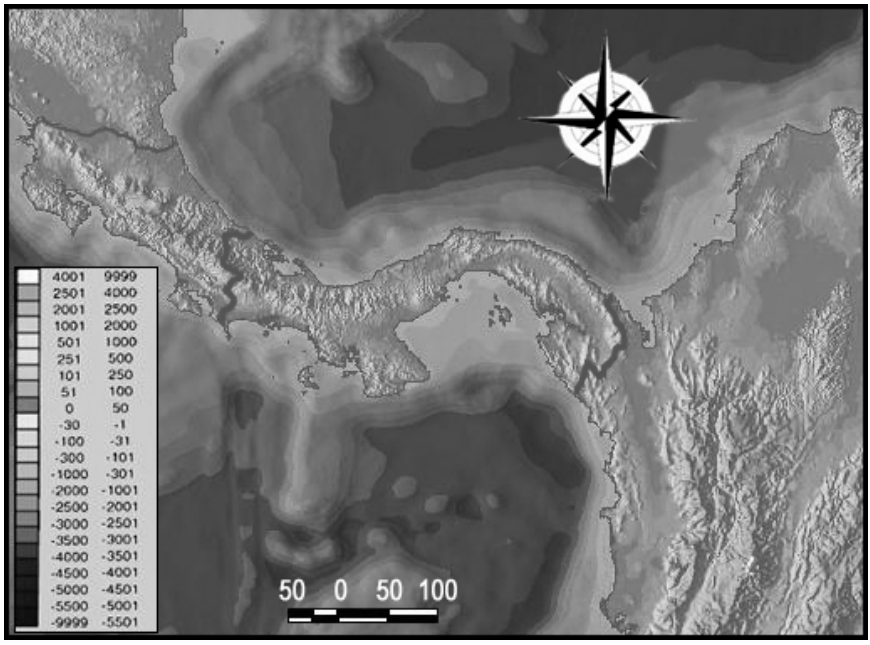

Figure 2. Relief map of southern Central America (USGS, 2001).

Perhaps the most clearly visible physiographic features on Panama's landscape are the mountain ranges and relict volcanoes (Fig. 3). The highest elevations occur in the vicinity of Mount Barú (3,475 m), - (formerly known as Volcán de Chiriquí) - a historically active volcano, which marks the eastern extremity of the Nicaragua volcanic belt in western Panama (Weil *et al*., 1972). Other smaller volcanic peaks are scattered along the Central Cordillera from the border with Costa Rica eastward to El Valle, near the Panama Canal. Although dormant for several centuries, volcanic ash and lava from Mount Baru have contributed to the formation of fertile, nutrient rich soils (Coates, 1997). The relict volcanoes of the Cordillera Central have also had a profound influence on the drainage patterns in the country.

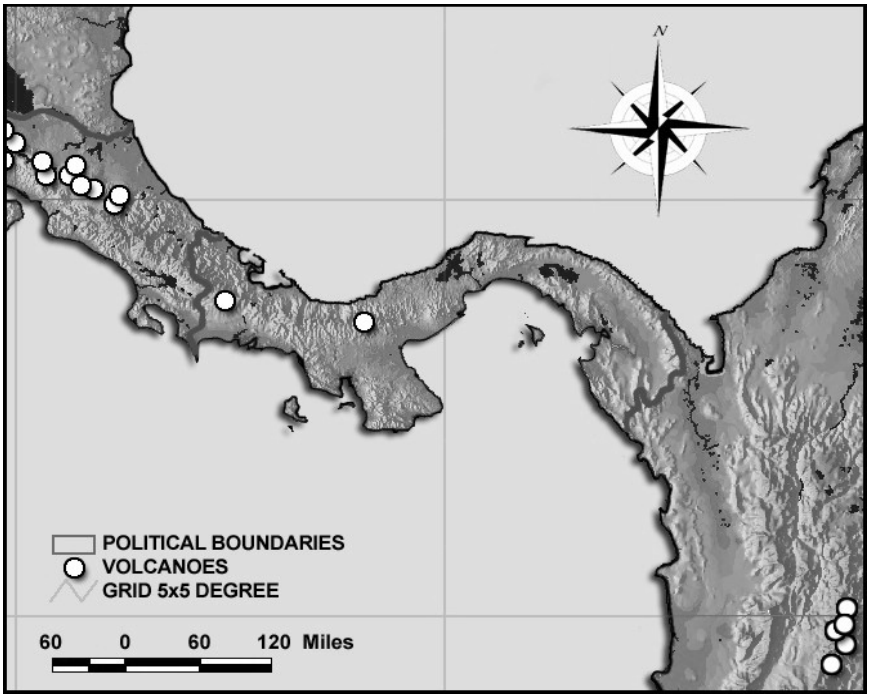

Figure 3. Volcanic activity across eastern Central America (USGS, 2001). White circles denote historically active volcanoes.

4.1 Volcanoes

Perhaps the most clearly visible physiographic features on Panama's landscape are the mountain ranges and relict volcanoes (Fig. 3). The highest elevations occur in the vicinity of Mount Barú (3,475 m), - formerly known

as Volcán de Chiriquí - a historically active volcano, which marks the eastern extremity of the Nicaragua volcanic belt in western Panama (Weil *et al*., 1972). Other smaller volcanic peaks are scattered along the Central Cordillera from the border with Costa Rica eastward to El Valle, near the Panama Canal. Although dormant for several centuries, volcanic ash and lava from Mount Baru have contributed to the formation of fertile, nutrient rich soils (Coates, 1997). The relict volcanoes of the Cordillera Central have also had a profound influence on the drainage patterns in the country.

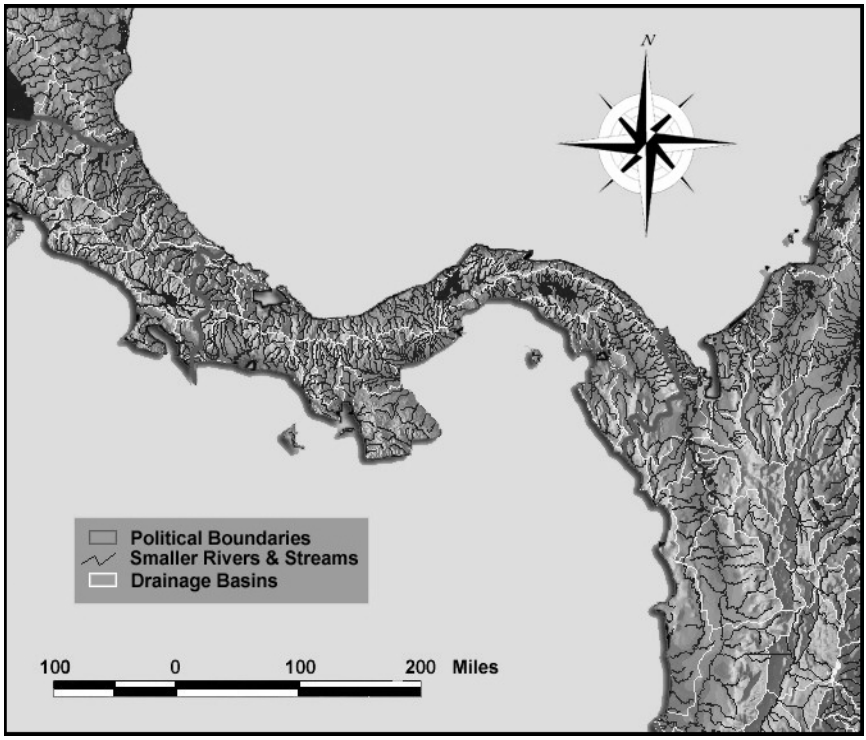

Figure 4. River drainages of Panama (USGS, 2001).

4.2 River Characteristics

Given the rugged nature of its relief and its tropical location, one would expect Panama to be well endowed with fresh water resources. The country has about 500 rivers by most accounts, about 350 of which discharge into the Pacific and the remaining 40% of which drain into the Atlantic (Fig. 4). Those rivers that flow into the Pacific are generally longer, of shallower gradient, and have longer, more developed basins. The steep, conical

character of many of Panama's mountains results in radial drainage patterns, within which streams extend outward in all directions from the mountain summit. The more prominent patterns, however, are the parallel streams that are associated with elongated, parallel mountain ranges of steep relief in close proximity to the coast. For example, the Río Chagres exhibits a parallel pattern (see Kinner *et al*., 2005, Chapter 5).

By several criteria, the Río Chagres is Panama's most important river (ANAM, 2000) and, uniquely, the only river in the world to flow into two oceans. Originally dammed in its lower section in 1914 to form Gatun Lake, a second dam was constructed in the lower portions of the upper basin in 1935 to form Lago Alajuela. Currently the Río Chagres provides about 40% of the water necessary to operate the Panama Canal and provides the drinking water for residents of Panama City and Colón, which amounts to nearly 50% of the country's population of 3 million (ANAM, 2000). Fortunately, the Chagres National Park was established in 1985 by Panama's Autoridad Nacional del Medioambiente (ANAM) to protect the hydrologic basin of this extremely significant river (ANAM, 2000).

4.3 The Panama Canal Watershed

The watersheds of the Panama Canal region (of which the Río Chagres basin is an integral part) comprise nearly 552,761 hectares, extending on both sides of the waterway into the provinces of Coclé, Panama, and Colón (ACP, 2001). Of the water withdrawn from these watersheds, 58% is used to operate the canal locks, 36% for generating electricity, and 6% for drinking water (ACP, 2001). The boundaries of the greater Panama Canal Watershed are defined by law within Panama's constitution because the watershed and its dense tropical rainforest constitute a critical natural resource for the country. The continuing health of the watershed and its rainforest are dependent upon favorable climate and compatible human activities.

5. CLIMATOLOGY

Climatology is the subfield of geography that examines the long-term conditions of the atmosphere and the interactions between the atmosphere and the earth's surface. Climate profoundly influences a host of environmental processes such as the growth of vegetation, soil formation, watershed hydrology, and geomorphic denudation. Climate also influences human activities ranging from agricultural to building practices. The term climate is often referred to as the 'average weather' of a location, but this can be overly simplistic and misleading. Depending on the spatial scale

considered or the timeframe used, a variety of different climatic patterns emerge in the analysis of any region, regardless of its size. As the spatial scope narrows and as the timeframe shortens, a host of factors internal to the climate system begin to play an increasingly important role in developing a clear analysis of 'average' atmospheric conditions. Factors such as topography, vegetation, regional pressure variability, and El Niño phases may play an important part in determining the climate for a particular season or year. This is especially true for Panama. Thus, geographers typically examine climate from both a regional and local perspective.

5.1 Regional Climate Patterns

Panama has a tropical climate that stems in part from its location between 7-10° N latitude. Using the Köppen climate classification system, Panama's climate is generally characterized as an ***A*** type (tropical climate with all monthly mean temperatures over 18 °C. More specifically, the country exhibits a regional pattern that includes an ***Af*** climate (sufficient precipitation all months) along the Atlantic coast, and an ***Aw*** climate (dry season during the winter) along the Pacific coast and on the south side of the continental divide.

Despite uniformly high temperatures and precipitation year round, temperatures on the Atlantic side of the isthmus are slightly higher, in general, than on the Pacific, and precipitation is of higher intensity on the Atlantic side. Average annual temperatures range from 23-27 °C in coastal areas throughout the country and average a milder 19 °C in the interior highlands (Microsoft, 2001). The rainfall pattern is more pronounced with an average of 2,970 mm on the Atlantic side and about 1,650 mm on the Pacific side of the continental divide (Microsoft, 2001).

5.2 Climate Controls and Localized Patterns

Climate controls influence a variety of variables such as temperature, temperature range, precipitation, and wind; and are the cause of the N-S and coastal-upland variations in Panama's climate. Controls such as insolation, pressure, ocean currents, maritime influence, altitude, and topographic barriers, all play a role in determining the climate of Panama, due to the country's mountainous terrain, equatorial proximity, coastal position between the Pacific Ocean and the Caribbean Sea, and its location relative to the inter-tropical convergence zone (ITCZ).

The amount of incoming solar radiation, or insolation, that Panama receives is primarily a function of its latitude. Located between 7-10 °N latitude, Panama is only a short distance north of the equator. As a result, the

country receives high amounts of insolation throughout the year, and maximum amounts during the summer, when the northern hemisphere is tilted towards the sun and periods of daylight are slightly longer. This results in year-round high temperatures with minimal seasonal and daily variation, especially at sea level locations.

The country's location on the Isthmus of Panama also contributes to the small annual and daily temperature range. The coastal orientation of the country subjects it to the moderating effects of the ocean and sea. This type of situation influences the temperature range between summer and winter, and even from day to night, regardless of latitudinal location. However, temperatures around the country can vary widely due to variations in elevation and rugged nature of the topography. Altitude has a dramatic effect on temperature. Air temperatures decrease with increasing elevation as a function of the dry environmental lapse rate, which averages about -10 °C per 1,000 meters increase in elevation. With much of Panama dominated by the continental divide, altitude must be considered carefully. Several peaks have elevations that exceed 3,500 m, so these mountains can experience temperatures that may vary by 10-15 °C over relatively short horizontal distances. Such temperature variability makes it very difficult to characterize broad regions as having uniform climate types. Moreover, elevation and orientation to prevailing winds can combine to produce microclimatic niches (Rees, 1997).

The influence of topographic barriers has a dramatic effect on precipitation regimes throughout the country. Orographic precipitation on the windward side of mountain ranges is common as moist air is forced upwards and cooled adiabatically. By contrast, air on the leeward side of mountain ranges descends and warms adiabatically resulting in a rain shadow effect where the air is warmer and much drier. The Atlantic coast of Panama experiences a sustained onshore flow of wind accompanied by orographic precipitation, except during the winter months. Thus, the Caribbean side has higher precipitation totals throughout the year, with only a short dry season during winter.

The Inter-Tropical Convergence Zone (ITCZ) has a significant impact on Panama's climate as the low-pressure system migrates seasonally across the country. Atmospheric pressure controls the amount and seasonality of precipitation. Parts of the country receive increased rainfall based on the presence of the ITCZ from May to December, and significantly less rain from January to April as the ITCZ migrates south.

Panama's climate is more complex than might be anticipated given the small territorial extent of the country. Attempting to characterize Panamanian climate regionally is difficult due to the interactions of several

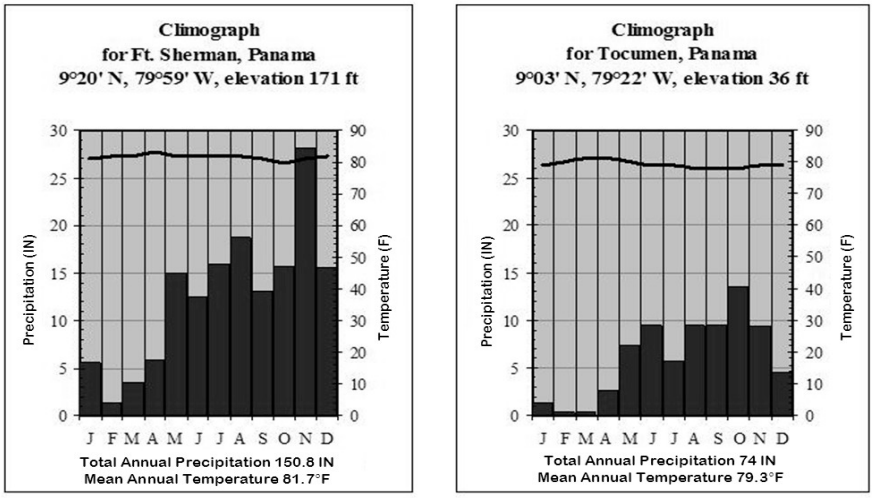

Figure 5. Climographs for two locations in central Panama demonstrating Atlantic versus Pacific variability – (left) for Ft. Sherman near the Atlantic coast and (right) for Tocumen near the Pacific coast (data from USAFCCC, 2003).

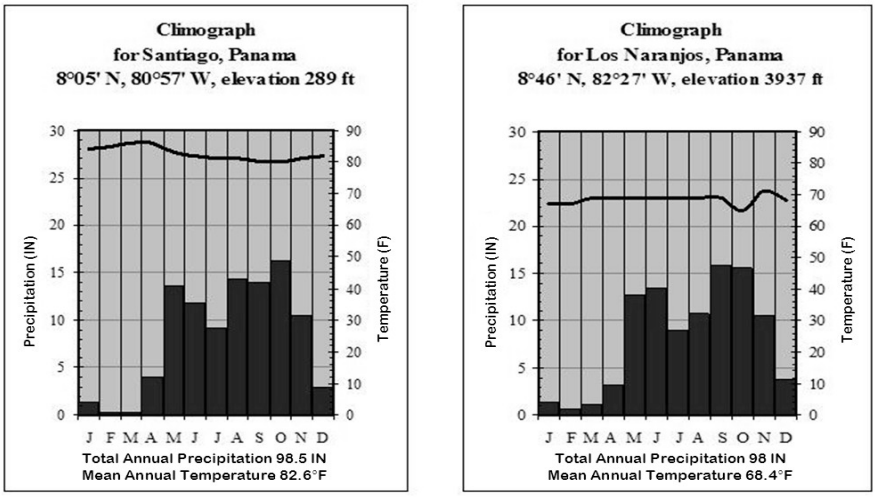

Figure 6. Climographs for two locations in central Panama illustrating interior lowland versus highland variability – (left) for Santiago a lowland site and (right) for Los Naranjos, a highland site (data from USAFCCC, 2003).

climate controls. Altitude and maritime location significantly affect temperature regimes, while pressure systems and topographic barriers influence precipitation patterns. The overall result is a tropical climate with local temperature and precipitation variations based on elevation, orientation, and proximity to the coast. Climographs, graphical representations of monthly mean temperature and monthly precipitation for a specific location, help to portray the impact of climate controls and provide a clearer picture of the climate diversity within the country (Figs. 5 and 6).

6. BIOGEOGRAPHY

Panama's biogeographic complexity stems from its geomorphology and climate. Biogeography is the study of the distribution of plants and animals, where these biotic entities occur, and why they occur at disparate locations. This field of study utilizes information derived from many other disciplines and subfields, such as meteorology, climatology, geomorphology, botany, zoology, ecology, and resource management. The biogeographic scale of study normally is regional to continental and global. However, based on being the focal point of the 'Great American Biotic Interchange' (Simpson, 1940), Panama's biogeography is as complex as any comparable area in the world.

6.1 Vegetation Patterns

Panama's incredible biodiversity is attributable to its tropical location and its position on the Central American land bridge. Webb (1997) provides a comprehensive statement of the 'Great American Biotic Interchange' noting that more than half of the present land mammals of South America came from North and Central America by way of the land bridge (Webb, 1997). Using Holdridge's (1967, 1974) classification scheme, Panama has twelve life zones, defined by climatic and soil conditions and associated forests. The biological diversity is highlighted by an estimated 10,000 species of plants (Labrut, 1993). More conservative surveys include up to 9,000 vascular plants, along with 218 species of mammals, 929 of birds, 226 of reptiles, and 164 of amphibians (Microsoft, 2001).

Natural vegetation zones include forested mountains, hills, lowlands, savannas, coastal mangrove swamps, and tidal flats. Dense tropical forests include multistory canopies that extend some 20-50 m above the ground in uncleared parts of the eastern and northwestern regions of the country (US DOD, 1999). Mangrove swamps are common along the Caribbean coast, with savannas and rolling foothills in other coastal locations. Land cover

estimates vary, but Tomaselli-Moschovitis (1995) concludes that some 54% of the country's 77,400 km² is classified as forest and woodland, 15% as meadows and pastures, 6% as arable mixed, 2% as permanent crops, and 23% as supporting other vegetative covers. Figure 7 provides a general picture of the country's land cover.

Panama's tropical rainforests deserve special mention because of their incredible biodiversity. Most forests are broadleaf evergreen that include more than 1,000 varieties of trees, including brazilwood, tropical cedars, ceiba, espave, jacaranda, laurel, lignumvitae, and rosewood (Weil *et al*., 1972). Deforestation, however, continues to be a major concern. One estimate identifies an average annual loss of 51,000 hectares of forest, with only three million hectares of forest remaining (Brokema, 1999). Other assessments indicate that tree cover has been reduced by 50% since the 1940s (Meditz and Hanratty, 1987).

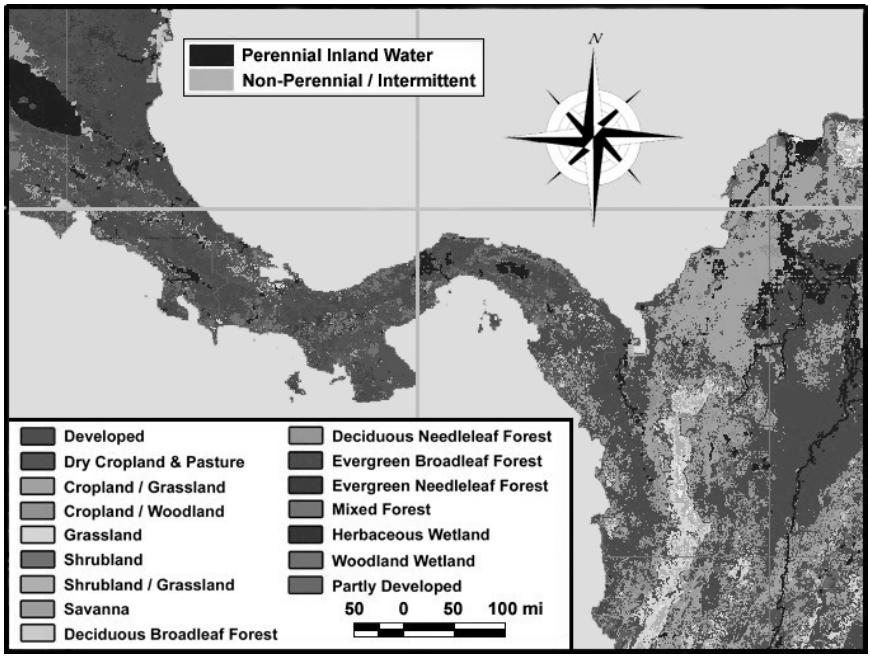

Figure 7. Land cover map of Panama (USGS, 2001).

7. CONCLUSION

Volcanism and tectonic activity have forged the territorial extent and physical relief of the Panama over the past 140 million years, with the most

visible development occurring during the past 10 million years (Coates, 1997; Harmon 2005, this volume). The effects of the 'Great American Biotic Interchange', which began in Central America less than 3 million years ago, still linger and have contributed significantly to Panama's remarkable biological diversity (Webb, 1997). The country's biodiversity is also enhanced by its tropical location, where warmer and wetter natural environments generally result in increased biological variety. Scholars agree that biodiversity is critical to the stability of ecosystems (such as Panama's tropical rainforest) because the health of the latter depends on their ability to withstand the loss of some of their members (Clawson, 2000). Additionally, researchers believe that nearly half of all life forms on the planet are associated with tropical rainforests, so these unique environments are important wherever they occur (Clawson, 2000).

Not to diminish the importance of its tropical rainforests, but some would argue that Panama's greatest natural resource is its relative location, which just over a century ago made the young Republic an attractive locale for constructing a canal to link the world's two major oceans. From this perspective, the Panama Canal holds the greatest promise for Panama's continued economic development and modernization, especially since the implementation of Carter-Torrijos Treaty on 31 December 1999 (see Heckadon, 2005, Chapter 3). To be sure, efforts to maintain and modernize the canal to promote economic development must recognize the concomitant need to protect the hydrological and biological integrity of the entire Panama Canal Watershed. In this regard, the upper Río Chagres hydrographic basin is a critical natural resource, whose forests supply 40% of the water necessary to operate the canal, as well as drinking water for nearly 50% of the country's population (ANAM, 2000). The multidisciplinary scientific study of this unique tropical watershed described in this volume is an important step towards ensuring that this irreplaceable natural resource is carefully managed, now and for future generations.

ACKNOWLEDGEMENTS

Thanks are extended to several colleagues for assistance with this chapter, particularly colleagues in the Department of Geography and Environmental Engineering at the US Military Academy. W. C. King and F. A. Galgano reviewed previous versions of this paper, J. Malinowski assisted with the graphics, and R. S. Harmon provided editorial expertise.

REFERENCES

Augelli, JP, 1986, The Panama Canal area: *Focus* 36: 20-29.

Autoridad Nacional del Ambiente de Panama, 2000, *Parques Nacionales de Panama*: Balboa, Panama.

Autoridad del Canal de Panama. 2002, *The Panama Canal: How the Canal Works*: Corporate Communications Division, Balboa-Ancon, Panama.

Autoridad del Canal de Panama, 2002, *The Panama Canal: Historical Background and Physical Features of the Waterway*: Corporate Communications Division, Balboa-Ancon, Panama.

Authoridad del Canal de Panama, 2001, *The Panama Canal, Information Brochure*: Corporate Communications Division, Balboa-Ancon, Panama.

Blouet, BW and Blouet, OM, 1997, *Latin America and the Caribbean: A Systematic and Regional Survey*: John Wiley Inc., New York, NY.

Blouet, BW and Blouet, OM, 2002, *Latin America and the Caribbean: A Systematic and Regional Survey*: John Wiley Inc., New York, NY.

Bonini, WE, Hargraves, RB, and Shagam, R, eds., 1984, *The Caribbean-South American Plate Boundary and Regional Tectonics*: Geol. Soc. Am., Boulder, CO.

Brokema, I, 1999, Position of the International Primate Sanctuary of Panama in the scheme of conservation areas: A report prepared to help clarify policy development at the International Primate Sanctuary of Panama.

Clawson, DL, 2000, *Latin America & the Caribbean: Lands and Peoples*: McGraw-Hill Inc., New York NY.

Coates, AG, ed., 1997, *Central America: A Natural and Cultural History*: Yale Univ. Press, New Haven, CT.

Coates, AG and Obando, JA, 1996, The geologic evolution of the Central American isthmus: in *Evolution and Environment in Tropical America* (JBC. Jackson, AF Budd, and AG Coates, eds.), Univ. Chicago Press, Chicago, IL: 21-56.

Goodwin, PB, 2000, *Global Studies: Latin America*: Dushkin/McGraw-Hill, Guilford, Canada.

Harmon, RS, 2005, The Geologic Development of Panama: in *The Río Chagres: A Multidisciplinary Perspective of a Tropical River Basin* (RS Harmon, ed.), Kluwer Acad. Press, New York, NY: 43-62.

Heckadon, S, 2005, Light and Shadows in the Management of the Panama Canal Watershed: in *The Río Chagres: A Multidisciplinary Perspective of a Tropical River Basin* (RS Harmon, ed.), Kluwer Acad./Plenum Pub., New York, NY: 29-44.

Holdridge, LR, 1967, *Life Zone Ecology*: Tropical Science Center, San Jose, Costa Rica:

Holdridge, LR, Renke, WC, Hathweay, WH, Liang, T, and Tofy, JA, 1974, *Forest Environment in Tropical Life Zones*: Pergamon Press, San Francisco, CA.

Kinner, D, Mitasova, H, Stallard, R, Harmon, RS, and Toma, L, 2005, GIS database and stream network analysis for the upper *Río* Chagres Basin, Panama: in *The Río Chagres: A Multidisciplinary Perspective of a Tropical River Basin* (RS Harmon, ed.), Kluwer Acad./Plenum Pub., New York, NY: 83-95.

Labrut, M, 1993, *Getting to Know Panama*: Focus Publications, El Dorado, Panama.

Longman, KA and Jenik, J, 1987, *Tropical Forest and its Environment*, Longman Ltd., London, UK.

Martinson, T, 1997, Physical Environments in Latin America: in *Latin America and the Caribbean: A Systematic and Regional Survey* (BW Blouet and OM Blouet, eds.), John Wiley Inc., New York, NY: 11-44.

Meditz, SW, and Hanratty, DM, eds., 1987, *Panama - A Country Study*: Library of Congress, Federal Research Division, Washington, DC.

Microsoft, Encarta, 2001, Interactive World Atlas: Panama.

Place, SE, ed., 1993, *Tropical Rainforests: Latin American Nature and Society in Transition*: Scholarly Resources Inc., Wilmington, DE.

Rees, P, 1997, Central America: in *Latin America and the Caribbean: A Systematic and Regional Survey* (BW Blouet and OM Blouet, eds.), John Wiley Inc., New York, NY: 237-271.

Simpson, GG, 1940, Mammals and land bridges: Jour. Wash. Acad. Sci., 30: 137-163.

Tomaselli-Moschovitis, V, ed., 1995, *Latin America on File*: Facts on File Inc., New York, NY.

Chapter 2

AN INTRODUCTION TO THE PANAMA CANAL WATERSHED

Russell S. Harmon
US Army Research Office

Abstract: The Panama Canal Watershed is a hydrologically complex, ecologically diverse managed natural-artificial managed water resource system composed of many sub-basins, rivers, and dammed lakes extending across 2,982 km^2 on both sides of the Panama Canal. The upper Río Chagres basin is the largest headwater unit in the watershed, occupying about one-third the total area but supplying almost half of the water needed for canal operation. Total runoff across the watershed is such that there is inadequate input of water during low-flow years to provide the all of $4.1x10^5$ m^3 of water needed to operate the canal, generate electricity, and provide public drinking water. At present, forest preservation is arguably the most important water resources management issue for the Panama Canal Watershed because deforestation causes enhanced soil erosion and reservoir sedimentation and also strongly affects the timing of the runoff. Overall, prospects for the long-term sustainability of the water resources of the Panama Canal Watershed are good, given the large percentage of land within the watershed that is federally protected. However, the challenge for the immediate future is to develop and enforce a consistent set of informed and enforced land management to ensure that the water resources will continue to be available to operate, if necessary, and expand the Panama Canal for the benefit of Panama and the world.

Key words: Panama, Panama Canal Watershed

1. THE PANAMA CANAL

The construction of the Panama Canal was one of the most profoundly important engineering and historic feats of the 20th Century (McCulloch, 1977). The canal is an 80 km long waterway that connects the Atlantic Ocean with the Pacific Ocean across the Isthmus of Panama (Fig. 1). To accomplish the building of canal and float ships across the continental divide, it was necessary to create Lake Gatun by building a dam across the lower reaches of the Rio Chagres and three sets of locks – at Gatun, Pedro

R. S. Harmon (ed.), The Río Chagres, Panama, 19-28.

Miguel, and Miraflores – that raise and lower ships 26 m from sea level to Lake Gatun and *vice versa.* On the Pacific side, Pedro Miguel is a single-step lock and Miraflores is a 2-step lock, whereas Gatun on the Atlantic side consists of a 3-step of lock (ACP, 2001). Smaller dams for operational water supply were also built at the Pedro Miguel and Miraflores lock sites and, subsequently a large dam was constructed across the upper Rio Chagres to create Lago Alhajuela (Fig. 2).

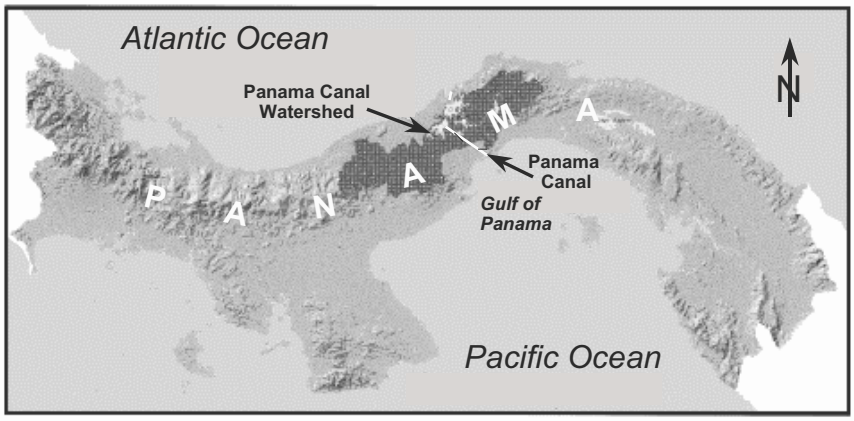

Figure 1. Topographic map of Panama sowing the location of the Panama Canal and the Panama Canal Watershed (modified from ACP, 2005)

With 38 ships making the ocean-to-ocean transit each day, the Panama Canal is an important contributor to the global economy as canal fees and related activities generate some 10% of the GDP of Panama (Cullen, 2005). The Panama Canal Watershed (Fig. 2) is a hydrologically and ecologically complex managed watershed that extends along both sides of the Panama Canal (ACP, 2001). Not only does the watershed provide the 1.91×10^5 m^3 of non-recycled water required for the passage of each ship through the canal, but its waters are also used to generate electricity and provide potable water for the more than one million residents of Panama City, Colon, and San Miguelito (Heckadon, 1993). With a large number of political, public, commercial, and individual interests presently competing for use and/or preservation of the varied resources of the basin, the of the Panama Canal Watershed represents one of the most high-profile examples of a sustainable land management challenge for the world in the 21st Century. Priority issues of immediate concern include water supply, population growth, deforestation, erosion, and reservoir sedimentation.

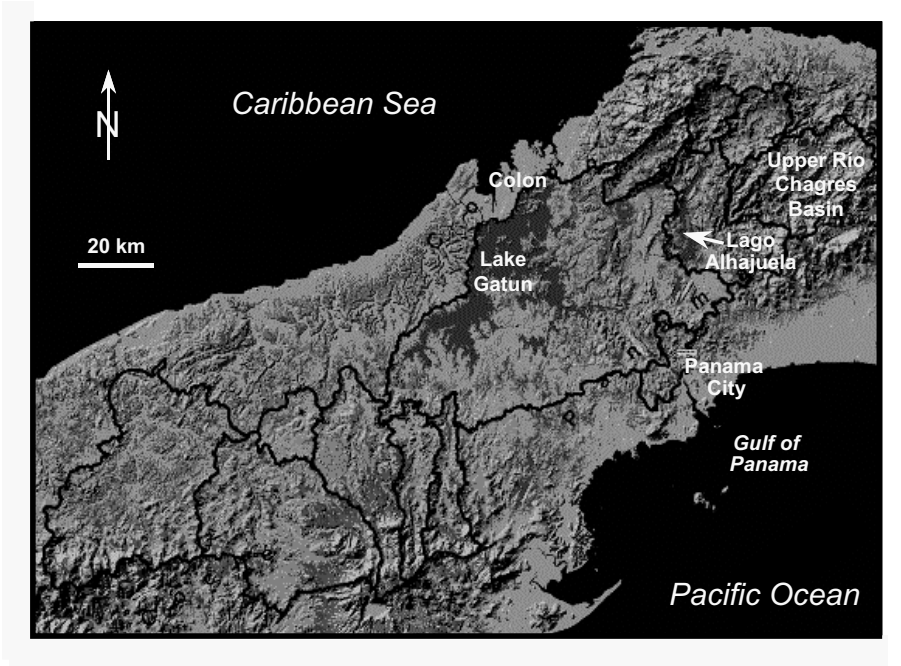

Figure 2. Topographic map of central Panama showing the location of the 13 sub-basins of the Panama Canal Watershed, Lake Gatun, Lago Alhajuela, and the upper Río Chagres basin (modified from ACP, 2005).

2. THE PANAMA CANAL WATERSHED

2.1 The Physical Watershed

As defined by Law 44 of the Panama Legislative Assembly enacted in August of 1999, which established the boundaries in law, the Panama Canal Watershed consists of 552,761 hectares (*i.e.,* 2,982 km^2) of land spread across 13 sub-basins in the provinces of Panama, Colon and Cocle (Fig. 2). Elevations across the Panama Canal Watershed range from sea level to about 1000 m, with most of the watershed at an elevation of <300 m. The construction of Lake Gatun in 1914 flooded a significant portion of the original Río Chagres basin (Fig. 3). This construction, together with the building of the Madden dam in 1936 to form Lago Alhajuela, divided the Río Chagres drainage into three parts, the upper basin above Lago Alhajuela, the lower basin, Gatun Lake, and river course between the dam and the Atlantic Ocean (Fig. 2). Today, Gatun Lake and Lago Alhajuela occupy about 14% of the total area of the Panama Canal Watershed. The upper Río Chagres basin, which occupies about one-third the area of total watershed, is

the largest headwater unit in the watershed, and arguably the most important of the 13 sub-basins, as it supplies almost half of the water needed for canal operation. This basin is a combined natural-artificial managed water resource system composed of many sub-basins, rivers, and dammed lakes. An understanding of the hydrometeorological characteristics of the watershed and interrelationships among different hydrometeorological variables (including: precipitation, evapotranspiration, soil storage, water losses, gross and net runoff, and water uses) are required for the upper Río Chagres basin as the foundation for sound water resources management across the entire watershed. Fortunately, the entire upper Río Chagres basin is included within the Chagres National Park, which presently serves to protect the hydrologic resources of this critical component of the Panama Canal Watershed.

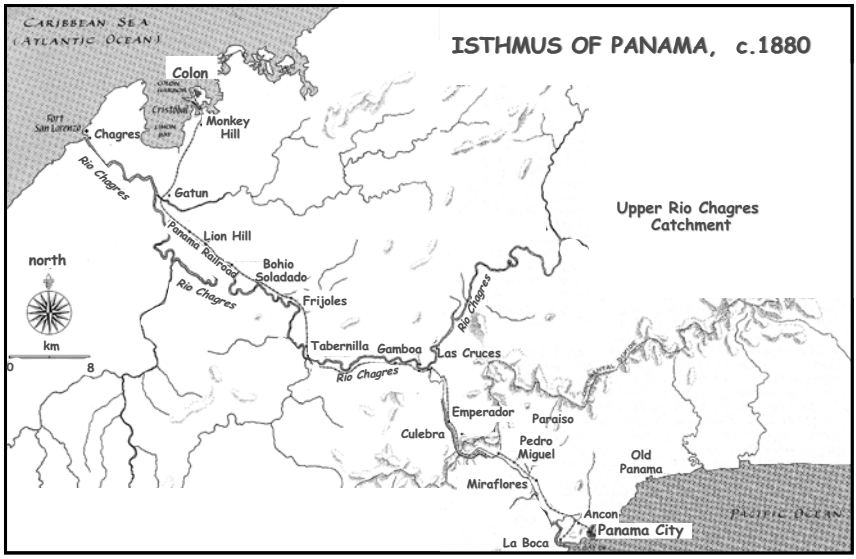

Figure 3. Map of central Panama, *c.* 1880, at the time of the unsuccessful French effort to build a sea-level canal across the Isthmus of Panama (modified from McCulloch, 1977).

2.2 Watershed Hydrometeorlogy

Central Panama is located in the moist lowland tropics where rainfall well exceeds evapotraspiration and has a distinct rainy season, typically lasting from May to mid-December, with wet season storms generated in the Caribbean. This situation produces a pronounced variation in annual rainfall and a strong rainfall gradient from one coast to the other, with the Atlantic side of the isthmus receiving an average of 3,000 mm as compared with

some 1,700 mm at the Pacific coast on the leeward side of the continental divide (Condit *et al.,* 2000). The total runoff across the watershed is $4.4x10^5$ m^3, which has been observed to decrease by up to 25% during low precipitation El Niño year years (Espinosa *et al*., 1997). This situation has caused concern because the current water budget is such that there is inadequate input of water during such low-flow years to provide all of $4.1x10^5$ m^3 of water needed to operate the canal, generate electricity, and provide public drinking water (Condit *et al.,* 2001). Hence, prudent management of the water resources within the Panama Canal Watershed is vital for the day-to-day operation of the Panama Canal and, therefore, the Panama Canal Authority also is considering the construction of a new lake in the western portion of the watershed and (Vargas, 2003).

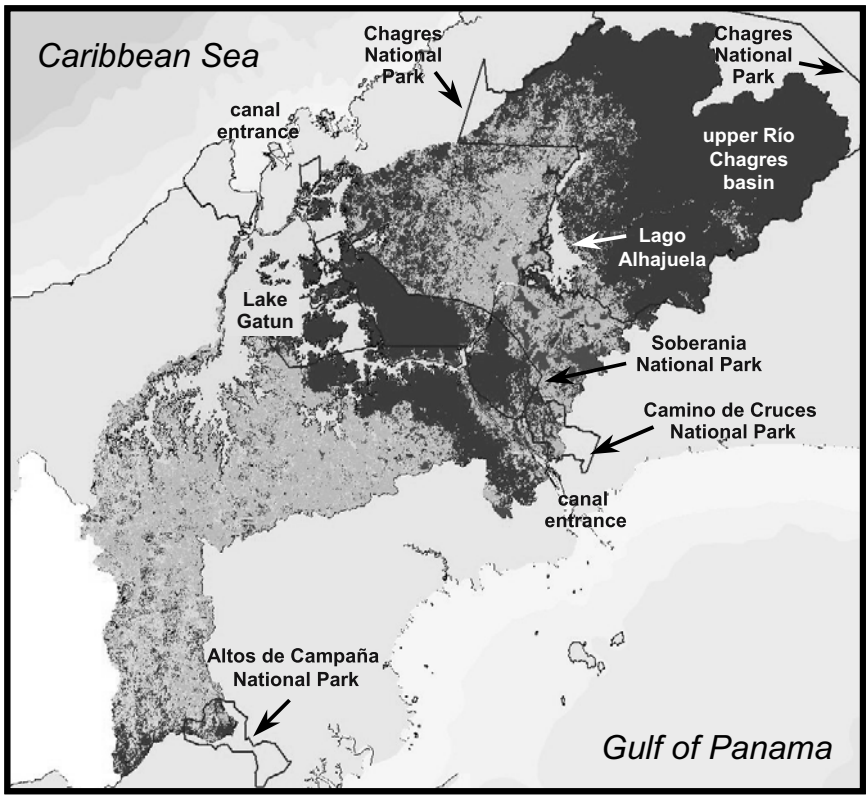

Figure 4. Land-cover map of the Panama Canal Watershed area (black = forest, dark grey = urban, light grey = agriculture, pasture, grassland, and shrubland). Also shown are the National Park boundaries, Lake Gatun, Lago Alhajuela, the upper Río Chagres basin, and the entrances to the Panama Canal (modified from Dale *et al.,* 2003).

2.3 Ecosystem Considerations

The ecosystem in central Panama, particularly that within the Panama Canal Watershed, is one of the most diverse anywhere around the world (Myers *et al.,* 2000; Condit *et al.,* 2001; Ibáñez *et al*., 2001). The long-term maintenance and sustainability of this biodiversity depends on the preservation of the tropical forest cover, which presently covers some 1570 km^2 of the watershed (Heckadon *et al*., 1999). Prospects for preservation are good, since almost 70% of this watershed cover is pristine, old-growth tropical forest contained in national parks and nature monuments located within two large blocks of land (Fig. 4) - one in a 16 km corridor along both sides of the former Canal Zone and the other in the sub-basins northeast of Lago Alhajuela, particularly the upper Río Chagres basin. These two areas of largely unbroken forest cover form a nearly continuous band across the isthmus. As illustrated in Figure 4, the vast majority of the agricultural, pasture, grasslands, and shrublands are concentrated in two zones - one between the forested canal corridor and the upper Río Chagres basin in the northeast sector of the watershed that contains a patchwork of forest fragments (Condit *et al.,* 2001) and the other in the southeast sector of the watershed.

2.4 Urbanization

Urbanization in central Panama is largely concentrated in the cities Panama City and Colon at both ends of the canal and along the Trans-Isthmusian Highway connecting these two urban centers. More than a million people reside in this narrow zone (Heckadon *et al*., 1999). However, as noted by the *Proyecto de Monitoreo de la Cuenca del Canal* (PMCC), a USAID program conducted from 1996-99, the rate of population growth was greater within the Panama Canal Watershed than anywhere else in the country (PMCC, 1999). Importantly, this study recognized that the high rate of population growth was not confined to the suburban areas of metropolitan Panama City, such as Chilibre and Las Cumbres, but was also affecting the area immediately to the south and west of Lago Alhajuela as well as rural areas of the western sector of the watershed. It was also noted that the number of people living within the boundaries of the national parks, where most people are engaged in subsistence agriculture, more than doubled during the census period from 1980 to 1990 (Condit *et al.,* 2001; Ibáñez *et al*., 2001). This high rate of population growth presents a major land management challenge because of the many different land use pressures exerted by the expanding number of people living within the Panama Canal Watershed.

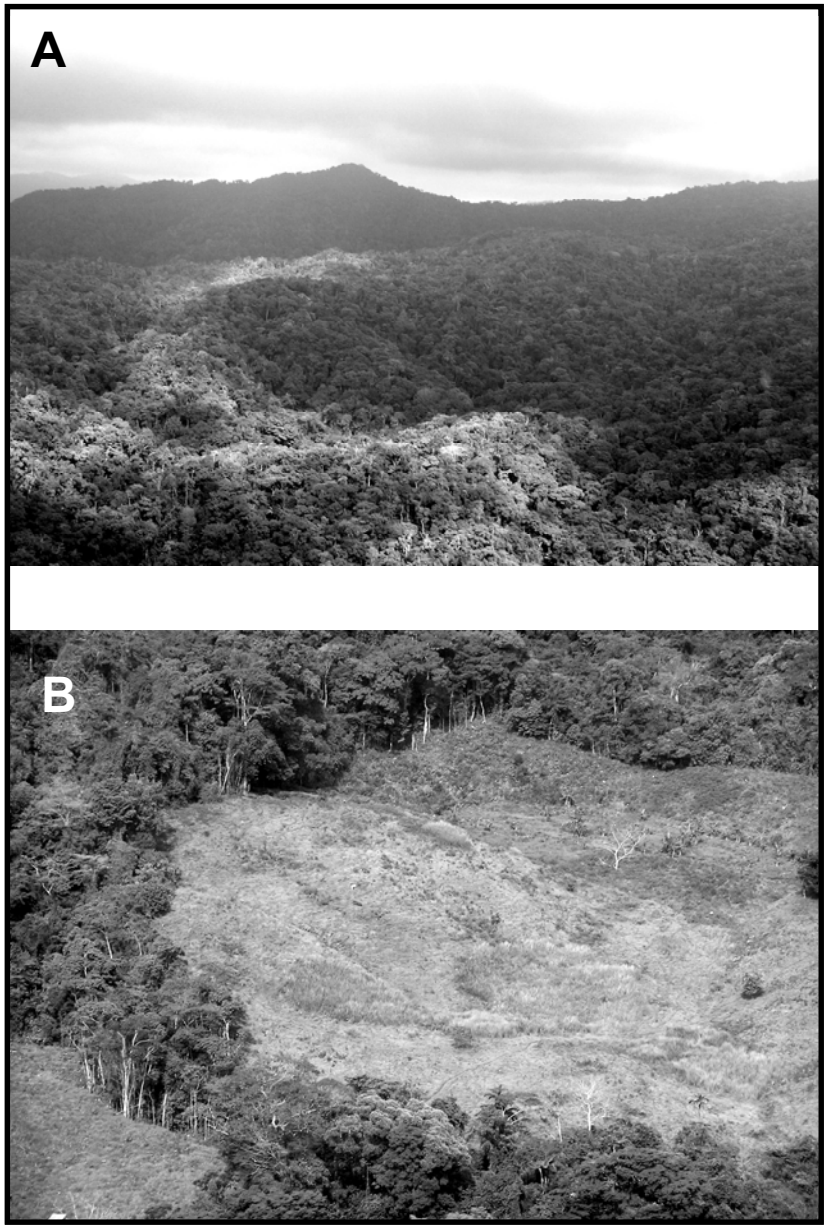

Figure 5. Example of (A) pristine tropical forest in the Chagres National Park and (B) of slash-and-burn clear cutting to create land for subsistence agriculture (photos by M. Kaplan).

2.5 Deforestation

One of the most important issues related to water resources management across the Panama Canal Watershed at present is ongoing deforestation of primary tropical rain forest (Ibáñez *et al*., 2001). In many of the more rural parts of the basin, as well within the national parks, deforestation is undertaken to clear land for agriculture (Fig. 5). Typically crops are planted for only few years on such cleared land parcels because of the low fertility of the soil, which leads to further cutting of forest in a repeated cycle of deforestation. Such land practice leads to erosion, landslides, sediment transport downstream by rivers, and ultimately reservoir siltation (Wadsworth, 1974; Nichols *et al.,* 2005, Chapter 21). Larsen (1984) estimated that 5% of the storage capacity of Lago Alhajuela had been lost to deforestation driven sedimentation by 1975. However, it is also very important to realize that deforestation has another important negative consequence in that it directly affects the timing of water delivery to channels following precipitation events, as runoff is more immediate in deforested areas. For example, for two adjacent basins of similar topography and geology within the Soberania National Park, Ibáñez *et al*. (2001) noted that 26% of rainfall in the deforested catchment was conveyed to streams almost immediately as compared with only 14% in the forested catchment. The implications of this observation is that continued deforestation within the Panama Canal Watershed has the potential to lead to increased flow volumes during the rainy season and, concomitantly, would cause reduced flow volumes during the dry season, the most critical time for canal operation. Other issues, such as the role deforestation in generating landslides and the extent to which deforestation enhances overall erosion, have not yet been studied in detail.

3. CONCLUDING REMARKS

Overall, prospects for the long-term sustainability of the water resources of the Panama Canal Watershed are good, given the growing awareness of the importance of this most valuable water resource and the large percentage of land within the watershed that is federally protected. However, there must be a understanding at all levels of society in Panama - within government, industry, and the public - that deforestation, with all of its many consequences, is the single most important threat to the long-term operability of the Panama Canal. Certainly, the challenge for the immediate future is to develop and enforce a consistent set of informed land management policies at all levels of government that are supported by

informed stakeholders to ensure that the water resources will continue to be available to operate, if necessary, and expand the Panama Canal for the benefit of Panama and the world.

ACKNOWLEDGEMENT

Thanks are due to V. Dale of the US DOE Oak Ridge National Laboratory for providing the land-cover map for the Panama Canal Watershed, M. Calderón of the Autoridad del Canal de Panama for redrafting the figure, and Micki Kaplan for the forest photographs of the Chagres National Park.

REFERENCES

Autoridad del Canal de Panama, 2005, The Panama Canal: www.pancanal.com/eng/ cuenca.

Autoridad del Canal de Panama, 2002, *The Panama Canal: How the Canal Works*: Corporate Communications Division, Balboa-Ancon, Panama.

Condit, R, Robinson, WD, Ibáñez, R, Aguilar, S, Sanjur A, Martínez, R, Stallard, RF, García, T, Angehr, G, Petit, L, Wright, SJ, Robinson, TR, and Heckadon, S, 2001, The status of the Panama Canal watershed and its biodiversity at the beginning of the 21st century. BioScience, 51: 389-398.

Condit, R, Pitman, N., Leigh, EG, Chave, J, Terbaugh, J, Foster, RB, Nuñez, PV, Aguilar, S, Valencia, R, Villa, G, Muller-Landua, H, Losos, E, and Hubbell SP, 2000, Beta-diversity in tropical forest trees: Science, 295: 666-669.

Cullen, B, 2005, Panama Rises: Smithsonian Magazine, 34: 44-55.

Dale, VH, Brown, S, Calderon, MO, Montoya, AS, and Martínez, R, 2003, Estimating baseline carbon emissions for the eastern Panama Canal Watershed: Mitigation Adapt. Strat. Global Change: 8: 323-348.

Espinosa, D, Méndez, A, Madrid, I, and Rivera, R, 1997, Assessment of climate change impacts on the water resources of Panama: the case of the La Villa, Chiriquí, and Chagres river basins: Climate Change, 9: 131-137.

Heckadon, S., Ibáñez, R, and Condit, R, 1999, La Cuenca del Canal: Deforestación, Urbanización, y Contaminación: Proyecto de Monitoreo de la Cuenca del Canal de Panama (PMCC), Sumario Ejecutivo del Informe Final, Smithsonian Tropical Research Institute.

Heckadon, S, 1993, The impact of development on the Panama Canal environment: Jour. Inter-Amer. Stud. World Affairs, 35: 129-149.

Ibáñez, R, Condit, R, Angher, G, Aguilar, S, Garcia, T, Martínez, R, Sanjur, A., Stallard, RF, Wright, SJ, Rand, AS, and Heckadon, S., 2001, An ecosystem report on the Panama Canal: Monitoring the status of the forest communities and the watersged: Env. Monitor. Assessment., 80: 65-95.

Larsen, MC, 1984, Controlling erosion and sedimentation in the Panama Canal watershed: Water Int., 9: 161-164.

McCulloch, D, *The Path Between the Seas: The Creation of the Panama Canal 1870-1924:* Simon and Shuster, New York, NY.

Myers, N, Mittermeier, RA, Mittermeier, CG, da Fonseca, GAB, and Kent, J, 2000, Biodiversity hotspots for conservation priorities: Nature, 403: 853-858.

Nichols, KK, Bierman, PR, Finkel, R, and Larsen, J, 2005, Long-term sediment generation rates for the upper Río Chagres basin: Evidence from Cosmogenic ^{10}Be: in *The Río Chagres: A Multidisciplinary Perspective of a Tropical River Basin* (RS Harmon, ed.), Kluwer Acad./Plenum Pub., New York, NY:

Vargas, CA, 2003, Panama Canal water resources management: Proc. Int. Sci. Symp. 'The Río Chagres: A Multidisciplinary Profile of a Tropical Watershed', Gamboa, Panama: 52.

Wadsworth, FH, 1974, Deforestation: Death to the Panama Canal: Proc. US Strategy Conf. on Tropical Deforestation, USAID, Washington, DC: 22-24.

Chapter 3

LIGHT AND SHADOWS IN THE MANAGEMENT OF THE PANAMA CANAL WATERSHED

Stanley Heckadon-Moreno
Smithsonian Tropical Research Institute

Abstract: This paper reviews the history of settlement in Panama and then summarizes the important findings of the Panama Canal Watershed Natural Resources Monitoring Project, a multidisciplinary study was conducted between 1996-1999.

Key words: Panama; Panama Canal Watershed; Río Chagres; Proyecto de Monitoreo de la Cuenca del Canal

1. INTRODUCTION

At midnight on 31December 1999, Panama assumed a challenge of global magnitude - that of managing the inter-oceanic canal, a critically important artery of international trade and commerce. Vital to the successful undertaking of such task is the sustainable management of the natural resources of a Caribbean river, the Río Chagres. Its waters, stored in lakes Gatún and Alhajuela (Fig.1), are used for the operations of the Panama Canal as well as used by six plants that provide water of optimal quality for human consumption to Panama City and Colón, urban centers that contain nearly 80% of Panama's urban population and industrial activity.

Herodotus once said that Egypt is a gift of the Nile. By analogy, it could also be said that Panama, a modern hub of global trade and commerce since the 1500's, is a gift of the Río Chagres. Strategically located in the narrowest and lowest portion of Central America, the complete Río Chagres catchmengt (or Panama Canal Watershed, as denoted in the other chapters of this volume) encompasses more than 3300 km^2 and is an extraordinary natural system for the production and storage of fresh water. This watershed

R. S. Harmon (ed.), The Río Chagres, Panama, 29-44.

is not located in the distant underdeveloped periphery of the isthmus, but within the metropolitan region of Panama City-Colón, were the processes and pressures of urbanization and industrialization are intense; thus there is an urgency to reconcile the rapid settlement and economic development of the region with the need to preserve the capacity of this fragile ecosystem to produce large quantities of high quality water. There is also a need to preserve, without degradation, the rich biological diversity of tropical forests of the watershed that, in the future, will sustain a novel and profitable industry of scientific and nature tourism.

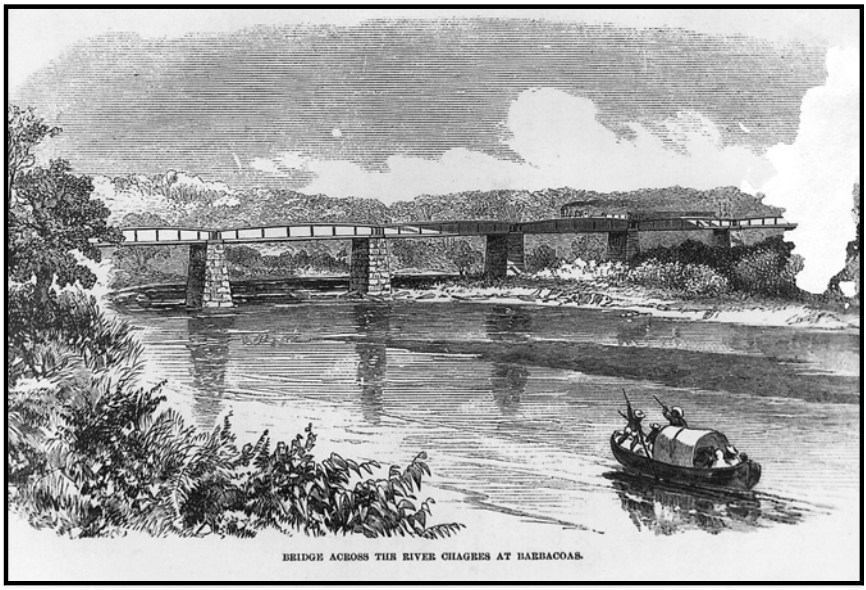

Figure 1. The old and new means of transport meet at the Barbacoas bridge on the Río Chagres, 1858. Construction of the Panama Railroad (1850-1855) ended the three hundred year reign of the dugout canoe as the main means of moving cargo and passengers across Panama (source: Harpers Monthly Magazine, 1858).

This paper summarizes important findings of the Panama Canal Watershed Natural Resources Monitoring Project, better known for it's Spanish acronym PMCC (Proyecto de Monitoreo de la Cuenca del Canal). This survey is perhaps the most ambitious applied research project led by the Smithsonian Tropical Research Institute (STRI). This multidisciplinary study was carried out between 1996-1999 by almost 40 researchers, in close collaboration with Panama's Autoridad Nacional del Ambiente (ANAM) and funded by the United States Agency for International Development (USAID). It's immediate forerunner was the Grupo de Trabajo de la Cuenca

del Canal, or Task Force on the Canal Watershed, that in 1985 and 1986 held a series of workshops to establish the status of development and conservation in the Río Chagres watershed.

The survey carried out by the PMCC offers a panorama of lights and shadows on the environmental health of the Río Chagres basin and the forces that act on it, in particularly during the last two decades of the 20th Century. As shall be seen, the achievements are the results of policy decisions gradually taken to protect forests, whereas the problems looming on the horizon are due to a lack of scientific data and political will to take decisions to insure water quality.

2. THE MIGRATORY WAVES

The Río Chagres is the river of interoceanic communication. People from around the world gathered on its banks to realize the old dream of linking the Atlantic and the Pacific Oceans. Geographers and historians like McKay (1977), Jaen (1981), and Lecompte (1984) stress that although human presence has a long history in the Chagres region, its environmental impact remained minimal throughout most of history. Their numbers were few and concentrated in small settlements along the so-called 'transit zone', a narrow strip of land of indefinite width parallel to the main trans-isthmus trade route. During the 300 years of the Spanish Colonial period, the population within the transit zone seldom rose above 1500 inhabitants, concentrated in the small '*pueblos'* and villages on the banks of the Río Chagres. Their livelihood was based on subsistence agriculture-rice, raising corn, root crops, plantains and bananas, and work as laborers in the transport of cargo and passengers across the isthmus by dugout canoes and mules.

In the second half of the 19th century, the population of the area grew substantially; first, due to the construction of the inter-oceanic railroad from 1850-1855 following the discovery of gold in California and then the French effort to build a sea-level canal across Panama from 1880-1890 (Figs. 1 and 2). This period of major engineering projects, gave rise to new types of settlements - train stations along the rail line (see Figure 3 of Harmon, 2005a, Chapter 2) and the work camps along the axis of the canal works. In the isthmus region, this area began to be generally referred to as *'La Línea'* (The Line).

By the end of the 19th Century, population of 'the Line' probably numbered about 20,000 inhabitants (Jaen, 1981). It represented, ethnically and culturally, a rainbow of mankind. Many inhabitants hailed from the small English and French speaking islands of the Caribbean, from the

northern coast of Colombia and Venezuela, from Europe, and even the far distant lands of China and India. Despite the intense activity generated by both projects, environmental changes remained confined to the neighborhood of the railroad and the canal (Fig. 3).

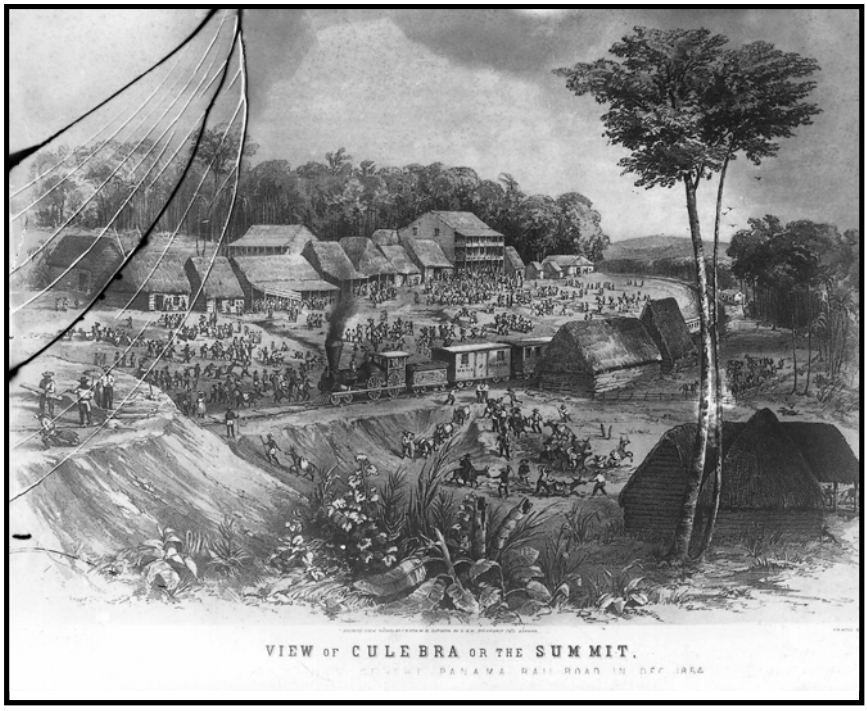

Figure 2. Culebra or Summit a village on the Line, 1854, at the height of the California gold rush (source: Archives, Panama Canal Commission).

In the 20th Century, the Río Chagres basin would be settled in three distinct waves. The first was during 20-year period just after the turn of the century, following the successful building of the Panama Canal by the United States. The number of people in the Chagres region during this time rose to over 40,000. Most of these people were immigrant workers who came to Panama from the Caribbean region. The population of Panama dwindled during the decades following the completion of the canal. The establishment of the Canal Zone by the United States led to the displacement of the native peasant population from the towns and camps of along the pathway of the canal.

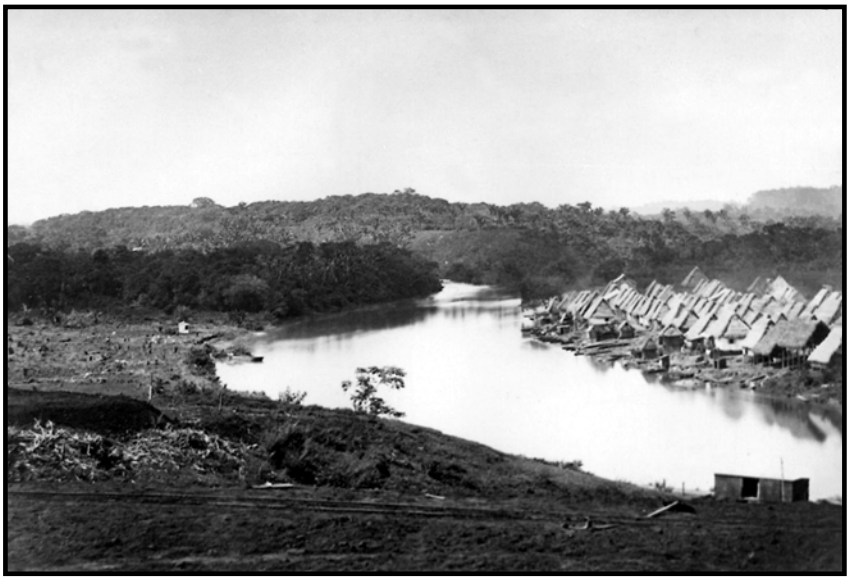

Figure 3. A village on the Río Chagres circa 1890, during the French Era of the Panama Canal. Image by the French photographer De Sablá (source: Archives, Panama Canal Commission).

Another reason for population decrease was the damming of the Río Chagres and the formation of Lake Gatún and later Lago Alhajuela (1930-1935). Their rising waters of these artificial lakes drowned over 500 km^2 of tropical forest and over 50 towns and villages (Figs. 4 and 5). Some of the families displaced by Lake Gatún built the first villages on the banks of the new lake, the '*pueblos del lago*', whose economy was based on the cultivation of root crops for self-subsistence and bananas for cash. Other early settlers of Lake Gatún were West Indians, a black, English speaking people of Protestant religion. Many were former canal diggers from the Caribbean who chose to remain in Panama rather than return to their densely-populated home islands. Thus, the town of Nueva Providencia (*i.e.,* New Providence) was created in 1916 on the banks of Lake Gatún by former laborers from Barbados. By the end of the 1930s it is estimated that the Río Chagres watershed held some 8,000 inhabitants.

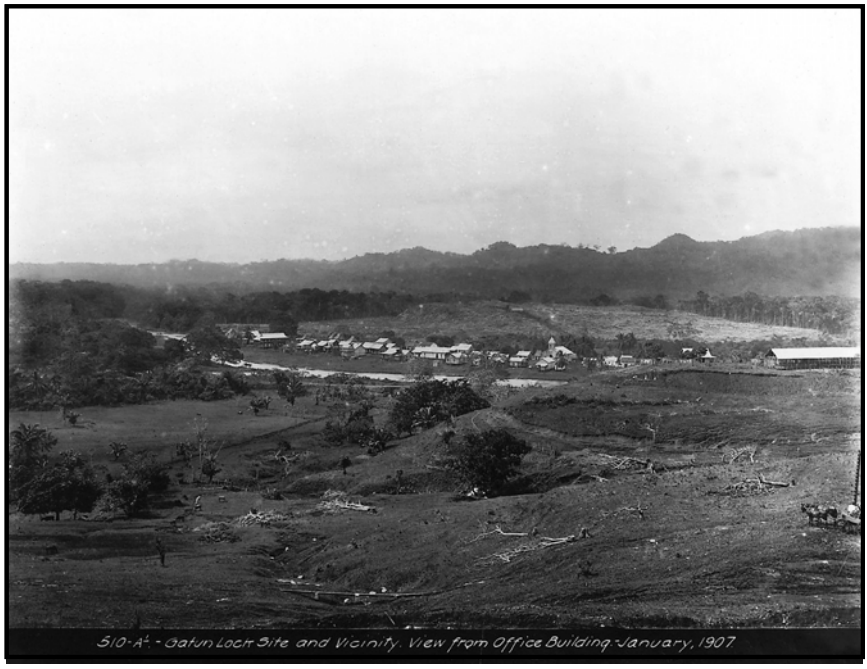

Figure 4. The old village of Gatún seven miles from the mouth of the Río Chagres in 1907 and soon to lie buried under the Gatún locks and dam (source: Archives, Panama Canal Commission).

The second wave of settlement of the canal watershed occurred after World War II. These settlers were primarily peasants from the interior and the western plains of the drier, Pacific side of Panama – namely from the provinces of: Coclé, Herrera, Los Santos, Veraguas and Chiriquí. Emberá Indians from the Río Bayano area in Darien and from the Chocó region in Colombia were also among those emigrating in this second wave of settlement.

The third, the contemporary wave of settlement, has had two root causes. The first was the growth of the population within the watershed. The second, and more important reason, was the intense migration of low income urban families from the cities of Panama and Colón, who have been seeking cheaper land for housing along the Trans-Isthmian Highway and proximity to local labor markets.

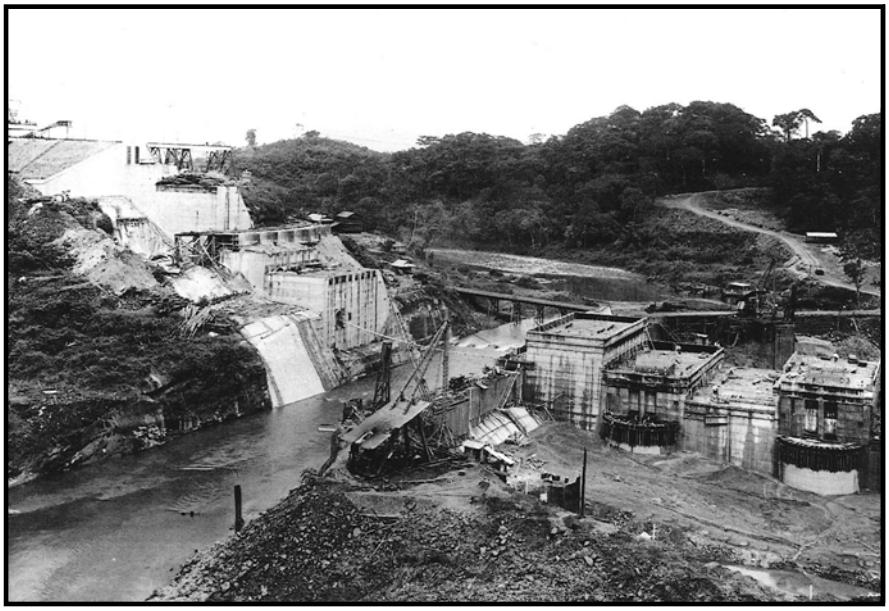

Figure 5. The construction of Madden Dam (1930-1935) across the Río Chagres gave birth to Lago Alhajuela. The dam had three purposes: flood control, storage of water for canal operations during the dry season, and the eneration of electricity for the Canal Zone and canal operations (Panama. Source: Archives, Panama Canal Commission).

3. THE TRANSISTHMIAN HIGHWAY: EPICENTER OF INDUSTRIALIZATION AND URBANIZATION

From the century between the 1850s to the 1940s, people and goods moved between the two population centers of the isthmus region, Panama City and Colón, by train. That changed in 1950 with the opening of the '*Transistmica',* or Trans-Isthmian Highway. As a result, the canal and the Río Chagres watershed became a colonization front for logging, 'slash-and-burn' agriculture, extensive cattle ranching, and an unplanned process of industrial and urban growth. From 1950 to 1990, the population of this area rose fivefold, from 21,000 to 113,00. Between 1980 to 1990, the annual growth rate stood at 3.8%, compared with the national average of 2.7%.

Today nearly 80% of the watershed's population is concentrated within a 2.5 km wide strip along the *Transistmica.* The other 20%, live on the west side of the canal in an overwhelmingly rural setting, depending on subsistence agriculture and cattle ranching.

Given the reasons outlined above for the ongoing settlement of the Chagres, the PMCC gave special attention to Chilibre, the largest '*corregimiento'* or administrative area. This area was subject to the most intense demographic and economic growth and the consequent effects of environmental degradation. The environmental deterioration of the Río Chilibre and one of its tributaries, the Río Chilibrillo, were selected as a the most relevant case studies. Almost 50% of the population of the Río Chagres watershed is crowded into the corregimiento of Chilibre. At the end of the 1990s, Chilibre had an estimated at 71,000 inhabitants.

At the turn of the 1950s, few industries existed on the Trans-Isthmian Highway; today there are hundreds; ranging from the industrial rearing of chickens and pigs for urban markets to metal foundries and factories for recycling paper, the fabrication of plastics and detergents, mosaics, cement blocks, and batteries. As private car ownership has rapidly increased, so has the number of mechanical garages to serve these vehicles and the ever-increasing number of buses that move passengers along the *Transistmica* between Panama City and Colón. In addition, Panama's most intensive mining activity takes place within the watershed, along or near the *Transistmica,* including the country's only two cement plants. The Río Chagres basin is the main source of raw materials for the vital construction industry in Panama City and Colón, which generates thousands of jobs and millions of dollars in bank loans. A core dilemma that has arisen is that the intense process of urbanization and industrialization in the watershed has taken place without the installation of systems for the collection and treatment of sewage and garbage.

4. A SOCIO-ECONOMIC SKETCH

Although the Río Chagres watershed has an extremely high water-production capacity and is rich in biological diversity, the socio-economic condition of its growing population is a cause for serious concern. In 1990, the region lacked a complete high school. To finish secondary education, students had to travel either to Panama City or Colón. Furthermore, the educational system is not preparing students with the skills demanded by the job markets of the 21st Century. For example, students are not provided with technical skills in areas such as information technology and computer sciences, foreign languages, environmental science, or such sectors as nature tourism and the hospitality industry that are required for the modern economy of Panama.

Unemployment amongst the watershed population stands at 16%, while the national average is over 13%. An additional 30% of people are underemployed. Many of those able to work do so as daily laborers. Men labor in the construction industry or hawk cheap wares in city streets and plazas. Women usually work as maids or waitresses. Unlike the middle and upper income groups, who shop in supermarkets on a weekly basis, the unemployed and underemployed buy in small quantities in tiny local stores paying higher prices. Winning the minds of such large mass of daily laborers is a challenge to societal goals, such as nature conservation that requires planning and a long-range vision of common benefits.

Until the early 1990s, most new houses were self-constructed by migrant families. It is estimated that housing by self-construction grows 4% yearly. Due to incentives to the construction industry, a boom presently is occuring in housing development by construction companies funded by the banking sector. In Chilibre and Chilibrillo, about 5000 housing units are planned for construction.

The plan for the development of the canal watershed, prepared by the Authority of the Interoceanic Region (ARI) and approved by the National Legislature of Panama, calls for slowing housing developments within the watershed. New housing is to be oriented to the pacific and Atlantic sides of the isthmus. However, this proposal faces major hurdles given large improvements to the transportation sector, such as the Panama-Colón Highway, the reconstituted Panama Railroad, and the building of modern ports at both ends of the canal.

5. FROM FOREST ‘CONQUEST’ TO PROTECTION

One of Panama’s greatest achievements is government legislation for the protection of the Río Chagres watershed. During the past two decades, there has been a slowdown in the aggressive expansion of cattle ranching towards the forests of the basin. The expansion of the pasture lands, a process started in the 1950s as part of a national development policy known as the ‘conquest of the jungle’, resulted in the loss of some 50% of the forest cover in the Río Chagres watershed. This policy seems to have come to an end. The percentage of existing forest cover is holding constant, and in some sectors, it is recuperating. Today, forest cover stands at some 158,000 hectares, or 47% of the total surface area of the basin. About 69% of the existing forests are under some form of protection. Most protected natural areas have been established since 1980.

A comparison of deforestation rates during the droughts caused by the last two *El Nino* events, indicates that there is a clear decrease in the annual rate of deforestation. In the 1982-1983 drought, some 3,000 hectares of forest were burned. However, in the dry period 1996-1997 the PMCC detected the destruction of less than 30 hectares of primary forest.

5.1 Forestry Plantations and Secondary Growth Recuperation

Since 1993, a significant change in land use has been taking place in the watershed. More people are planting trees for commercial purposes. The land planted covers well over 3000 hectares. This move toward the cultivation of commercial timber species by the private sector is due to new fiscal policy incentives to forestry. Another factor has been the forestry concessions granted by ARI to companies to reforest degraded areas within the old Canal Zone, mainly in land occupied by canal grass or '*Paja canalera'*.

In addition, there is a perceptible expansion in land covered by secondary growth or '*rastrojo*'. This is taking place in areas under state protection and on private lands. A growing number of landholders are allowing vegetation recovery along stream banks, hillsides, and ridges. This change partly reflects a new environmental awareness on behalf of the community. Slowly, but gradually, people are placing greater value on the positive benefits of trees and greater tree cover.

The reduction in deforestation rate, and gradual regeneration of the tree cover, can also be attributed to changes in loan policies by the Banco Nacional de Panama. Since 1990, the bank began to refuse loans for livestock if it led to the conversion of forest to pastures. This measure has been paired with a program to raise the environmental awareness of cattle ranchers, including a stress on the importance of saving farm forest cover. Protecting secondary forest cover is perhaps one of the most sensible and economical ways of reforesting degraded lands and protecting biodiversity in the Río Chagres watershed.

5.2 Protected Forests

Today, Panama is harvesting the fruits of decisions made 10 to 15 years ago to save the forests of the Río Chagres Watershed in support of the long-term well being of the Panama Canal. A crucial role was played by both Panamanian and United States researchers to facilitate the conservation measures enacted by Panamanian government decision makers. Among the

most notable of these actions was the creation of Soberania National Park in 1980, during the tenure of President Aristides Royo, which resulted in the protection of some 20,000 hectares of forest on the east bank of the Panama Canal. The direct forerunner of the Soberaniá Park was the old Madden Road Forest Reserve from the former Canal Zone days. Also of critical importance was the action by President Eric A. del Valle in 1985 to establish the Chagres National Park (see Figure 4 of Chapter 2), at the insistence of the Task Force on the Panama Canal Watershed. This action safeguarded nearly 130,000 hectares of forest in the upper Río Chagres basin, the headwater area for the rivers that provide the bulk of the water for operation of the Panama Canal: the Río Chagres and its major tributaries, Río Pequení, and Río Boquerón. It can be said that, with this legislation, Panama bought the life insurance policy for the canal and the water plants of Panama City and Colón.

Also of crucial importance to the protection of the natural areas within the Panama Canal Watershed were the creation of the Metropolitan Natural Park within Panama City and the Gatun Recreation Park in Colón. In 1993, during the term of President Guillermo Endara, and thanks to the strong lobbying of the Panamanian civil society, the National Legislature established the Cruces Trail National Park, encompassing some 4000 hectares of dry forests contained within the former U.S. military bases at Albrook and Clayton. Through these various land preservation actions, a trans-isthmian environmental green belt was created that crosses central Panama from the Pacific to Atlantic paralleling the canal. More recently, the lowland humid forests of the Fort Sherman and the old Spanish Fort San Lorenzo areas on the Caribbean entrance to the canal were added to this green belt. To conclude this recounting of the steps to protect the forests of the Canal Watershed, mention also should be made of the creation of Altos de Campaña National Park in 1966, by Ruben Dario Carles, then Minister of Agriculture. The suggestions of scientists at the Smithsonian Tropical Research Institute (STRI) had a positive influence in this decision.

Together with the consolidation of this system of natural protected areas, the development, expansion, and improvement of a corps of park rangers has taken place within ANAM and the National Police. This natural resources protection force is supplemented by the wardens of Barro Colorado Natural Monument. Established in 1923 by Jay Morrow, Governor of the Canal Zone, at the petition of the international scientific community, and in particular, by men of science like James Zetek and Thomas Barbour, Barro Colorado is Latin America's oldest wildlife protection area.

5.3 Flattening the Pyramid: The Administration of Protected Areas

For 500 years, Panama developed a major institutional disease: a highly centralized public administration system that concentrated all political powers with the central government in Panama City. This bureaucratic structure resembles a pyramid and is tends to be very inefficient, as the management of the growing number of protected areas has been almost the exclusive concern of the central government, first, under the agency RENARE, later INRENARE, and currently ANAM (Autoridad Nacional de Ambiente de Panama). In the future, it will be vital for proper environmental management to flatten the administrative pyramid and essential to incorporate local governments, the private sector, and the civil society into both the decision-making process and the management of Panama's important environmental resources. New and creative ways of citizen participation need to be explored.

In 1994, for the first time in Panama, mayors were elected directly by the voters, thus becoming accountable to their constituency. It is the start of a new process of '*municipalizacion', i.e.*, the empowerment of the municipalities and decentralization of state power. New municipal responsibilities ultimately will include the use and protection of natural resources. In the 21st Century, it becomes a matter of sound government, to strengthen the capacity of local governments to manage the environment.

In the Panama Canal Watershed, it is vital to promote and strengthen the existence of both municipal and privately held protected areas. It will also be necessary to garner community support for environmental stewardship. A pioneering example of the new forms of participation that are developing is the Patronato, or Board, that manages the Metropolitan Natural Park. This Patronato represents institutions of the central government and the private sector and is led by the Mayor of Panama City.

5.4 Roads, Highways, and Soils

Increased protection of primary and secondary forests is leading to a gradual and continuing reduction in the rate of soil erosion and silting of rivers and lakes. However, the PMCC was still able to detect a substantial level of sediment transport in river courses, especially in those with larger water flows such as the Río Chagres and Río Pequeni. This is directly attributable to the construction of rural access roads, poorly built and with out proper maintenance. The same process is also evident on the west side of the canal, in the Río Trinidad and Río Ciri Grande basins that flow into Lake

Gatun. In the future, road construction in the watershed should only be carried out after sound environmental impact studies, followed by the implementation of sediment erosion mitigation measures.

However, by far the most worrisome situation regarding soil erosion within the Canal Watershed are the major roads, the Corredor Norte and the Panama-Colón Highway. These 4-lane cement highways have cut a path across such protected areas as the Metropolitan Natural Park, the Cruces Trail Park, and Soberania National Park (see Figure 4 of Chapter 2) Additionally, these developed transportation corridors are generating additional pressure for new settlements and economic development across the greater Panama Canal Watershed.

5.5 On Water Quantity

As the Panama Canal and cities of the metropolitan region demand more water, it is possible to envisage that the peak water production capacity of the Canal Watershed will be reached within a limited number of years. This would then require Panama to tap other Caribbean rivers, damming them and diverting part of their flow towards Lake Gatun, a costly but perhaps inevitable measure that would fall to the Panama Canal Authority (ACP). On 31 August 1999, the National Legislative Assembly passed Law 44, which enlarged the boundaries of the Panama Canal Watershed by an additional 2000 km^2. This area covers portions of three rivers: the Río Indio, Río Cocle del Norte, and Río Cano Sucio.

An irreplaceable priceless resource of Panama has been the exceptional water quality of the Río Chagres watershed. Sanitation engineers have labeled this water as 'Panamanian champagne'. This water is treated at a low cost and offered to urban consumers at a rate of 13 gallons/cent. Appropriate measures to stop and reduce water contamination need be taken soon so that the population of the metropolitan region will not have to buy bottled water in stores at $4-5/gallon. The economic and social costs of water quality loss within the Río Chagres basin would lead to severe consequences for all Panamanians.

Thus, Panama needs to establish a modern water quality monitoring system and support this critical infrastructure for the long term by strengthening its academic capacity in environmental engineering. Although water quality near city water plants is still favorable, the number of contaminated streams is gradually growing. Such degradation is more serious along the 'Transistmica', measured by such indicators as organic, inorganic, and microbiological contamination. Unlike deforestation, which is visually arresting and affects the erosion potential of an area over the long

term, water contamination is far more dangerous and insidious. Among its most readily detectable symptoms are an expansion of the mass of aquatic vegetation that results from increased levels of detergents, fertilizers, and human waste in rivers and streams. Such vegetation is thicker and larger in the mouths of streams flowing into lakes Gatun, Alhajuela, and Miraflores than elsewhere. In some rivers, swimming is causing skin irritations. It is also imperative to take preventive measures along the new Panama-Colón Highway and the Panama Railroad, so as not to repeat the ecologically destructive style of development that previously occurred place on the 'Transistmica'.

5.6 Science, Policy, and Water Husbandry

A prevalent social myth among Panamanians in the 20th Century was that, irregardless of the style of development that took place in the Panama Canal Watershed, a landscape of steep hillsides and nutrient poor soils, it would always yield endless volumes of high quality water. Until recently, it has been the custom to first undertake development projects and then later ascertain the negative environmental impacts, or at the most, to study their effects while a project is underway. A message from the work of the PMCC is that this approach, in some cases, might be overstepping the boundaries of tolerance of tropical natural system.

Just as in the past measures were successfully taken to protect Canal Watershed forests, it would be a matter of good governance, for the immediate future, to establish policies for water husbandry. This will require new forms of institutional cooperation among public and private organizations to establish water quality norms and long term environmental monitoring programs. Like the concept of maintenance, monitoring has been absent from the national dialogue. A change in this attitude is urgently needed.

6. SUMMARY AND CONCLUSIONS

Protecting and monitoring water quality in the Panama Canal Watershed is a national priority and one of the greatest challenges to Panama for the 21st Century. The health and well being of almost a million people ultimately depend such action. Success or failure will hinge in the national capacity to generate a critical mass or researchers, technical cadres, and environmental mangers. It was an unstated aspiration of the PMCC that the results of the study of the relationships between man and nature in the setting of the Río

Chagres tropical river system would be useful in the decision-making process to safeguard this extraordinary natural heritage.

REFERENCES

Jaen, O, 1981, Hombres y Ecología en Panama. Editorial Universitaria y Smithsonian Tropical Research Institute, Panama City, Panama.

The Canal Record, 1907, Matachín: An Interesting History of the Name: Written for the Canal Record by General Davis, First Governor of the Canal Zone. Isthmian Canal Commission, Ancon, Canal Zone, Panama: 1: 133.

The Canal Record, 1908, Removal of Gatun Village: Isthmian Canal Commission, Ancon, Canal Zone, Panama, 1: 249.

The Canal Record, 1908, Crossing the Isthmus in 1852: Report of the Regimental Surgeon, Fourth Infantry, U.S. Army, Isthmian Canal Commission, Ancon, Canal Zone, Panama, 1: 347.

The Canal Record, 1911, The Lake Villages: Hamlets and Towns Whose Sites will be Covered by Gatun Lake: Isthmian Canal Commission, Ancon, Canal Zone, Panama, 5: 120-121.

The Canal Record, 1913, Movement of Squatters in Canal Zone: Isthmian Canal Commission, Ancon, Canal Zone, Panama, 6: 321.

The Canal Record, 1913, Emigrants from the Lake Area.: Isthmian Canal Commission, Ancon, Canal Zone, Panama, 7: 22.

The Canal Record, 1913. Health Conditions in the Chagres River Villages: Isthmian Canal Commission, Ancon, Canal Zone, Panama, 7: 21.

The Canal Record, 1920, Commercial Woods Native of Canal Zone and Republic of Panama and in Structural Use by the Panama Canal: Isthmian Canal Commission, Ancon, Canal Zone, Panama, 13: 315-319.

Harmon, RS, 2005a, The Panama Canal Watershed: in *The Río Chagres: A Multidisciplinary Perspective of a Tropical River Basin* (RS Harmon, ed.), Kluwer Acad./Plenum Pub., New York, NY: 19-28.

Heckadon-Moreno, S, 1981, Sistemas de producción campesina y recursos naturales en la Cuenca del Canal de Panama: Dirección de Recursos Naturales Renovables y Agencia para el Desarrollo Internacional, Panama.

Heckadon-Moreno, S (ed.), 1986, La Cuenca del Canal de Panama: Actas de los Seminarios Talleres, Grupo de Trabajo sobre la Cuenca del Canal de Panama, Panama City, Panama.

Heckadon-Moreno, S (ed.), 1986. Informe del grupo de trabajo sobre la Cuenca del Canal de Panama (Sumario Ejecutivo): Grupo de Trabajo sobre la Cuenca del Canal de Panama, Panama City, Panama.

Heckadon-Moreno, S, 1987, Impacto Ambiental del Desarrollo de La Cuenca del Canal de Panama. Pensamiento Iberoamericano: Inst. Cooperación Iberoamericana y Comisión Econ. para la América Latina, Madrid, Spain, 12: 167-177.

Heckadon-Moreno, S, 1993. Impact of development on the Panama Canal environment. Jour. Interamerican Studies, 35: 129-149.

Heckadon-Moreno, S, 1998, Naturalistas del Istmo de Panama: Smithsonian Tropical Res. Inst. y Fundación Santillana para Iberoamérica, San Jose, Costa Rica.

Heckadon-Moreno, S; Ibáñez, R, and Condit, R, 1999, La Cuenca del Canal: deforestación, urbanización y contaminación: Smithsonian Tropical Res. Inst., Panama City, Panama.

Lecompte, D, 1984, Transformación del Medio Geográfico en la Región Canalera. Tierra y Hombre: Revista Dept. Geogr.. Univ. Panama, Panama City, Panama: 57-76.

McKay, A, 1977, Salud Comunitaria y Colónización rural en Panama: el caso de Cerro Cama: in *Colónización y Destrucción de Bosques en Panama. Asociación Panameña de Antropología* (S Heckadon-Moreno and A Mckay, eds.), Panama, City, Panama: 50-75.

Minter, JE, 1948, *The Chagres: River of Westward Passage*: Rinehart, New York, NY.

Mollien, GT, 1944, Viaje por la República de Colombia en 1823: Biblioteca de la Cultura Colombiana, Bogotá, Colombia.

Nelson, W, 1889, *Five Years at Panama: The Trans-Isthmian Canal:* Belford, New York, NY.

Pereira, B, 1960, *Biografía del Río Chagras*: Imprenta Nacional, Panama City, Panama.

US Department of Commerce, 1924, The Republic of Panama (Agricultural Products, bananas): Trade Information Bulletin, No 257, US Gvmt. Print. Office, Washington, DC: 1-115.

Chapter 4

GEOLOGICAL DEVELOPMENT OF PANAMA

Russell S.Harmon
US Army Research Office

Abstract: The Panama that geologists see today is a young landscape that in form comprises a reclined S-shaped, generally E-W oriented isthmus produced through complex geotectonic processes that created and assembled a diverse suite of geological units since late Cretaceous/early Tertiary time. The geological development of Panama is a consequence of the relative motions of the North and South American continental plates and four oceanic plates over the past 150 million years, and is a part of the larger story of the tectonic development of the Caribbean basin and Central America. The igneous rocks that comprise much of present-day Panama formed during Tertiary time as an oceanic plateau associated with the Galapagos plume and from an oceanic volcanic island arc complex that presently extends from the southern margin of Nicaragua to the northwestern Colombia. About 10 million years ago, the Panama-Costa Rica arc began to collide with northwestern South America, cutting off the deep-water circulation between the Pacific and the Caribbean. Development of Central America was completed around 3 million years ago, creating the land bridge between North and South America and terminating the shallow marine circulation between the Pacific and Caribbean.

Key words: Panama; geological history; Caribbbean basin; plate tectonics

1. INTRODUCTION

The thin isthmus of land that comprises Panama is geologically young and its development can only be described and understood within the framework of plate tectonics, the unifying theory for modern geology. This concept, which is well described in current physical geology textbooks (see *e.g.,* Davidson et al, 1997; Skinner and Porter, 2000), holds that the lithosphere (*i.e.,* the solid outer portion of the Earth) is divided into seven major and many minor plates about 100 km thick that are in motion relative

R. S. Harmon (ed.), The Río Chagres, Panama, 45-62.

to one another due to thermal convection deep within the Earth. These plates are rigid and move on the curved surface of the Earth as integral physical entities and interact with one another along three types of margins.

Divergent plate margins are found where two plates have ruptured, are spreading apart as magma rises up from the Earth's mantle to form new oceanic crust (*e.g.,* the mid-Atlantic ridge). Transform margins occur where two fractured plates are sliding past one another and generating earthquakes when built-up stresses are released and movement occurs (*e.g.,* the San Andreas fault in California).

Convergent margins are located where two plates are moving toward one another. Where two plates containing continents converge, a Himalayan-type mountain range will be produced during collision of the two continental land masses. Where two oceanic plates or an oceanic plate and a continental plate collide, one plate will be subducted beneath the other back into the mantle. As the subducted oceanic lithosphere is being pushed slowly down into the mantle at an oceanic trench, it is progressively heated. This heating releases water and other volatiles, previously acquired during deep-sea hydrothermal alteration and weathering, from the subducting oceanic crust and fluxes the ovberlying convecting mantle wedge to cause melting. This melting produces magmas that coalesce and rises to the surface to form a linear array of volcanoes on the opposite plate oriented parallel to the zone of subduction (either an oceanic-island arc like the Lesser Antilles or a continental-margin arc like the Andes).

Table 1. A Portion of the Geological Time Scale that relates to the geological development of Panama (Numerical ages for the Period boundariesare derived from radiometric dating).

ERA	PERIOD	EPOCH	Time - Millions of years before present (Ma)
Cenozoic	Quaternary	Holocene	0.1
		Pleistocene	2.0
	Tertiary	Pliocene	5.1
		Miocene	24.6
		Oligocene	38.0
		Eocene	54.9
		Paleocene	65.0
Mesozoic	Cretaceous		144.0
	Jurassic		

Elongate sedimentary basins are common features behind volcanic island arcs. Frequently, plate motions will transport a section of geologic crust (*e.g.,* a seamount, an island arc complex, or a fractured piece of continental margin) that formed in one place to a far distant location and juxtapose it in a geologic context that is totally unrelated to its origin. Such units are called 'exotic terranes'. Occasionally, a upwelling heat plume develops deep within the Earths mantle and produces a 'hotspot' beneath a an oceanic or continental plate that remains stationary for tens of millions of year. When such plumes occur under an oceanic plate, the result can be a large oceanic volcanic chain, like the Hawaiian islands, or a large ocean floor plateau, such as that associated with the Galapagos plume. The geological development of Panama can be understood within this general plate tectonic framework and global plate motions over the past 150 million years (Table 1; Fig. 1).

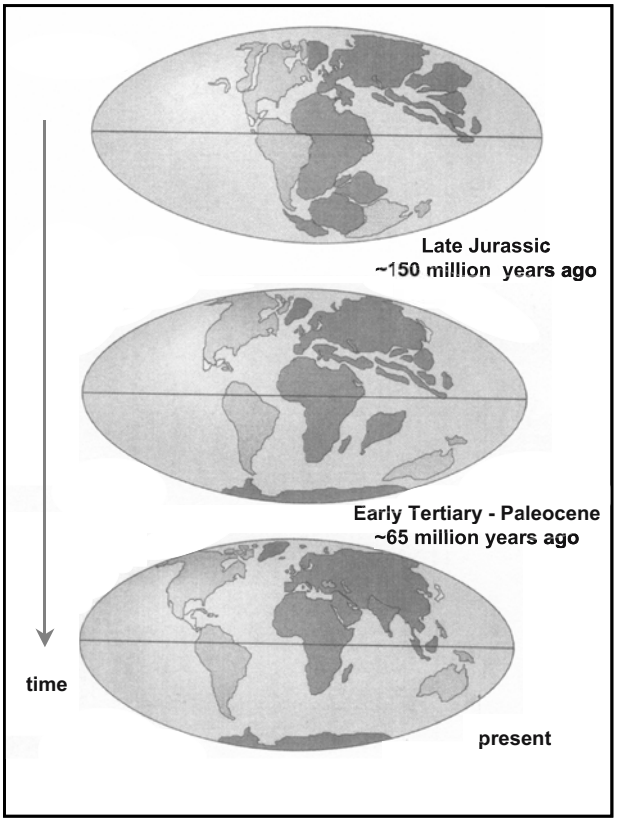

Figure 1. Plate motions in the Western Hemisphere over the past 150 million years (after Davidson *et al.,*1997).

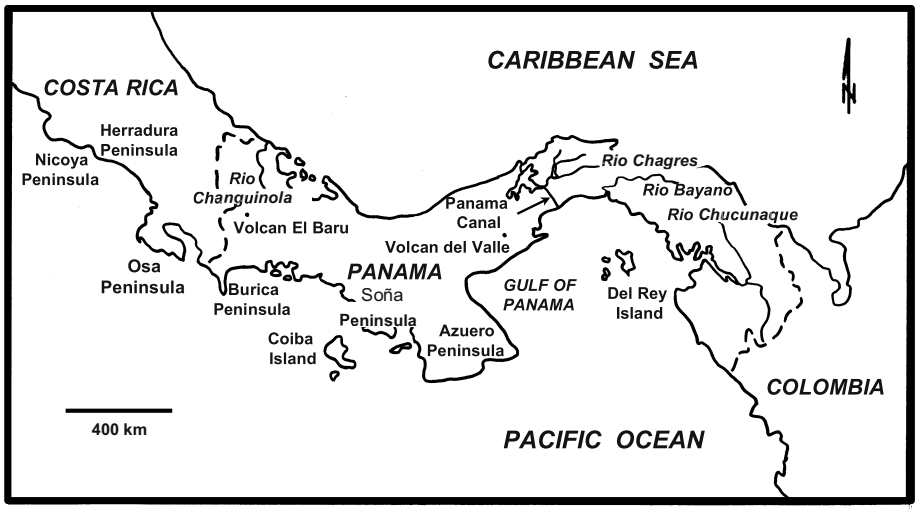

Figure 2. Map of southern Central America showing the locations of geographic features mentioned in the text.

2. THE PANAMA OF TODAY

As the southernmost portion of Central America, Panama (Fig. 2) forms the last and youngest segment of the land bridge between North and South America. The development of this land bridge, which only occurred during late Pliocene – early Pleistocene time around 3.5 million years ago with the closure of the Caribbean-Pacific seaway (Fig. 3), had profound biological, oceanographic, and climatological consequences (Duque-Caro, 1990; Coates *et al.,* 1992). Not only did it profoundly change the distribution of flora and fauna across the Americas and in adjacent oceans, but this event also affected the pattern of ocean circulation and global climate.

Together, Panama and Costa Rica presently define a small, northward-moving microplate (the 'Panama block' of Kellogg *et al.,* 1995) that is situated between the Nazca and Caribbean oceanic plates and occupies a geographic position between the foreland of continental South America and the Chortis block of Nicaragua that defines the continental basement of Central America (Fig. 4). This southern region of Central America has asymmetric geological character such that the Pacific side is a geologically active margin characterized by a deep oceanic trench, a narrow marine shelf, active subduction and consequent volcanic activity and earthquakes, whereas the Atlantic side is a passive, stable margin with a broad marine shelf.

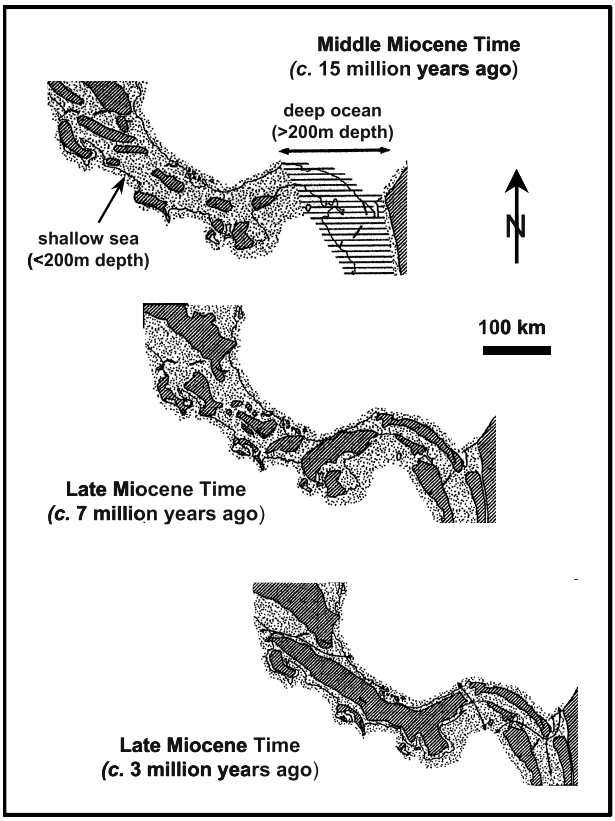

Figure 3. Paleographic reconstruction of the development of the Central American isthmus since Middle Miocene time. The lined pattern denote deep ocean conditions with the sea floor at a depth in excess of 200m and the stippled pattern indicates the inferred position of the marine shelf with water depth of less than 200m (modified from Coates, 1998).

Early studies recognized the geological complexity of Central America, noticed the complicated structural patterns present across the region, and described the stratigraphic patterns developed within narrow elongate sedimentary basins (Vaughn, 1918; Woodring, 1928; Schubert, 1935). Of particular note were the distinct differences in stratigraphy and structural character between northern and southern Central America. Subsequent studies (Lloyd, 1963; Dengo, 1969) placed Guatemala, Honduras, and most of Nicaragua into a geological province or terrane of continental affinity termed the Chortis block. Although subsequently subdivided into two different geological terranes (Fig. 4), the Chortega block and the Chocó block (Dengo, 1962) on the basis of a sharp gravity difference in central Panama at the narrowest part of the isthmus (Case, 1974; Dengo, 1985), the

remainder of southern Central America from southernmost Nicarauga, to northwestern Colombia was observed to have a similar geological character that was quite distinct from that of the Chortis block. This region, termed the 'Panama microplate' (Fig. 4), has been subdivided into two different, but geologically similar geological terranes the Chortega block and the Chocọ block (Dengo, 1962) on the basis of a fault inferred from a sharp gravity difference in central Panama at the narrowest part of the isthmus (Case, 1974; Dengo, 1985).

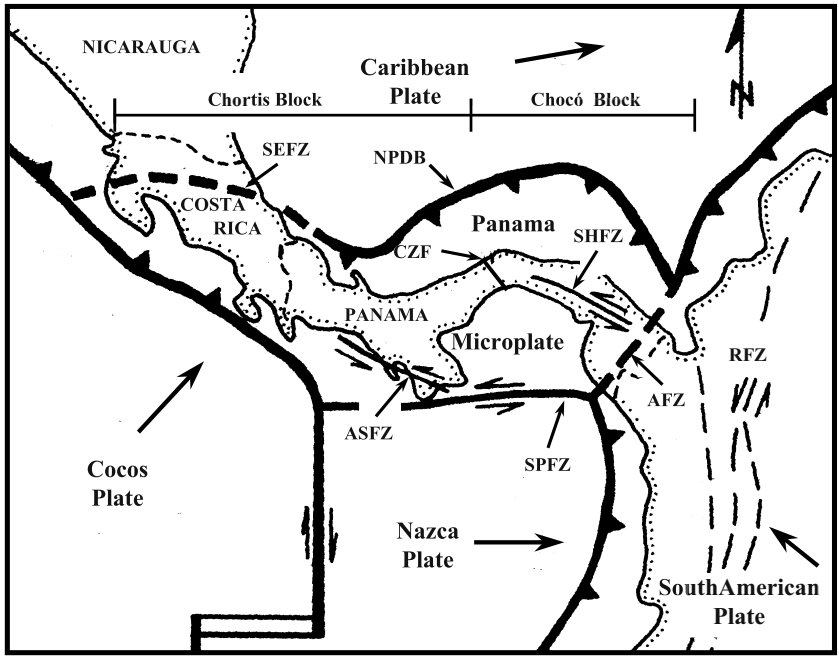

Figure 4. Present-day tectonic setting of southern Central America and northwestern South America, showing the area defined as the Panama block. The northern boundary of this microplate is defined by the North Panama Deformed Belt (NPDB), the southern boundary by the South Panama Fault Zone (SPFZ), the western boundary by the Santa Elena suture (SEFZ) with the continental Chortis terrane of northern Central America, and the eastern boundary with South America by the Atrato Fault Zone (AFZ), a southwestward extension of the South Caribbean Fault. The bar in the upper center of the figure indicates the division of the Panama microplate into the Chortega block and Chocọ́ block, which are separated by the Canal Fracture Zone (CFZ). The large arrows represent the direction of plate convergence. The active volcanism of Nicarauga, Costa Rica and western Panama is a result of the near orthogonal convergence of the Cocos plate with the Panama microplate, whereas the lack of volcanism in central and eastern Panama is attributed to the highly oblique motion between the Panama microplate and the Nazca plate (after Duque-Caro, 1990; de Boer *et al.,* 1995; Kellog *et al.,* 1995; Mann and Kolarsky, 1995).

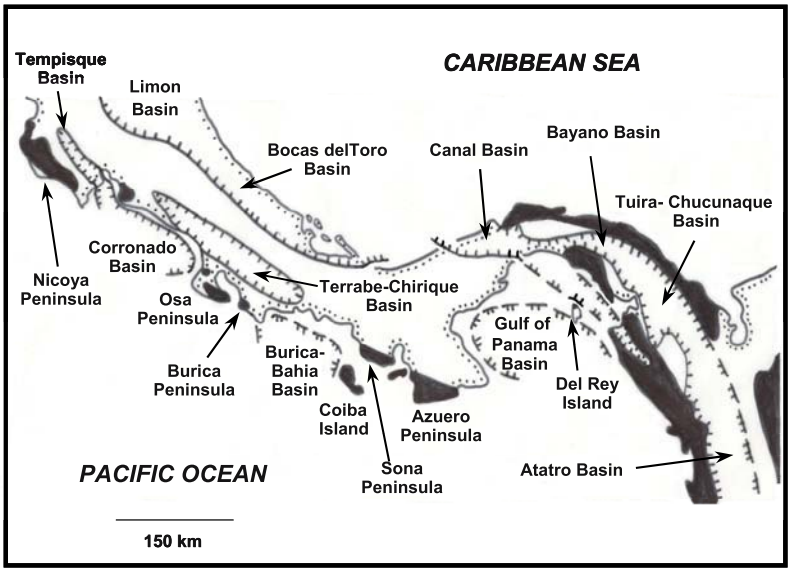

Figure 5. Location of obducted ophiolitic basement rocks (in black) and sedimentary basins (hatchured boundaries) in southern Central America and northwestern South America (after Escalante, 1990).

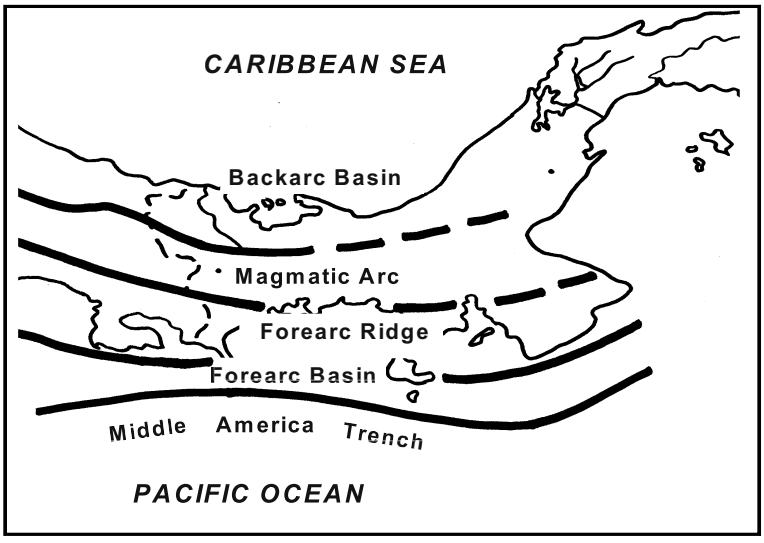

Figure 6. A portion of the Chortega block of eastern Costa Rica and western Panama showing the approximate locations of the structural components of the Panama-Costa Rica arc (after Escalante, 1990).

The Chortis block is a fragment of continental crust that was translated into its present position from a location beyond northern Mexico (see Fig. 7 below). By contrast, the basement of the Chortega and Chocó Blocks of southern Central America and northwestern Colombia consists predominantly of oceanic mafic igneous rocks of ophiolitic affinity and associated cherts and silicious limestones that form a tectonic belt (Fig. 5) along the Pacific side of Costa Rica and western Panama and on both the Pacific and Caribbean sides of eastern Panama and western Colombia (Weyl, 1969; Case, 1974; de Boer, 1979; Wildberg, 1984). Pichler *et al.* (1974) recognized that these mafic rocks belonged to a single, coherent association and Escalante (1990) speculates that this ophiolitic suite may comprise a single stratigraphic unit that extends as far southward as Ecuador.

Overall, the Panama that geologists see today is a young landscape that in form comprises a reclined S-shaped, generally E-W oriented isthmus (Fig. 2) constructed during the recent geological past (Fig. 3) as the result of a complex set of geotectonic processes that created and assembled a diverse suite of geological units over the past 150 million years. Much of present-day Panama formed in Tertiary time from a calc-alkaline oceanic volcanic island arc complex that presently extends from the southern margin of the Chortis Block in Nicaragua to the northwestern end of the South American continent (Fig. 6). The volcanic arc, deposits of related volcaniclastic sediments, and shallow marine sediments deposited in narrow back-arc basins (Escalante, 1990), together, were developed upon a plateau of late Cretaceous to early Cenozoic age oceanic crust (Bowland and Rosencrantz, 1988). A significant portion of the Chortega block and more than half of the Chocó block in eastern Panama, particularly the region east of the former Canal Zone (Case, 1974), consists of intrusive and extrusive mafic igneous rocks generated in the Paleoocene-Oligocene volcanic island arc (Kesler *et al.,* 1977; de Boer *et al.,* 1995; Grosser, 1988; Maury *et al.,* 1995). A single carbonate marine sequence of Cretaceous age has been mapped on the Pacific side of Panama (Fisher and Pessagano, 1965), and both carbonate and clastic marine sequences of equivalent age outcrop in Costa Rica (Escalante, 1990). Marine basins filled predominantly with clastic materials and volcaniclastic sequences extend across southern Central America. Some of the younger marine sedimentary basins, such as the Bocas del Toro and Bayano and Tuira-Chucunaque basins of Panama and the Limon basin in Costa Rica, have been uplifted over the past few million years to be included in the present-day landscape.

Significant additions to the southern, Pacific margin of the developing arc volcanic terrane also occurred on the fore-arc side of southern Central America. This occurred through both the obduction of local Cretaceous-age oceanic crust (Berrange *et al.,* 1988) and the docking of younger exotic

terranes consisting of oceanic rises and plateau, seamounts, and primitive oceanic arcs (Bowland and Rosencranrz, 1988; Escalante, 1990) that had been transported from locations far to the south and west. The most notable areas are the Azuero, Soná, and Burica peninsulas of Panama and the Osa, Herradura, Nicoya, and Santa Elena peninsulas in Costa Rica (Figs. 5). These ophiolitic sequences date back to late Jurassic – early Cretaceous time (Bourgois *et al.,* 1984) and are the oldest exposed rocks in southern Central America. In such areas, it is not uncommon to find strikingly diverse geological strata which bear no common genetic relationship or stratigraphic continuity spatially juxtaposed. Subduction-related volcanism occurred throughout the Cenozoic development of Panama and has continued into historic time at Volcán El Baru and Volcán El Valle. Subduction of the Cocos Ridge beneath southern Central America has been responsible for the continuing uplift of southern Costa Rica and western Panama during Quaternary time.

3. GEOLOGICAL DEVELOPMENT OF PANAMA

As illustrated in Figures 1 and 7, the geological development of Panama is a direct consequence of the relative motions of the North and South American continental plates and four oceanic plates over the past 150 million years (Adamek *et al.,* 1988; Bandy and Casey, 1973; Case and Holcombe, 1980; Case *et al*., 1971; Coates *et al.*, 1992; de Boer *et al.,* 1986; Donnelly*,* 1989; Duncan and Hargreaves, 1984; Duque-Caro, 1990; Escalante, 1990; Gardner *et al.,* 1992; Hoernle *et al.,*2002; Keigwin, 1982; Keller *et al.,* 1989; Lonsdale and Kiltgord, 1978; Mann *et al.,* 1990; Mann and Kolarsky, 1995; Pindell and Barrett, 1990; Vergara-Muñoz, 1988; Wadge and Burke, 1983).

The development of Panama is but one small part of the larger story of the tectonic development of the Caribbean basin and Central America. The paragraphs that follow briefly summarize this story within the framework of the geological time scale presented in Table 1. The starting point for this story is the supercontinent of Pangea (the amalgamated land mass of North America, South America, Eurasia, Africa, India, Australia, and Antarctica) which and began to breakup during the Jurassic some 200 million years ago It was at this time that North America began to separate from South America, a processes would ultimately lead to the present continental geography of the Western Hemisphere that we see today (Fig. 1).

3.1 Late Jurassic (*c.* 140 Ma, Fig. 7a)

By this time, the rifting separating North and South America was sufficient for a proto-Caribbean seaway to have developed along the E-W trending mid-ocean ridge system between the continents. The Yucatan block had rotated eastward into the Gulf of Mexico and the continental fragments underlying the Bahamas had moved southeastwards to be in their present positions relative to North America as this separation proceeded. A backarc basin opened within the Mexican terrane, an oceanic volcanic arc extending along the west coast of North America and the western margin of the Chortis terrane that, together with Jamaica, was moving southeastwards toward the Mexican peninsula. The proto-Greater Antilles arc began to develop at the eastern, subducting margin of the Farallon plate and another volcanic arc extended along the western margin of South America.

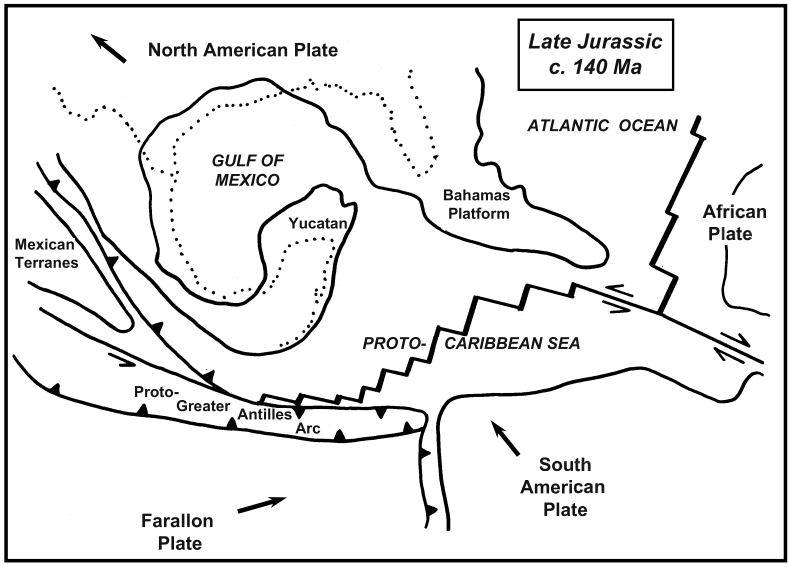

Figure 7a. Plate tectonic reconstruction for late Jurassic time at about 140 Ma. The dotted in this and subsequent figures denote the present-day coastline of North and Central America; the solid line indicates the inferred coastlines at the specific time in the past.

3.2 Middle Cretaceous (*c.* 100 Ma)

A very wide proto-Caribbean-Pacific seaway had developed through continued sea-floor spreading, which had also begun in the equatorial Atlantic initiating the separation of South America and Africa. Arc volcanism continued along the western margins of North and South

America. In the eastern Pacific, southward-dipping subduction began along the north side of what was to become the Caribbean plate and Greater Antilles arc, initiating in the progressive migration of the arc northeastwards into the Caribbean basin.

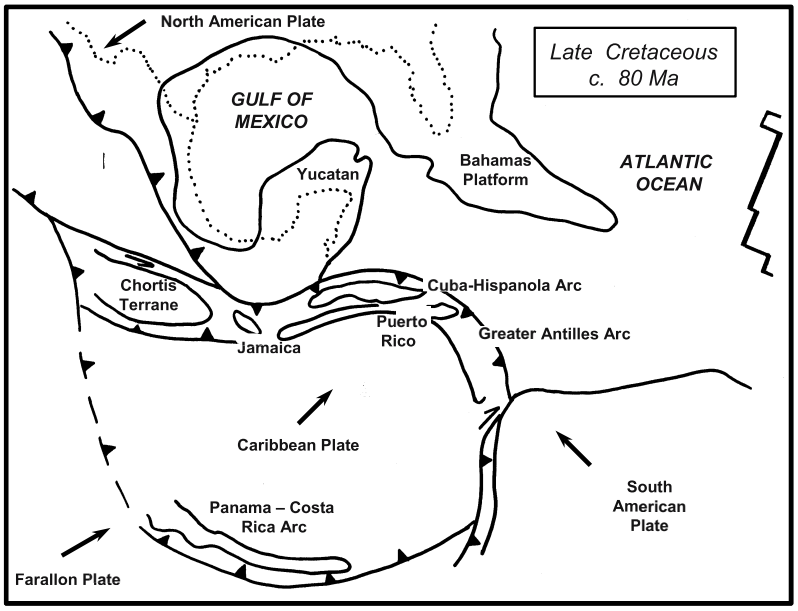

Figure 7b. Plate tectonic reconstruction for Late Cretaceous time at about 80 Ma.

3.3 Late Cretaceous (*c.* 80 Ma, Fig. 7b)

Sea-floor spreading between North and South America reached its maximum extent during this time. Suduction-generated volcanism continued along the western margins of South and North America, including the Chortis block. At this time, the Galapagos hotspot was established in the east-central Pacific Ocean and began the emission of voluminous amounts of mafic basaltic magma. This magmatism generated a vast lava plateau that that ultimately would extend over an area of 3 million km^2, form the floor of the Caribbean Sea, and produce the ridges that presently are being underplated beneath Central America as a result of subduction of the Cocos plate (see Fig. 7b below). The Caribbean plate had begun to move northeastwards, with subduction-related volcanic activity developing along the leading edge of the Caribbean plate. The Greater Antilles and Cuba-Hispanola arcs began to develop at the leading edge of the plate margin and the continental Chortis terrane was moving southeastwards. Accretion of oceanic rocks to the western margin of South America was initiated

Collision of the Greater Antilles arc with the North American continent had begun with the emplacement of ophiolites along the southern margin of Yucatan. Large quartzose turbidite sequences developed off northern South America from sediments shed from the northwestern edge of the continent and oceanic rocks of were accreted to the continental-margin arc. Sea-floor spreading had begun in the central Pacific. In the eastern Pacific, this led to the initiation of subduction of the Farallon plate beneath the western edge of the Caribbean plate and inception of the Costa Rica-Panama volcanic arc that was ultimately to produce the Chortega and Chocó terranes.

3.4 Paleocene (*c.* 60 Ma)

Arc volcanism continued along the western margins of South and North America, including the southeastward-moving Chortis block. The Caribbean plate continued to move northeastward. The leading edge of the Cuban arc suite began to run up against the Bahamas platform. With the initiation of the Yucatan and Grenada back-arc basins, the Greater Antilles arc was able to enlarge to ring the entire Caribbean basin. Convergence between the Chortis block and the Costa Rica-Panama arc continued.

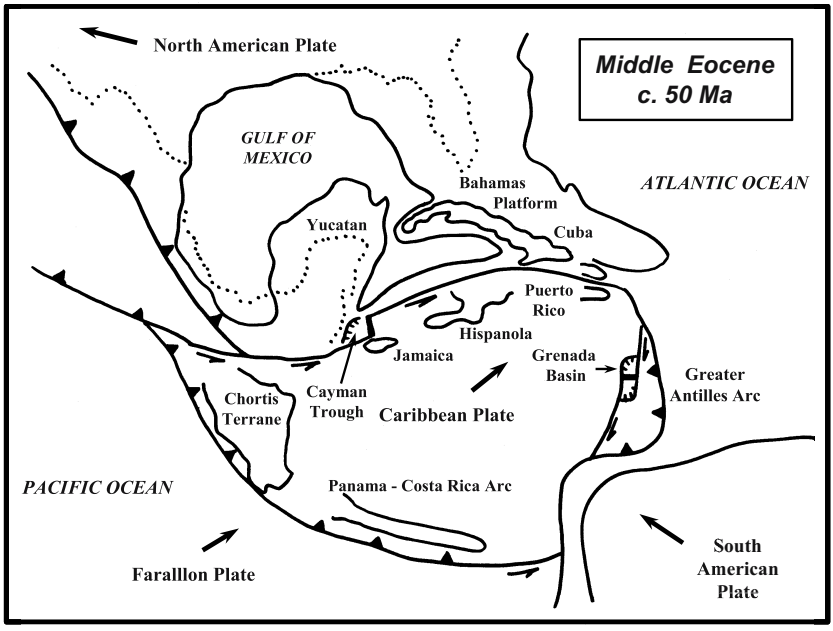

Figure 7c. Plate tectonic reconstruction for Middle Eocene time at about 50 Ma.

3.5 Middle- Late Eocene (*c.* 50-40 Ma, Fig. 7c)

The collision of the Cuba- Hispañola arc with the Bahamas platform was complete, which prevented further northeastward movement of the Caribbean plate. This initiated an eastward migration of the Caribbean plate, leading to the development of a new subduction zone and, subsequently, the Lesser Antilles volcanic arc. Eastward subduction continued along the western margins of South and North America, including the Chortis block. In the north, the Farallon plate was almost entirely subducted beneath North America and the Pacific mid-ocean ridge had intersected the continent. The Chortis block was beginning to impinge on southern Mexico and the Chortis block and the Costa Rica-Panama arc became aligned to form the proto-Central America magmatic arc. The emplacement of the ophiolite complexes and the docking of exotic terranes consisting of oceanic ridges and seamounts that had been transported from locations far to the south and west that ultimately would form the basement of the Chortega and Chocó Blocks was completed by middle Eocene time.

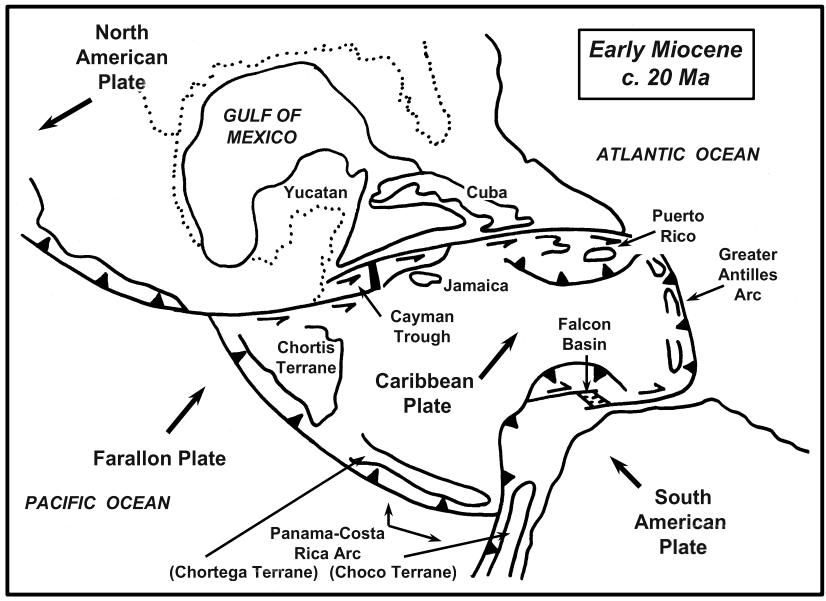

Figure 7d. Plate tectonic reconstruction for Early Miocene time at about 20 Ma.

3.6 Early Miocene (*c.* 20 Ma, Fig. 7d)

Eastward movement of the Caribbean plate continued, with Puerto Rico separating from Hispanola and Jamaica continuing its eastward migration.

The East Venezuela basin formed in response to foreland loading along the southern margin of the Caribbean plate. The remainder of the Farallon plate separated into two plates, a southern Nacza plate and a northern Cocos plate, divided by a small E-W trending mid-ocean ridge and N-S trending transform faults (the South Panama Fracture Zone). Proto-Central America was formed as the Chortis block collided with southern Mexico and the Panama - Costa Rica arc was fully aligned with the Chortis Block.

3.7 Mid-Late Miocene (*c.* 10 Ma)

Eastward movement of the Caribbean plate continued, with compressional deformation occurring along the continental margins of the basins. The Panama-Costa Rica arc, which was to become the Chortega and Chocó blocks, collided with the Western Cordillera of South America, cutting off the deep-water circulation between the Pacific and the Caribbean. This collision initiated uplift of the Andean arc and the migration of Andean terranes (*i.e.,* the Andean Orogeny) in northern Colombia. Volcanic islands developed along the Panama-Costa Rica arc in the present location of southern Central America. The doubly-curved shape of present-day Panama (began to develop as the E-W trending volcanic arc (Fig. 3). The doubly-curved shape of present-day Panama began to develop as the E-W trending volcanic arc began to be internally deformed and northwestward-trending strike-slip faulting was initiated as a result of this collision (Fig. 4).

3.8 Present (Fig. 8)

Eastward movement of the Caribbean plate continued, with increased compressional deformation continuing along the continental margins of the basins. This movement is being accommodated through left-lateral strike slip faults along its northern boundary within continental lithosphere at the edge of the North American plate and right lateral strike-slip faults within the oceanic and continental lithosphere along the margin of the South American plate. Development of Central America was completed, creating the land bridge between North and South America and the termination of shallow marine circulation between the Pacific and Caribbean in latest Pliocene – early Pleistocene time. N-S compressive stresses between North and South America have created the Panama block microplate (Fig. 4), which is defined on the north by the North Panama Deformed Belt, on the south by the Middle America Trench, the Santa Elena Fault System on the western side of the Chortega Block and the Atrato Fault Zone on the eastern side of the Chocó Block.

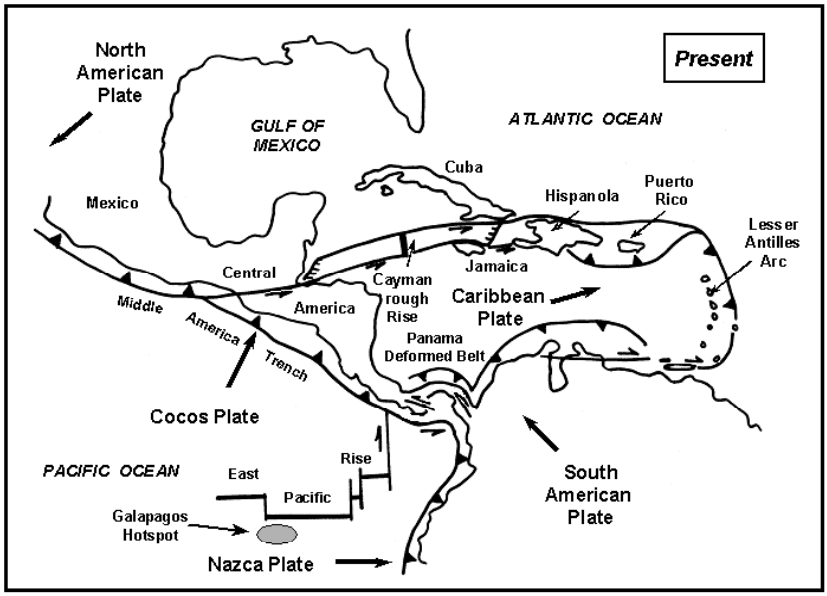

Figure 8a. Present plate tectonic configuration of the Caribbean region.

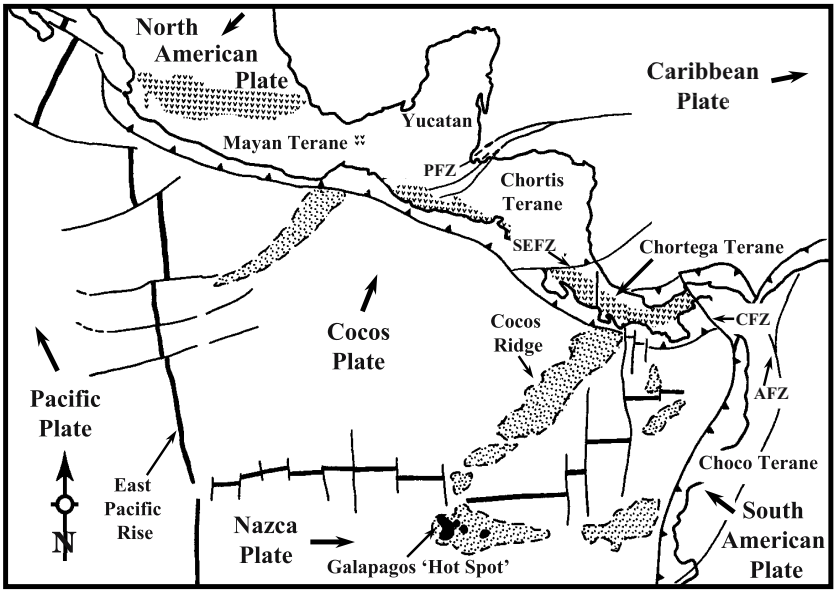

Figure 8b. Present plate tectonic configuration of the southern Central America region (after de Boer *et al.,*1995).

Having separated from the Caribbean Plate in late Tertiary or early Quaternary time, the Panama microplate is currently moving northward as a result of collision of the Panama-Costa Rica volcanic arc with South America to the east and the indenting of the Chortega block by the Cocos Ridge to the south. Together, the basinwide compressive stress regime and northern movement of Panama have led to regional uplift, the oroclinal bending, and the left-lateral strike-slip faulting that that generated the Panama foldbelt and led to the curved Panamanian isthmus. Near orthogonal subduction of the Cocos plate beneath Central America has resulted in an active and well-defined continental-margin volcanic arc extending from Guatemala to Costa Rica. The shallow subduction of the Cocos Ridge, a thick sequence of oceanic crust formed by submarine volcanic activity associated with the Galapagos hot spot, beneath the central portion of the Chortega block during the Plio-Pleistocene time has resulted in the rapid uplift of the Cordillera de Talamaca in Costa Rico and western Panama. The E-W movement of the Nacza plate along the margin of Panama is sub-parallel to the direction of motion of the Caribbean plate so subduction beneath Panama is restricted and volcanic activity limited, although not entirely absent.

REFERENCES

Adamek, S, Frolich, C, and Pennington, W, 1988, Seismicity of the Caribbean-Nazca boundary: Constraints on microplate tectonics of the Panama region: Jour. Geophys. Res., 93: 2053-2075.

Bandy, OL and Casey, R., 1973, Relector horizons and paleobathymetric history, eastern Panama: Geol. Soc. Amer. Bull., 84: 3081-3086.

Berrange, J, Bradley, D, and Snelling, N., 1988, K-Ar dating of the ophiolitic Nicoya complex of the Osa peninsula, southern Costa Rica, Jour. South Amer. Earth Sci., 2: 49-59.

Bourgois, J, Azema, J, Baumgartner, PO, Bournon, J, Desmet, A, and Aubboin, J, 1984, The geologic history of the Caribbean-Cocos plate boundary with special reference to the Nicoya ophiolite complex (Costa Rica) and D.S.D.P. results: A synthesis: Tectonophys., 108: 1-32.

Bowland C and Rosencrantz, E, 1988, Upper crustal structure of the western Colombian Basin, Caribbean Sea: Geol. Soc. Amer. Bull., 100: 534-536.

Case, JE, 1974, Oceanic crust forms basement of eastern Panama: Geol. Soc. Amer. Bull., 85:645-652.

Case, JE and Holcombe, TL, 1980, Geologic-tectonic map of the Caribbean region: US Geol. Surv. Misc. Inv. Series Map 1-1100, scale 1:2, 5000,000.

Case, JE, Duran, LG, Alfonso, Lopez, RA, and Moore, WR, 1971, Tectonic investigations in western Colombia and eastern Panama: Geol. Soc. Amer. Bull., 82: 2685-2712.

Coates, AG, 1998, The Forging of Central America: in *Central America: A Natural and Cultural History*, (AG Coates, ed), Yale Univ. Press, New Haven, CT: 1-39.

Coates, AG, Jackson, JBC, Collins, LS, Cronin, TM, Dowsett, HJ, Bybell, LM, Jung, P, and Obando, JA, 1992, Closure of the Isthmus of Panama: The near-shore marine record of Costa Rica and western Panama: Geol. Soc. Amer. Bull., 104: 814-829.

Davidson, JP, Reed, WE, and Davis PM, 1997, *Exploring the Earth: An Introduction to Physical Geology:* Prentice-Hall Inc., Upper Saddle River, NJ.

de Boer, JZ, 1979, The outer arc of the Costa Rica orogen: Oceanic basement complexes of the Nicoya and Santa Elena peninsulas: Tectonophys., 56:221-259.

de Boer, JZ, Drummond, MS, Bourdelon, MJ, Defant, MJ, Bellon, H, and Maury, RC, 1995, Cenozoic magmatic phases of the Costa Rican island arc (Cordillera de Talamanca): in *Geologic and Tectonic Development of the Caribbean Plate Boundary in Southern Central America* (P Mann, ed.), Geol. Soc. Amer. Spec. Paper 295: 35-55.

Dengo, G, 1969, Problems of tectonic relations between Central America and the Caribbean: Trans. Gulf Coast Assoc. Geol. Soc., 19: 311-320.

Dengo, G, 1962, Tectonic-igneous sequence in Costa Rica: in *Petrologic Studies – A Volume to Honor AF Buddington*, (AEJ Engel, H.L James, and BF Leonard, eds.), Geol. Soc. Amer.: 133-161.

Dengo, G, 1985, Mid America; Tectonic setting for the Pacific margin from southern Mexico to northwestern Colombia: in *The Ocean Basins and Margins* (AEM Nairn and FG Stehli, eds.), Plenum Press, New York, NY, 7: 123-180.

Donnelly, TW, 1989, Geological history of the Caribbean and Central America: in *The Geology of North America – An Overview* (AW Bally and AR Palmer, eds.), Geol. Soc. Amer., A: 299-321.

Duncan, RA and Hargraves, RB, 1984, Plate tectonic evolution of the Caribbean region in the mantle reference frame: in *The Caribbean-South American Plate Boundary and Regional Tectonics* (WE Bobini, RB Hargraves, and R Shagam, eds.), Geol. Soc. Amer. Mem. 162: 81-84.

Duque-Caro, H, 1990, Neogene stratigraphy, paleoceanography, and paleobiogeography in northwest South America and the evolution of the Panama Seaway: Jour. South Amer. Earth Sci., 4: 262-269.

Escalante, G, 1990, The geology of southern Central America and western Colombia: in *The Geology of North America,* Vol. H, The Caribbean Region, (G Dengo and JE Case, eds.), Geol. Soc. Amer.: 201-230.

Fisher, DM.; Gardner, TW; Marshall, JS, and Montero, PW, 1994, Kinematics associated with late Cenozoic deformation in central Costa Rica; western boundary of the Panama Microplate: Geology, 22: 263-266.

Fisher, SP and Pessagano, EA, 1965, Upper Cretaceous strata of northwestern Panama: American Association of Petrooeum Geologists Bulletin, 49: 433-444.

Gardner, TW, D Verdonck, N M Pinter, R Slingerland, K P Furlong, TF Bullard, and SG Wells, 1992, Quaternary uplift astride the aseismic Cocos Ridge, Pacific coast, Costa Rica: Geol. Soc. Amer. Bull. 104: 219-232.

Grosser, JR, 1989, Geotectonic evolution of the Western Cordillera of Colombia: New aspects from geochemical data on volcanic rocks: Jour. South Amer. Earth Sci., 2: 1449-1458.

Keigwin, L, 1982, Isotopic paleoceanography of the Caribbean and East Pacific: Role of Panama uplift in late Neogene time: Science, 217: 350-353.

Kellogg, JN and Vega, V, 1995, Tectonic development of Panama, Costa Rica, and the Colombian Andes: Constraints from global positioning system geodetic studies and gravity: in *Geologic and Tectonic Development of the Caribbean Plate Boundary in Southern Central America* (P Mann, ed.), Geol. Soc. Amer. Spec. Paper 295: 75-90.

Keller, G, Zenker, C, Stone, S, 1989, Late Neogene history of the Pacific-Caribbean gateway: Jour. South Amer. Earth Sci., 2: 73-108.

Kesler, SE, Sutter, JF, Issigonis, J, Jones, LM, and Walker, RL, 1977, Evolution of porphyry copper mineralization in an oceanic island arc, Panama: Econ. Geol., 72: 1142-1153.

Lloyd JJ, 1963, Tectonic history of the south Central American orogen: Amer. Assoc. Petrol. Geol. Mem. 2: 88-100.

Lonsdale, P and Kiltgord, KD, 1978, Structure and tectonic history of the eastern Panama basin: Geol. Soc. Amer. Bull., 89: 981-999.

Mann, P and Kolarsky, RA, 1995, East Panama deformed belt: Structure, age, and neotectonic significance: in *Geologic and Tectonic Development of the Caribbean Plate Boundary in Southern Central America* (P Mann, ed.), Geol. Soc. Amer. Spec. Paper 295: 111-130.

Mann, P, Schubert, C, and Burke, K, 1990, Review of Caribbean neotectonics: in *The Geology of North America,* Vol. H, The Caribbean Region, (G Dengo and JE Case, eds.), Geol. Soc. Amer.: 307-338.

Maury, RC, Defant, MJ, Bellon, H, Stewart, RH, and Cotte, J, 1995, Early Tertiary arc volcanics from eastern Panama: in *Geologic and Tectonic Development of the Caribbean Plate Boundary in Southern Central America* (P Mann, ed.), Geol. Soc. Amer. Spec. Paper 295: 29-34.

Pichler, H, Stibane, FR, and Weyl. R, 1974, Basischer Magmatismus und Krustenbau in südlichen Mittelamerika, kolumbien, und Ecuador: Neues Jahrbuch fur Geol. Palëontol. Monatschefte, 2: 102-126.

Pindell, JL and Barrett, SF, 1990, Geological evolution of the Caribbean region: A plate tectonics perspective: in *The Geology of North America,* Vol. H, The Caribbean Region, (G Dengo and JE Case, eds), Geol. Soc. Amer.: 405-432.

Skinner, BJ and Porter, SC, 2000, *The Dynamic Earth: An Introduction to Physical Geology*, John Wiley and Sons Inc., New York, NY.

Schubert, C, 1935, *Historical Geology of the Antillean-Caribbean Region*, John Wiley and Sons Inc., New York, NY.

Vaughn, TW, 1918, Geological history of Central America and the West Indies during Cenozoic time: Geol. Soc. Amer. Bull., 29: 615-630.

Vergara-Muñoz, A, 1988, Tectonic patterns of the Panama block deduced from seismicity, gravitational data, and earthquake mechanisms: Implications to the seismic hazard: Tectonophys,, 154: 253-267.

Wadge, G, and Burke, K, 1983, Neogene Caribbean plate rotation and associated Central American tectonic evolution: Tectonics, 2: 633-643.

Weyl, R, 1969, Magmatische Forderpahsen and Gesteinschemisimus in Costa Rica: Neues Jahrbuch für Geologie und Palëontologie, 7: 423-446.

Wildberg, H, 1984, Der Nicoya-Komplex, Costa Rica, Zentralamerika: Magmatismus und Genese eines polygenetischen Ophiolith-Komplexes: Münstersche Forschung. Geol. Palëontol., 62: 123p.

Woodring, WP, 1928, Tectonic features of the Caribbean region: Proceedings 3rd Pan-Pacific Sci. Congress, Tokyo: 401-431.

Part II: The Upper Río Chagres Basin

Chapter 5

IGNEOUS GEOLOGY AND GEOCHEMISTRY OF THE UPPER RÍO CHAGRES BASIN

Gerhard Wörner[1], Russell S. Harmon[2], Gerald Hartmann[1], and Klaus Simon[1]
[1]Universität Göttingen, [2]US Army Research Office

Abstract: The geological basement of the upper Río Chagres basin (RCB) is primarily a mixture of Cretaceous to Upper Tertiary age volcanic and intrusive rocks. Exposed rocks consist of highly deformed mafic basalts, basaltic andesites, gabbros, diorites as well as chemically more evolved granodiorites, tonalities, and granites. Ultramafic rocks, that would provide evidence for an oceanic basement/lithospheric mantle basement to the RCB, are absent. Primary stratigraphic relations and contacts are generally obscured, either tectonically or by deep weathering. Most rocks, in particular the volcanics, volcaniclastic sediments, and granites are all strongly deformed and chemically altered. Mafic and granitic rocks have distinct weathering characteristics that influence stream channel morphologies throughout the RCB. The mafic complexes are most resistant to weathering and mechanical erosion, producing narrow river channels, rapids, and deeply cut gorges. Granitic lithologies are most easily weathered and generate straight and wide river courses. Massive altered basalts are intermediate in their style of weathering. Dike swarms crosscut all lithologies and strongly influence river channel form and orientation. The geochemical composition of the rocks suggest that the majority are derived from extensive volumes

Key words: Panama; Río Chagres; igneous geology; geochemistry

1. GEOLOGICAL SETTING

The Central American land bridge between the Santa Elena transform fault in northern Costa Rica, the boundary with the continental Chortis terrane of northern Central America, and the Atrato Fault Zone in northern Colombia, a southwestward extension of the South Caribbean Fault is characterized by a distributed series of mafic complexes that form the

R. S. Harmon (ed.), The Río Chagres, Panama, 65-82.

foundation of the Central American land bridge (Fig.1; see also Harmon, 2005, this volume; Figs. 2 and 4). These mafic terranes have been tectonically amalgamated onto an early Tertiary tholeiitic volcanic island arc system (Goossens *et al.,* 1977), which subsequently evolved from tholeiitic to a more mature calc-alkaline volcanic arc from the Oligocene to present (Alvarado *et al.,* 1993; de Boer *et al.,* 1995; Hoernle *et al.,* 1995, and references therein).

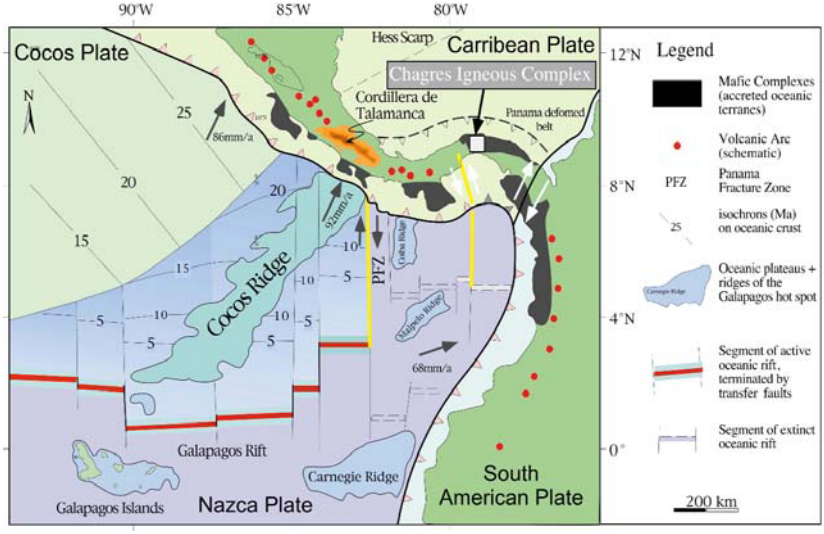

Figure 1. Plate tectonic setting of the Central American land bridge following Gutscher *et al*. (1999) and Meschede and Barckhausen (2001) with accreted mafic complexes from Gossens *et al.* (1978).

Presently, active volcanism in Costa Rica, western Panama, and northern Colombia is associated with the northwestward subduction of the Cocos Plate beneath Central America (Fig. 1). Two volcanic gaps exist, one where the Cocos Ridge has collided with the arc in southern Costa Rica, and the other in eastern Panama, where convergence has been taken up since the mid-Miocene time by movement along the N-S trending Panama Fracture Zone. As a consequence, the convergent plate boundary in central Panama has locked, arc volcanism has ceased, and related northward displacement of central and eastern Panama has been accommodated by strike-slip motion, oroclinal bending, and extension (Fig. 1). The result of this complex tectonic situation is the low topography of the central Panama in the canal region as compared to mountainous landscapes generated by the compressional regime

operating to the west of the Panama Fracture Zone and transpressional deformation occurring in northern Colombia.

The history of tectonic deformation of the mafic basal complexes in north-central Panama is documented by unconformably overlying shallow marine sediments. Abundant large displacements of these rocks (*e.g.,* the SW-NE trending Río Gatun Fault in the Gatuncillo Fm. of Middle to Upper Eocene age) date the last major displacements older than about 15 Ma (where 1 Ma = 10^6 years B.P.). By contrast, the Gatun Fm. and Chagres Fm. were deposited by about 8 Ma and 6 Ma, respectively, in a narrow, inter-oceanic strait about 200-500m deep (Collins *et al.,* 1996). Their exposure along the present coast directly overlying the RCB mafic igneous complex supports the idea that uplift in the Panama Canal area since Miocene time has been minor and restricted to the emergence of shallow marine sediments by no more than a few hundred meters.

Rocks directly underlying the upper Chagres basin belong to a series of mafic complexes that occur throughout southern Central America and northern Colombia (Fig. 1). These mafic complexes are thought to have been accreted onto the convergent plate margin during Tertiary time (Escalante, 1990; Hoernle *et al.,* 2002). Goossens *et al.* (1977) noted their age range from the Cretaceous to the Eocene, described the distribution, lithology and geochemistry of these rocks, recognized the tholeiitic character, and proposed their correlation from northern Costa Rica to the northern Colombian Andes. More recently, Hoernle *et al.* (2002) suggested the term "Carribean Large Igneous Province" (CLIP) for this region and linked the CLIP-rocks to the thickened oceanic crust of the Carribean Plate and to the abundant Pacific aseismic ridges offshore along the western coast of Central America. They also confirmed previous evidence of a continuous age range from the Cretaceous to Miocene for these mafic complexes. The ultimate origin of all these occurrences was proposed to be the Cretaceous plume head and subsequent trace of the Galapagos hot spot on the Nazca plate.

In general, CLIP lithologies are dominated by submarine lava effusions. Although intrusive equivalents of these submarine volcanics also have been described within the Central America region, the mafic igenous complex of the upper Río Chagres basin (RCB) is characterized by an abundance of intrusive lithologies, gabbros and granites. This suggests a similar geological setting, but a relatively deeper level of erosion for the rocks of the RCB compared to other CLIP mafic complexes.

This paper describes the lithologies that are exposed across the RCB, examines their distribution, and discusses the geological control that these rocks exert on the drainage system of the upper Río Chagres watershed and its tributaries (see Fig.1 of the Introduction). Geochemical data are used to

consider possible correlatives in other terranes of the CLIP in Central America as well as the ultimate origin of the magmas that produced igneous rocks of the RCB.

2. ROCK TYPES OF THE RCB

Bedrock exposures within the RCB are strictly limited to the river channels. Thus, it is impossible reconstruct in any detail the areal extent and structural relations between the rock suites or their stratigraphic framework. Observed contacts between lithologies either are continuous, tectonic, or obscured by deep erosion. Because lithologies have a major control on the river courses at least at a 10 m to 100 m scale, the different rock types are discussed below according to their erosional resistance and their relation to riverbed morphology.

Three basic rock types have been observed within the upper Río Chagres basin:

(i) volcanic rocks that were erupted as submarine lava flows,
(ii) volcaniclastic rocks derived from the submarine eruption and fragmentation of lavas, and
(iii) coarse-grained igneous rocks that intruded into the volcanic pile and cooled slowly.

Compositionally, two broad classes of igneous rock are distinguished across the upper Río Chagres basin – *mafic* lithologies and *felsic* lithologies. Mafic rocks are those with a silica (SiO_2) content of <52% (basaltic lavas and gabbros) that are rich in magnesium (Mg) and iron (Fe). These mafic rocks represent original magmas generated by partial melting of a source within the Earth's mantle. Magmatic evolution by fractional crystallization of silicate and oxide solid phases will produce geochemically evolved *silicic* compositions that are enriched in silica (SiO_2), alumina (Al_2O_3), and alkali elements (Na and K). Within the RCB, the differentiation of mafic magmas produced more silica-rich products andesites (if the magmas were erupted as lavas) or diorites and various types of granites and tonalites (if intruded and crystallized at depth).

Figure 2 is a map of the river network of the upper Río Chagres basin showing the locations of different lithologies observed. Figure 3 shows typical examples of the prevalent lithologies in river channel outcrop.

2.1 Basalts, Andesites, and Related Volcanic Rocks

Basalts and related volcanic rocks of the RCB with <52% SiO_2 are mostly fine-grained and contain rare phenocrysts of pyroxene or plagioclase. Only three in-situ outcrops of amphibole-bearing volcanic rocks (younger dikes), a lithology expected in a volcanic island arc setting, have been found within the RCB.

Vesicles in the volcanic rocks are very rare and, when present, are spherical in shape. The majority of RCB volcanics are massive and non-vesicular. Breccias of aphyric dense clasts up to 15 cm in diameter occur rarely. Pillow lavas and related volcaniclastic rocks (pillow breccias), which are unequivocal evidence for submarine eruptions, are rare in the RCB. However, more abundant occurrences have been described from related stratigraphic sequences in Central Panama (Mapa Geologico de Panama, 1:250.000). Also outside the limits of the RCB watershed to the north, abundant volcaniclastic submarine debris flows have been observed that contain clasts with sizes up to several meters in diameter. These sediments contain strongly vesicular volcanic clasts and red-oxidised, subaerial scoria.

The observed association of volcanic rocks suggests a submarine emplacement, mostly well below the vesiculation depth of about 200 m. The persistently massive nature of the basalts (>90% in volcanic terrain) and their rare but recurrent intercalations with submaine volcaniclastics reflects their eruption as thick submarine sheet lava flows. Such sheetflows form as the result of massive submarine effusive events at high eruption rates. The chemical composition of all basaltic and low-K andesitic rocks has been affected by submarine alteration (*e.g.,* the secondary formation of albite and chlorite during submarine hydrothermal alteration – see section 3.1 below) and, more recently, by deep tropical weathering.

Extensive areas of volcanic rock are found in the headwaters of the upper Río Chagres and the Río Chagresito (Fig. 2). These basalts and andesites are observed to be more resistant to river incision than granites, except where strongly cross cut by faults.

2.2 Intermediate to Mafic Intrusive Rocks (Diorites and Gabbros)

Mafic intrusive rocks are variable in composition and texture, ranging from fine-grained (sub-mm) micro-diorites with 52-63% SiO_2 to coarse-grained (*c.* 5 mm) gabbros with <52% SiO_2, that sometimes exhibit schlieren textures of mixed mafic and silicic lithologies. These rock types are often

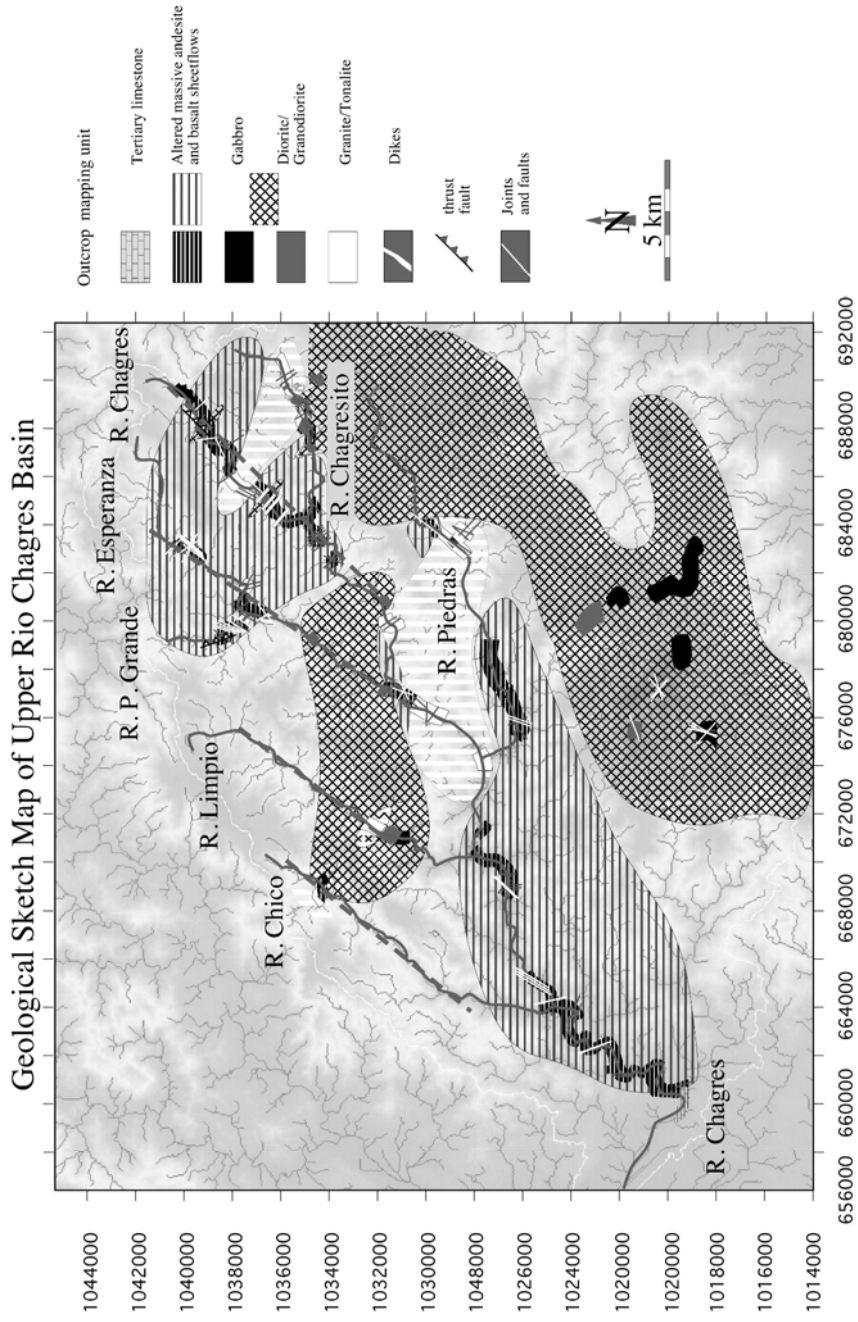

Figure 2. Preliminary geological map of the the upper Río Chagres basin showing the distribution of different lithologies described in the text.

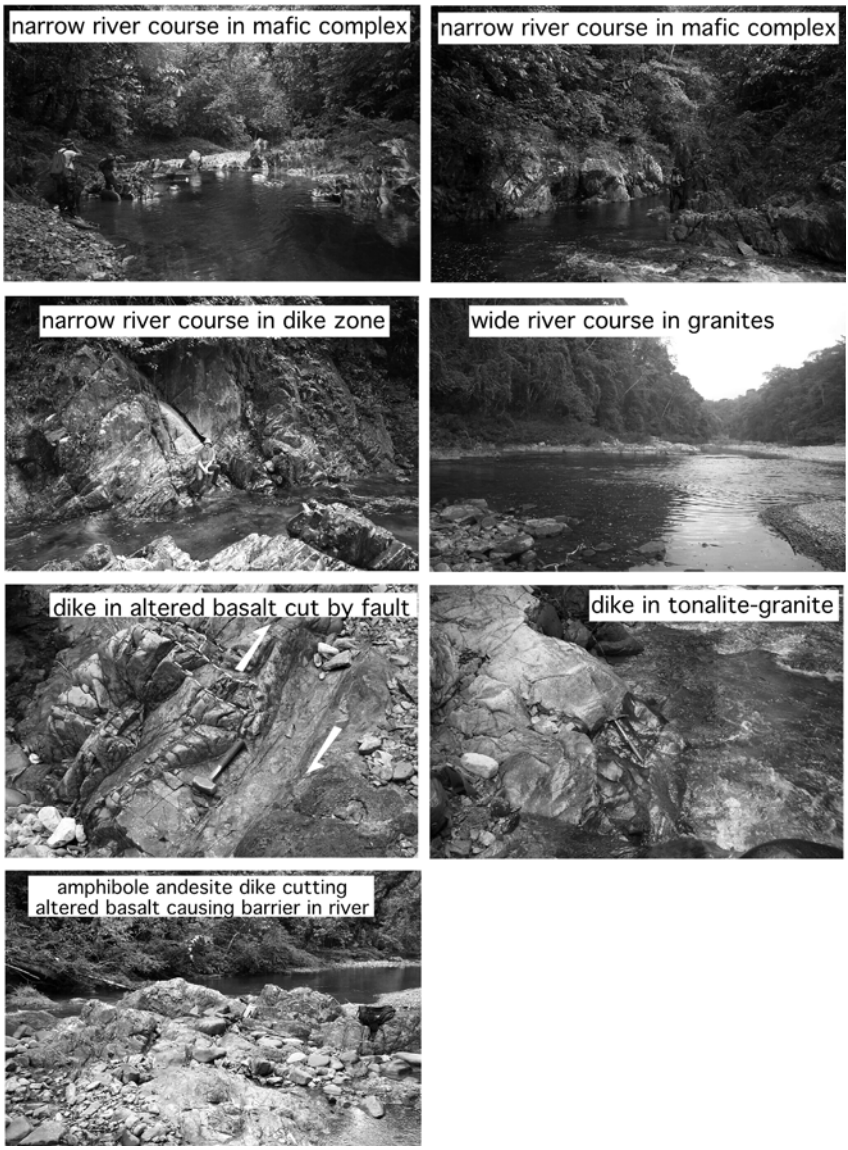

Figure 3. Examples of typical lithologies observed along the Río Chagres and its tributaries.

closely associated in localized "mafic complexes", which range from a few tens of meters to up to >1 km in size. Contacts are always obscured, but given the lensoid shape of the smaller bodies, tectonic fragmentation of competent mafic rocks within a package of more easily deformed volcanic rocks is likely. It is not possible to structurally relate mafic intrusive

complexes to the basalts and andesites. However, their geochemical fingerprints are identical (see section 3.2 below) and, therefore, a genetic link is confirmed. It is likely that these mafic complexes represent the tectonized equivalents of the magma chambers related to submarine volcanism that produced the basalt sheet flow extrusions.

Mafic complexes are the most resistant to erosion of all RCB lithologies. These rocks typically form narrow rapids and waterfalls up to tens of meters in height, as is observed, for example, in the headwaters of Río Chico (Figs. 2 and 3).

2.3 Granites and Tonalites

The most evolved intrusive rocks observed are plagiogranitic in composition with a silica content of >68%. Transitional granodiorite with 58-68% SiO_2 is frequently observed in association with the granitic rocks. These intrusive rocks are abundant in the upper reaches of the Río Piedras, Río Chagres, and the Río Esperanza-Playa Grande area, as well as to the south in the middle course of the upper Río Chagres (Figs. 2 and 3). All of these evolved coarse-grained rocks (tonalites, granites, and plagiogranites) are here denoted by the collective field term of 'granite'.

Both, the coarse-grained character and the abundance of easily-weathered sheet silicates and feldspars as primary mineral constituents make these rocks particularly sensitive to chemical alteration and softening by deep tropical weathering. In addition, granites, like all rocks of the RCB, are affected by strong tectonic movements and abundant faults. As a result, river courses in granitic lithologies are typically of low gradient, uniformly meandering, and without narrow reaches and rapids.

2.4 Dikes

Dikes of basaltic to andesitic composition up to 1-3 m in width are abundant across the RCB and often form dike swarms that occasionally form the bedrock of the river channel for several tens of meters. Dikes are observed to cross cut all all other lithologies, but tend to be more abundant in the basaltic and andesitic volcanics than in the mafic intrusive or granite terrains. This is probably due to the fact that the volcanic rock pile is fed by dikes, whereas the intrusive rocks represent discrete magma chambers from which many of the dikes originate. Chilled, previously glassy dike margins are now deeply altered to clay. Vesicles have not been observed in dike rocks. With few exceptions, these dikes are sub-vertical in orientation (Fig. 3). Conjugate sets of dikes at an angle of about 60° are often observed but are usually strongly biased to one of the directions. Swarms of dikes are

observed, as are multiple dike-in-dike injections. Such dike swarms may comprise > 90% of the exposed bedrock along a reach of river for several tens of meters and sometimes more. On a larger (>km) scale, there appears to be no systematic orientation of dikes that can be related to a regional tectonic fabric. This is mostly due to the fact that younger strike-slip fault motions have displaced and rotated both the dikes and their host rocks. The abundance of dikes and dike swarms confirms the assertion from the sheet flows, that the RCB is characterized by high eruption rates.

Dike swarms into basalts and mafic intrusive rocks tend to form narrow (< 50 m) and steep-sided river sections and one or more series of rapids. In silicic lithologies, andesite and granite, occasional dikes often form small isolated rapids when crossing at a high angle. Crossing at lower angles, the dike swarms may determine river reach orientation for 100 m or more.

2.5 Deformation

Limited exposures and missing lithological differentiation prohibit the observation of strata and depositional boundaries. Observations of tectonic deformation, therefore, are restricted to types and patterns of faults. Exposed faults are characterized by intensively deformed zones, which occur often in sub-parallel swarms (Fig. 2). Individual faults are no more than 50 cm wide and are generally part of fault swarms over tens of meters wide (Fig. 3).

Deformation locally produced thinly stretched mylonites, which are and layered at a mm-scale and sometimes show internal folding. Vertical fold axes prove the strike-slip nature of observed displacements. These fault zones are characterized by pronounced weathering and bleaching by fluids and, sometimes, by secondary mineralization (pyrite). With few exceptions, faults are generally steep, mostly vertical.

The observed association of volcanic rocks suggests a submarine emplacement, mostly well below the vesiculation depth of about 200 m. The persistently massive nature of the basalts (>90% in volcanic terrain) and their rare but recurrent intercalations with submaine volcaniclastics reflects their eruption as thick submarine sheet lava flows. Such sheetflows form as the result of massive submarine effusive events at high eruption rates. The chemical composition of all basaltic and low-K andesitic rocks has been affected by submarine alteration (*e.g.,* the secondary formation of albite and chlorite during submarine hydrothermal alteration – see section 3.1 below) and, more recently, by deep tropical weathering.

Extensive areas of volcanic rock are found in the headwaters of upper Río Chagres and the Río Chagresito (Fig. 2). These basalts and andesites are

observed to be more resistant to river incision than granites, except where strongly cross cut by faults.

3. GEOCHEMISTRY

3.1 Alteration

Fluid-rock interactions associated with submarine emplacement and subsequent strong tectonic deformation resulted in high degrees of chemical alteration even before exposure of the RCB rock suite to tropical weathering in the near-surface environment. Primary textures are preserved in all rock types. However, primary mineralogies are restricted to rare fresh phenocrysts (pyroxenes, feldspars and amphibole) in volcanic rocks and occasionally the cores of large pyroxene grains in the intrusive rocks. Chloritization of biotite and amphibole, sassuritization of feldspars in granites, and the almost complete alteration of finer-grained mafic lithologies to albite and chlorite attest to the profound chemical changes. These resulted from a combination of of early hydrothermal processes during and after submarine emplacement and chemical alteration from present-day low-temperature tropical weathering. Deformed rocks tend to become silicified.

Sampling was restricted to the least weathered rocks, but the effects of hydrothermal alteration could never be completely avoided. Consequently, the mobile 'Large-Ion-Lithophile Elements' (LILE), *e.g,* Cs, Ba, Rb and K, are affected by this process and, thus, show a large variation in geochemical composition (Fig. 4). As such, these elements cannot be used as geochemical tracers of magma source. By contrast, the 'Rare Earth Elements' (REE) and 'High Field Strength Elements' (HFSE), *e.g.* Nb, Ta, Hf, Zr and Ti, are known to be largely immobile during alteration. These elements show systematic behavior and can be used for petrogenetic interpretations.

3.2 Major and Trace Element Compositions

Concentrations of major element vary on a water-free normalized basis from (rare) ferro-gabbros with 45% SiO_2 to granites that have 78.5% SiO_2. Potassium contents are generally below 1%, often much lower. This attests both to the initially low K_2O contents of many rocks and the strong post-emplacement, low-temperature hydrothermal alteration that affected these rocks. The majority of rocks (60% of the samples analyzed) have SiO_2 contents that range between 48-57%. Rocks of intermediate composition,

such as the amphibole-bearing andesites, are rare. In essence, the RCB igneous assemblage is bimodal in composition consisting of basalts, basaltic andesites, and their intrusive counterparts on the one hand and granodiorites and granites on the other.

Trace elements are reported here as conventional "spider-diagrams" where trace concentrations have been normalized to primordial mantle values (Fig. 4). The advantage of such diagrams is the representation of the full spectrum of trace element patterns that facilitates rapid comparison between different rock types.

All RCB rocks are characterized by a large scatter for K, Sr, Rb, and, to a lesser extent, Ba (Fig. 4a, b) as expected for elements that are affected by hydrothermal alteration. The REE, HFSE, Th and U appear to be more stable throughout the RCB rock suite. Their patterns, however, are rather inconclusive as regards identifying the source of the RCB magmas. No clear subduction zone signature, *e.g.* negative Nb and Ta troughs associated with high Pb and Sr peaks, is displayed in Figure 4. While the latter do indeed show positive spikes, there are no clear depletions in Ta and Nb over immobile neighboring elements (such as La). However, none of the RCB rocks analyzed show a clear indication of a typical intra-plate, ocean island basalt (OIB) signature, *e.g.* relative enrichment of Nb and Ta. By comparison, the data published by Hoernle *et al.* (2002) from accreted mafic complexes in Central America (Fig. 1) do show, at least for one group of rocks, such OIB patterns (Fig. 4c). By contrast, early Tertiary rocks from the Darien mafic complex, located to the northeast of the RCB (Fig. 1), have trace element patterns with low Nb, leading Maury *et al.* (1995) to infer their origin from an island arc volcanism generated by a Cretaceous/Tertiary subduction zone.

Figure 5 attempts to resolve the ambiguity by plotting trace element ratios of mantle-normalized compositions. Typical intra-plate basalts (OIB) and oceanic crust (MORB) are indicated in the figure, as well as the compositional trends expected from dehydration of subducted oceanic crust

Figure 4. (overleaf). Trace element ratios (a, b, normalized values) of igneous rocks from the upper Río Chagres basin. The fields of typical basalts from different tectonic settings are indicated. The field in the lower left of (a) could be considered the forbidden quadrant of this plot: rocks with low La/Ta (i.e. positive Ta anomaly = enriched pattern) should not have a low La/Yb ratio (depleted pattern).

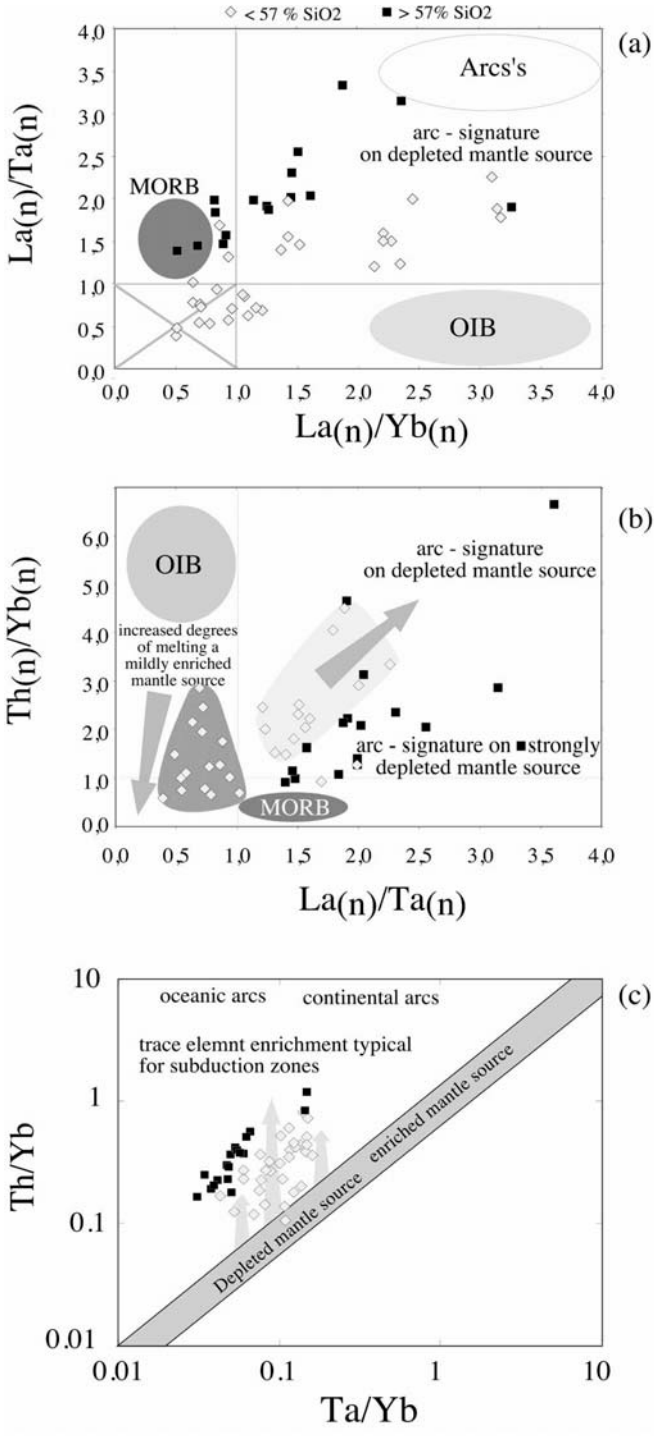
◇ < 57 % SiO2 ■ > 57% SiO2
(a)
Arcs's
arc - signature
on depleted mantle source
MORB
OIB
La(n)/Ta(n)
La(n)/Yb(n)
(b)
OIB
arc - signature
on depleted mantle source
increased degrees
of melting a
mildly enriched
mantle source
arc - signature on strongly
depleted mantle source
MORB
Th(n)/Yb(n)
La(n)/Ta(n)
(c)
oceanic arcs
continental arcs
trace elemnt enrichment typical
for subduction zones
Depleted mantle source
enriched mantle source
Th/Yb
Ta/Yb

in an island arc setting. Considering only mafic rocks (*i.e.,* rocks with <57.5 % SiO_2), there is one group of RCB samples that lies close to the arc trend. These rocks have slight characteristics of subduction zone magmas.

This evidence, together with that from the Th/Yb-Ta/Yb diagram (Fig. 5c) suggests that the mantle source of the Chagres rocks was rather depleted, with some RCB rocks having a slight subduction zone character. Importantly, not a single sample exhibits a trace element character that could be taken as evidence for a typical (trace element-depleted) mid-ocean ridge basalt (MORB) spreading center origin.

Considering the close association of the RCB with the island arc rocks of the nearby Darien belt in Panama (to the north of the RCB) studied by Maury *et al.* (1995), we conclude that the mafic complex of central Panama and the rocks of the upper Río Chagres basin do not represent oceanic crust and the accretion of ocean floor (ophiolites). Rather, the link between undepleted intraplate tholeiites, rare OI-type basalts (OIB), and arc tholeiites in the RCB suggests a different origin. Lithologies suggest massive eruptions at rather deep subaerial conditions. Intrusive rocks attest a focused intrusion of large mafic accretion of ocean floor (ophiolites). Rather, the link between undepleted intraplate tholeiites, rare OIB basalts, and arc tholeiites in the RCB suggests a different origin. Lithologies suggest massive eruptions at rather deep submarine levels (>200 m), occasional emergence to shallow and even subaerial conditions. Intrusive rocks attest a focused intrusion of large mafic as well as geochemically-evolved magma chambers into the volcanic pile (for a schematic reconstruction see Fig. 5). The geochemistry of most rocks suggests melting from an undepleted (plume-type) mantle source. This is the typical setting for an intra plate oceanic plateau with high melting and eruption rates

The starting point in the evolution of the CRB basement thus was likely the accretion of such an oceanic plateau, probably derived from intra-plate (OIB-type) magmatism associated with initiation of the Galapagos hot spot (Hoernle *et al.,* 2002) during Upper Cretaceous time. This was followed by the onset (and further evolution) of an early tholeiitic island arc system near the Cretaceous-Tertiary boundary. This volcanic island arc was largely submerged below sea level. Further construction of the arc and closure of the Caribbean-Pacific seaway resulted from continued arc magmatism, deposition of volcaniclastic and marine sediments, and tectonic uplift and transform faulting over the past 20 My. The volcanic pile was thus severely

deformed and dismembered (Fig. 5). Volcanism ceased at about 8-6 Ma, and since then large compressive movements have all but stopped in the Canal Zone region and the nearby upper Río Chagres basin.

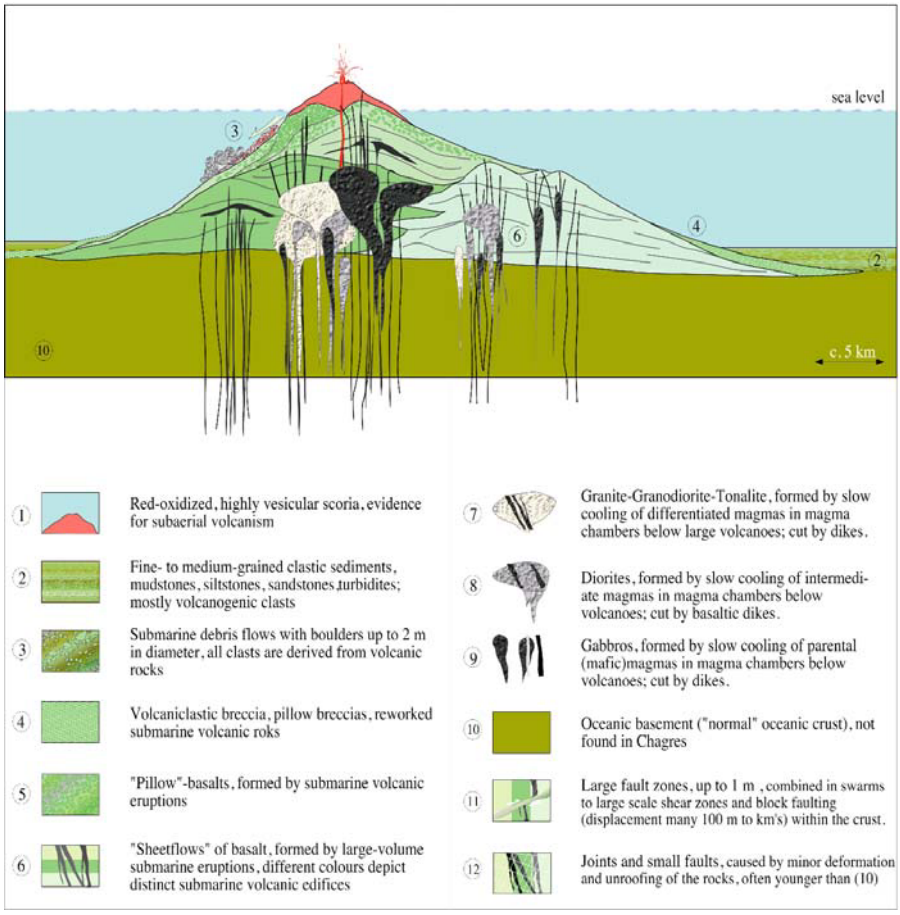

Figure 5a: Schematic representation of the volcanic and instrusive geological associations of the upper Río Chagres basin igneous complex 2:1 vertical exaggeration). This conceptual model is based on the lithological, geochemical, and structural observations discussed in the text.

4. SUMMARY & CONCLUSIONS

Exposed rocks of the upper Río Chagres basin comprise highly deformed basalts and basaltic andesites, gabbros, diorites, granodiorites, and granites. Intercalated volcaniclastic breccias and sandstones are also observed. Most rocks, in particular the volcanic and volcaniclastic sediments and granites,

are all strongly deformed and chemically altered. Mafic intrusive rocks are relatively fresh and form less-deformed domains surrounded by more deformed lithologies. Primary structures and contacts are generally obscured, either tectonically or by deep weathering. Consequently, the basement rocks have very distinct compositions and weathering characteristics.

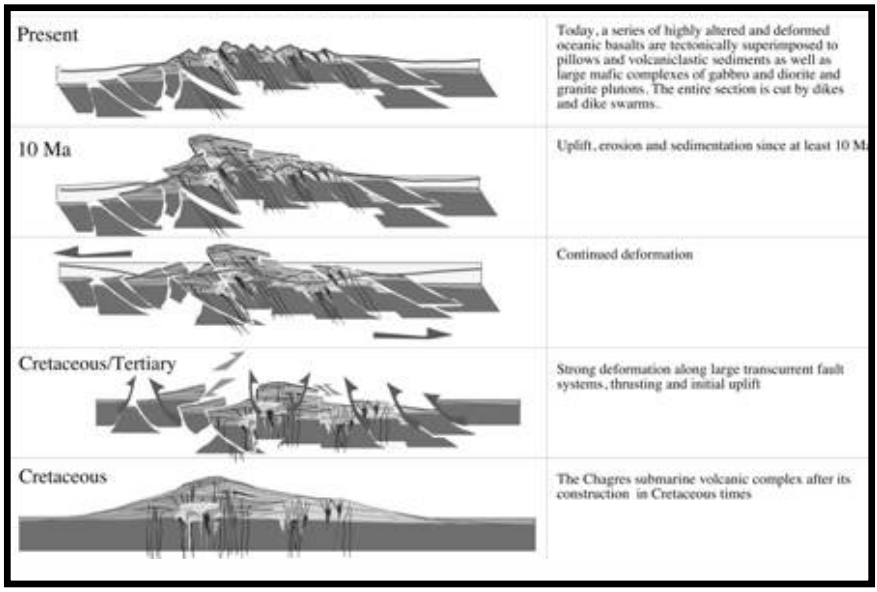

Figure 5b. Schematic illustration of the geological evolution of the original upper Río Chagres submarine volcanic complex of Figure 6a through deformation, sedimentary vcover, and erosion to produce the geology observed today in the upper Río Chagres basin (no vertical exaggeratrion).

The assemblage of lithologies observed within and immediately adjacent to the RCB is interpreted as package of (i) volcanic structures with submarine lava flows, (ii) dikes associated with breccias and sediments, and (iii) intrusive complexes of variable composition (magma chambers). Evidence for subaerial or shallow marine emplacement is lacking. The mafic complexes, followed by mafic dike swarms, are the most resistant to weathering and mechanical erosion. Fluvial erosion in these lithologies results in deeply cut gorges and narrow rapids. Granite lithologies are most easily weathered and produce straight and wide river courses during erosion. Massive altered basalts are intermediate in their style of weathering.

Geological correlation and geochemical compositions suggest that the mafic complex belongs to the series of Cretaceous to Early Tertiary mafic igneous suite, which characterize Central America from northern Costa Rica to the Colombian Andes. These mafic rocks have been accreted and incorporated into the Central American landbridge since Oligocene time. Geochemically, the igneous rocks belong to the tholeiitic series. Mobile elements (Cs, Ba, Rb, K, Sr) are highly variable. Immobile trace elements show a pattern intermediate between the typical depleted MORB patterns and enriched ocean island basalts (OIB). A trace element signature typical of a subduction zone setting is not supported by the data. These patterns and the lithological observations support the model of an origin from an oceanic plateau that was probably formed by the Galapagos plume.

ACKNOWLEDGEMENTS

We are grateful for helpful comments by an anonymous reviewer and compelled to acknowledge the skills of chief helicopter pilot Thomas Exenberger of Helipan, Inc. who facilitated much of our fieldwork by landings at almost impossible places, leaving both us, and the nearby waterfowl, deeply impressed. This work was funded by the Leibniz-Award of the DFG (German Science Foundation to GW) and an Army Research Laboratory Fellow award (to RSH).

REFERENCES

Alvarado, GE, Kussmaul, S, Chiesa, S, Gillot, PY, Appel, H, Wörner, G, and Rundle, C, 1993, Resumen crono-estratigrafico de las rocas igneas de Costa Rica basada en dataciones radometricas: J. South Am. Earth Sci., 6: 151-168.

Collins, LS, Coates, AG, Berggren, WA, Aubry, MP, and Zhang J, 1996, The Late Miocene Panama isthmian strait: Geology 24: 687-690.

DeBoer, JZ, Drummond, MS, Bordelon, MJ, Defant, MJ, Bellon, H, and Maury, RC, 1995, Cenozoic magmatic phases of the Costa Rican island arc (Cordillera de Talamanca), in *Geologic and Tectonic Development of the Carribean Plate Boundary in Southern Central America (*Mann P, ed.): Geol. Soc. Am. Spec. Paper 295: 35-55.

Escalante, G, 1990, The geology of southern Central America and western Colombia: in *The Geology of North America,* Vol. H, The Caribbean Region, (G Dengo and JE Case, eds.), Geol. Soc. Amer.: 201-230

Goossens, PJ, Rose, WI, Flores D, 1977, Geochemistry of tholeiites of the Basic Igneous Complex of northwestern South America, Geol. Soc. Am. Bull., 88: 1711-1720.

Gutscher, MA, Malavieille, J, Lallemand, S, Collot, JY, 1999, Tectonic segmentation of the North Andean margin: Impact of the Carnegie Ridge collision. Earth Planet. Sci. Lett. 168: 255-270.

Harmon, RS, 2005, The geological development of Panama: in: *The Río Chagres: A Multidisciplinary Perspective of a Tropical River Basin* (RS Harmon, ed.), Kluwer Acad./Plenum Pub., New York, NY: 45-62.

Hoernle, K, Bogaard, vdP, Werner, R, Lissinna, B, Hauff, V, Allvarado, G, and Garbe-Schönberg, D, 2002, Missing history (16-71 Ma) of the Galapagos hotspot: Implications for the tectonic and biological evolution of the Americas: Geology 30: 795-798.

Maury, RC, Defant, MJ, Bellon, H, deBoer, JZ, Stewart ,RW, and Cotten, J, 1995, Early Tertiary arc volcanics from Eastern Panama. in *Geologic and Tectonic Development of the Caribbean Plate Boundary in Southern Central America* (P Mann, ed.): Geol. Soc. Am. Spec. Paper 295: 29-34.

Meschede, M, and Barckhausen, U, 2001, The relationship of the Cocos and Carnegie ridges: age constraints from paleogeographic reconstructions: Int. J. Earth Sci. 90: 386-392.

Sun, SS, and McDonough, WF, 1989, Chemical and isotopic systematics of oceanic basalts: implications for mantle composition and processes, in: *Magmatsim in the Ocean Basins* (AD Saunders and MJ Norry, eds), Geol. Soc. London Spec. Publ. 42: 313-345.

Chapter 6

GIS-BASED STREAM NETWORK ANALYSIS FOR THE UPPER RÍO CHAGRES BASIN, PANAMA

David Kinner[1,2], Helena Mitasova[3], Robert Stallard[1], Russell S. Harmon[4], and Laura Toma[5]

[1]US Geological Survey, [2]University of Colorado, [3]North Carolina State University, [4]Army Research Office, [5]Duke University

Abstract: To support a number of projects focused on diverse biological and physical science aspects of the upper Río Chagres basin, a detailed stream network was extracted from digital elevation data obtained by interferometric radar survey. The elevation data represented the bald earth surface plus a forest canopy of varying height. Therefore, different algorithms for stream network extraction were qualitatively evaluated in terms of their capability to extract accurate stream locations from this challenging type of elevation data. The programs based on a shortest path algorithm and an imposed gradients constraint provided stream locations that were closer to on-ground GPS measurements than the tools based on depressions filling and iterative linking. The influence of different spatial resolutions on network structure and orientation was also explored.

Key words: Radar topography; DEM; stream network extraction; GIS

1. INTRODUCTION

The multidisciplinary study conducted in 2002 included investigators with a diverse set of interests and goals. The common objective of participants was to provide information about geology, hydrology, and ecosystems within the upper Río Chagres basin (Fig. 1). This region of the Panama Canal Watershed was mapped at a relatively coarse resolution until the mid 1990s. In the most-detailed map available, major stream channels were shown at a resolution 1:50,000, but little topographic information was included on the map. The relative inaccessibility of this mountainous

R. S. Harmon (ed.), The Río Chagres, Panama, 83-95.

tropical rain forest watershed and a persistent cloud cover over the basin's western edge have inhibited mapping of this region. A recent Interferometric Synthetic Aperture Radar Elevation (IFSARE) survey by the United States Army, LANDSAT imagery, and subsequent field investigations have provided new, more detailed information about the topography, land cover, and streams in the basin. To support continuing research, this paper describes existing and new geospatial data integrated within a common Geographic Information System (GIS) database. This integration creates a spatial framework for the field observation data obtained along the main channel of the upper Río Chagres during fieldwork in Feburary-March of 2002.

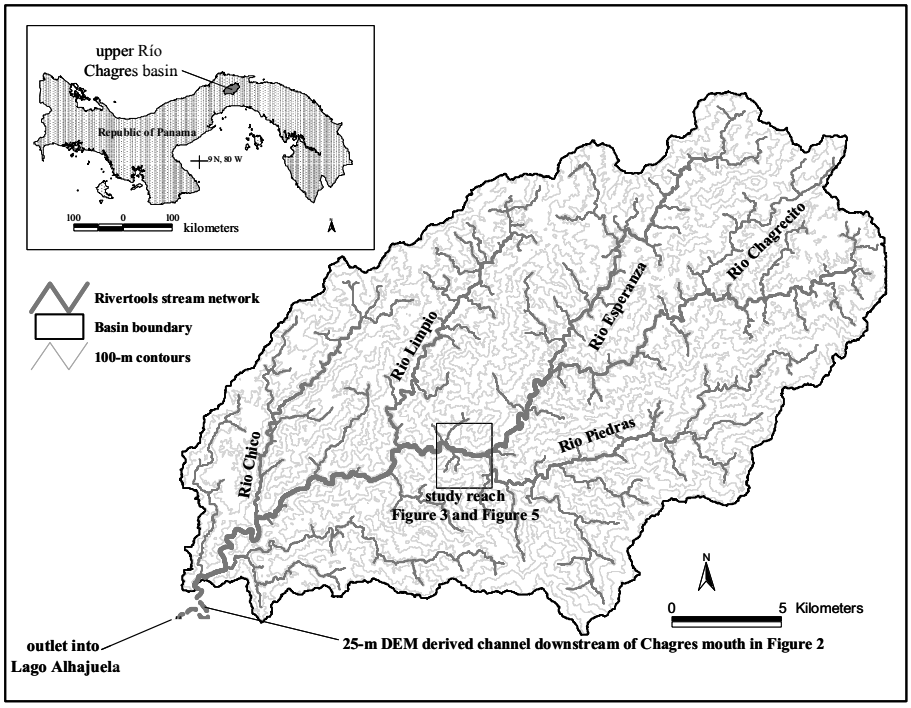

Figure 1. Map of the upper Río Chagres basin showing contours, rivers and the catchment boundary, all derived from an IFSARE DEM.

The GIS database provided an environment for deriving secondary map layers with valuable information both for fieldwork and modeling. One of the most important derived map layers for a hydro-geologic study is a watershed stream network. In a tropical forested landscape, it is usually impossible to map the locations of streams from satellite or aerial imagery,

particularly those of a lower-stream order. The only recourse is to apply terrain analysis algorithms to a Digital Elevation Model (DEM) to determine the channel network. Various approaches have been developed to perform this task, most of them designed for application to the bare ground 30-m USGS DEM product (see *e.g.,* O'Callahan and Mark, 1984; Peckham, 1998; Garbrecht and Martz, 1997; and Jenson and Domingue, 1988). However, IFSARE-based elevation models have different properties than the DEMs used for the development of the stream extraction tools. Therefore, it is necessary to evaluate different methods and identify the one most suitable for the data available and the type of terrain in a particular study area. Georeferenced stream and geology data were collected at selected sites along the upper Río Chagres and its tributaries, providing on-ground data for verification of the quality of the IFSARE data set and the extracted stream network and evaluation of flow routing algorithms. The modeled and observed data are qualitatively compared in this work.

2. STREAM NETWORK ANALYSIS

Generating river networks using digital-elevation data is a multi-step, interpretive process. The assumptions that resolve flow directions on DEMs will ultimately affect the locations of the derived-stream network. Properties like contributing area, length, and bifurcation ratios may be influenced by choice of stream delineation algorithm. Accuracy in stream network position is particularly critical in the case of the upper Río Chagres basin because there has not been extensive mapping of the river channels and the analysis output provides the 'best-available' map of the river network. Moreover, the elevation data - the 10 m resolution digital surface model (DSM) based on the IFSARE survey - represents the surface of the earth with vegetation rather than bare ground, posing additional challenges for stream extraction. Two systems with tools for watershed analysis were used to extract the stream network (i) *RiverTools v. 2.4* and (ii) *GRASS GIS*.

River Tools v. 2.4 (Rivix LLC, 2001) is a commercially-available terrain analysis system for analyzing DEM-derived river basin characteristics (the use of trade, product or firm names is for descriptive purposes only and does not imply endorsement by the US Government). It includes single and multiple flow direction (SFD, MFD) algorithms, visualization tools, and tools for extracting statistical properties of river networks (*i.e.,* bifurcation ratio, statistical similarity, *etc.*). *GRASS GIS* is an Open Source/Free software general purpose GIS; it includes a number of modules for basin analysis. We have used the SFD-based *r.watershed* and SFD/MFD-based

r.terraflow for massive DEMs. The Panama Canal Watershed DEM with approximately 11,000x11,000 pixels is an example of a 'massive' DEM. In general, the stream extraction algorithms compute the stream network by routing flow through the DEM and using a selected threshold of stream-order or contributing upslope area to determine which cells are stream cells.

2.1 Filling Sinks in IFSARE Data

The first step used by *RiverTools* and *r.terraflow* in determining the location of river networks is creating a depression-free landscape by removing sinks. Sinks are DEM pixels that have a lower elevation than all surrounding pixels. These sinks can be hydrologic features like lakes, natural depressions or sinkholes, or they could be artefacts of the DEM-construction process (Jenson and Domingue, 1988). For the upper Río Chagres basin DSM, an intermittent canopy overhanging stream channels may have generated at least some of the depressions. In some locations, the radar survey may measure the distance to the riverbed; in other locations the top of the canopy is measured. This discontinuity means that areas that have no cover may appear to be sinks and, for some algorithms, they have to be filled to the level of the surrounding cells in order to route flow through topography. In a radar-based DSM, this filling may be a source of additional error in the stream delineation process.

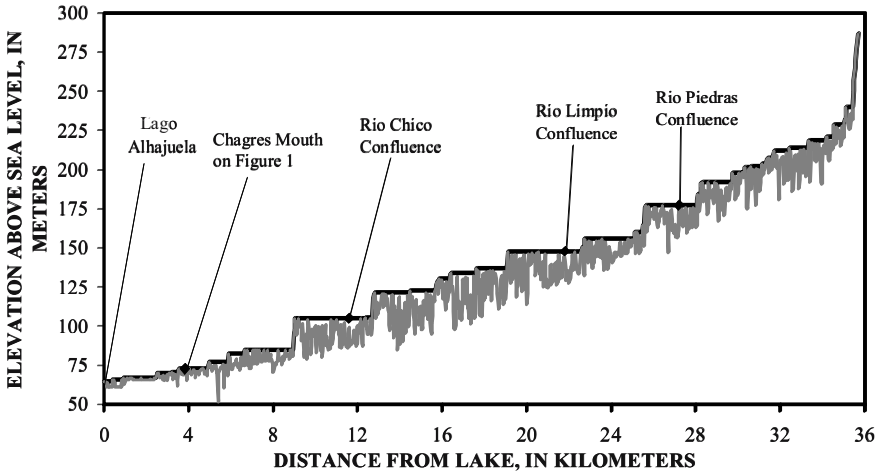

Figure 2. Comparison of filled topography (dark line) and IFSARE original topography (gray line) for a 35 km reach of the upper Río Chagres basin. The reach begins on the DEM at Lago Alhajuela at the shoreline on the land-cover map and traverses upstream.

Figure 2 shows a longitudinal profile comparison of the initial and *RiverTools* filled IFSARE DSMs at a 25 m grid cell resolution. As shown in the figure, the filling process creates a step-like stream profile, but the non-filled, DSM-based stream profile has many elevation spikes. Also, elevation errors are dampened on the upper Río Chagres near Lago Alhajuela (a distance of 0-4 km on the x-axis in Fig. 2). Land-use data indicates shrubs and grass along the channel through this reach, a feature confirmed by on-site inspection that would likely cause fewer elevation errors than an overhanging forest canopy. The average filling necessary to route water through the reach in Figure 2 is 8.37 m. To put this value in context, the average filling for 40 km long headwater reaches in the Nishnabotna River Basin in Iowa and for the Boulder Creek Watershed in Colorado are 0.48 m and 0.99 m respectively. These estimates were created using USGS 1:25,000, comparably scaled, 30 m resolution grid cell DEMs that were constructed from topographic maps. The combined effects of IFSARE radar and the forest canopy appear to significantly increase the number, depth, and spatial extent of sinks in the DSM.

It is necessary to make a cautionary note about the IFSARE-based DSM. Sinks may affect slope, curvature, and other terrain analysis calculations. It is necessary to average stream slope estimates over a large enough area to remove the effects of these discontinuities in elevation. Smoothing of topography also may be useful to better compute average gradients terrain characteristics.

2.2 Computing Flow Direction and Resolving Flats

A core step in stream network analysis is resolving the flow directions of water on the landscape for each cell in a DEM. Except for *r. terraflow* (see section 2.5 below), a single-direction flow algorithm (SFD) with eight possible directions of flow (D-8) was used (O'Callahan and Mark, 1984). For a given grid-cell, the center to center slope from that cell to an adjacent cell is calculated for all cells in an 8-cell neighborhood. 'Flow' proceeds in the direction of the cell with the greatest slope. Contributing areas for each pixel are determined recursively in a down gradient direction and represent the number of cells that 'flow' into a given cell.

Using the D-8 algorithm, flow direction is easy to compute in areas where slope is well defined. As the size of a river basin increases, channels become larger and the river gradient decreases. Areas where the gradient magnitude is zero are called 'flats', for which the flow direction is undefined. In DEMs represented with centimeter to millimeter vertical precision, areas with zero slope are rare (*e.g.,* in the currently used floating

point DEMs as opposed to older integer DEMs that had vertical precision of 1 m) and most flats are created by filling large, multi-pixel depressions like the ones shown in Figure 2. Several approaches have been developed to route flow through flats, of which only the 'iterative linking' and 'imposed gradients' methods are considered here.

Iterative linking (Jenson and Domingue, 1988) defines the flow direction for all of the cells in a flat. The method starts from the spill points of flat areas and iteratively assigns flow directions to the neighbours of the spill points. The program then proceeds to the neighbours of the neighbours, and continues recursively until all of the flow directions in a flat are defined. The final form of the network therefore depends heavily on the order that cells are defined (cells could be defined along a row for example) rather than any physically based criteria. There is no physical basis to iterative linking, but it resolves flow direction and can be numerically efficient. *RiverTools*, *r.watershed,* and *r.terraflow* all use iterative linking for flats. *R.watershed* does not fill sinks to create multi-pixel flat areas, but applies iterative linking only in areas that are flat on the original DEM.

The imposed gradients method is a second flat resolution approach described by Garbrecht and Martz (1997). In this method, artificial topography is created over flat areas by adding micrometer increments to the elevations of the flat. This addition is completed both longitudinally and laterally such that topography slopes downstream and from the sides of the flats towards the outlet. Of the software used here, imposed gradients has only been implemented in *RiverTools.*

Topography is not filled in the *r.watershed* program; rather flow is routed through sinks (Ehlschlaeger, 1989). The *r.watershed* flow direction algorithm is based on the A^T search algorithm for finding the 'least cost' path between an upstream cell and a downstream cell. The sum of the elevations along a given path represents the 'cost' of the path. The algorithm begins at the watershed outlet or any internal sinks, like a lake, and it begins working upslope (Ehschlaeger, 1989).

In the case of programs that fill sinks before determining flow directions like *RiverTools*, flow can only be routed to cells of a lower elevation. Because of this requirement, sinks must be filled so that the slope from any grid cell is at least zero. Negative slopes are not permitted along a flow path. In the A^T method, flow directions can proceed in the direction of negative slope. Because sinks are not removed from the dataset, more of the original information from the DEM is preserved in deriving final flow grid. This preservation may enhance the accuracy of flow paths in areas that are filled by other algorithms because some of the filled data could be close to the actual elevations of stream channels.

2.3 Algorithm Comparison

Figure 3 is a comparison of channels generated using *RiverTools* iterative linking and imposed gradient methods and the *GRASS r.watershed* program with GPS point locations of the upper Río Chagres channel for the section labeled 'study reach' in Figure 1. The vector representations of the stream network in the figure were created by converting the raster stream network to a vector format. All three methods seem to track the observed channel fairly well for most of the measured reach. However, both the imposed gradients and the shortest path methods seem to match the channel better than iterative linking. The difference suggests that, qualitatively, the combined use of filling sinks and iterative linking for a complex DSM, with spatially variable vegetation cover implemented in *RiverTools,* reduces the accuracy of stream extraction and was not fully robust. Several upper Río Chagres basin sub-watersheds were excluded from the river basin when the imposed gradients approach was used. This is probably because the topography constructed on the large flats becomes higher than the surrounding terrain and creates sinks in the already filled topography. The imposed gradients method was designed for USGS 1-m vertical scale DEMs and not the floating point, millimeter precision DEMs like the upper Río Chagres watershed DSM (Peckham, personal communication). However, this problem does not appear to affect the delineation of the main channel in Figure 3.

In this work, two different methods were used to differentiate grid cells that represent streams and those that are part of the surrounding landscape. After completing the flow direction step in *RiverTools*, the flow paths were used to compute Strahler stream order. This process starts at ridge cells and follows flowpaths down gradient. The flow paths that begin at ridges are considered first order streams; if two streams of the same order *n* converge, then Strahler ordering rules dictate that the stream below the convergence has a stream order of *n+1* (Strahler, 1957). This process continues in a downstream direction until all streams receive a Strahler order. *RiverTools* was used to prune the stream network by cutting all streams below a given Strahler order threshold, which for the 10-m DEM, was a third-order stream.

To differentiate between hillslope and channel cells in *r.watershed*, a threshold contributing area of 100 cells was used. To compare the impact of resolution on the level of detail and structure of the extracted stream network we performed the analysis at 10-m, 25-m, 50-m, 100-m and 200-m resolutions, so the selected threshold area increased with increased cell size, leading to effective generalization of the resulting network. The selection of the 100-unit threshold was arbitrary, based on cartographic rather than

physical criteria. This leads to fewer major streams being extracted at lower resolutions. The resulting series of stream networks extracted from DSM at 50-m, 100-m, and 200-m resolutions is in Figure 4.

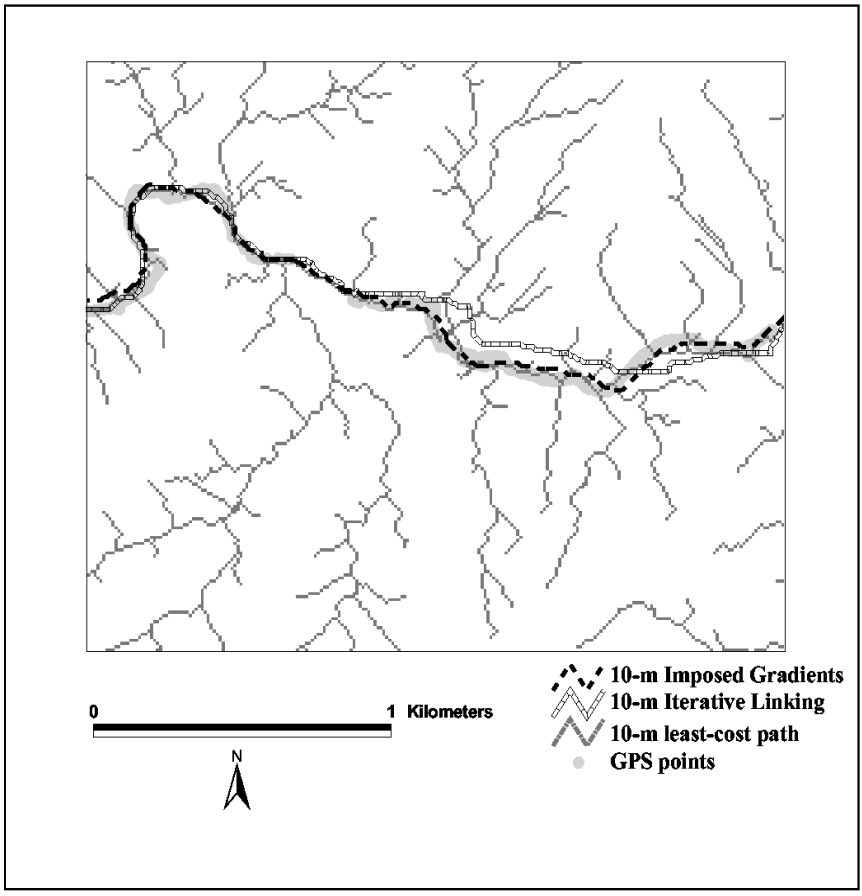

Figure 3. Comparison of observed GPS data (light gray symbols in background) and flow networks derived using the *GRASS r.watershed* shortest path approach (light gray).

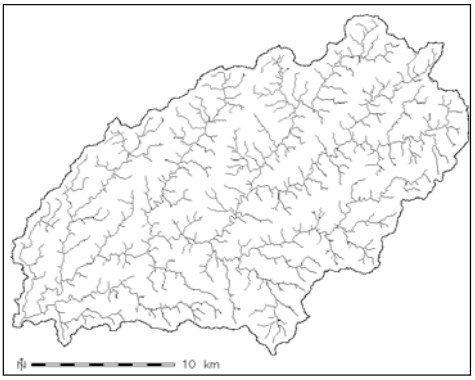

Figure 4a. Stream network derived using *r.watershed* and 50-m grid cells.

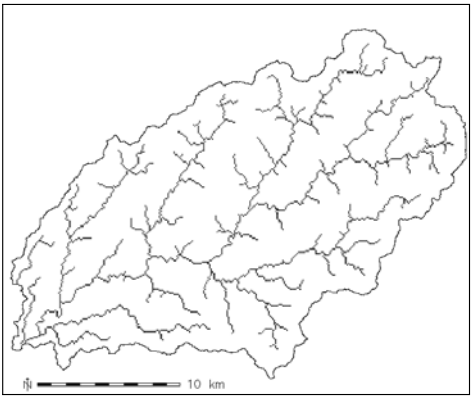

Figure 4b. Stream network derived using *r.watershed* and 100-m grid cells.

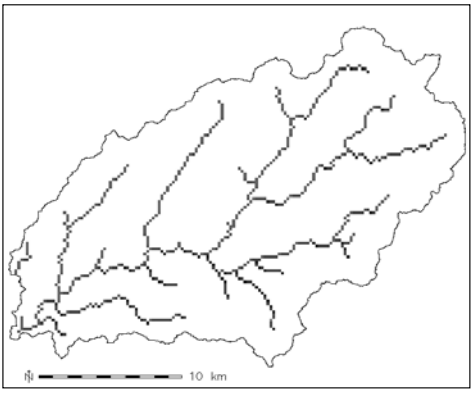

Figure 4c. Stream network derived using *r.watershed* and 200-m DEM.

2.4 Extracting the Stream Network

Extraction of stream networks at a series of decreasing resolutions shown in Figure 4 reveals the stream network geometry at different scales and levels of detail. The coarser-scale resolution highlights the difference between the northern half-basin with clearly parallel stream orientation and the southern half-basin with greater variability of stream orientation and lengths. It is unclear from this work what may control the fundamental differences in stream structure between the northern and southern halves of the river basin. However, the coarser data more readily resolve the underlying network structure.

The density and structure of stream network derived from the 10-m resolution DSM and 100 cells = 10,000 m^2 threshold by *r.watershed* was practically identical with the stream network extracted by *RiverTools* with the Strahler stream order 3 at the same resolution; the most significant differences were in the areas with large filled sinks. New field data will allow us to set the threshold more accurately and to determine whether contributing area, stream order or curvature provides the best method to determine where channels begin.

2.5 Computing the Stream Network for the Upper Río Chagres Basin and the Panama Canal Watershed

As is apparent from the multi-algorithmic comparison, the program *r.watershed* works fast and produces reasonable matches to observed data when applied to small datasets. However, this algorithm is not efficient on larger datasets. For example, the computation of the stream network for the upper Río Chagres basin at 10-m resolution (3200x3600 pixels) took 12 hours. Computation of the stream network for all of the Panama Canal Watershed (~11,000X11000 pixels) is not readily feasible using *r.watershed.*

The inefficiency is likely due to the *r.watershed* design assumption that data are small enough to fit in the internal memory of the computer. If datasets are large, they do not meet this requirement and reside on disk instead. Because program execution using external disks is much slower than when using the computer main memory, the bottleneck during analysis of large datasets is typically the movement of information between main memory and disk rather than the CPU computation time.

The *r.terraflow* module was recently implemented in GRASS GIS for computing flow direction and flow accumulation. It was designed and optimized for massive digital elevation datasets and was tested here as an efficient alternative to *r.watershed.* The *r.terraflow* design uses the standard

ideas for computing flow direction and flow accumulation described above, but encodes them using scalable Input/Output (I/O)-efficient algorithms. As a result, *r.terraflow* is scalable to very large datasets. For instance, it computes flow direction and flow accumulation for the entire Panama Canal Watershed dataset in approximately 3 hours.

The module *r.terraflow* can compute both SFD and MFD flow routing. It can also use a combination of the two by switching to SFD, if contributing area exceeds a user-defined threshold. In flat areas, *r.terraflow* uses the iterative linking process proposed by Jenson and Domingue (1988) that was incorporated into *RiverTools*. In depressions, *r.terraflow* routes flow by computing the lowest-height path from each cell outside the terrain. It can be formally shown (Arge *et. al*., in press) that computing lowest-height paths for all cells in the terrain can be done using a bottom-up plane sweep of the terrain which simulates the process of flooding the terrain (or rather of uniformly raising a water table).

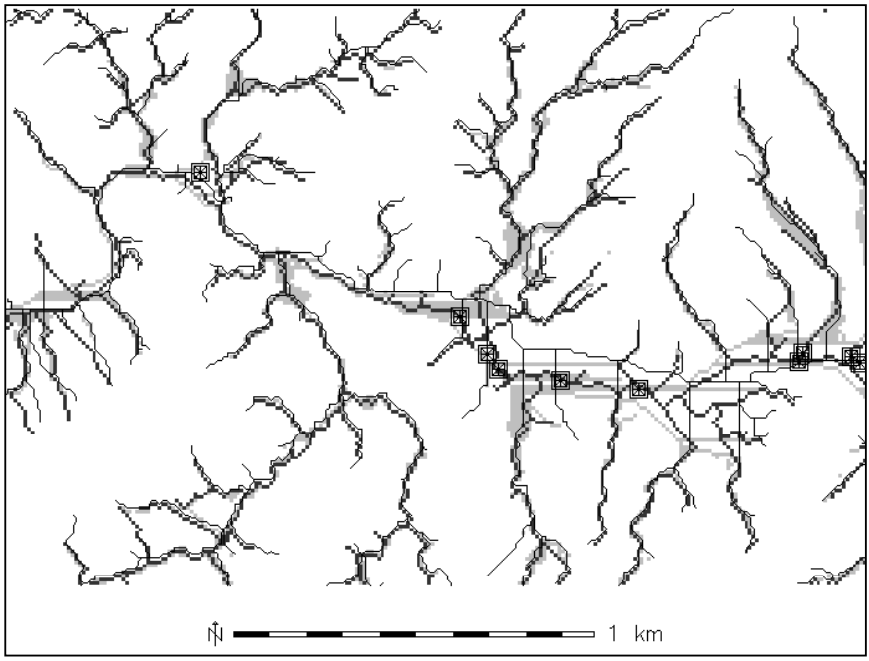

Figure 5. Comparison of stream channel output from *r.terraflow* (light gray), *r.watershed* (dark gray), river tools with sink filling (black line) and observed data (square symbols) for a 2km segment of the Chagres river. The streams were extracted from 10-m resolution DSM.

A detailed analysis of the accuracy of *r.terraflow* is under investigation. Figure 5 indicates that for some parts of the DSM, *r.terraflow* is remarkably similar to the other algorithms. Because it uses iterative linking, it has many of the same issues with flats, including the parallel flow paths indicated in Figure 5. Additionally, *r.terraflow* often diverges from the more accurate *r.watershed*-generated stream channels. The stream networks produced by extracting cells with flow accumulation larger than 100 cells look different for MFD and SFD flow routing. With either method the stream network contains big wet areas in the flat parts of the terrain. The *r.terraflow* output is therefore more suitable for identifying areas susceptible to floods, than to narrowly delineating the stream network. Further work is necessary to incorporate into *r.terraflow* a procedure for refining the stream network.

3. CONCLUSIONS

For most of the portions upper Río Chagres basin examined in this study, all algorithms tested produced a realistic stream network in locations that were identical or very close to the observed streams. The results were surprisingly accurate given the fact that the flow was traced on top of vegetation cover that was several tens of meters high throughout most of the basin, rather than on the bare ground. The most significant artefacts, in the form of long straight stretches of stream channels located tens of meters away from the observed stream locations, were produced by the tools that fill in the depressions caused by gaps in tree cover creating large artificial flats and then use iterative linking to overcome these flats. The algorithms that use the shortest path or imposed gradients generated more accurate results for these areas.

The software tools tested also differed in computational efficiency. While *r.watershed* provided the most accurate results it was slower than *r.terraflow.* The computed the stream network for the upper Río Chagres basin at 10-m resolution was computed almost ten times faster using *r.terraflow* than *r.watershed.* Furthermore, *r.terraflow* extracted the stream network from the DSM for the entire Panama Canal Watershed in 3 hours where the other *r.watershed* had not completed this task after running a full day. The efficiency of algorithms in *RiverTools* have not been systematically compared to the *GRASS GIS* algorithms *r.watershed* and *r.terraflow*; this comparison remains the subject of future work.

Identification of stream origin and first order stream location remains an open research question due to the fact that it is a dynamic phenomenon. Therefore, the resulting 10-m resolution stream network based on 10,000 m^2

upslope area threshold (or third order Strahler threshold) should be interpreted as a map of all potential streams, rather than actual streams. Field data are needed for sound selection of thresholds defining the stream origin instead of using the arbitrary threshold methods reported in this work.

ACKNOWLEDGEMENTS

We would like to acknowledge the generous funding of this research by the US Geological Survey, National Research Council, and US Army Research Office. The Panama Canal Monitoring Project provided land use data that helped in analysis. We would also like to thank J. Syvitski and S.Peckham for providing computer and other resources that aided in completion of the *RiverTools* work. D. Mixon, S. Murphy and D. Lashlee provided helpful reviews of this manuscript. S. Howe and E. Wohl kindly provided their field survey data.

REFERENCES

Arge, L, Chase, J, Halpin, P, Toma, L, Urban, D, Vitter, J, Wickremesinghe, R, 2005, Flow computation on massive grid terrains: Geoinformatica, in press.

Ehlschlaeger, CR, 1989, Using the AT search algorithm to develop hydrologic models from digital elevation data: Proc. Int. Geogr. Inf. Sys. (IGIS) Symp., Baltimore, MD, 275-281.

Garbrecht, J and Martz, LW, 1997, The assignment of drainage directions over flat surfaces in raster digital elevation models: Jour. Hydrol., 193: 204-213.

Jenson, SK and Domingue, JO, 1988, Extracting topographic structure from digital elevation data for geographic-information system analysis: Photogram. Eng. Remote Sens., 54: 1593-1600.

O'Callahan, J and Mark, D, 1984, The extraction of drainage networks from digital elevation data: Comput. Vision Graph. Image Proc., 28: 323-344.

Peckham, SD, 1998, Efficient Extraction of River Networks and Hydrologic Measurements from Digital Elevation Data: in *Stochastic Methods in Hydrology: Rain, Landforms and Floods* (EO Barndorff-Nielsen, ed.), World Scientific, Singapore: 173-203

Rivix Limited Liability Company, 2001, RiverTools™ - User's Guide, release 2001: Research Systems, Inc., Boulder, CO.

Strahler, AN, 1957, Quantitative analysis of watershed geomorphology: EOS, Trans. Am. Geophys. Union, 38: 913-920.

Chapter 7

SOILS OF THE UPPER RÍO CHAGRES BASIN, PANAMA

Soil Character and Variability in Two First Order Drainages

J. Bruce J. Harrison[1], Jan M.H. Hendrickx[1], David Vega[2], Lucas E. Calvo-Gobbetti[2]

[1]New Mexico Institute of Technology, [2]Universidad Tecnológica de Panama

Abstract: Understanding the relationship between rainfall, and stream flow in mountain terrain requires the quantifying of rates of water movement into and through regolith covered hillslopes. General theory holds that infiltration rates in humid tropical are higher than rainfall intensities so surface runoff is minimal. However, soil profile characteristics can vary significantly on a hilslope, with concomitant changes in soil hydrologic characteristics. The pattern of soils within two small first order drainages was evaluated within the upper Río Chagres basin. Two main influences on soil distribution were identified. Mass movements primarily translational sliding and treefall result in stripping of the upper soil horizons and exposure of weathered saprolite. Soils forming in the deposits are characterized by higher infiltration rates and a more uneven surface topography than the stable soils. A catenary relationship was also observed with stable, oxidizing soil profiles in upper slope positions and reduced (gleyed) soils at the outlet of the drainage basin.

Key words: Panama; Río Chagres; tropical soil catenas; saprolite; mass movements

1. INTRODUCTION

A fundamental question when studying streamflow in tropical and humid environments is the role that hillslope characteristics play in determining streamflows. The hydrologic properties of soils developed in the unconsolidated regolith in first order drainage basins can have a major influence on how rainfall is translated into steamflow. If the infiltration rate of the soil is low, then surface runoff becomes a major factor in streamflow response to rainfall (Ridolfi *et al.,* 2003). By contrast, if the infiltration rate on steep hillslopes is high, then subsurface flows will be an important component of streamflow (Montgomery and Dietrich, 2002). Within the soil

R. S. Harmon (ed.), The Río Chagres, Panama, 97-112.

profile, the depth to bedrock or a less permeable layer and the soil porosity become important factors influencing water movement through the regolith and into the stream channel.

Detailed measurements of soil hydrologic properties are time consuming and only represent a point estimate of hydrologic properties of the soil. The hydrologic properties of a hillslope result from an integration of the hydrologic properties of the different soil units on the hillslope. Thus, it is important to characterize the range of hydrologic properties on a hillslope and to determine the proportion of the drainage basin hillslope characterized by the individual soil units. Measured infiltration rates on hillslopes in the Luquillo Mountains of Puerto Rico ranged from 0-106 mm/hr (Harden and Scruggs, 2003), which largely exceeded the rainfall rates in this area. However, no estimate was made of the proportion of the hillslope characterized by each infiltration measurement. Determining the spatial variation of soils on a forested hillslope is also a time consuming and difficult process. There are logistical constraints to developing a statistically significant, randomly sampled, data set of soil hydrologic properties within a drainage basin. One approach to determining variability of soil properties is to identify the major controls on the spatial variability within the drainage basin. From this starting point, it is possible to locate soil sampling sites in a pattern which will encompass the major range of soil profile characteristics.

Hillslopes can be broadly classified as stable or unstable systems. Unstable hillslopes occur in geomorphically active drainage basins, where patterns of erosion and deposition are reflected in the distribution of eroded and buried soil profiles. The pattern of soil variability is determined by pattern of erosion and deposition and the degree of soil development is determined by the age of the land surface. This has been described as temporal soil variability (Tonkin, 1993).

On stable hillslopes, topography produces systematic changes in soil profile characteristics with the two main influences being slope orientation and the position of a soil profile within the drainage basin. Slope orientation results in differences in solar radiation and/or exposure to eolian or atmospheric deposits of dust or salts. (Birkeland, 1999). On stable hillslopes, throughflow in the regolith produces systematic changes in soil properties in the direction of water movement. Usually, soils in upper slope positions are more leached than soils in lower slope positions because they are not receiving any replenishment from upslope soils. However, while major differences in soil morphology can be determined, the boundaries between the different soils are usually gradual (Young, 1988). This pattern of soil variability has been described as a soil catena. (Milne, 1935; Birkeland, 1999). Thus, the pattern of soil distribution is different according to whether the drainage basin is stable or unstable. The goal of the soil studies in the

upper Río Chagres drainage basin described here was to determine the controls on soil variability and to identify the range and spatial extent of soil profiles present.

2. TROPICAL SOILS

The distinct features of tropical soils are a reflection of the moist warm climate typical of tropical regions of the world. This climate promotes strong weathering resulting in the formation of deeply weathered bedrock or unconsolidated regolith termed saprolite. The strong weathering environment results in a soil with a high clay content, with the common mineralogy being kaolinitic, and enriched in the more residual elements such as Fe, Si, and Al. Organic matter levels are usually low, often only a thin organic layer is found at the soil surface and low (<4%) organic carbon is found within the soil profile. These soils usually are classified within the Oxisol and Ultisol orders of the USDA soil taxonomy (USDA, 1994).

3. METHODS

The upper Río Chagres watershed is a strongly dissected, densely forested landscape with most hillslopes bearing first and second order streams. Two small first order drainages were chosen for detailed soil studies, one developed on a granitic lithology in the upper portion of the Río Chagrictio drainage and the other in altered rhyolite in the upper reaches of the Río Piedras drainage (see Fig. 1 of the Preface for the site locations).

Soil pits were described down the axis of the drainage, from the intersection of the drainage basin with a main ridge, down to where a perennial stream issued from the regolith. Pits were hand dug into the underlying saproloite to a depth of at least 50 cms. Soils were described following the standard procedures (USDA, 1993). Samples were taken from every pedogenic horizon and, where the horizon was greater than 20 cm thick, sampled at 20 cm intervals. Subsequently, each soil sample was analyzed in the laboratory. Particle size was determined using the pipette method and bulk density by the paraffin clod method (Singer and Janitzky, 1986). The clay mineralogy was determined for selected samples, which covered the range of weathering observed in the field. Infiltration studies were carried out at different depths for each of the soils described here by Hendrickx *et al.,* (2005, this volume).

4. OBSERVATIONS AND RESULTS

The drainage basins have similar morphologies; both are small, narrow, and steep. The Río Chagrecito basin has a 2 m scarp at the head of the basin, where it connects to the dissected ridge. Saprolite is exposed at the base of the scarp. The upper Río Piedras drainage lacks a scarp at the head of the basin. However, the soil at this point in the drainage is shallow and weakly developed. Both drainages have irregular downslope topographic profiles, with up to 2 m of relief developed through mass movements. The mass movement erosion scars expose saprolite, indicating that the failure plane occurs at the soil/saprolite boundary. Erosion scars are widespread along the upper slopes of the drainage. but almost totally lacking in the lower part of the drainage**.** Trees are rafted in an upright position downslope with mass movements so that it is often difficult to identify areas of mass movement. Large cracks at the soil surface in both drainages appear to be tension cracks related to the mass movements.

Treefall is a common feature in both drainages, but occurs more frequently on the ridge crests into which the drainages are developing. This process produces a pit and mound topography, which can create a preferred pathway for water to enter a soil (Schaetzl *et al.,* 1990).

4.1 The Río Chagrecito Study Site

The first order drainage basin studied along the middle reaches of the Río Chagrecito is at an elevation of 1391 m. It is 150 m from ridge crest to the point of free flowing water, and approximately 50 m wide. The drainage is developed in deeply weathered granitic bedrock. Slope angles range from 55^{o} at the head of the basin to 20^{o} at the toe of the slope. Soils from three sites were described down the axis of this first order drainage basin. The relative thickness and horizonation of each soil profile are shown in Figure 1 and compositional characteristics of the three soils examined are listed in Tables 1 and 2.

The Chagrecito-1 soil is from the edge of an erosion scarp near the ridge crest. This soil is strongly developed and overlies deeply weathered bedrock or saprolite (Fig. 2a). It has a thin A horizon and several B horizons of clay and iron accumulations that grade into saprolite at 3 m depth. A large pipe, probably an old root channel, at 30 cm depth is lined with dark humus and clay coatings. The soil has a coarse angular blocky structure in the upper part of the profile, with large soil ped faces coated with humus and clay. This soil is very fine textured, containing less than 10 % sand and having high silt and clay contents. There is a marked change in the texture at the soil/saprolite

contact where the sand and clay contents decrease and the silt content of the profile increases significantly (Table 2).

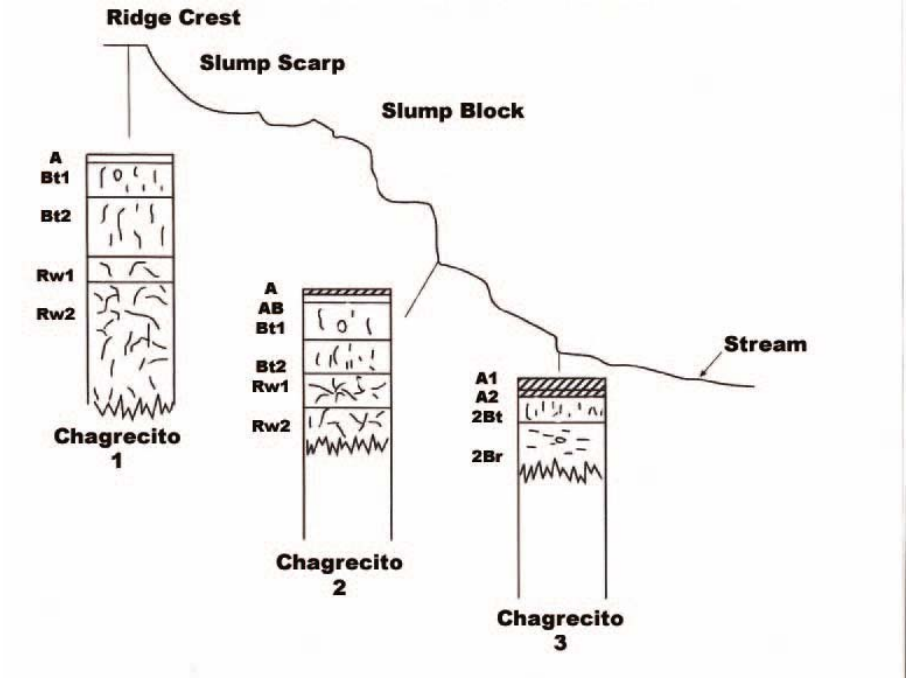

Figure 1. Diagrammatic representation of the Río Chagrecito soil profile locations.

The Chagrecito-2 soil (Fig.2b) is from a midslope in an area of uneven surface topography. It has a similar A horizon to the Chagrecito-1 soil, but the B horizons are not as strongly developed. This soil contains more weathered clasts and has less red coloring than the Chagrecito-1 soil. A coarse blocky structure occurs in the top 60 cm, with humic and clay coatings on ped faces. The sand content of this profile is higher and the clay content a little lower than in the Chagrecito-1 soil (Table 2).

The Chagrecito-3 soil is developed at the base of the hillslope. It has a very weakly-developed A horizon and contains gravely B horizons. The presence of gleyed colours and iron oxide concretions indicates that a reduced soil environment exists for periods of time during the year (Fig 2c). As this soil was being described, water was flowing from pores and old root channels (Fig 2d). This soil has the highest sand content and a lower silt content than the other soils in this drainage (Table 1).

Table 1. Morphological description of Chagrecito site soils.

Soil	Slope Position	Horizon	Color (moist)	Depth (cm)	Texture	Structure	Consistency (dry)
CH-1	crest						
		litter		5-0			
		A		0-5	SiCl	3mcr	h
		AB		5-10	Cl	3lsbk	h
		B1		10-50	Cl	3msbk	h
		B2		50-120	Cl	M	vh
		Rw		120-150	SiCl	M	h
		Rw2		150-300	SiL	M	sh
CH-2	back	litter		5-0			
	slope	A	7.5YR3/3	0-5	SiClL	3msbk-3Lcr	sh
		AB	7.5YR4/6	5-15	Cl	3msbk-3Lcr	h
		B1	5YR4/6	15-60	Cl	3msbk-3Lcr	h
		B2	5YR5/6	60-100	Cl	3msbk-3Lcr	
		Rw1	2.5YR4/8	100-140		M	
		Rw2	10YR5/6	140-280+		M	
CH-3	foot	Litter		5-0			
	slope	A1	10YR4/4	0-10	Cl	3msbk	h
		A2	10YR4/3	10-20	grSCl	2msbk	sh
		2B1	2.5YR6/1	20-50	Cl	3msbk	h
		2B2	5BG4/6	50-100+	Cl	3msbk	h

Soil	Slope Position	Consistency (moist)	Roots	Pores	Comments
CH-1	crest				
		ss,sp	3vf,f,m,l	2l	pores 5-6 cm diam
		s,p	2vf2f2m1l		large cracks
		s,p	1vf1f2m		large cracks
		s,p	1vf1f1m1l		large root burrows
					transition to
		s,sp	1f1m		saprolite
		nsnp	1vf1f		
CH-2	back				
	slope	ss,sp	3vf3f3m	3f2m	animal burrows,
		s,p	1vf2f2m	cracks+2L	35%wk-st w'd clasts
		s,p	1vf2f1m	cracks 1m	10%wk w'd rocks
		s,p	1f1m	10-0.5cm pores	
					strongly weathered
					bedrock (saprolite)
					strongly weathered
					bedrock, more
					homogeneous
					color than above)
CH-3	foot				
	slope	s,p	1vf2f	large cracks	
		s,p	2vf2f1m	3m	
		s,p	2f2m1l	5cm pipe, cracks	
					strongly gleyed,
		s,p	2f2m1l	pipes and cracks	mottled

Figure 2a. Chagricito-1 soil.

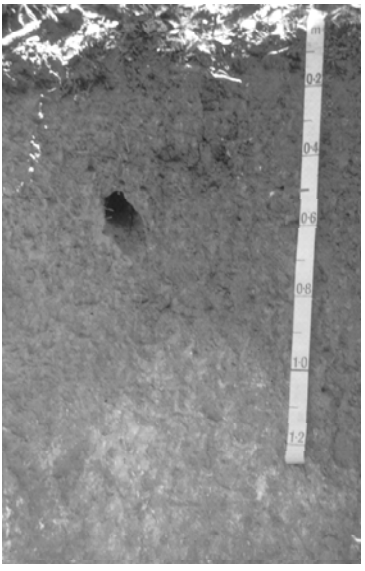

Figure -2b. Chagricito-2 soil.

Figure 2c. Chagricito-1 soil.

Figure 2d. Water flowing from former root channel in Chagrecito-3 soil.

Table 2. Particle size and bulk density data for the Chagrecito site soils.

Soil	Slope Position	Horizon	Bulk Density (g/cm^3)	Sand %	Silt %	Clay %
CH-1	crest	Litter				
		A	1.2	9.1	67.9	23
		AB	1.3	7.8	54	38.2
		B1	1.36	5.9	53.6	40.4
		B1	1.4	6.1	57.8	36
		B2	1.38	6.4	59.7	33.8
		B2	1.45	6.7	44.4	48.8
		B2	1.45	4.7	52	43.4
		RW1	1.47	6	61	32.9
		RW1	1.4	8.9	87.6	3.5
		RW2	1.3	9.2	68.9	22
		RW2	1.25	9.2	72.8	22
		litter				
CH-2	backslope	A	1.21	16.7	67.9	15.4
		AB	1.27	15.4	63.2	21.4
		B1	1.38	16.9	65.1	18
		B2	1.5	14.5	72.4	13
		Rw1	1.38	11.1	71.8	17.1
		Rw2	1.2	15	70.8	14.2
CH-3	footslope	Litter		25.6	67	8
		A1		42.3	40.9	17
		A2		48.2	35.1	16.7
		2B1		9.2	68.8	22
		2B2		14.6	69.7	15.7

4.2 Upper Río Piedras Drainage

The first order basin examined in the upper Río Piedras drainage is similar to the upper Río Chagrecito study area in size and slope angle. The drainage basin is developed off a major ridge, but lacks the steep head scarp found in the Chagrecito drainage. Four soils were described down the axis of this drainage basin. The relative thickness and horizonation of each soil profile are shown in Figure 3 and the morphological and compositional characteristics of the four soils examined are listed in Tables 3 and 4.

The Piedras-1 soil is described in a ridge crest position. It is a shallow soil developed over strongly fractured and weathered granite bedrock. The weathering is located primarily along joints and fractures. A weak A horizon overlies a transitional AB horizon which grades to a strong clay rich Bt horizon extending into the fractures. The bedrock fractures in the upper 40 cm of the profile are tilted in a downslope direction suggesting gradual creep

downslope. The sand content of this soil is similar to that of the lowest soil in the Chagrecito drainage (Table 4).

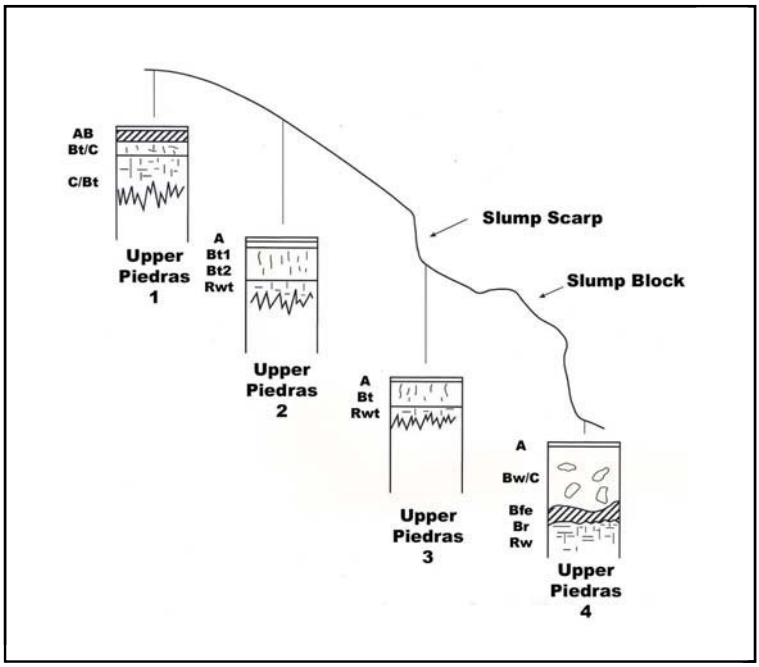

Figure 3. Diagrammatic representation of the Río Piedras soil profile locations

The Piedras-2 soil was from the steep backslope. It is the deepest soil of the four sampled in this drainage basin. Large fractures are found at the surface, which is covered in litter. This soil has a well developed A horizon and thick clay rich B horizons which overlie strongly weathered granite bedrock. A large root channel in the Bt horizon has clay and organic matter coatings suggesting that this is a conduit for water movement through the soil. The sand content of this soil is the highest of any soil in this drainage with equal amounts of silt and clay.

The Piedras-3 soil pit is located on the edge of a head scarp (45^{o}) of a landslide. The soil has a thin weakly developed A horizon overlying 37 cm of yellow Bt on strongly weathered granite bedrock. Large fractures and joints in the bedrock are filled with clay and organic matter. The sand silt and clay contents are similar to that of the Piedras-1 soil.

The Piedras-4 soil is from a site at the base of the small drainage and consists of a large slump block. There is evidence of mixing of soil and unweathered regolith with weakly weathered and unweathered clasts

juxtaposed. The soil regolith is loosely packed with numerous large pores and cracks with clay and organic matter staining along the edges. Parts of the soil profile have developed under reducing conditions, indicated by gley coloring and the formation of a weakly developed iron pan at the base of the reduced zone. This soil has a fine texture with 40 % sand, and equal amounts of silt and clay.

Table 3. Morphological description of the Piedras drainage soils.

Soil	Slope Position	Horizon	Color (moist)	Depth (cm)	Texture	Structure	Consistency (dry)
PD1	crest	litter		5-0			
		A1	10YR3/4	0-5	SiCl	3fcr	sh
		AB	10YR4/6	5-20	Cl	3msbk-3mcr	sh
		Bt/C	10YR5/8	20-40	Cl	M/3msbk	h
		C/Bt	10YR5/8	40-90	Cl	M/3msbk	h
PD-2	backslope	litter		5-0			
	(upper)	A	10YR3/6	0-5	Sil	3mcr	sh
		Bt	10YR6/6	5-15	Cl	3msbk	sh
		Bt2	7.5YR6/4	15-60	Cl	3lsbk	sh
		Ct	7.5YR5/8	60-80+	SiCL	M	sh
PD-3	backslope	litter		3-0			
	(middle)	A	10YR4/4	0-3	SiCL	3mcr	sh
		Bt1	10YR5/8	3-40	Cl	3msbk	sh
		Coxt		40-60	strongly weathered bedrock, fractures filled with clay, decrease with depth.		
PD-4	backslope	A	10YR4/3	0-3	SiCl	3fcr	s
	(lower)	Bw/C	10YR4/6	3-100	Cl	3msbk	s
		Bfe	thin 3 cm iron pan at boundary with underlying gleyed horizon				
		Br	5BG4/7	103-120	Cl	M	NA
PD-5	terrace	A	10YR3/3	0-15	SiL	3mcr	sh
	25m	Bw/A	10YR4/6	15-27	SSiL	3msbk	sh
	above	2Ab	10YR3/6	27-45	SiCL	3msbk	sh
	river	2Btb	10YR5/6	45-80	CL	3msbk	sh
		2Coxrb	10YR6/4	80-120	SiCL	M	NA

The Piedras-3 soil pit is located on the edge of a head scarp (45^{o}) of a landslide. The soil has a thin weakly developed A horizon overlying 37 cm of yellow Bt on strongly weathered granite bedrock. Large fractures and joints in the bedrock are filled with clay and organic matter. The sand silt and clay contents are similar to that of the Piedras-1 soil.

The Piedras-4 soil is from a site at the base of the small drainage and consists of a large slump block. There is evidence of mixing of soil and unweathered regolith with weakly weathered and unweathered clasts juxtaposed. The soil regolith is loosely packed with numerous large pores

and cracks with clay and organic matter staining along the edges. Parts of the soil profile have developed under reducing conditions, indicated by gley coloring and the formation of a weakly developed iron pan at the base of the reduced zone. This soil has a fine texture with 40 % sand, and equal amounts of silt and clay.

Table 3. (cont.). Morphological description of the Piedras drainage soils.

Soil	Slope Position	Consistency (moist)	Roots	Pores	Comments
PD1	crest	ss,sp	2vf2f1m1l	3f large inter-granular spaces	
		ss,p	2vf3f2m1l	2f2m plus inter-granular spaces	
		s,p	1f1m	1m1l plus 4cm pipe	
		s,p	1f1m1l	1m root channel	
PD-2	backslope	so,sp	2vf2f2m	2vf2f	abundant worm burrowing
	(upper)	s,p	1vf1f1m1l	1f1m1l	3cm root channels
		s,p	1f1m1l	1vf1l	cracks from surface
		s,p	1m	1m	
PD-3	backslope	ss,sp	3vf3f2m1l	abundant inter-granular spaces	large factures with clay fims
	(middle)	s,p	1f2m2l	4 5-6 cm pipes	large fractures with clay Plus OM cutans
		ss,sp	2f1m1l	2f2m2l	several large pipes 4-5 cm diameter
PD-4	backslope	s,p	1f1m	2f2m2l	disturbed soil mass
	(lower)	s,p	2f2m	2m	
		so,po	2vf2f2m1l	2f	
PD-5	terrace	ss,sp	1vf2f1m1l	2vf2f	charcoal fragments
	25m	ss,sp	1vf1f1m	1vf1f	
	above	s,p	1f1m	1f1m	
	river	ss,sp	1m	1f	mottled plus concretions 2.5YR4/6

4.3 Clay Mineralogy

Six soil horizons were analysed to determine the dominant clay mineralogy of these soils. Three samples were from the Chagrecito-1 soil, the A, B1 and Cw horizons. All samples had the same dominant clay mineral, kaolinite or halloysite, the non-expanding halloysite. Three samples were taken from the Piedras-2 soil, A, B, and Cw horizons. These soils showed some variability in clay mineralogy but all were dominantly

halloysite. The lowest horizon contained trace amounts of illite, smectite and interlayered illite/smectite.

Table 4. Particle size and bulk density data for the Chagrecito site soils.

Soil	Slope Position	Horizon	Bulk Density (g/cm3)	Sand %	Silt %	Clay %
Piedras-1	crest	litter				
		A1	1.2	45.4	28.5	26.1
		AB	1.42	45.4	24.6	29.8
		Bt/C	1.5	38.5	21.1	40.4
		C/Bt	1.42	41.1	23	35.8
Piedras-2	backslope	litter	1.33	66.1	24.3	9.5
	(upper)	A	1.37	55.1	21.9	22.9
		Bt	1.5	33.3	26.1	40.6
		Bt2	1.48	24.1	35.9	39.9
		Ct	1.46	49.8	32.1	18.1
Piedras-3	backslope	litter				
	(middle)	A	1.22	43.9	33.1	23
		Bt1	1.7	44.4	24.9	30.8
		Bt1	1.3	37	42.8	20.2
		Coxt	1.3	53.8	37.3	9
Piedras-4	backslope	A	2.05	43.9	33.1	23
	(lower)	Bw/C	1.37	44.4	24.9	30.8
		Bfe	N/A	N/A		
		Br	1.4	37	42.8	20.2
Piedras-5	Terrace	A		50.3	27.4	22.3
	25m above	Bw/A		55.7	22.2	22.1
	river	2Ab		50.8	25.9	23.2
		2Btb		36.1	20.7	43.2
		2Coxrb		31.8	21.5	46.7

5. DISCUSSION

5.1 Soil Development

In the absence of numerical ages for the landsurfaces in the study area, the degree of soil development can be used to determine the relative age of the regolith. Soil development in tropical regions is strongly controlled by the rate of weathering. The warm temperatures and abundant moisture mean that chemical weathering is rapid and is mostly occurring under oxidizing conditions. Characteristic changes in soil morphology and chemistry occur as a soil profile weathers over time. In general, a soil progressively loses the

more mobile cations (*e.g.* Na, K, Ca) from exchange sites, which become dominated by Fe, Mg, Al, and silica. The particle size will decrease, and the soil texture will become more clay rich and there will be fewer unweathered clasts in the regolith. Soil horizonation will be more pronounced, especially with strong clay and red iron rich B horizons (Birkeland 1994). Generally tropical soils lack well developed A horizons as most the organic material is rapidly oxidized.

The soils can be ranked in order of increasing development based on the characteristics listed above – for the Chagrecito site: C-2 < C-3 < C-1 and for the Piedras site: P-4 = P-3 < P-1 < P-2 = P-5. Although the soils in the different drainage basins have similar morphology, there is insufficient data to determine if rates of soil development are similar on different lithologies in the two areas. In the Chagrecito drainage, the most strongly developed soil is at contact between the drainage basin and the main ridge. This soil has the greatest depth to saprolite, the strongest red color in the B, and the highest clay content of any soil. The other two soils in this basin are developed on transported regolith. They contain unweathered clasts and have a lower clay content. At the upper Piedras site, the most strongly developed soil is UP-2, on the upper part of the basin. The soil at the top of the basin is shallow, weakly developed, and is developing into weakly weathered bedrock, suggesting that pedogenesis is of short duration. The other two Piedras soils are both forming in transported regolith, have a significant proportion of unweathered clasts. The range of development of the soils in the study area is a reflection of different ages of site stability. This indicates that the landsurface in the drainage basins is diachronous, *i.e.* consists of individual soil elements of different age. The soil developed on a terrace surface in the upper Piedras location shows a similar degree of soil development as the most strongly developed soil on the hillslopes

5.2 Landscape Stability

The hillslopes in both drainages show evidence of extensive mass movement. At the Chagrecito site, the top of the drainage basin has a 2m head scarp exposing the most strongly developed soil in this drainage basin. Weathered saprolite is exposed at the base of the scarp in a linear erosion scar. This is the scar of a translational mass movement, which occurs at the boundary between the soil profile and saprolite. Vepraqskas *et al.* (1996) describe the physical changes that occur at the contact between the soil profile and saprolite that are reflected in the minimum K_{sat} determined in deeply weathered soil. They found that soil pores become blocked with clay and organic coatings, significantly reducing the saturated hydraulic conductivity at this point. Such physical changes may determine the failure

plane for translational mass movements. Translational mass movements are slides that occur on shallow planar surfaces. The failure plane appears to be below the rooting depth of many of the trees and, therefore, trees may be moved while remaining in an upright position. The depositional part of the mass movement is reflected in the uneven topography and more weakly developed soils in the lower part of the basin. The two lowermost soils in this drainage contain numerous partially weathered clasts and weaker horizon development, which indicates less overall weathering and younger soils. Large trees are growing on the uneven topography, indicating that mass movement is predominantly translational and the trees are being episodically rafted downslope.

5.3 Pattern of Soil Variability

Although the soil pattern is determined by the frequency of disturbance, the mode of disturbance - translational flows - means that there is evidence of catenary relations as well within the drainage basins. The most stable soils were observed in upper slope positions, soils in the mid-slope and toe-slope positions were always forming in transported regolith. However, the lowermost soils in both drainages were strongly gleyed, indicating that reducing conditions exist in the soil for considerable periods of time. This was also the point where throughflow was observed exiting the hillslope regolith through pores, fractures, and root channels in the soil. In-situ soil profiles occupied an estimated 10-15% of the total area of the drainage basin in both study areas, with exposed saprolite incorporating another 10%, and the rest of the area consists of mass movement debris and disturbed soils.

5.4 Hydrologic Significance of Soil Properties

Soil properties influence the ease with which water enters and moves through the soil. The uppermost soil horizon for all soils is a weakly developed and thin A horizon. It contains little organic matter and the horizon has a high clay content. Large fractures were frequently found underneath the litter layer leading to the high infiltration rates measured in this part of the soil (Hendrickx *et al.,* 2005, this volume). Such features are not uncommon in soils with high clay contents, but the clay mineralogy of these soils is predominantly the non-expanding halloysite, kaolinite. The fractures may be tension cracks produced by the frequent mass movement occurring on these steep hillslopes. The fractures and uneven topography create preferred pathways for water movement from the surface. The mass movement deposit appears to have a lower bulk density and the regolith is loosely packed indicating increased macroporosity. The role of macropores

in influencing streamflows in steep forested drainages has been described by Mozley (1982) and Casanova *et al.,* (2003). This work suggests that infiltration rates will be greater in the mass movement deposits than in soils higher on the hillslope. Another avenue for water entry into the soil is through the uneven topography created by mass movement and tree fall. Tree fall was observed frequently throughout the two drainage basins, but was more prevalent on the ridges - the more stable parts of the landscape. The process of tree fall produces a pit and mound topography, which persists in the landscape long after a tree, has disappeared. The upper soil horizons are removed and large fractures develop where tree roots have been torn out of the soil, creating preferred pathways into the subsoil. In temperate regions, enhanced leaching has been described as occurring in the pits indicating increased water movement through this part of the landscape (Schaetzl *et al.,* 1990).

In all soils of the upper Río Chagres basin study areas, preferred pathways for water movement were observed. Soil structure was mostly large angular blocky in the upper 50 cm. Along the faces of these soil peds, clay and organic staining was observed indicating water movement along these structural features. In each soil large former root channels, which were also coated with clay and organic staining, were observed.

6. CONCLUSIONS

The pattern of soil variability within two upper Río Chagres drainages reflects elements of both stability and instability. Translational mass movements, which raft weathered soil regolith downslope, are the dominant geomorphic process in both areas. The base of the translational mass movements appears to be the contact between the pedogenic soil profile and saprolite. Soils developed in transported regolith form the majority of the landsurface within the drainages, estimated at 60%. More stable soil profiles with higher clay contents and deeper weathering profiles are present in upper slope positions and form an estimated 10% of the total landsurface area. Catenary soil relations are observed in both drainages, with the stable soils in upper slope positions and gleyed soils occupying the lowermost parts of the drainages making up less than 5% of the area.

Soil properties strongly influence the entrance of water into the regolith and the stability of the regolith. The high clay content of even the less well-developed soil profile means that the soils will have high moisture retention values and the tree roots and disturbances due to mass movement mean that the soils should also have high macroporosity.

ACKNOWLEDGEMENTS

The 2002 fieldwork in the upper Río Chagres watershed was funded by the Tropical Regions Test Center (US Army Yuma Proving Ground), and we thank the organizers for their support. Other support was provided by the Universdad Technologica de Panama and New Mexico Institute of Technology.

REFERENCES

Birkeland PW, 1999, *Soils and Geomorphology*: Oxford Univ. Press, New York, NY.

Casanova, M, Messing, I, Abraham, J, 2000, Influence of aspect and slope gradient on hydraulic conductivity measured by tension infiltrometer: Hydrol. Proc., 14: 155-164.

Harden, CP and Scruggs, PD, 2003. Infiltration on mountain slopes: a comparison of three environments. Geomorph., 55, 5-24

Milne G, 1935, Some suggested units for classification and mapping, particularly for East African soils: Soil Res., 4: 183-198.

Mosley, MP, 1982, Subsurface flow velocities through selected forest soils, South Island, New Zealand: Jour. Hydrol., 55: 65-92.

Montgomery, DR and Dietrich, WE, 2002, Runoff generation in a steep, soil-mantled landscape: Water Resour. Res., 38: 1168, doi:10.1029/2001WR000822

Schaetzl, RJ, Burns, SF, Small, TW, Johnson, DL, 1990, Tree uprooting: Review of types and patterns of soil disturbance: Phys. Geogr., 11: 277-291.

Singer, MJ and Janitzky, PJ, eds., 1986, Field and Laboratory Procedures used in Soil Chronosequence Study: USGS Bull. 1648.

Tonkin, PJ, 1994, Principles of soil-landscape modelling and their application in the study of soil-landform relations within drainage basins. in Soil-landscape modelling in New Zealand: (TH Webb, ed.), Manaaki Whenua Press, Canterbury, NZ: 21-37.

USDA Soil Conservation Service, 1994, Keys to Soil Taxonomy: US Government Printing Office, Washington, DC.

USDA Soil Survey Staff, 1993, Soil Survey Manual: USDA Handbook No 18, US Government Printing Office, Washington, DC.

Vepraskas M.J., Guertal, W.R., Kleiss, H.J., Amoozegar, A., 1996, Porosity factors that control the hydraulic conductivity of soil-saprolite transitional zones: Soil Sci. Soc. Am. Jour., 60: 192-199.

Young, AW, 1988, A catena of soils on Bealey Spur, Canterbury, New Zealand. PhD Dissertation, Univ. Canterbury, NZ.

Chapter 8

HYDROLOGY OF HILLSLOPE SOILS IN THE UPPER RÍO CHAGRES WATERSHED, PANAMA

Jan M.H. Hendrickx[1], David Vega[2], J. Bruce J. Harrison[1], Lucas E. Calvo Gobbetti[2], Pedro Rojas[3], and Timothy W. Miller[1]

[1]New Mexico Institute of Technology, [2]Universidad Tecnológica de Panama, [3]Autoridad Nacional de Ambiente dePanma

Abstract: Soil hydrologcal processes determine how precipitation is partitioned into infiltration, runoff, evapotranspiration, and ground water recharge in the upper Río Chagres basin. The focus of this study is to investigate the soil hydrological processes by which precipitation excess on first order drainage basins enters the streams feeding the upper Río Chagres and its major tributary rivers. Infiltration rates, water retention curves, and water repellency of surface soils have been measured. These measurements together with the soil morphological observations by Harrison *et al.* (2005, Chapter 7) and hydrological observations by Calvo *et al.* (2005, Chapter 9) and Niedzialek and Ogden (2005, Chapter 10) are used to formulate a comprehensive conceptual model of runoff production in the upper Río Chagres watershed.

Key words: Panama, Panama Canal Watershed; upper Río Chagres basin; hillslope processes; soil hydrology

1. INTRODUCTION

The partition of precipitation into infiltration, runoff, evapotranspiration, and groundwater recharge in watersheds with steep slopes depends to a large extent on hillslope soil water dynamics (*e.g.,* Dingman, 2002; Anderson and Burt, 1990; Kirkby, 1978). These processes are not well understood, particularly in tropical rainforests. Bonell (1993) reviews the runoff generation process in forests, with an emphasis on tropical rainforests and states... "the varying runoff responses in tropical environments hinge on the delicate balance of rainfall intensity-soil hydraulic properties-topography".

R. S. Harmon (ed.), The Río Chagres, Panama, 113-138.

Calvo *et al*. (2005; Chapter 9) and Niedzialek and Ogden (2005; Chapter 10) present data that confirm Bonell's findings for the tropical upper Río Chagres basin. These investigators observed a disproportionably large volume of runoff during storms occurring immediately after the dry season and larger than normal runoff volumes during the wettest periods of the year. In addition, Niedzialek and Ogden (2005, Chapter 10) report that the discrete quasi-stable baseflows in the upper Río Chagres are not observed in the internal Río Piedras drainage which exhibits a more ephemeral behavior. The objective of this study was to identify the soil hydrological processes that cause the temporal variability in the rainfall-runoff relationships observed in the upper Río Chagres watershed.

2. SOIL HYDROLOGICAL PROCESSES THAT PRODUCE STREAM RESPONSES

This section presents an overview of the soil hydrological processes that may affect stream responses to precipitation events. Immediately after the start of a storm a large proportion of the precipitation contributes to 'surface storage'; later after infiltration of water into the soil, there is also soil 'moisture storage'. Two types of surface storage are recognized: retention and detention. Retention is storage held for a long period of time and depleted by evaporation; detention is short-term storage depleted by flow away from the storage location (Chow *et al.,* 1988). As the detention storages are filling up, flow away from them starts: surface runoff over the land surface, saturated flow through aquifers underlying the hillslope, and unsaturated flow through the soil near the land surface. The precipitation that becomes stream or channel flow reaches the stream either by falling directly into the channel or by surface runoff and/or subsurface flow.

Dingman (2002) classifies flow mechanisms that produce stream event responses with a focus on the soil hydrological processes. This classification has been slightly with the inclusion of water repellency in Table 1, which presents the soil hydrological processes contributing to stream flow during and after precipitation events on steep hillslopes.

Surface runoff or overland flow is caused either by saturation from above or by saturation from below. Runoff resulting from saturation from above has been first described by Horton (1933, 1945) and is also named 'Hortonian overland flow'. This type of runoff occurs when the rain intensity exceeds the infiltration capacity of the soil. Since the infiltration capacity of soils is in most cases higher than observed rainfall intensities, it is generally accepted that Hortonian overland flow occurs rarely on vegetated surfaces in humid regions (Chow *et al.,* 1988; Dingman, 2002). Saturation from above

occurs mainly on impervious surfaces in urban areas, and on natural surfaces with thin soil layers and low infiltration capacity as in some semiarid and arid lands.

Table 1. Classification of soil hydrological processes contributing to stream flow in a first order drainage basin.

I. Surface Runoff or Overland Flow
A. Saturation from Above (*i.e.,* Hortonian overland flow)
1. Precipitation rate exceeds soil hydraulic conductivity
2. Water repellent soil surface
B. Saturation from Below
1. Decreasing soil hydraulic conductivity with depth
II. Subsurface Flow
A. Saturated Subsurface Flow to Stream
1. Flow from ground water mounds in shallow aquifer
a. Gradual mound development
b. Sudden mound development
2. Flow from perched saturated zones
a. Darcian flow through soil matrix
b. Pipe and macropore flow
B. Unsaturated Flow
1. Darcian flow through soil matrix
2. Macropore flow

One important soil condition that can affect surface runoff is water repellency. It has been reported to occur worldwide: Australia, Canada, Colombia, Egypt, India, Italy, Japan, New Zealand, Poland, Portugal, South Africa, Spain, The Netherlands, and the USA (Jaramillo *et al.,* 2000). However, no reports were found on its occurrence in tropical lowland rainforests. In wettable 'normal' soils the initial infiltration rate is highest immediately after wetting and then decreases with time. In water repellent or hydrophobic soils the infiltration rate is lowest immediately after wetting and then increases with time (*e.g.,* Feng et al., 2002). The negligible to low infiltration rates after the start of a storm may cause water repellent soils to exhibit Hortonian behavior. Almost forty years ago, Krammes and DeBano (1965) argued that water repellency is a neglected factor in watershed management. In the late 1980s, Burch *et al.* (1987, 1989) report the occurrence of saturation from above due to water repellency in eucalypt forests. Yet, today water repellency is still not considered in most hydrology textbooks (*e.g.,* Chow *et al.,* 1988; Dingman, 2002; McCuen, 1998) and handbooks (*e.g.,* ASCE, 1996; Maidment, 1992). The effect of water repellency on surface runoff is most dramatically demonstrated after forest

fires. Neary *et al*. (2003) summarize what is known about the effects of fire on watershed resources in the southwestern USA. Flood flows after wildfires often increase considerably due to factors such as combustion of vegetation and forest floor cover, development of water repellent layers in the soil, and accelerated development of post-fire thunderstorms. Increases in storm flows of 1.5 to 2,300 times the measured pre-fire flood peaks have been documented. The effect is especially severe in steep watersheds. Since the senior author observed water repellency during a previous visit in Panama, one important objective of this study was to systematically explore whether water repellency plays a role in the rainfall-runoff relations of the upper Río Chagres watershed.

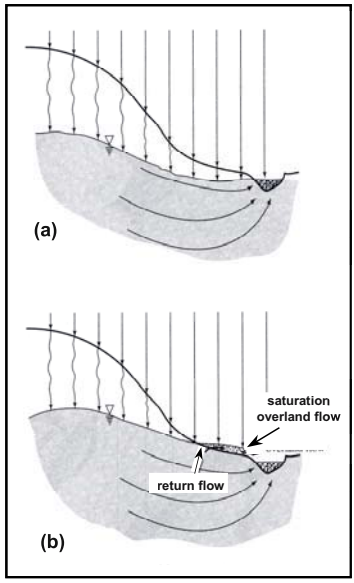

Figure 1. Saturation overland flow and sub-surface event flow due to near-stream ground water mounding. (a) Early stages of event; overland flow is absent and only regional ground water flow is (base flow) occurring. (b) Later, water table has risen to the surface in near-stream areas due to local and upslope recharge, infiltration ceases, and saturation overland flow results along with subsurface event flow. Return flow is the portion of saturation overland flow contributed by 'breakout' of ground water. Flow contributing to mounding results from both vertical recharge and downslope flow in the saturated zone (modified from Dingman, 2002; after Ward, 1984).

Runoff resulting from saturation from below occurs when the soil profile contains horizons with relatively low permeability or is underlain by a shallow ground water table. Once the soil becomes saturated, infiltration ceases and detention storage fills up resulting in surface runoff on hillslopes.

Surface runoff is the result of precipitation on saturated parts of the hillslope plus the contribution of ground water 'break-out' from upslope (Fig. 1).

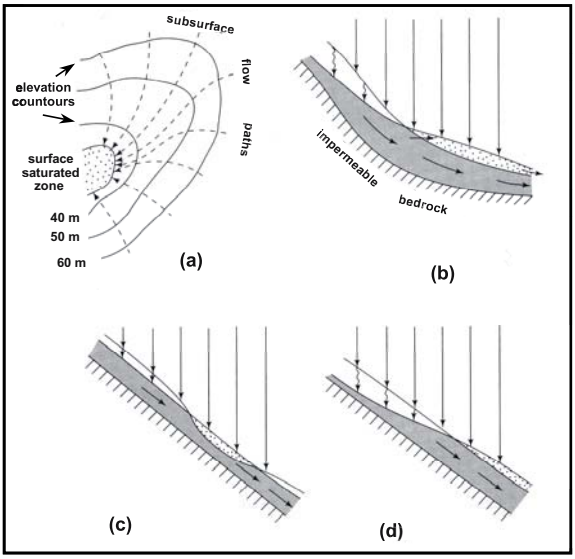

Figure 2. Situations in which saturation overland flow may arise on hillslopes outside of near-stream areas. (a) Plan view showing convergence of subsurface flow paths. (b) Cross-section showing downslope reduction in hydraulic gradient associated with slope break. (c) Cross-section showing local area of thin soil. (d) Cross-section showing formation of perched saturated zone above low-conductivity layer with constant slope and soil thickness. (modified from Dingman, 2002; after Ward, 1984).

Field studies (Dunne and Black, 1970; Dunne, 1978; Ward, 1984) and modelling (Freeze 1972, 1974) have shown that this mechanism is important in humid areas. Although saturation from below will most likely occur in drainage basins with concave hillslope profiles and in flat valleys, it is not restricted to near-stream areas. Ward (1984) describes four different scenarios where surface runoff may arise on hillslopes away from the streams (Fig. 2): (a) Convergence of water flow paths into slope concavities; (b) Downslope reduction in hydraulic gradient associated with slope break; (c) Subsurface flow conducted through thin soil layers; and (d) Zones of perched ground water 'break-out' at soil surface. Within a watershed the extent of areas saturated from below varies greatly with time. In many regions this temporal variability of overall watershed wetness causes a large temporal variability in storm runoff (Dingman, 2002).

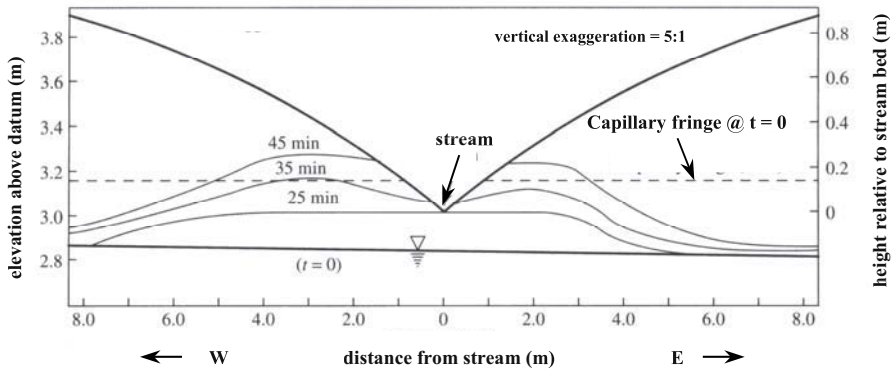

Figure 3. Quick response of a near-stream water table due to pressurization of the capillary fringe during a simulated rain of 2 cm/hr in a sandy soil. Lines show position of ground water table at successive times after onset of the rain (modified from Dingman, 2002; after Abdul and Gillham, 1989).

Saturated subsurface flow is generally considered the source of most streamflow between precipitation events, *i.e.* the base flow. It is recognized that the travel times of regional ground water flows are so large that the short-term pulses of precipitation are damped out before reaching the streams. However, tracer studies have revealed that under certain conditions ground water can be a significant part of short-term stream response to precipitation events (*e.g.,* Sklash and Farvolden, 1979; Space *et al.,* 1991).

Saturated subsurface flow to streams can occur due to local gradual ground water mound development near streams as well as from flow through perched saturated zones. Ground water recharge during rainfall events can produce a mound that increases the hydraulic gradient toward the stream and so produces a prompt contribution to streamflow. A special case is where sudden pressurization of the capillary fringe and unsaturated zone above shallow ground water tables causes an almost instantaneous formation of sudden ground water mounds (Abdul and Gillham, 1984, 1989; Jayatilaka *et al.,* 1996). The streamflow contribution generated by this mechanism may greatly exceed the amount of water needed to pressurize the capillary fringe and unsaturated zone from negative to positive pressure (Fig. 3).

Unsaturated subsurface flow can never be a direct source of water to a stream. Soil water pressures in unsaturated flow are negative, whereas water pressures in a stream are positive. Only when soil water pressures build up in a soil to slightly positive pressures, can water leave the unsaturated zone and enter the shallow aquifer or move through a seepage face into the stream.

During wetting events infiltration on hillslopes is nearly vertical for most soils, while shallow unsaturated flow tends to become parallel with the slope during drying events (Jackson, 1992). This phenomenon typically leads to

two distinct flow regimes on steep hillslopes: one during wet episodes and another during dry periods. During wet periods, infiltrating water can cause a perched saturated zone that feeds the stream on hill slopes that consist of a thin permeable soil layer overlying a relatively impermeable layer, (Fig. 4).

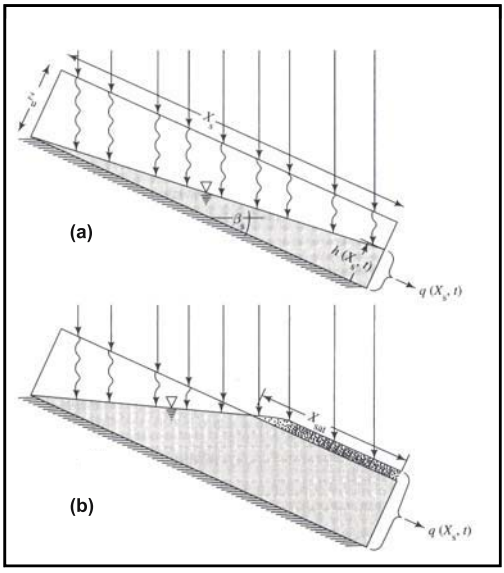

Figure 4. Formation of a perched saturated zone on a hill slope in which a soil horizon with relatively high hydraulic conductivity overlays a soil horizon with relatively low hydraulic conductivity. (a) Subsurface storm flow from basal saturated zone at slope base. (b) Sloping slab with 'breakout' water near the stream, producing saturation overland flow with subsurface storm flow (from Dingman, 2002).

The response time of this runoff process on steep slopes can be evaluated using simple conceptualisations and is on the order of hours (Dingman, 2002). During dry periods on steep hillslopes, the near-surface soil water equipotential lines become normal to the slope which causes unsaturated water flow parallel to the slope and accumulation in the 'toe' (Fig. 5). Since unsaturated flow parallel to a hillslope is a slow process, this flow will not contribute to event response but it can be a main source of base flow during the dry season (*e.g.,* Anderson and Burt, 1977; Hewlett and Hibbert, 1963; Nutter, 1975; Weyman, 1970).

Hewlett and Hibbert (1963) demonstrated the potential for base flow maintenance by unsaturated flow from uplands with an illustrative experiment. They saturated a confined column soil (1m x 1m x 15m) of homogeneous sandy-clay-loam, covered it to prevent evaporation, tilted the

soil column at a 40° slope, and its discharge was measured at the slope base. Since unsaturated flow parallel to a hillslope is a slow process, this flow will not contribute to event response, but it can be a main source of base flow during the dry season (*e.g.,* Anderson and Burt, 1977; Hewlett and Hibbert, 1963; Nutter, 1975; Weyman, 1970). As expected, the discharge rates declined very rapidly during the first five days from *c.* 620 to *c.* 50 liters per day. However, drainage persisted until the experiment was terminated on day 145. After three months (*i.e.,* the approximate length of the dry season in the upper Río Chagres watershed), the discharge was still about 1 liter/day.

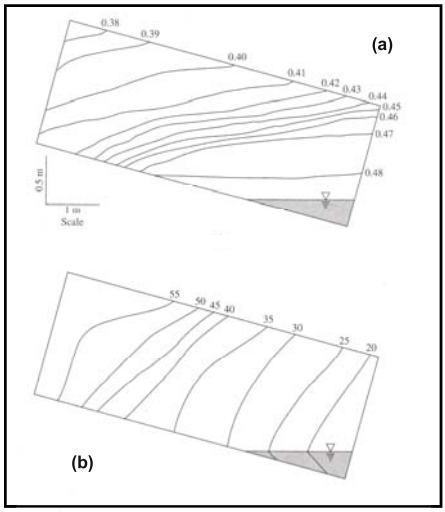

Figure 5. (a) Water content and (b) hydraulic head distribution in a sloping slab after 749 hours of drainage. The slope is 15°. The equal head lines are perpendicular to the soil surface indicating slope parallel flow, which is typical for draining conditions between storm events. Also, note the saturated wedge at the toe slope (from Dingman, 2002; after Nutter, 1975).

Macropores and pipes are produced by roots, soil fauna, or desiccation cracking. Their sizes can vary from a few millimetres to more than 100 mm. Stresky (1991) observed in a New Hampshire forest that macropore networks were generally oriented downslope and were interconnected over distances of at least tens of meters. Therefore, these features provide pathways for water to bypass the soil matrix and to move downslope to the shallow aquifer at velocities of several millimetres per second (*e.g,* Beven and German, 1982; Hendrickx and Walker, 1997; Mosley 1979, 1982). In many cases, it is unclear whether the soil matrix surrounding the macropores was saturated or unsaturated, but for water to enter larger macropores and pipes soil water pressures need to become slightly positive at the point of entrance. Once water is inside the macropore network, it can be transported

downslope through otherwise unsaturated soils. Many studies indicate that the importance of macropore flow increases with the amount of precipitation in an event (Dingman, 2002). German (1986) analysed drainage responses to storms observed during a 7-year period in the Coshocton monolith lysimeters (Northeast Experimental Watershed, USDA-ARS, Coshocton, Ohio). Rains of only 10 mm/day caused a drainage response at 2.4 m depth on the same day as precipitation when volumetric water content in the upper meter of the undisturbed soil profile exceeded a threshold value of 0.3 m^3/m^3, whereas at soil water contents below this threshold value storms greater than 50 mm per day were found not to cause any drainage flow. This demonstrates that macropore flow also increases with soil water.

3. METHODS AND MATERIALS

Most of the data for this study have been obtained during the upper Río Chagres field campaign of 4-16 March 2002. The field work was conducted in two small, narrow, and steep first order drainage basins with similar morphologies: at a site in the upper Río Chagrecito drainage (approximate coordinates: 9°22′ N latitude, 79°19′ E longitude) and the upper Río Piedras drainage (approximate coordinates: 9°18′ N latitude, 79°20′ E longitude). Harrison *et al.* (2005, Chapter 7) describe the methods for soil morphology and geomorphological observations in the field. In addition, to these qualitative observations we have also measured infiltration rates and water repellency in the field.

Tension disc infiltrometers (*e.g.,* Clothier and Scotter, 2002) were taken to the field. However, these instruments of choice could not be employed for the following reasons: (1) Even during the dry season the upper Río Chagres basin receives frequent showers wetting the river sand beds. Since moist sands cannot be sieved, it was difficult to obtain the supply of fine sand needed to install the infiltrometer on the soil; (2) Especially in the upper soil layers roots tend to damage the sensitive membrane; (3) Each infiltration measurement in the fine textured soils would have taken a long time, thus limiting the total number of measurements possible. For these reasons, the crude method of 'test pits' (USBR, 1984) had to be used. A small test pit (0.3x0.3 m with depth 0.2 m) was dug out in the soil horizon of interest. After filling it with water to a depth of about 0.15 m, the fall of the water level in time, *i.e.* the infiltration rate, was monitored by reading a ruler placed in the bottom of the pit (Fig. 6). When the water level had fallen by about 0.05 m, the water level was brought back to its original level. This method definitively overestimates the infiltration rates but it yields

information on the relative infiltration rates of representative soil horizons. Measurements were made in four soil pits at the Piedras drainage site (RP-1, RP-2, RP-3, and RP-4) and in two soil pits at the Chagrecito drainage site (C-1 and C-2). A full description of these soil profiles is given by Harrison *et al.*, 2005, Chapter 7).

Figure 6. Measurement of upper limit of infiltration rates in small test pits.

Soil water repellency in the field and in the laboratory is determined with the empirical 'Water Drop Penetration Time' (WDPT) test described by several investigators (*e.g.,* Dekker and Jungerius, 1990; King, 1981; Krammes and DeBano, 1965; Letey *et al*., 1975). Three drops of water from a standard medicine dropper are placed on the smoothed surface of a soil sample, and the time that elapses before the drops are absorbed is determined. Using the WDPT test on dried samples in the laboratory gives the persistence of the potential water repellency while its use on field-moist samples yields the actual water repellency (Dekker and Ritsema, 1994). Different classification systems for water repellency are used (King, 1981; Dekker, 1998). A soil is considered wettable if the penetration time is less than 5-10 sec; slightly water repellent if the penetration time is 10-60; water repellent if the penetration time is 60-90 sec; and strongly water repellent at longer penetration times.

In the field, 1-m long transects were selected close to the soil profile pits described by Harrison *et al.* (2005, this volume). Along each transect, the litter was carefully removed to expose the surface soil. Next, 20 soil rings (diameter = 0.05 m; height = 0.05 m) were inserted side by side. Then, the WDPT test was administered on the soil surface within each of the rings. The soil sample within each ring was put in a plastic bag for transport to the

hydrology laboratory at New Mexico Tech. There, the soil water content was measured. In addition, the WDPT test was repeated after air drying the samples for several weeks. Soil ring samples (diameter = 0.05 m; height = 0.05 m) were collected in six of the representative soil horizons described by Harrison *et al.* (2005, this volume), for determination of the soil water retention curve at New Mexico Tech using the hanging water column technique (Dane and Hopmans, 2002).

4. RESULTS AND DISCUSSION

This section discusses what has been learned about the soil hydrological processes that contribute to stream flow response in the upper Río Chagres basin. The discussion is structured along the soil hydrological processes presented in Table 1, based upon both field and laboratory measurements as well as the field observations described by Harrison *et al.* (2005, this volume).

4.1 Surface and Soil Moisture Storage

The shapes of the first order drainage basins in the upper Chagrecito and upper Río Piedras drainages are similar to those shown in Figures 2a and 2b. Slope angles in the two basins vary from approximately 55^{o} at the head of the basin to approximately 20^{o} at the toe. Harrison *et al.* (2005, Chapter 7) observed extensive mass movement in both drainages that generated an uneven topography, especially in the lower slope areas. They also observed frequent tree fall (Fig. 7), especially on the higher, more stable, parts of the drainages.

After a tree has fallen a pit and mound topography will persist in the landscape long after the tree has disappeared. Despite the steep slopes the uneven topography creates many local depressions that provide a considerable volume for surface storage of precipitation and run-on water from upslope. Some of the detained water will evaporate, but most will infiltrate into the soil to increase soil moisture storage and, therefore, the propensity for macropore flow. Ponding of surface water in small depressions will result in small positive water pressures that also allow water to enter the macropore and pipe system. It will be hypothesized below how the combination of these local depressions with water repellent soil surfaces after the dry season could create a system of bypass flow that allows quick downward transport of storm water into the pipe network through an unsaturated soil matrix.

Figure 7. Fallen tree - a common occurrence throughout the upper Río Chagres basin.

4.2 Surface Runoff Caused by Saturation from Above

Saturation from above occurs when the precipitation intensity exceeds the infiltration capacity of the soil. The upper limits of the infiltration rates measured in the different soil profiles are presented in Table 2. The infiltration rates measured near the soil surface appear to be relatively high given the amount of clay in the soil (Harrison *et al*., 2005, this volume). However, the blocky soil structure and the large number of cracks and macropores close to the soil surface often result in high infiltration rates in tropical forest soils (*e.g.,* Bonell *et al*., 1981). These high infiltration rates will make the occurrence of Hortonian flow most unlikely as long as the soil surface is wettable, i.e. not water repellent.

Water repellent soil surfaces have a much lower infiltration rate than the same soil surface under wettable conditions. Since water repellency is enhanced when the soil becomes dry, it is expected that the effect of water repellency on runoff is the strongest immediately after the dry season. The degree of water repellency has been measured in the field and in the laboratory. The results are presented in Tables 3 and 4.

Table 2. Upper limits of infiltration rates in selected profiles of the upper Río Piedras (RP) and upper Río Chagrecito (C) drainages. See Harrison *et al.* (2005, Chapter 7) for full soil profile descriptions.

Profile	Depth (cm)	Horizon Description	Upper Limit Infiltration Rate (cm/day)
RP-1	10	A/B	5,760
	40	C/Bt Clay in fractures	26
	80	C/Bt Clay in fractures	19
RP-2	40	Bt2	9
	80	Cox/t Saprolite with clay in fractures	55
RP-3	40	Cox/t Saprolite with clay in fractures	180
	80	Cox/t Saprolite with clay in fractures	160
RP-4	10	Bw/C Disturbed horizon	14,400
C-1	10	Bt	60
	120	Saprolite	180
	300	Saprolite	85
C-2	50	Bt	85

The 'Water Drop Penetration Test' (WDPT) measurements show that water repellency does occur in the upper Río Chagres watershed, but the areal extent of water repellency is not at all clear. At the Chagrecito-1 site, four of the laboratory dried samples are water repellent (Table 3), two samples are slightly water repellent at Chagrecito-2, and at Chagrecito-3 no sample shows any degree of water repellency. The field measurements on 7 March 2002 at the Chagrecito-1 site resulted in 17 out of 20 samples water repellent or strongly water repellent. However, on 8 March 2002, the field measurements at the Chagrecito-2 and Chagrecito-3 sites documented no water repellency. This negative result was probably caused by the moist soil conditions, as measured gravimetric water contents ranged from 0.54 to 1.77 kg/kg following heavy showers which occurred during the previous night. At the Piedras-1 site, 13 field samples exhibit strong water repellency and the other samples some degree of water repellency, At the Piedras-2 site, 11 field samples were water repellent, whereas at the Piedras-3 only a single field sample was slightly water repellent. By contrast, samples from the Piedras-1 and Piedras -2 sites were much less water repellent when measured under laboratory conditions.

Table 3. Gravimetric field soil water content and results of Water Drop Penetration Test (WDTP) on soil surface samples from the Chagrecito drainage. Wettable = 0-10 sec, slightly water repellent = 10-60 sec, water repellent = 0-90 sec, strongly water repellent = >90 sec. WDPT of field is average of three drops; WDPT lab is average of five drops.

Site	**Chagrecito - 1**			**Chagrecito - 2**			**Chagrecito - 3**		
----------	Field	Field	Lab	Field	Field	Lab	Field	Field	Lab
Distance (cm)	wc (g/g)	WD PT (sec)	WD PT (sec)	wc (g/g)	WD PT (sec)	WD PT (sec)	wc (g/g)	WD PT (sec)	WD PT (sec)
5	0.55	8	1	1.08	1	1	0.72	1	1
10	0.58	58	1	1.29	2	4	0.80	2	1
15	0.54	12	3	1.21	6	1	0.85	1	1
20	0.62	21	3	1.36	4	1	0.76	1	2
25	0.59	2	75	1.41	3	6	0.86	1	2
30	0.57	20	95	1.41	3	10	0.65	1	1
35	0.61	203	13	1.33	2	14	0.73	1	1
40	0.65	27	3	1.27	3	2	0.67	1	0
45	0.65	3	8	1.30	1	1	0.70	1	1
50	0.64	20	1	1.28	1	7	0.80	1	1
55	0.64	151	1	1.28	2	2	0.82	1	1
60	0.64	236	2	1.42	2	4	0.83	1	1
65	0.62	92	4	1.49	1	1	0.75	1	1
70	0.61	161	1	1.53	4	2	0.72	1	1
75	0.64	46	10	1.73	2	6	0.59	1	1
80	0.63	93	1	1.77	2	3	0.89	1	1
85	0.63	286	6	1.18	2	5	0.65	1	1
90	0.61	186	2	1.49	1	2	0.63	1	2
95	0.63	34	2	1.29	2	3	0.64	1	1
100	0.64	26	1	1.32	2	1	0.65	1	1
Average	0.61	84	12	1.37	3	4	0.73	1	1

The dynamic behavior of soil water repellency is not yet understood. In general, the degree of soil water repellency decreases with soil moisture content. It also has been reported that the degree of water repellency changes with different drying temperatures. For example, Dekker (1998) found for 4 out of 7 sandy soil sites in The Netherlands that water repellency was greater after drying at 65ºC relative to 25ºC, whereas it decreased for 2 others, and remained unchanged for one. Doerr *et al.* (2002) found that an increase in relative humidity from typical ambient laboratory conditions, *i.e.,* 40-50% relative humidity, to 98% for a time period of less than one day increased the degree of water repellency strongly. This finding may explain the large differences observed between field and laboratory WDPT values observed at Chagrecito-1 site and the Piedras-1 and Piedras-2 sites. The much lower degree of water repellency measured in the laboratory compared to that

determined in the field, may have been caused by the low humidity in arid New Mexico versus the high humidity in the field in Panama.

The field and laboratory measurements, together with observations of water repellency made by the senior author during the dry season of 2001, leave no doubt that water repellency does occur in the in the upper Río Piedras watershed. It is hypothesized that a combination of dry soil surfaces and high relative humidity create patches of severe water repellency just before the first storms after the dry season. Instead of precipitation filling up the dry soil profiles – as is assumed by many hydrological models – it will run off into the many depressions created by the uneven topography of the drainages. At the lowest points in these depressions, a slightly positive water pressure will develop that allows the runoff water to enter the system of macropores and pipes. As soon as the water starts flowing in this natural drainage system, it can bypass the large dry soil mass on the hillslope and move downward at a high velocity. At the toe of the hillslope, this water contributes to the shallow aquifer feeding the stream. After the surface soils have been wetted at the start of the rainy season, water repellency probably does not any longer affect the relation between precipitation and runoff.

4.3 Surface Runoff Caused by Saturation from Below

Saturation from below occurs when the soil profile contains less permeable layers or is underlain by a shallow ground water table. Our infiltration measurements (Table 2) and the observations by Harrison *et al.* (2005, Chapter 7) show that the occurrence of a less permeable B horizon is a typical feature of the hillslope soils in the watershed. At the Piedras site, the upper limits of the infiltration rates in the B horizon are two to three orders of magnitude less than those of the overlying soil horizons. Therefore, it is expected that saturation from below is a common feature during the wet season when soil water content is high and precipitation frequent (Fig. 2d). The severe decrease of saturated hydraulic conductivity with depth seems to be not uncommon in tropical watersheds, having been reported in tropical Australia (Bonell *et al.,* 1981) and in the Amazon (Elsenbeer *et al.,* 1992). Saturation from below due to a shallow ground water table may occur during wet periods at the toe slope (Fig. 1b) or where the ground water table breaks out the slope due to a reduction in hydraulic gradient associated with slope break or local areas of thin soil (Fig. 2b, c).

Table 4. Gravimetric field soil water content and results of the 'Water Drop Penetration Test' on soil surface samples from the Piedras drainage. Wettable 0-10 s, slightly water repellent 10-60 s, water repellent 60-90 s, strongly water repellent >90 s. WDPT of field is average of three drops; WDPT lab is average of five drops.

Site	Upper Río Piedras-1			Upper Río Piedras-2			Upper Río Piedras-3		
---	Field	Field	Lab	Field	Field	Lab	Field	Field	Lab
Distance (cm)	wc (g/g)	WDPT (sec)	WDPT (sec)	wc (g/g)	WDPT (sec)	WDPT (sec)	wc (g/g)	WDPT (sec)	WDPT (sec)
5	0.28	54	43	0.25	4	2	0.31	1	1
10	0.27	334	101	0.24	29	2	0.30	2	1
15	0.26	337	94	0.23	27	1	0.32	2	1
20	0.33	55	92	0.21	64	20	0.32	1	1
25	0.30	11	23	0.23	93	12	0.32	2	2
30	0.26	31	14	0.22	103	6	0.32	3	2
35	0.29	59	16	0.23	121	2	0.30	8	1
40	0.28	33	62	0.25	20	12	0.32	2	1
45	0.37	307	7	0.22	21	10	0.30	8	1
50	0.30	513	10	0.22	99	2	0.32	2	1
55	0.26	767	150	0.22	21	2	0.31	2	1
60	0.28	1127	87	0.30	6	1	0.30	2	1
65	0.30	775	71	0.29	5	1	0.30	2	1
70	0.29	351	32	0.29	2	1	0.29	12	1
75	0.29	632	96	0.29	3	1	0.27	7	1
80	0.31	428	81	0.27	3	2	0.28	5	1
85	0.30	470	24	0.29	2	22	0.28	3	1
90	0.29	232	47	0.31	19	3	0.27	3	1
95	0.30	78	67	0.28	2	2	0.30	3	1
100	0.33	251	38	0.26	2	1	0.29	2	1
Average	0.30	342	58	0.26	32	5	0.30	4	1

4.4 Saturated Subsurface Flow

The presence of (almost) permanently saturated flow in soil profiles is marked by reduced conditions that lead to distinctive blue-greyish gley mottles. Harrison *et al.* (2005, Chapter 7) have observed such gley mottles in the soil profiles at the toe slopes of the drainages. No gley mottles have been observed in any of the soil profiles on either the hill crests or backslopes, which indicates that saturated subsurface flow is not a permanent condition on the hillslope. Although saturated through flow as a result of perched water tables almost certainly will occur during wet periosds, such flow events will have a short duration. Most likely, the network of macropores and pipes on the hillslope will act as a subsurface drainage system that

quickly evacuates large volumes of water to the shallow aquifer under the toe slope adjacent to the stream.

The inflow of water into the shallow aquifer will lead to the build up of a groundwater mound and an increased discharge into the stream (Figs. 1b, 2b, 4b). The steep soil water retention curves presented in Figure 8 indicate that a relatively small amount of water can cause a large sudden change in soil water pressure along the hillslope resulting in sudden ground water mounds (Fig. 3). For example, under moist conditions (*i.e.,* soil water pressure about 250 cm), the soil in the B horizon of Chagrecito-1 at depth 120 cm needs only 2-3 cm of infiltration to raise the ground water level 250 cm.

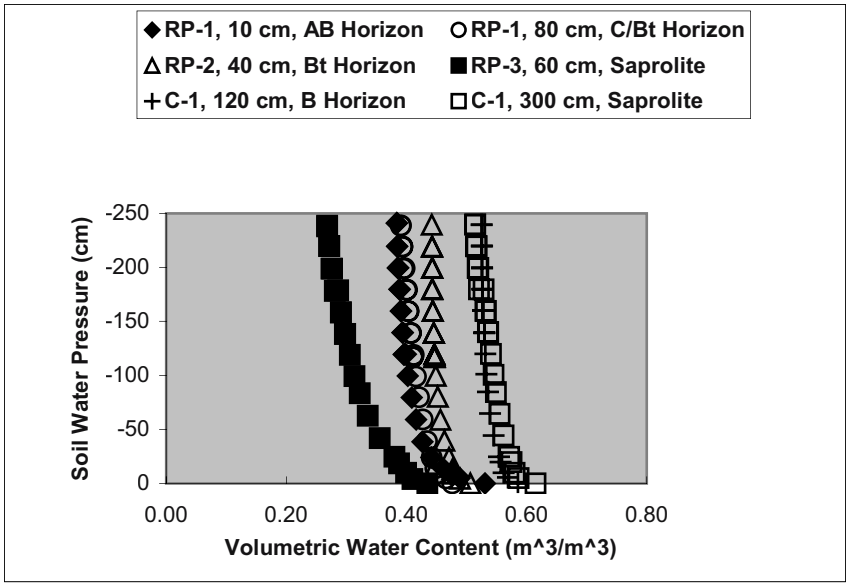

Figure 8. Soil water retention curves from different soil horizons in the Chagrecito and Piedras drainages.

Saturated shallow subsurface flows appear to be periodic in nature with the exception of the waters seeping from toe slopes. However, deep saturated subsurface flows in the aquifers underlying the hillslopes are a permanent feature of the upper Río Chagres basin, as is observed in the 10 to 20 m deep wells used by the local population for drinking water. These deep ground water supplies are expected to become important for the future development of water resources in the watershed especially during episodic periods with scarce water supplies. Since little is know about the hydrogeology of the watershed the investigation of aquifers, recharge, and

the ground water volumes available for exploitation should have a high priority.

4.5 Unsaturated Subsurface Flow

Three types of unsaturated subsurface flow are recognized along the hill slopes in the two drainages: (i) a vertical downward flow from the soil surface into the soil matrix after the start of and during precipitation events, (ii) a continuous vertical downward flow leaving the less permeable B horizons and entering into weathered and unweathered bedrock, and (iii) a lateral downhill flow component parallel to the soil surface after precipitation has ceased.

As has been discussed above, the unsaturated downward flow from the soil surface will be overtaken by saturated flow during storm events due to saturation from below at the interface of the A and B horizons, which is caused by the lesser permeability of the Bt horizons. This phenomenon is well recognized in surface water hydrology. However, it also should be acknowledged that the less permeable B horizon is not completely impermeable and, therefore, a substantial volume of water will pass through it to become ground water recharge. The volume of ground water recharge in the upper Río Chagres watershed is a major unknown; quantification of this component of the water balance is critical for the development of water resources management strategies during drought periods.

It is hypothesized that the lateral downhill unsaturated flow component is critical to maintain base flow during the dry season and in between major precipitation events. Support for this idea is found in the large water holding capacity of the hillslope soils, which varies from about 60 to 45 vol. % (Fig. 8). These water holding volumes are similar to those observed in the soils for the lateral unsaturated flow experiments by Hewitt and Hilbert (1963) described in Section 2. Further evidence is provided by the discharge measurements made for one of the springs exiting from the toe slope of the Chagrecito site at the end of the 2002 dry season. Before the heavy rain during the night of 7-8 March 2002, the spring discharge measured 5.5 liters/min; on the morning after the rain it measured 6.5 litres/min. The relatively small effect of the precipitation on spring discharge during the dry season indicates that the springs are mainly fed by unsaturated flow (Fig. 5), which is a slow process. Thus, contrary to many other watersheds where the source of base flow is the regional aquifer, baseflow in the upper Río Chagres basin between storm events and during the dry season is mainly fed by downward- seeping unsaturated flow. As shown by the experiments of Hewlitt and Hibbert (1963,) this kind of flow can maintain considerable discharge where precipitation events occur on a regular basis. At the

Chagrecito site, where drainage covers about 1 hectare; 2 to 3 springs were estimated to yield a total discharge of about 15 litres/min from the drainage. Extrapolating this discharge to the entire approximately 400 km^2 of the upper Río Chagres watershed yields a discharge of 600 m^3/min or 10 m^3/sec. The latter discharge is quite similar and certainly at the same order of magnitude as the estimate presented by Niedzialek and Ogden (2005, this volume) during the dry season of 2001.

4.6 Macropores and Pipes

An abundance of macropores, cracks, and pipes was observed in each of the eight soil profiles described by Harrison *et al.* (2005, this volume). The diameter of the pipes could be up to about 10 cm (Fig. 9), a dimension similar to subsurface drains used in agriculture.

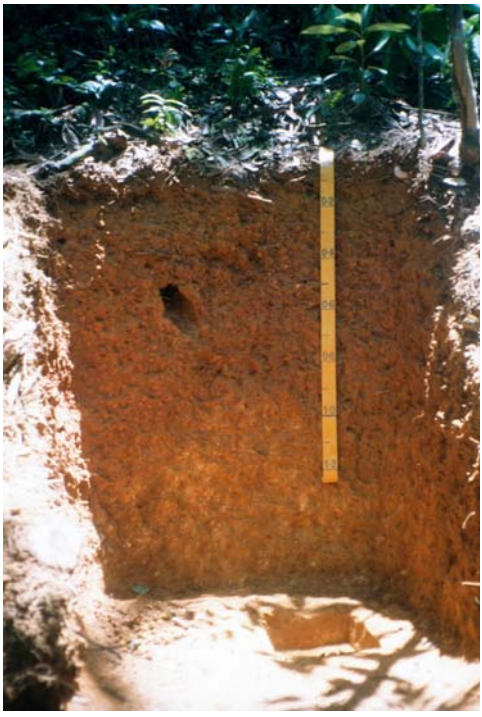

Figure 9. A typical soil pipe with diameter 12 cm in soil profile RP-2.

For water to enter the pipes and macropores a positive water pressure is required. Two mechanisms are recognized for a positive water pressure to

develop along the hill slope. The first is the situation where saturation from below leads to saturated conditions, *i.e.* a positive water pressure, around soil pipes. This mechanism could develop very quickly, especially in moist soil where only a small amount of infiltration is needed to make soil water pressures positive due to the steep water retention curves measured in the hill slope soils (Fig. 8). The second mechanism would operate where water accumulation in small soil surface depressions leads to ponding and positive water pressures. This mechanism will convey runoff water into the soil pipe network even when the hill slope soils are unsaturated. Critical factors for the latter mechanism are the uneven topography and the occurrence of water repellency after dry periods.

Co-author Rojas, a ranger in the Parque Nacional Chagres (Chagres National Park), has often observed that the pipes release jets of water during heavy precipitation events. This not only indicates that some pipes carry water under considerable pressure at full flow condition, but also that a water drop may travel downhill through a sequence of surface runoff and pipe flowpaths. The exfiltration of water from pipes on tropical hill slopes has also been reported by Bonell *et al.* (1984) and Elsenbeer and Cassel (1990).

5. CONCEPTUAL RUNOFF PRODUCTION MODEL

Calvo *et al.* (2005, Chapter 9) and Niedzialek and Ogden (2005, Chapter 10) have analysed preciptation-runoff relations in the upper Río Chagres basin and found anomalously high runoff production at the start of the wet season and discrete quasi-stable baseflows during the hydrologic year. The soil hydrology observations discussed here form the basis for the formulation of a hypothetical, comprehensive conceptual model for runoff production that explains the apparently anomalous precipitation-runoff situation observed in the upper Río Chagres watershed.

The key factors that affect runoff production along the tropical hill slopes of the upper Río Chagres watershed are: steep gradients, extensive macropore and pipe networks, soils with high water retention, B horizons with relatively low permeability overlain by A/B horizons with relatively high infiltration capacity, the occurrence of water repellency and cracks when soil surface dries out, uneven topography with many small surface depressions, and high precipitation events.

The model discussion begins at the start of the wet season when the soil surfaces are relatively dry and soil cracks have developed. At this time, the water content of the upper layers of the soil profile is relatively low. The relatively few water content measurements made suring this study indicate

that at least 20 vol. % pore space is available for soil water storage. The measurements presented in Tables 3 and 4 indicate the occurrence of a state of water repellency after the dry season.

Calvo *et al.* (2005, this volume) and Niedzialek and Ogden (2005, this volume) report anomalously high runoff volumes during the first storms of the subsequent wet season. Obviously, bypass flow carries a large volume of precipitation quickly downhill without wetting the soil matrix. Since about 20 vol. % of the soil is available for water storage, saturation from below has to be excluded as a possible runoff mecihanism. Overland flow is also unlikely given the relatively high infiltration rate of the soil surface and the uneven topography. The only other quick response flow pathway is the macropore and pipe network. However, for water to enter this network a positive water pressure is needed.

Therefore, it is hypothesized that the uneven topography caused by mass movement along the unstable slope and tree fall results in a large number of small surface depressions which provide the necessary source of water. These surface depressions accumulate water relatively quickly as rains begin due to the water repellency that prevents infiltration into the soil surface and enhances the runon towards the lowest points in the depressions. Here, almost immediately a positive water pressure develops that allows the runon water to enter the pipe network. Once the water is in the pipes it moves rapidly downhill. Niedzialek and Ogden (2005, Chapter 10) argue that dry season soil cracks would lead to increased soil storage [and reduced runoff, *sic*]. This is true for cracks without an outlet. However, along the hill slopes in the two drainages, the cracks would fill up with water swiftly and create additional water sources with positive water pressures that feed into the pipe network. Thus, the quick filling of small depressions and cracks due to a water repellent soil surface allows the development of water sources with positive water pressures that feed immediately into the downhill pipe network. It is this process that is envisaged to cause the anomalously high runoff volumes observed for the upper Río Chagres basin at the start of the wet season.

Once the wet season has started, the moist soil surface causes the water repellency disappear and infiltration into the soil matrix starts to fill the soil water storage reservoir. In addition, most soil cracks will have disappeared due to swelling of the clay minerals upon wetting. As a consequence, the volume of runon water towards the lowest points in the small surface depressions will decrease. This, in turn, leads to lower positive water pressures and less water entering the downhill pipe network. Therefore, it is expected that the amount of runoff for a given storm will decrease as compared to the runoff observed at the start of the wet season. Indeed, Calvo

et al. (2005, Chapter 9) report a sharp decrease in the 'Curve Number', *i.e.* a measure of the runoff volume, immediately after the first storms of the wet season. Their analysis supports our hypothesis.

During the wet season, two critical sequential threshold values of soil moisture are recognized: one where the macropores and pipes become active due to localized saturation inside the soil profile around the pipes and another where saturation from below reaches the soil surface and starts to enhance surface runoff. The steep water retention curves of the soils along the hill slopes (Fig. 8) create a situation where a small amount of water added to a moist soil can generate the rapid development of a positive water pressure around macropores and pipes. This will cause water to enter the pipe network and leads to an increased runoff volume. The soil moisture content at which this process starts is the 'critical soil moisture threshold for macropore flow'. For example, German (1986) found a threshold value of 30 vol. % water which is well below saturation.

Finally, during the peak of the rainy season and during prolonged storms soil moisture conditions will reach saturation throughout the soil profile at the 'critical soil moisture threshold for saturation from below'. Now, not only the pipe network will be conveying water downhill, but also surface runoff that is caused by saturation from below. As a consequence, the runoff volume for a given storm will increase as compared to the events occuring earlier in the wet season when soil water contents were lower. The increase of the 'Curve Number' during periods of high soil moisture (see Fig. 3 of Calvo *et al.,* 2005, this volume) supports this hypothesis.

The increasingly higher quasi-stable base flows reported by Niedzialek and Ogden (2005, this volume) can be explained, at least in part, by inspecting the experimental work by Hewlett and Hibbert (1963). The more moist the soil, the higher the unsaturated hydraulic conductivity and, therefore, the higher the unsaturated flow parallel to the slope towards the shallow aquifer at the toe slope which feeds the stream. However, it is not clear what causes the step-wise increase in base flow during the wet season. This may be a caused by the soil hydraulic properties and/or components of saturated ground water flow.

Niedzialek and Ogden (2005, Chapter 10) observed that the runoff behavior for the upper Río Chagres basin differs from that in the Río Piedras sub-basin. They discuss possible causes for the almost ephemeral flow regime of the Río Piedras, including the contributions of ground water to base flow and the change in land use that has occurred on part of the Río Piedras catchment. Another possible cause is the unsaturated flow regime along the hill slope. A small difference in soil moisture storage and/or unsaturated hydraulic conductivity could easily lead to a dramatic stop of baseflow during the dry season and between storms. Harrison *et al.* (2005,

Chapter 7) observed that the soils at the Piedras site are much thinner that those in the Chagrecito site. If this observation holds for the entire upper Chagrecito and Piedras sub-catchments, then it would indicate that soil moisture storage in the upper Río Piedras sub-catchnment is much less than in the upper Río Chagrecito sub-catchment. As a consequence, the water level of the upper Río Chagres watershed falls dry in the dry season due to a lack of water supply by unsaturated flow down the hill slope.

6. RESEARCH NEEDS

Much progress has been made with the development of a conceptual model that describes all aspects of runoff production in the upper Río Chagres watershed. However, more research is required to quantify all components of the runoff process and verify the conceptual model and hypotheses posed in Sections 4 and 5 of this paper. Specifically, we see the following research needs:

(i) Determination of (i) exactly how and over what distance macropores and soil pipes are connected, (ii) if soil pipes and macropores start at the soil surface or inside soil profile, and (iii) what is the connection between pipes and small surface depressions.

(ii) Measurement of runoff rates to study the occurrence of Hortonion runoff due to lower infiltration rates caused by water repellency and a measurement of infiltration rates to investigate the effects of macropores and cracks.

(iii) Determination of the degree of water repellency in the field as a function of soil moisture, air temperature, and relative humidity.

(iv) Determination of what part of dry season base flow is a result of soil drainage (unsaturated subsurface flow) and what part is from inflowing ground water (saturated subsurface flow) in order to quantify how future groundwater exploitation in the basin will affect base flow.

(v) A hydrologic characterization of the behaviour of aquifers underlying the upper Río Chagres basin and the amount of ground water recharge, about which little is presently known. Since these aquifers are an important and accessible source of water during periods of water scarcity in El Niño years, their assessment should have a high priority.

ACKNOWLEDGEMENTS

This study was partly funded by US Army Research Office, Terrestrial Sciences Program. Other support was provided by the Universidad Tecnológica de Panama and New Mexico Tech Support for the fieldwork was provided by the Yuma Proving Ground Tropic Regions Test Center.

REFERENCES

Abdul, AS and Gilllham, RW, 1984, Laboratory studies of the effects of the capillary fringe on stream flow generation: Water Resour. Res. 20:691-698.

Abdul, AS and Gillham, RW, 1989, Field studies of the effects of the capillary fringe on streamflow generation: Jour. Hydrol., 112:1-18.

ASCE, American Society of Civil Engineers, 1996, Hydrology Handbook. Second Edition. ASCE Manuals and Reports on Engineering Practice No. 28, New York, NY.

Anderson, MG and Burt, TP, 1977, A laboratory model to investigate the soil moisture conditions on a draining slope: Jour. Hydrol., 33:383-390.

Anderson, MG and Burt, TP, eds., 1990, *Process Studies in Hillslope Hydrology*, John Wiley and Sons, New York, NY.

Beven, K and Germann, P, 1982, Macropores and water flow in soils: Water Resour. Res., 18:1311-1325.

Bonell, M, Gilmour, DA, and Sinclair, DF, 1981, Soil hydraulic properties and their effect on surface and subsurface water transfer in a tropical rainforest catchment: Hydrol. Sci. Bull. 26:1-18.

Bonell, M, Hendricks, MR, Imeson, AC, and Haselhoff, ., 1984, The generation of storm runoff in a forested clayey drainage basin in Luxembourg: Jour. Hydrol., 71:53-77.

Bonell, M, 1993, Progress in the understanding of runoff generation dynamics in forests: Jour. Hydrol., 150:217-275.

Burch, GJ, Bath, RK, Moore, ID, and O'Loughlin, EM, 1987, Comparative hydrologic behaviour of forested and cleared catchments in south-eastern Australia: Jour. Hydrol., 90:19-42.

Burch, GJ, Moore, ID, and Burns, J, 1989, Soil hydrophobic effects on infiltration and catchment runoff: Hydrol. Proc., 3:211-222.

Calvo, LE, Ogden, FL, and Hendrickx, JMH, 2005, Infiltration in the Upper Río Chagres Basin – The Soil Conservation Service "Curve Numbers": in *The Rio Chagres: A Multidisciplinary Perspective of a Tropical River Basin* (R.S. Harmon, ed.), Kluwer Acad./Plenum Pub., New York, NY: 139-147.

Chow, VT, Maidment, DR, and Mays, LW, 1988, *Applied Hydrology*, McGraw-Hill, Inc., New York, NY.

Clothier, B and Scotter, D, 2002, Unsaturated water transmission parameters obtained from infiltration: in *Methods of Soil Analysis. Part 4. Physical Methods. Soil Science* (JH Dane and GC Topp, eds.), Soil Sci. Soc. Amer., Madison, WI: 879-898.

Dane, JH, and Hopmans, JW, 2002, Hanging water column: in *Methods of Soil Analysis. Part 4. Physical Methods. Soil Science* (JH Dane and GC Topp, eds.), Soil Sci. Soc. Amer., Madison, WI: 680-683.

Dekker, LW, 1998, Moisture variability resulting from water repellency in Dutch soils: PhD Thesis, Wageningen Agricultural Univ., The Netherlands. 240p.

Dekker, LW and Jungerius, PD, 1990, Water repellency in the dunes with special reference to the Netherlands: Catena Suppl., 18:173-183.

Dingman, SL, 2002, *Physical Hydrology*, Prentice-Hall, Inc., Upper Saddle River, NJ.

Doerr, SH, Dekker, LW, Ritsema, CJ, Shakesby, RA, and Bryant, R, 2002, Water repellency of soils: the influence of ambient relative humidity: Soil Sci. Soc. Amer. Jour., 66:401-405.

Dunne, T, 1978, Field studies of hillslope flow processes, in *Hillslope Hydrology* (MJ Kirkby, ed.), John Wiley and Sons, New York, NY: 227-293.

Dunne, T and Black, RD, 1970, Partial area contributions to storm runoff in a small New England watershed: Water Resour. Res., 6:1296-1311.

Elsenbeer, H and Cassel DK, 1990, Surficial processes in the rain-forest of western Amazonia: IAHS Publ., 192:289-297.

Elsenbeer, H, Cassel, K, and Castro, J, 1992, Spatial analysis of soil hydraulic conductivity in a tropical rain forest catchment: Water Resour. Res., 28:3201-3214.

Feng, GL, Letey, J, and Wu, L, 2002, The influence of two surfactants on infiltration into a water-repellent soil: Soil Sci. Soc. Amer. Jour., 66:361-367.

Freeze, RA, 1972, Role of subsurface flow in generation surface runoff: 2. Upstream source areas: Water Resour. Res., 8:1272-1283.

Freeze, RA, 1974, Streamflow generation: Rev. Geophys. Space Phys., 12:627-647.

German, PF, 1986, Rapid drainage response to precipitation: Hydrol. Proc., 1:3-13.

Harrison, JBJ, Vega, D, Calvo-Gobbetti, LE, Rojas, P, and Hendrickx, JMH, 2005, Spatial variability of soil in two small first order drainage basins, Río Chagres watershed, Panama: in *The Rio Chagres: A Multidisciplinary Perspective of a Tropical River Basin* (R.S. Harmon, ed.), Kluwer Acad./Plenum Pub., New York, NY: 97-112.

Hendrickx, JMH and Walker, G, 1997, Recharge from precipitation. in *Recharge of Phreatic Aquifers in (Semi)-Arid Areas.* (I. Simmers,ed.), Balkema, Rotterdam, The Netherlands.

Hewlett, JD and Hibbert, AD, 1963, Moisture and energy conditions within a sloping soil mass during drainage: Jour. Geophys. Res., 68:1081-1087.

Horton, RE, 1933, The role of infiltration in the hydrologic cycle: Trans. Am. Geophys. Union, 14:446-460.

Horton, RE, 1945, Erosional development of streams and their drainage basins: hydrophysical approach to quantitative morphology: Bull. Geol. Soc. Amer., 56:275-370.

Jackson, CR, 1992, Hillslope infiltration and lateral downslope unsaturated flow: Water Resour. Res., 28:2533-2539.

Jaramillo, DF, Dekker, LW, Ritsema, CJ, and Hendrickx, JMH, 2000, Occurrence of soil water repellency in arid and humid climates: Jour. Hydrol., 231-232:105-114.

Jayatilaka, CJ, Gillham, RW, Blowes, DW, and Nathan, RJ, 1996, A deterministic-empirical model of the effect of the capillary fringe on near-stream area runoff. 2. Testing and application: Jour. Hydrol., 184:317-336.

King, PM, 1981. Comparison of methods for measuring the severity of water repellency of sandy soils and assessment of some factors that affect its measurement: Aust. Jour. Soil Res., 19:275-285.

Kirkby, MJ, ed, 1978, *Hillslope Hydrology*, John Wiley and Sons, New York, NY.

Krammes, JS and DeBano, LF, 1965, Soil wettability: a neglected factor in watershed management: Water Resour. Res., 1:283-286.

Letey, J, Osborn, JF, and Valoras, N, 1975, Soil water repellency and the use of non-ionic surfactants: Calif.Water Resour. Center Contr. No. 154, Univ. California, Davis CA.

McCuen, RH, 1998, *Hydrologic Analysis and Design*: Prentice Hall, Inc., Upper Saddle River, NJ.

Mosley, MP, 1979, Streamflow generation in a forested watershed, New Zealand: Water Resour. Res., 15:795-806.

Mosley, MP, 1982, Subsurface flow velocities through selected forest soils, South Island, New Zealand: Jour.Hydrol., 55:65-92.

Neary, DG, Gottfried, GJ, and Folliott, PF, 2003. Post-wildfire watershed flood responses: 2nd Int. Wildland Fire Ecology and Fire Mgmt. Congress; Session 1B, Fire effects on soils/watershed. Orlando, FL.

Niedzialek, JM, and Ogden, FL, 2005, Runoff production in the Upper Río Chagres Catchment, Panama: in *The Rio Chagres: A Multidisciplinary Perspective of a Tropical River Basin* (R.S. Harmon, ed.), Kluwer Acad./Plenum Pub., New York, NY: 149-168.

Nutter, WL, 1975, Moisture and energy conditions in a draining soil mass: Atlanta, GA: Georgia Inst.Tech. Env. Resour. Center ERC 0875.

Sklash, MG and Farvolden, RN. 1979, The role of groundwater in storm runoff: Jour. Hydrol., 43:45-65.

Space, MI, Ingraham, NI, and Hess, JW, 1991, The use of stable isotopes in quantifying groundwater discharge to a partially diverted creek: Jour. Hydrol., 129:175-193.

Stresky, SJ, 1991, Morphology and flow characteristics of pipes in a forested New England hillslope: M.Sc. Thesis, Univ. New Hampshire, Durham, NH.

USBR, 1984, *Drainage Manual: A Water Resources Technical Publication*. USDI Bureau of Reclamation, Denver CO.

Ward, RC, 1984, On the response to precipitation of headwater streams in humid areas: Jour., Hydrol. 74:171-189.

Weyman, DR, 1970, Throughflow on hillslopes and its relation to the stream hydrograph: Int. Assoc. Sci. Hydrol. Bull., 15:25-32.

Chapter 9

INFILTRATION IN THE UPPER RÍO CHAGRES BASIN, PANAMA:

The Soil Conservation Service "Curve Numbers"

Lucas E. Calvo[1], Fred L. Ogden[2], and Jan M.H. Hendrickx[3]
[1]Universidad Tecnológica de Panama, [2]University of Connecticut, [3]New Mexico Institute of Technology

Abstract: Annual runoff hydrographs recorded by the Panama Canal Authority in the upper Río Chagres basin indicate several peculiar features. First, the annual hydrograph is strikingly seasonal, with very few signs of direct runoff and a continuous decay in base flow during the dry season. Secondly, there are signs of anomalously high runoff production efficiencies early in the wet season. Thirdly, the base flow from the catchment exhibits up to three different "quasi-stable" base flow discharges as the wet season progresses. This study examined runoff generation in the upper Río Chagres basin using the US Department of Agriculture, Natural Resources Conservation Service '*Curve Number*' *(CN)* methodology. Specifically, variation curve of the *CN* was analyzed using rainfall and runoff observations from the basin. Results indicate significant influence of seasonality on the *CN*. Furthermore, there are significant inter-seasonal changes in the *CN* that invalidate the applicability of the *CN* approach in this tropical watershed.

Keywords: Panama; Río Chagres; rainfall-runoff; hydrograph analysis

1. THE UPPER RÍO CHAGRES BASIN

The upper Río Chagres basin is one of the most important hydrologic catchments in Panama. Runoff from this basin represents a significant fraction of the water used to transit ships through the Panama Canal. Furthermore, this catchment provides drinking water for a large fraction of the population of Panama City. The basin is located on the eastern edge of the Panama Canal Watershed, as shown in Figure 1 (Panama Canal Commission, 1994).

R. S. Harmon (ed.), The Río Chagres, Panama, 139-147.

According to Robinson (1985): …"A large portion of the basin is covered with thick, tropical rainforest. The terrain found along the river is probably the most rugged found in the entire Panama Canal Watershed. Landslides are seen in many places and indicate that even with thick foliage, erosion does occur. High hills with 45 degree slopes are common and the divide elevation rises up to 2500 ft (760 m) near the headwaters."

Rainfall and streamflow have been continuously recorded since 1933 at the Chico gage, located at the outlet of the upper Río Chagres basin, which has a drainage area of 411 km^2. A second gage, located in the downstream reaches of one of the major Río Chagres tributaries - the Río Piedras - has been recording rainfall and river stages since 1985. However a stage-discharge relation for the Piedras gage was not developed until after December, 2000 (Ogden, 2003, see CD accompanying this volume). Beginning in 1998, additional five rain gaging stations were installed in or near the boundary of the catchment at places called: Candelaria, Esperanza, Limpio, Río Piedras and Vista Mares. Figure 1 shows also the location of these stations inside the upper Río Chagres basin.

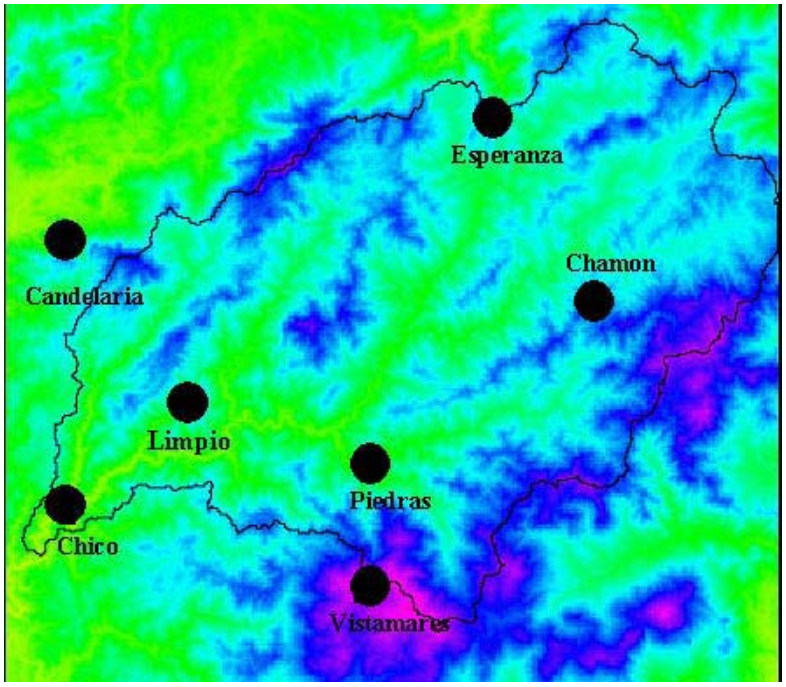

Figure 1. The upper Río Chagres basin, showing major rivers and streams.

2. DETERMINATION OF CURVE NUMBERS

Design rainfall runoff hydrology and environmental impact analysis draws heavily on the *'Curve Number' Method'* (USDA-SCS, 1972). The centerpiece of the method is the *'Curve Number'* coefficient (or *CN*), a measure of a watershed's hydrologic response potential, and usually selected from handbooks based on soils, cover, and land use. It can be shown that, when used to calculate rainfall excess and synthesis of composite hydrographs, the *CN* value is the most influential factor that determines flood peaks and volume,

The *CN* concept has been around for a considerable length of time (Ponce and Hawkins, 1996). The longevity of the approach lies in its simplicity. It has been re-interpreted several times (Steenhuis *et al.,* 1995), and has been the subject of much discussion. Limited comparisons elsewhere have suggested significant departures between handbook and data-defined *CN*s. In addition, the primary reference for the *CN* method, National Engineering Handbook#4, suggests that the soils-based table values are only guides, and that local values should be used if possible. A joint workgroup was formed by the US Department of Agriculture to review the *CN* procedure in terms of current field measurements. As a result of this workgroup much of the National Engineering Handbook has been rewritten to improve consistency and clarity (Hjelmfelt *et al.,* 2000). Furthermore, an asymptotic method was developed for determining *Curve Numbers* from rainfall-runoff data.

One of the principal modifications done by the group was to remove reference to the antecedent moisture conditions (AMC). Variability is incorporated by considering *CN* as a random variable and the AMC-I and AMC-III conditions as bounds on the distribution.

The equation utilized by the Soil Conservation Service for direct runoff estimation is:

$$Q = \frac{\left(P - 0.2S\right)^2}{\left(P + 0.8S\right)} \tag{1}$$

for $P > 0.2S$, where Q and P are the direct runoff and rainfall depths, and S is a storage index, all in inches. *CN* is a transformation of *S*, or:

$$CN = \frac{1000}{S + 10} \tag{2}$$

The runoff equation can be solved via the quadratic formula to yield:

$$S = 5\left(P + 2Q - \sqrt{4Q^2 + 5PQ}\right) \tag{3}$$

If values for *Q* and *P* are available from local watersheds, then *S* and *CN* can be calculated for every event with $0 < Q < P$. *CN* may vary from 0 to 100, although *CN*s are typically in the range of 55-95.

The above procedure works well using "ordered" *P* and *Q* data (Hawkins, 1993). That is, when *P* and *Q* are matched by rank order. This unnatural pairing matches the frequency of each, in keeping with the dominant usage of the method. That is, to estimate the (for example) 100-yr runoff from the100-yr rainfall. When this is done, often times a strong secondary relationship remains between the *CN* and *P*. For most cases, this relationship is well described by the function:

$$CN = CN_\infty + (100 - CN_\infty)e^{-kP} \tag{4}$$

where CN_∞ and k are coefficients to be determined. A least squares procedure for fitting the above equation can be developed. As CN_∞ is the asymptotic stable value approached as *P* grows larger, it is more appropriate for large events, such as design storms, and thus CN_∞ is taken as the defining *CN* for the watershed.

3. DETERMINATION OF CURVE NUMBERS FOR THE UPPER RÍO CHAGRES BASIN

A total of 31 storm events were selected for which precipitation and discharge were recorded from 1998 to 2000 in the upper Río Chagres basin (Table 1). Within this period at least five rain gauges were working in the basin. Discharge measurements were used from the Chico gage, at the basin outlet.

The Thiessen Polygon Method was used to estimate the average rainfall depth, *P*, in the basin. For the 1998 and 1999 storms, data were available from six rain gage stations; for 2000 no data were available for the Limpio gage. After constructing the polygons and measuring the areas, the weights shown in Table 2 were obtained. Care should be taken in the determination of *P* to include only those precipitation intervals that corresponds in fact to the analyzed event.

The total direct runoff, *Q*, is obtained by separating the baseflow from the total hydrographs measured on Chico gage. Baseflow was separated by a

Table 1. Selected storm events and estimated CNs

Date (dd/mm/yy)	**P** (inches)	**Q** (inches)	**S** (inches)	**CN**	**Q_i** (ft^3/sec)
23/07/99	2.83	0.76	3.70	73.01	2000
25/05/98	2.03	0.71	2.05	82.96	1700
11/08/99	1.69	0.27	3.13	76.16	1210
26/08/99	1.94	0.44	2.87	77.69	1670
19/08/98	2.54	0.29	5.58	64.20	773
17/05/98	2.34	2.15	0.17	98.35	290
27/09/98	1.07	0.23	1.65	85.87	1052
22/11/98	0.89	0.22	1.24	89.00	1100
04/07/98	1.68	0.29	3.01	76.89	521
03/08/98	0.61	0.16	0.81	92.52	975
25/09/99	1.72	0.37	2.64	79.09	1003
11/07/99	1.42	0.52	1.38	87.91	1619
10/11/99 I	0.25	0.07	0.31	96.99	1440
10/11/99 II	1.09	0.32	1.31	88.40	1980
31/08/99	0.81	0.18	1.22	89.15	1424
26/09/99	1.56	0.18	3.41	74.58	1392
13/11/99	0.87	0.13	1.69	85.58	2110
25/04/98	1.05	0.68	0.41	96.06	290
15/06/98	1.27	0.19	2.44	80.39	700
25/08/99	1.18	0.22	2.01	83.26	1336
22/06/99	2.98	0.61	4.75	67.80	1296
08/10/00	2.02	0.98	1.37	87.95	2150
11/09/00	2.42	0.43	4.21	70.37	1040
03/08/00 I	2.60	0.49	4.36	69.63	720
03/08/00 II	1.37	0.16	3.01	76.86	1890
21/10/00	2.22	0.29	4.57	68.62	1344
17/02/99	2.15	0.33	4.07	71.07	635
07/09/98	0.51	0.09	0.89	91.82	685
11/11/99	0.20	0.07	0.19	98.16	2200
27/07/99 I	1.80	0.21	3.96	71.65	1595
27/7/99 II	0.76	0.09	1.67	85.72	2500

The values of *S* and *CN* in Table 1 were calculated using equations (3) and (2), respectively. Figure 3 shows the calculated *CN* values plotted versus the total rainfall *P* used in the calculations. Contrary to what was proposed by Hawkins (1993), the natural *P* and *Q* pairs were used in the calculation of the *CNs*, *i.e.,* those *P* and *Q* values that belong to the same hydrologic event. By choosing natural *P* and *Q,* better reproductions of the registered hydrographs were obtained.

straight line projection of the flow prior to the flood runoff (initial discharge, Q_i on Fig. 2) with a slight rise to intersect the recession curve. The surface runoff hydrograph is obtained by subtracting the baseflow ordinates from the total runoff hydrograph ordinates. The area under this hydrograph curve represents the surface runoff volume, Q. This volume was obtained by adding up the average ordinates of the surface runoff hydrograph and multiplying the result by the 15-minute time interval. Finally, this volume is expressed in inches of runoff over the drainage area.

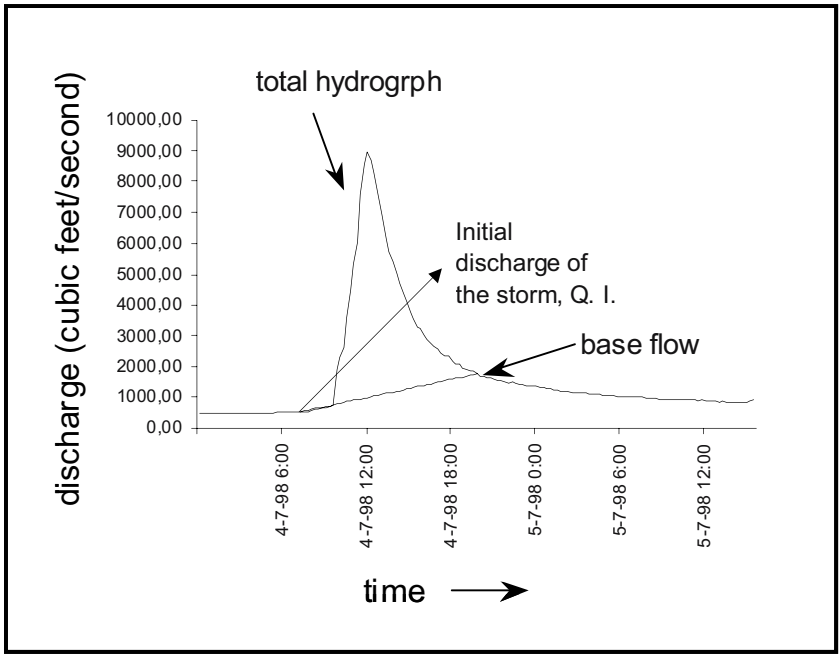

Figure 2. Registered total hydrograph for the storm of 4/7/98.

Table 2. Rain gage rainfall weights for 1998-2000

Rain Gage	1998-1999	2000
Chico	0.0563	0.1158
Río Piedras	0.2461	0.3056
Esperanza	0.4046	0.4343
Limpio	0.2080	-
Vista Mares	0.0729	0.0729
Candelaria	0.0119	0.0714

As observed in other studies, the *CN* values decline with increasing total storm precipitation *P* and then approach and/or maintain a near constant value with increasingly larger storms. Hjelmfelt *et. al.* (2000) call this the most common scenario.

The influence of the soil moisture, or the so-called antecedent moisture condition (AMC), can be considered in the effective determination of *CN*s. Three different antecedent moisture conditions have been previously defined. The AMC is identified by using the baseflow at the initial moment of the runoff event, Q_i, as a guide. A high Q_i value would indicate that a lot of water had been infiltrated recently in the basin to produce high soil moisture conditions. A low Q_i would indicate that no significant precipitation events have occurred in some time, so the soil moisture state would be low.

As shown on Figure 3, when Q_i was less than 300 ft^3/sec, as for the events of 25/04/98 and 17/05/98 (Table 1) that occurred in the dry season, the resulting *CN* values were unusually high. This suggests some process that increases runoff production efficiency, such as hydrophobicity due to water- repellent soils, with the very first rains at the end, or in the middle, of the dry season. When the Q_i was between 500 and 1600 ft^3/sec the *CN* values varied regularly with the total precipitation, which corresponds to the normal soil moisture conditions AMC-II described in the National Engineering Handbook #4. The moisture state equivalent to AMC-III was observed for Q_i >1600 ft^3/sec. In this case the *CN* values were higher than those on the previous case indicating elevated soil moisture.

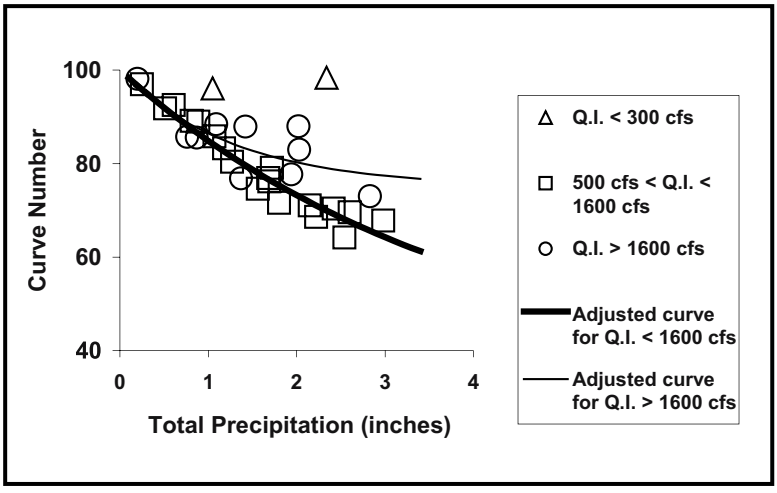

Figure 3. Variation of *CN* with total precipitation *P* for the upper Río Chagres basin.

The asymptotic exponential curve of the equation (4) was adjusted for the following cases: 500 $ft^3\ s^{-1} < Q_i < 1600\ ft^3\ s^{-1}$ and $Q_i > 1600\ ft^3\ s^{-1}$ with the help of the least squares method. The values for CN_∞ and k obtained on both cases were: $CN_\infty = 34$; k = -0.26 and $CN_\infty = 75$; k = -0.78, respectively. If the "ordered pairs" proceeding would have applied over all the storm events of Table (1), the resulting values would be CN_∞ = 66; k = -0.68. Thus, a recommended *CN* value for extreme storm events on the upper Río Chagres basin is: *CN* = 75 during the wet season.

4. CONCLUSION

The infiltration coefficient *CN* was determined using rainfall and discharge data from the Chico stream gage on the upper Río Chagres basin. This analysis used *P* and *Q* pairs belonging to the same event, and different infiltration behaviors were investigated according to the different antecedent moisture conditions, AMC, defined using the baseflow at the initial discharge prior to a runoff event, Q_i. The AMC conditions evaluated are, to a strong degree, influenced by the seasonality of the Panamanian climate.

Unusually-high runoff *CNs* were calculated (>0.95) for two events that occur very early in the wet season, during April and May 1998 (denoted by the open diamonds on Fig. 3). It is not known exactly why these anomalously-high values of *CN* occur. Possible explanations include water repellent soils (hydrophobicity) that may arise in the upper Río Chagres basin in the presence of hard rains at the beginning of the wet season (*e.g.,* Hendrickx *et al.*, 1993; Jaramillo *et al.,* 2000). In fact, water repellent soils were observed on several instances during dry season field investigations. Other explanations might include errors in rainfall estimation, or some other unknown phenomena.

5. FUTURE RESEARCH DIRECTIONS

The role of rainfall interception by vegetation is poorly understood in triple-layer tropical forest canopy under the seasonal climatic conditions of Panama. Similarly, the role of evaporation from interception is poorly understood for Panamanian conditions. Finally, quantification of evapotranspiration is complicated by the triple layer canopy, large canopy heights, and rugged terrain.

Discharges to the river due to deep groundwater circulation have not been quantified to date, which adds considerable uncertainty to our base flow separation technique. Rainfall observations from the existing network

of gages in the catchment may not adequately describe the true spatial distribution of rainfall, as it seems highly dependent upon both elevation and latitude (Knox *et al.,* 2005, this volume).

The issue of hydrophobic soils remains unsettled. The exact process or compounds that cause hydrophobicity or their persistence into the wet season is not known for the conditions that exist in Panama. Furthermore, the soils in the watershed have been observed to exhibit significant cracking during the dry season due to shrinking. Undetermined at this time are both the spatial extent of soils with high shrink/swell potential and the role of soil cracking on hydrology in this tropical watershed.

REFERENCES

Hawkins, RH, 1993, Asymptotic determination of runoff curve numbers from data: Jour. Irrig. Drainage Eng., 119: 344-345.

Hendrickx, JMH, Dekker, LW, and Boersma, OH, 1993, Unstable wetting fronts in water repellent field soils: Jour Envi. Qual., 22: 109-118.

Hjelmfelt, AT, Woodward, DA, Conaway, G, Plummer, A, Quan, QD, Van Mullen, J, Hawkins, RH, and Rietz, D, 2000, Curve Numbers, Recent Developments: USDA Nat. Resour. Cons. Serv., Washington, DC.

Jaramillo, DF, Dekker, LW, Ritsema, CJ, and Hendrickx, JMH, 2000, Occurrence of soil water repellency in arid and humid climates: Jour. Hydrol., 231/232: 105-114.

Knox, R, Ogden, FL, and Dinku, T, 2005, Using TRMM to Explore Rainfall Variability in the Upper Río Chagres Catchment, Panama: *The Río Chagres: A Multidisciplinary Perspective of a Tropical River Basin* (RS Harmon, ed.), Kluwer Acad./Plenum Pub., New York, NY: 211-226

Ogden, FL, 2003, Rating Curve Development for the Río Piedras Stream Gaging Station Upstream from the Río Chagres in the Panama Canal Watershed: Project report submitted to the US Army Res. Office and Panama Canal Authority, Dept. Civil Env. Eng., U-2037, Univ. Connecticut, Storrs, CT.

Panama Canal Commission. 1994, Panama Canal Watershed Hydrology 1993: Balboa, Panama.

Ponce, VM and Hawkins, RH, 1996, Runoff curve number: has it reached maturity?: Jour. Irrig. Drainage Eng., 1:1-19.

Robinson, F, 1985, A Report on The Panama Canal Rain Forest: Meteorol Hydrog. Branch, Eng. Div., and Eng. Const. Bureau, Panama Canal Commission.

Steenhuis, TS, Winchell, M, Rossing, J, Zollweg, JA, and Walter, MF, 1995, SCS runoff equation revisited for variable-source runoff areas, Jour. Irrig. Drainage Eng., 121: 234-238.

USDA Soil Conservation Service, 1972, National Engineering Handbook, Section 4: Hydrology, US Dept. Agriculture Nat. Resour. Cons. Serv. (formerly SCS), Washington, DC.

Chapter 10

RUNOFF PRODUCTION IN THE UPPER RÍO CHAGRES WATERSHED, PANAMA

Justin M. Niedzialek and Fred L. Ogden
University of Connecticut

Abstract: Runoff production in tropical watersheds is governed by a wide variety of potential sources and there have been few rigorous studies to date. The 414 km^2 upper Río Chagres basin offers a unique opportunity to better understand the runoff production mechanisms in tropical watersheds through data analysis and modeling with rainfall and runoff data. Flow data and tipping bucket rain gage data are available at both the basin outlet (Chico gage) and for an 80.6 km^2 internal basin location (Piedras gage). Modeling is performed using the Sacramento Soil Moisture Accounting Model (*SAC-SMA*), calibrated using data from 2000 and verified using data from 2001. The flood event of 28-31 December 2000 was examined in detail. Data analysis and modeling reveal critical threshold storages in the catchment, and anomalously high runoff production at the start of the wet season. This conclusion is supported by field studies that reveal evidence of high storage capacity and dry season water repellency. Observation of discrete quasi-stable baseflows in the upper Río Chagres is not seen in the internal Rió Piedras drainage, which is shown to exhibit ephemeral behavior year-round. New data collection and monitoring is proposed for the upper Río Chagres catchment, including measurements of rainfall above canopy, cloud stripping, stemflow, throughfall, soil moisture, interflow, and overland runoff measurements.

Key words: Panama; Río Chagres; tropical runoff production; hydrologic modeling; hydrologic monitoring;

1. INTRODUCTION

The 414 km^2 upper Río Chagres basin offers a unique opportunity to better understand runoff production mechanisms in tropical watersheds through data analysis and modeling using rainfall and runoff data. This paper examines the hydrologic properties and quantifies runoff production mechanisms relevant to the upper Río Chagres basin.

R. S. Harmon (ed.), The Río Chagres, Panama, 149-168.

The hydrology of tropical, forested watersheds varies significantly from that of their well-studied, temperate counterparts. Therefore, detailed field studies of the hydrologic cycle at the watershed scale are of significant interest to the hydrologist. Results of field studies to quantify the various components of tropical forest hydrology have provided mixed results to date. According to Fournier (1978), throughfall by leaf drainage of water reaching the ground has been estimated to be approximately 60-80% in the tropics. Stemflow in tropical forests has been shown in to vary between 1-18% in Puerto Rico and interception by the tree canopy observed to be about 5% in Costa Rica. Variations in these results highlight how difficult it is to quantify the many factors that need to be considered in tropical watershed hydrology. Not surprisingly, results vary considerably from one study watershed to another. Thus, generalizations of tropical runoff production mechanisms should be made with care.

Analysis of the upper Río Chagres from the Chico gage (Fig. 1) discharge record suggests the presence of discrete quasi-stable baseflow levels. Conversely, small and intermittent baseflow levels are observed at the internal Piedras gage, a station located in the lower reaches of the Rió Piedras sub-basin (Fig. 1). Providing an acceptable explanation of the baseflow differences is not a trivial task. There is evidence for several conflicting runoff production mechanisms within the upper Río Chagres basin. On one hand, there is evidence of dry season soil cracking in parts of the watershed, which would imply that there is an increased storage volume for rainfall during the dry season. However, qualitative results of simple field studies indicate that there is evidence of dry season soil water repellency (Hendrickx *et al.,* 2005, Chapter 8) that would tend to increase runoff in the dry season and perhaps early wet season.

Modeling of the upper Río Chagres basin to gain further insight into the exact runoff mechanisms is accomplished with the use of the Sacramento Soil Moisture Accounting Model, *SAC-SMA* (Burnash *et al.,* 1973). Gan and Burges (1990a, b) performed a comparison of *SAC-SMA* with a fully distributed, physics-based hydrologic model to evaluate the physical interpretation of SAC model parameters. Gan and Burges (1990a. and 1990b) concluded that SAC model parameters provided little meaning in the way of hydrologic reality and performed poorly when predicting extreme events. Their advice was heeded regarding *SAC-SMA* parameter interpretation, however when the immense distributed model data sets are not available *SAC-SMA* can still be a valuable resource when used with careful consideration. In fact, *SAC-SMA* is the hydrologic component used in the National Weather Service (NWS) river forecast system and has been implemented by the Autoridad del Canal de Panama (ACP). Future research is envisioned using a distributed modeling framework.

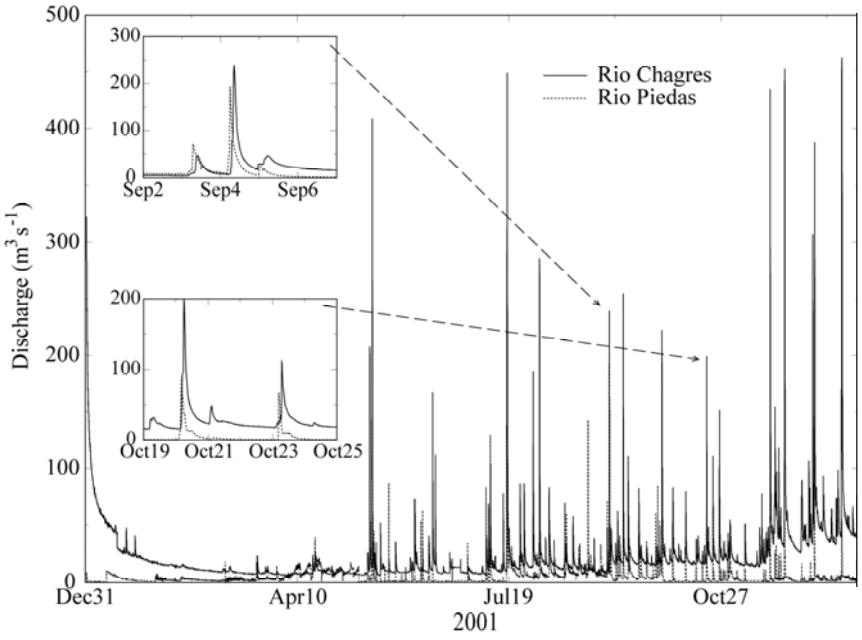

Figure 1. Discharge record for 2001 from the Rió Piedras and the upper Río Chagres. Inset figures illustrate the detailed hydrograph hs for two arbitrarily chosen runoff producing events.

2. DATA ANALYSIS

In and around the upper Río Chagres basin, there is a wide range of data sources available to facilitate a detailed hydrologic analysis. ACP operates seven rain gages, two of which provide a historical record almost 50 years in length. Two stream gages have been continuously monitored for an extended period, one gage is at the Chico station located in the lower reaches of the upper Río Chagres basin just above the outflow to Lago Alhajuela. The other, the Rió Piedras station, is located within an internal sub-basin just upstream of the Rió Piedras confluence with the Río Chagres. The locations of these stations and rain gage locations within the upper Río Chagres basin are shown in Figure 2.

There is a well-established rating curve for the Chico stream gage that defines the upper Río Chagres watershed. River stage levels have been continuously monitored at the Rió Piedras gage station for nearly 50 years, however a traditional rating curve was never developed to relate the stage

level to discharge. The Piedras stream gage rmonitors a catchment area of approximately 80.6 km^2. A combination of river cross-sectional surveys, velocity measurements, and the US Army Corps of Engineers *HEC-RAS* software package was used to develop an approximate rating curve (Ogden, 2003). The rating curve was developed using survey data from February 2001, thus any significant sediment deposition or changes in channel geometry, from an extreme event, since that time will create errors in the rating curve. Further, the rating curve should only be applied to stage data from 2001 to the present as there was an extreme runoff producing event in December 2000. Periodic re-surveying should be performed to minimize errors. The rating curve should be accurate to within 50% for flows less than 10 cm and within 10-15% for larger flows. A copy of the report and the rating curve is provided on the CD that accompanies this volume.

Comparison of the Chico gage discharge records for the Río Chagres with those for the internal Piedras gage for the Rió Piedras tributary provides a unique opportunity to study the runoff production mechanism within each catchment. Discharge data for both gages are plotted together in Figure 1. Precipitation in Panama consists of a distinct rainy season, typically lasting from early May until mid-December, this trend is observed in the runoff record shown in Figure 1. A further description of the relevant climatology of Panama is given by Espinosa (2003) and Palka (2005, Chapter 1).

There are several interesting features of the two catchments shown in Figure 1. As would be expected for an internal catchment, the timing of discharge is offset and there is an overall smaller volume of discharge for the Rió Piedras. This is particularly easy to see with the insets of Figure 1 that focus on two arbitrarily selected runoff-producing events. It is also interesting to note that the first inset event shows that the Rió Piedras contributes nearly all of the runoff of the upper Río Chagres basin whereas this behavior is not observed in second inset. The upper Río Chagres discharge record from the Chico station exhibits periods of quasi-stable baseflow that are seemingly triggered by critical threshold storages. The Rió Piedras, by contrast, does not exhibit the same baseflow behavior; in fact, its character more closely resembles that of an ephemeral stream.

Why are there such different baseflow responses for the upper Río Chagres and the Rió Piedras? There are several possible explanations for the differences in groundwater discharges as seen at these two different spatial scales. Perhaps there is a larger, regional groundwater circulation from the headwaters of the upper Río Chagres to the outlet bypassing the Rió Piedras. In the upper parts of some catchments, tributary streams are often perched above the regional groundwater table (Foster, 1993).

Ward (1984), from the results of Hewlett and Hibbert (1967), points out that the majority of precipitation infiltrates the soil surface and enters the

stream channels through a mechanism referred to as 'quickflow.' Ward (1984) concluded that the distribution of these variable source areas is related to subsurface flow convergence.

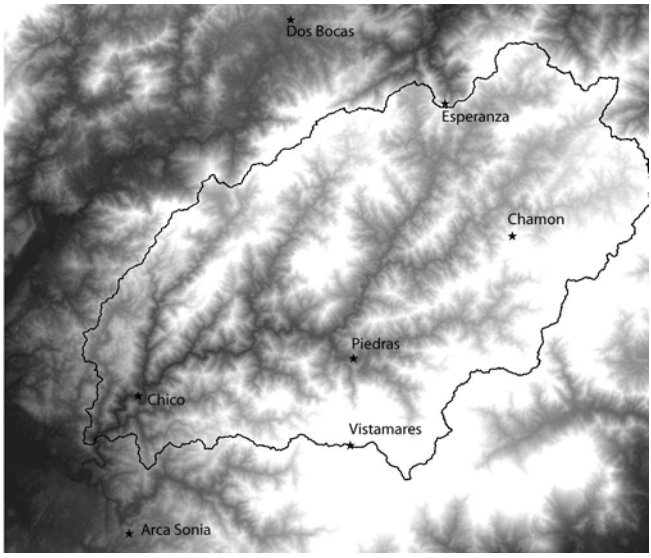

Figure 2. The location and name of rain gages in the upper Río Chagres basin. The sites designated 'Piedras' and the 'Chico' indicate the approximate locations of the two stream gages discussed in the text.

Bonnel (1993) concludes that compaction of cleared lands makes Hortonian runoff more likely and decreases groundwater recharge. There is also qualitative evidence that increased overland and subsurface flows result in increased peaks during the wet season and smaller baseflows in the dry season (Lal, 1993). This explanation is one possible explanation for the curious baseflow behavior of the Rió Piedras. However, the overall percentage of developed and deforested land seems to be rather small. There is conflicting evidence and it would be hard to quantify the effect of land use changes on baseflow. In either case, it is a potential explanation that should not be discounted.

Runoff efficiencies were computed for each basin to examine runoff response to varying rainfall inputs. The runoff efficiency of an event is

defined as ratio of the volume of runoff to the volume of rainfall. Runoff efficiencies computed for selected upper Río Chagres and Rió Piedras precipitation events during 2001 are shown in Tables 1 and 2. Runoff efficiencies for the extreme event of December 2000, are also included in Table 3, as defined by Figure 3.

Table 1. Runoff efficiencies for selected rainfall-runoff events in the upper Río Chagres watershed during 2001.

Julian Day(s)	Rainfall (mm)	Runoff (mm)	Runoff Efficiency (%)
102	28.0	1.8	6
112	18.0	1.2	7
122-128	109.0	18.0	17
130-131	56.0	32.0	57
137-138	91.0	14.0	15
156-160	78.0	22.0	28
165-168	53.0	20.0	38
209-212	88.0	52.0	59
221-222	66.0	30.0	45
249	73.0	22.0	30
270-276	140.0	61.0	44
290-297	264.0	104.0	39

Table 2. Runoff efficiencies for selected rainfall-runoff events in the Rió Piedras watershed during 2001.

Julian Day(s)	Rainfall (mm)	Runoff (mm)	Runoff Efficiency (%)
106-110	302.3	84.1	28
154-157	78.7	20.5	26
258-260	78.7	14.9	19
309-312	55.9	9.6	17
326-328	119.3	18.3	15
334	106.7	16.3	7

Runoff efficiencies for the upper Río Chagres basin are generally lower during the dry season indicating large storage potential in all compartments. There is one notable exception near day 130-131, where the runoff production efficiency is anomalously high compared with all times during the dry season. During the wet season, runoff efficiencies are higher, with values averaging slightly over 40%. As seen in Table 3 for the extreme event of 2000, there is a wetting period during the beginning of the event and runoff efficiencies increase. This is followed by a marked decrease in efficiencies, as the subsurface must have drained somewhat, before runoff

efficiencies again increase with increasing rainfall. This final increase in runoff production is culminated by the largest runoff event on 31 December 2000.

Table 3. Computed runoff efficiencies in the upper Río Chagres at the Chico gage for the extreme event of December 2000.

Event	Rainfall (mm)	Runoff (mm)	Runoff Efficiency (%)
1	225.0	95.7	43
2	39.8	24.3	61
3	10.7	6.5	61
4	41.4	15.0	36
5	113.0	64.4	57
6	177.0	137.0	77

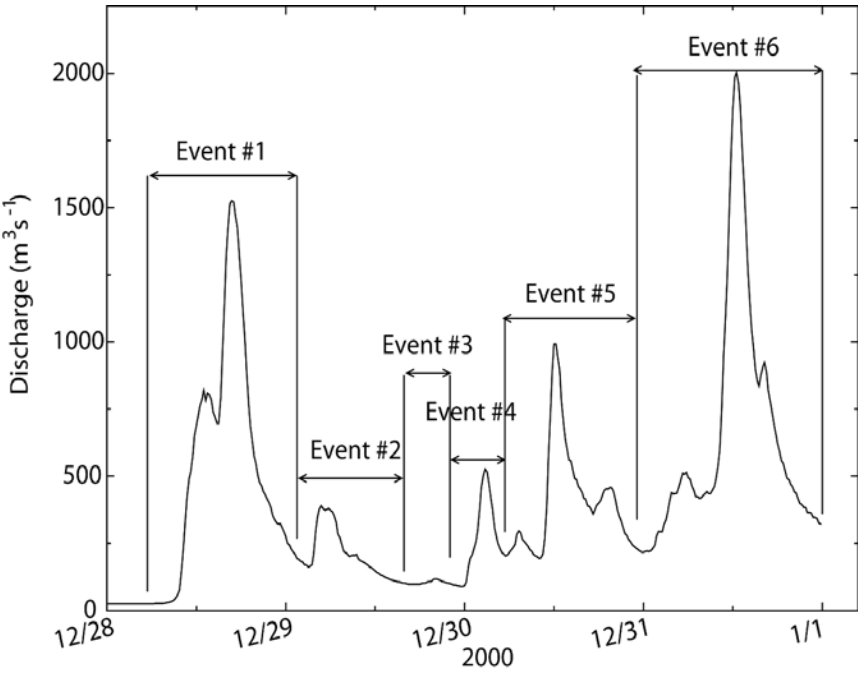

Figure 3. Definitions for the extreme runoff event of late December 2000.

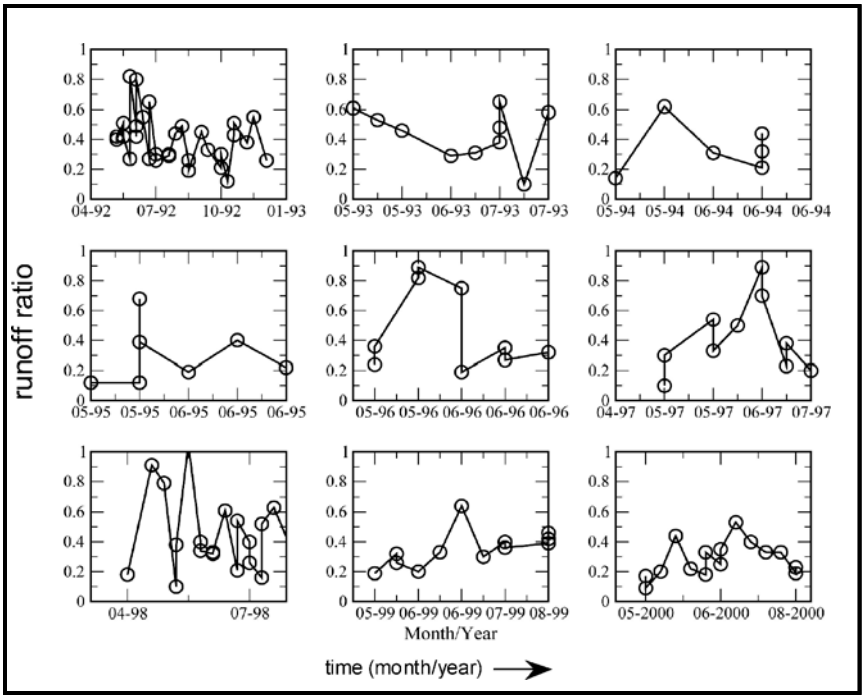

Figure 4. Historical record of runoff efficiencies calculated for the upper Rio Chagres watershed above the Chico gage.

Although a smaller sample of runoff efficiencies was computed for the Rió Piedras, significant differences are observed in Table 2. Runoff efficiencies actually decrease later in the year as the wet season progresses. On average during the dry season, runoff production efficiency for the Rió Piedras appears to be a bit larger than for the upper Río Chagres, as observed at the Chico gage. This type of response would seem to indicate increased overland flow. More analysis needs to be performed before any statistically meaningful comparisons can be made.

The anomalously high runoff efficiency observed near day 130-131 spurned interest in a further examination of several years worth of data for the Chico gage. During a typical year the largest runoff efficiencies were usually seen shortly after the start of the wet season, such as all of 1992 plotted in Figure 4. Computation of runoff efficiencies encompassing the transition from the dry to wet season were tabulated for several years and are shown in Figure 4, which illustrates that the runoff ratio frequently approaches 80%. A qualitative study showed that the high runoff ratios early in the wet season were more or less insensitive to rain rate.

3. MASS BALANCE AND SOIL MOISTURE STORAGE

A simple mass balance model reflecting the major processes of rainfall, runoff, soil moisture storage, and evapotranspiration was applied to the upper Río Chagres basin. The following form was chosen to represent each of these processes:

$$S_{t+1} = P_t - Q_t - AET_t + S_t \tag{1}$$

where S is the storage, P is the precipitation, Q is runoff, AET is the actual evapotranspiration, and t is the time resolution which will be months in this case. Each term in the mass balance equation has units of length; in particular mm will be used in the following discussion. In this simple mass balance the actual evaporation is not exactly known, therefore the following approximation based on potential evapotranspiration and soil moisture is applied:

$$AET_t = PET_t \left[\frac{S_{t+1} + S_t}{2S_{Max}} \right] \tag{2}$$

where AET is the actual evapotranspiration, PET is the potential evapotranspiration, and S_{Max} is the maximum storage. Thus the approximation of AET is based on the change in storage scaled by the maximum storage. Substituting (2) into (1) and then solving for the storage at the next month yields the final form of the mass balance equation:

$$S_{t+1} = \frac{P_t - Q_t + S_t(1 - PET / 2S_{Max})}{\left(1 + \frac{PET}{2S_{Max}}\right)} \tag{3}$$

This particular form was chosen because the only unknowns in the final form are the storage terms. Rainfall and runoff are known from gage data and the PET can be approximated as 6.0 mm/day or in this application 180.0 mm/month (Hendrickx *et al.,* 2005, this volume). A simple optimization, such as Excel solver can be applied to minimize the residuals of delta S and solve for S_{Max}. An initial guess is required for S_t, which has little influence beyond the first few months of the model, this parameter can also be included in the optimization.

Results of the mass computations using 16 years of data and averaged for each month of the year are shown in Figure 5 along with the average runoff. Figure 5 illustrates how the watershed starts with some residual storage in January from the recent cessation of the wet season and decreases as the dry season progresses. The model seems to indicate the watersheds' storage tendency to wet or dry unless a major perturbation, such as the start or the end of the wet season is applied. While this modeling exercise is lumped into a monthly temporal resolution, this observation is analogous to observations of runoff efficiencies previously mentioned and other studies at the hillslope scale, such as Dykes (2000). It must be noted that the storage terms will have some error terms built in such as interception and subsequent re-evaporation, which was not built into this simplistic representation.

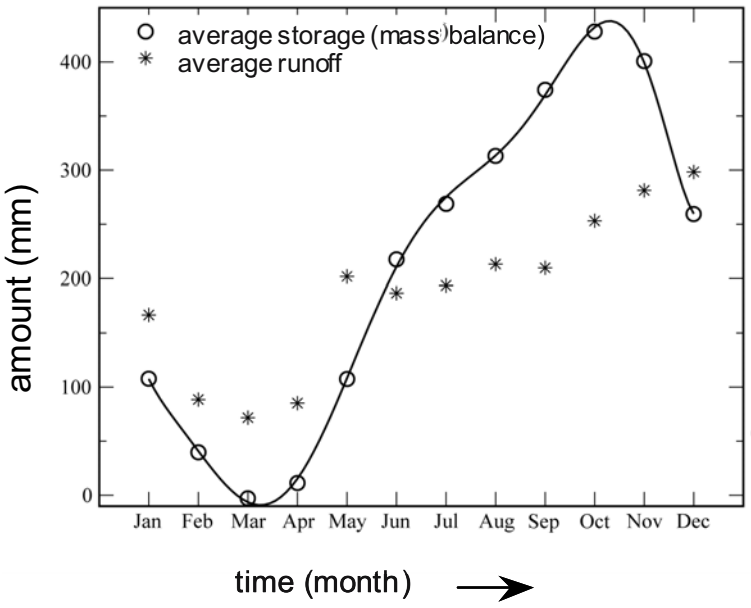

Figure 5. Monthly average values of relative soil moisture storage based on the mass balance calculations, average runoff shown for comparison.

Because the mass balance exercise hinted at a tendency for insignificant runoff perturbations during the dry season a means of quantifying such transitions was examined. One simple method of testing this theory is to determine if there is an approximately constant storage that must be filled in order to trigger a rise in baseflow. Computation of the storage required to raise baseflow was accomplished by examining upper Río Chagres hydrographs that had a clear transition in baseflow levels shortly after the

wet season onset, such as Figure 1. The date of this transition was recorded and was then plotted against the cumulative depth of rainfall thus far in the wet season. The results are shown in Figure 6a, along with a trend line inserted for visualization purposes. This analysis reveals that a mean storage of 363 mm is required to trigger an increase in baseflow with a standard deviation of appoximately 60 mm.

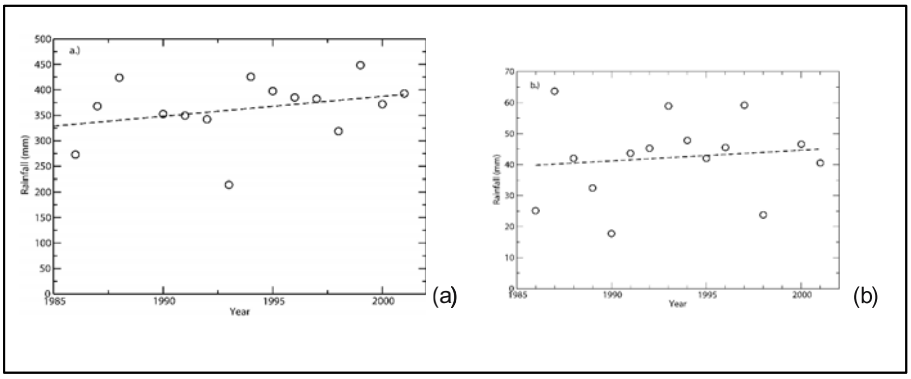

Figure 6. Historical record of the amount of rainfall required to (a) elevate the baseflow level and (b) trigger substantial runoff following the onset of the wet season as seen at the Chico gage. The trend lines are shown for visualization purposes.

The upper Río Chagres at the Chico gage rarely has significant runoff events during the dry season. The obvious explanation is the paucity of large rainfall events during this time of year. Clearly, there is enough rainfall to frequently produce flashy hydrographs once the wet season begins. A typical annual upper Río Chagres hydrograph, such as that in Figure 1, shows a sharp transition from gradually decaying baseflow during the dry season to frequent large runoff producing events early in the wet season. The date of the first large runoff event was determined and the cumulative amount of rainfall required to produce the first significant runoff was evaluated for 16 years of record. On average, approximately 42 mm of rainfall, with a standard deviation of 4.6 mm, is required to produce the first signs of significant runoff. Wheras a large spread in the data is expected due to the dynamic nature of storm events, it is instructive to note that there is a hydrologic storage that must be filled to produce the observed rises in the hydrograph at the onset of the wet season. Certainly, these observations raise many implications for the actual runoff production mechanisms, but the main point is that there is some storage that must be filled before the dynamics of runf are initiated.

4. SACRAMENTO MODELING

Watershed modeling is performed with the Sacramento Soil Moisture Accounting Model (*SAC-SMA*). The *SAC-SMA* model is a conceptual, lumped-parameter, soil moisture accounting hydrologic model included in the US National Weather Service river forecast system. Details of the model formulation are given by Burnash *et al.* (1973). Model inputs consist of rainfall and evaporation from which model output is compared against observed hydrographs. *SAC-SMA* contains a total of eight input parameters and six state variables, many of which must be computed by calibrating the model to observed data.

In *SAC-SMA*, soil-moisture storage of the watershed is conceptualized by dividing the soil into an upper and lower zone. The upper zone is sub-divided into two distinct components of storage - referred to as tension water storage, which must be filled before moisture becomes available to enter other storages, and free water storage. Percolation from the upper to the lower zone storage is partitioned similarly into a tension and free water storage. However, within the lower zone there are two storage compartments available to percolation, primary and supplementary free water storage. This sub-division allows for groundwater drainage at two different rates. The *SAC-SMA* formulation can conceptually simulate surface water runoff, direct runoff, lateral interflow, and baseflow.

Owing to the large number of *SAC-SMA* parameters and its conceptual formulation, it was decided to use an automated calibration procedure to fully explore the model parameter space. The Shuffled Complex Evolution (SCE) optimization method of Duan *et al.* (1992) was selected for this purpose. The SCE method was developed specifically for the automated calibration of lumped parameter hydrologic models. The SCE method requires the computation of a cost function; the hydrograph Root Mean Square Error (RMSE) is subjectively used as a goodness of fit indicator.

The importance of spatially varied rainfall on the performance of the upper Río Chagres basin modeling was also investigated. There is a significant amount of spatial rainfall variability within the upper Río Chagres catchment. It was initially hypothesized that a general Precipitation-Elevation (P-E) relationship existed in the watershed, perhaps due to an orographic enhancement effect. Evidence exists for this hypothesis because the higher elevation rain gages in the watershed receive significantly more rainfall than gages at lower elevations. Initially, an area-weighting scheme was applied to bins of basin elevation. For the case of the Rió Piedras sub-basin, a weighting scheme was applied using the Piedras and the Chamon rain gages. The Piedras, Chamon, Chico, Vista Mares, Dos Bocas, and Arca Soñia rain gages initially were used for the upper Río Chagres basin. In

reality, the situation is more complex (Knox *et al.,* 2005, Chapter 13). Thus, the area-weighting scheme initially applied was only an approximation. However, because of the geographic distribution of elevations and the NE-SW orientation of the two gages in the Rió Piedras catchment, the area-weighting scheme used seemed to closely mirror that of the true spatial rainfall distribution. A compromise in weighting schemes was needed and the Rió Piedras area-weighting scheme was used for testing of *SAC-SMA*. Using area-weighted rainfall, as compared to a single-gage rainfall, both the calibration and verification results for the upper Río Chagres watershed are improved. The year 2000 was chosen as a calibration year due to the limited availability of rainfall records at several of the newer rain gages.

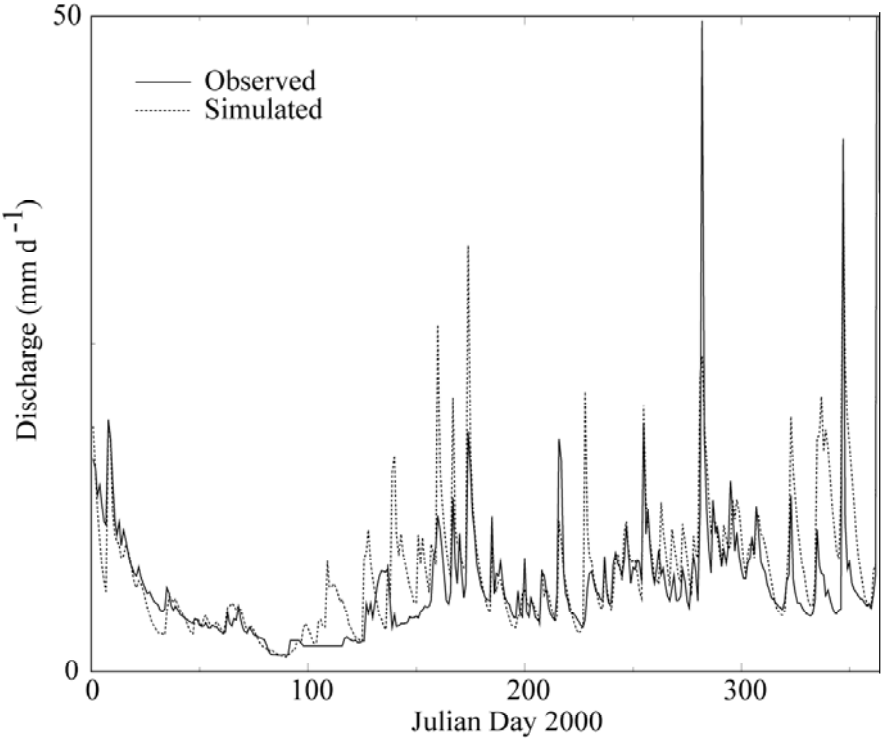

Figure 7. Sacramento model calibration results on the upper Río Chagres at the Chico monitoring station using multiple gage average rainfall.

Figures 7 and 8 show results of *SAC-SMA* calibration to the upper Río Chagres watershed with both the spatially varied rainfall and the single gage

rainfall inputs. RMSE values are improved from 26.0 to 22.7% for the calibration event and the baseflow levels are accurately simulated. Furthermore, the timing and the peak discharge for many of the runoff events are more closely matched.

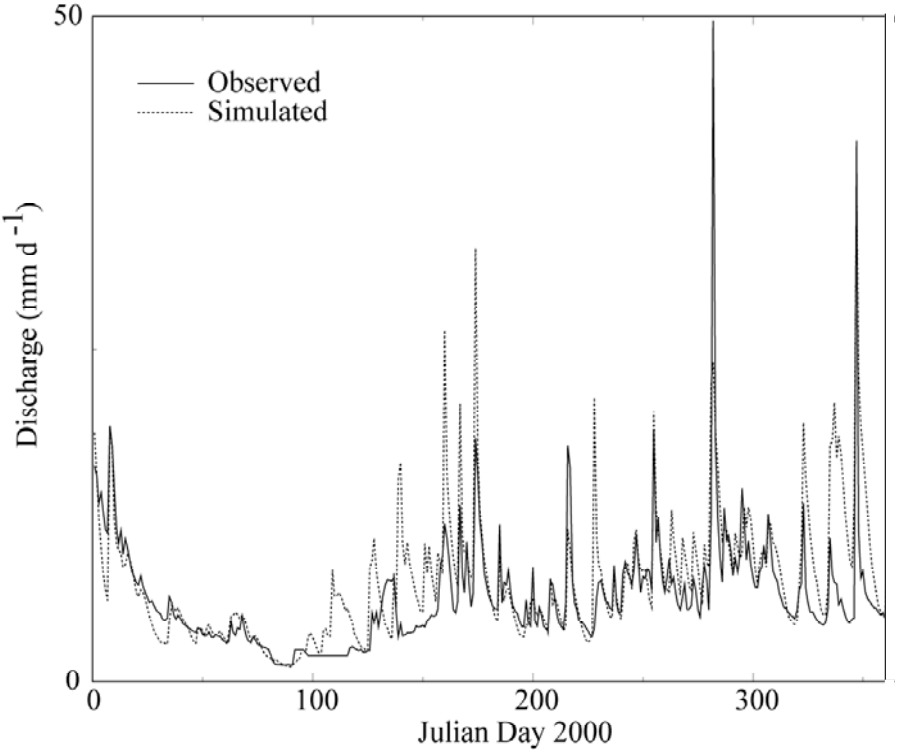

Figure 8. Sacramento model calibration results for the upper Río Chagres at the Chico gage using multiple gage average rainfall.

Results from the verification runs in Figure 9 and 10 show an improvement of the RMSE from 31.1 to 25.9%. Simulations using both the single-point and spatially-varied rainfall inputs had some trouble predicting runoff in the wet season of 2001. Particularly problematic for *SAC-SMA* are the shifts in baseflow levels exhibited during the wet season. Furthermore, the Sacramento model could not accurately reproduce the runoff observed at the Rio Piedras gage, as shown in Figure 11. The predicted baseflow is much higher than the observed data mirroring the differences in baseflow between the upper Río Chagres and Rió Piedras basins.

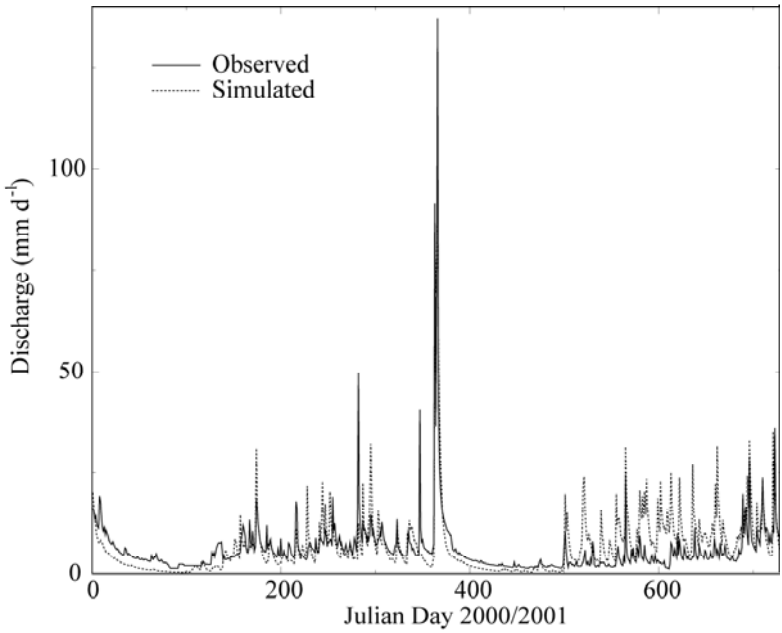

Figure 9. Upper Río Chagres verification for the single gage case.

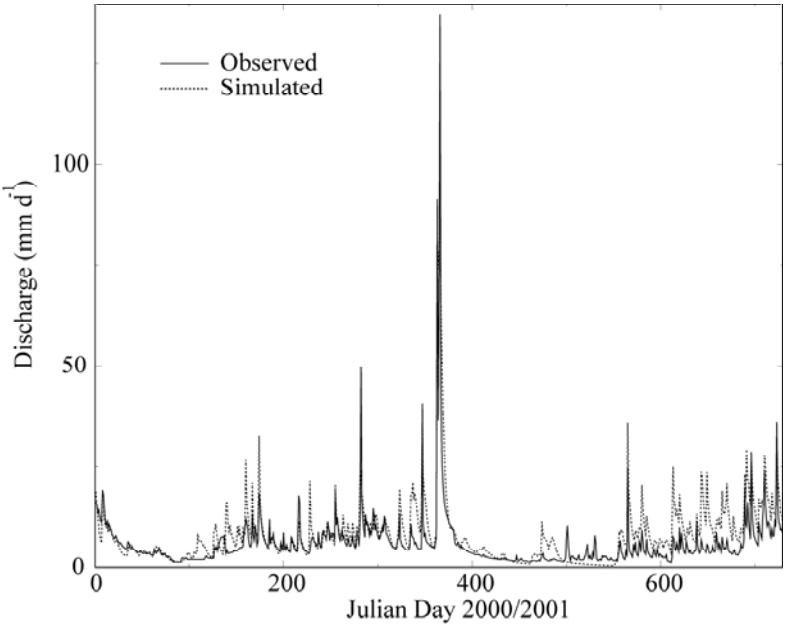

Figure 10. Upper Río Chagres verification using multiple rain gage input.

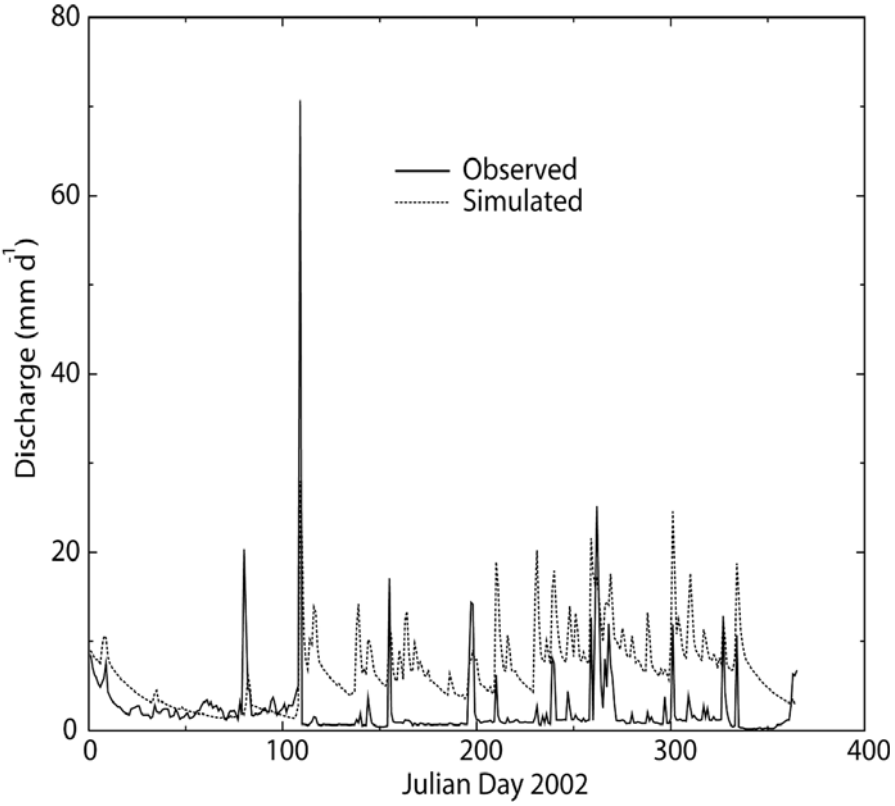

Figure 11. Sacramento modeling results for the Rió Piedras catchment using the parameter set derived from calibration of *SAC-SMA* on the upper Río Chagres at the Chico gage.

5. CONCLUSION

Results from our study of the upper Río Chagres basin indicate that rainfall climatology consideration is essential for accurate rainfall runoff simulation. Analyses from this study and by Knox *et al.* (2005, Chapter 13) in this volume indicate large rainfall gradients primarily oriented from north to south, but also increasing with elevation. Therefore, use of a single point measurement in the upper Río Chagres can lead to erroneous assumptions in the volume of rainfall input. Both model calibration and verification results showed marked improvement when a spatially distributed rainfall field was used as input.

Contribution of groundwater to streams in the Rió Piedras catchment (80.6 km^2) is much less than the entire upper Río Chagres basin (414 km^2). Unfortunately, there is no obvious explanation as to the exact mechanism.

Possible explanations include large scale, regional groundwater flows from the headwaters that bypass much of the Rió Piedras sub-basin. Potential changes in runoff production mechanisms that accompany land use changes in the Rió Piedras area should also be further examined. The latter explanation is considered less likely as the percentage of land use changes in the Rió Piedras are relatively small, but cannot be discounted because of growing clear-cutting of the tropical forest for subsistence farming and development along its southern margin.

A simple mass balance computation considering the processes of rainfall, runoff, and evaporation does a relatively good job in predicting the average soil moisture storage of the watershed. While the mass balance was performed at a monthly timescale, results indicate that dry season rainfall has little lasting effect on runoff or soil moisture. This notion is further supported by an analysis of discrete baseflow levels that were observed for the upperRío Chagres, such as Figure 1.

There was evidence to suggest that on average a constant storage of 360 mm must first be filled before large changes in the baseflow runoff are observed. Furthermore, a storage of 42 mm on average must be filled at the onset of the wet season for significant runoff to initiate in the watershed. Examination of several years of rainfall and runoff data indicates that the highest runoff ratios during the year occur shortly after the transition to the wet season. These high runoff ratios also roughly correspond to the time between wet season initiation and the 360 mm storage limit. The exact mechanism responsible for this abnormal behavior must be examined in further detail.

There is a lack of Sacramento model parameter transferability between the upper Río Chagres basin and the Rió Piedras sub-basin. In general, calibrated model parameter transfer should provide meaningful results when applied to an internal basin. This lack of transfer between the two watersheds tends to further support the notion that there may be inherent differences in the runoff production mechanisms in each catchment.

6. AREAS OF FURTHER RESEARCH

As the conclusions from this paper suggest, there is still much hydrological research needed in the upper Río Chagres watershed to better characterize runoff production. Thus, the inclusion and the importance of this section is to highlight the potential means of answering many of the questions posed by this paper. Work is presently underway to identify and install two additional stream gages in the upper Río Chagres basin. Ideally,

the two would be situated at *c.* 20 km^2 and the other at *c.* 180 km^2, which would result in the placement of four gages at varying spatial scales for data analysis and modeling of sub-catchments.

There are parts for two weather stations in Panama that could be installed within the upper Río Chagres basin. Elevations of approximately 180 m and 700 m would be used as criteria in site selection. One site that has already been preliminarily identified due to its ease of access is Gamboa (see Fig 3 of Chapter 2). Potentially, both weather stations could be sited together, one above and the other below the canopy with the use of a tower. Evapotranspiration measurements above the canopy will also be helpful in closing the land-atmosphere water balance. New data monitoring is proposed in the upper Río Chagres catchment to be patterned after the CSIRO Tropical Forest Research Instrumentation, Queensland, Australia. CSIRO Instrumentation includes measurement of rainfall above the canopy, cloud stripping, stemflow, throughfall, soil moisture, and overland runoff measurement. Such a study would be conducted in a small (*i.e.,* approximately <1 km^2) watershed to further quantify the contributions of various runoff production mechanisms.

Development of a combined *SAC-SMA* modeling framework with the distributed model, *GSSHA* (Downer and Ogden, 2004), will allow the distributed modeling of the overland flow plane, river network, and land surface atmosphere interactions. This combined framework development should be completed by the end of summer, 2003, and will undergo rigorous testing on several watersheds including the upper Río Chagres basin.

Further quantification of the spatial distribution of rainfall is essential for continued modeling efforts. This consideration will become particularly relevant with a distributed modeling framework. Radar data, such as that described by Georgakakos and Sperfslage (2005, Chapter 22) usually represents the best possible means of specifying rainfall rates at a very fine resolution throughout a study watershed, a perfect fit for distributed watershed modeling. Finally, other data sets from tropical watersheds could be useful for comparisons of runoff production and further hydrologic model research, development and testing efforts.

ACKNOWLEDGEMENTS

This study was funded by the Army Research Office, Terrestrial Sciences Program Grant DAAD19-01-1-0629. The authors would like to thank R. Harmon for organizing the Chagres Scientific Symposium that produced this volume. The Army Research Office, Autoridad del Canal de Panama, and Universidad Technologica de Panama. C. Vargas and M. Hart from ACP

graciously supplied stream and rain gage data. R. Knox and J. Zahner from the University of Connecticut provided insightful discussions and assistance with data processing and the Sacramento-SMA model.

REFERENCES

Bonell, M and Balek, J, 1993, Recent Scientific Developments and Research Needs in Hydrological Processes of the Humid Tropics: in *Hydrology and Water Management in the Humid Tropics*, UNESCO, Div. Water Sci., Paris, France: 167-260.

Burnash, RJC, Ferral, RL, and McGuire, RA, 1973, A Generalized Streamflow Simulation System: in *Conceptual Modeling for Digital Computers*, U.S. National Weather Service, Sacramento, CA.

Downer, CW, and Ogden, FL, 2004, GSSHA: A model for simulating diverse streamflow generating processes, Jour. Hydrol. Engrg., 9:161-174.

Duan, Q, Sorooshian, S, and Gupta, V, 1992, Effective and efficient global optimization for conceptual rainfall-runoff models: Water Resour. Res., 28: 1015-1031.

Dykes, A.P. and Thornes, J.B., 2000, Hillslope hydrology in tropical rainforest steeplands in Brunei, *Hydrol. Process.*, 14: 215-235.

Espinosa, JA, 2003, The Climatology of Panama: *The Río Chagres: A Multidisciplinary Profile of a Tropical Watershed*, Proc. Chagres Int. Sci. Symp.: 10.

Foster, SSD and Chilton, PJ, 1993, Groundwater systems in the humid tropics: in *Hydrology and Water Management in the Humid Tropics*, UNESCO, Div. Water Sci., Paris, France: 261-272.

Fournier, F, 1978, Water Balance and Soils: in *Tropical Forest Ecosystems a State of Knowledge Report*, UNESCO, Div. Water Sci., Paris, France: 256-269.

Gan, TW and Burges, SG, 1990, An assessment of a conceptual rainfall-runoff model's ability to represent the dynamics of small hypothetical catchments 1. Models, models properties, and experimental design: Water Resour. Res., 26: 1595-1604.

Gan, TW and Burges, SG, 1990, An assessment of a conceptual rainfall-runoff model'sability to represent the dynamics of small hypothetical catchments 2. Hydrologic responses for normal and extreme rainfall: Water Resour. Res., 26:1695-1619.

Georgakakos, KP and Sperfslage, LA, 2005, Operational rainfall and flow forecasting for the Panama Canal Watershed: in *The Río Chagres: A Multidisciplinary Profile of a Tropical Watershed* (RS Harmon, ed.), Kluwer Acad./Plenum Pub., New York, NY: 323-333.

Hendrickx, JMH, Vega, D, Harrison, JBJ, Calvo, LE, and Miller, TW, 2005, Soil Hydrology Along Steep Hillslopes in the Río Chagres Watershed: in *The Río Chagres: A Multidisciplinary Profile of a Tropical Watershed* (RS Harmon, ed.), Kluwer Acad. Pub., New York, NY: 113-138.

Hewlett, JD and Hibbert, AR, 1967,Factors Affecting the Response of Small Watersheds to Precipitation in Humid areas: in *Forest Hydrology*, Peragamon Press, Oxford, UK: 275-290.

Knox, R., Ogden, F.L., and Dinku, T., 2003, Use of TRMM observations to develop precipitation-elevation relations for the Río Chagres catchment, Panama: in *The Río Chagres: A Multidisciplinary Profile of a Tropical Watershed* (R.S. Harmon, ed.), Kluwer Acad. Pub., New York, NY: 211-226.

Lal, R, 1993, Challenges in Agriculture and Forest Hydrology in the Humid Tropics: in *Hydrology and Water Management in the Humid Tropics*, UNESCO, Div. Water Sci., Paris, France: 395-404.

Ogden, FL, 2003, Rating Curve Development for the Rió Piedras Stream Gaging Station Upstream from the Río Chagres in the Panama Canal Watershed: Report for U.S. Army Research Office, Univ. Connecticut Dept. Civil Env. Eng., Storrs, CT: 18 p.

Palka, EJ, 2005, A geographic overview of the republic of Panama: Pathway to the continents and link between the seas: in *The Río Chagres: A Multidisciplinary Profile of a Tropical Watershed* (RS Harmon, ed.), Kluwer Acad./Plenum Pub., New York, NY: 1-18.

Ward, RC, 1984, On the response to precipitation of headwater streams in humid areas: Jour. Hydrol., 74: 171-189.

Chapter 11

DOWNSTREAM HYDRAULIC GEOMETRY ALONG A TROPICAL MOUNTAIN RIVER

Ellen Wohl
Colorado State University

Abstract: The upper Río Chagres basin drains 414 km^2 of mountainous topography in central Panama. Hillslopes exceed 45^o in over 90% of the basin and are highly dissected by a predominantly bedrock channel network. A variety of igneous bedrock lithologies are exposed discontinuously along the channels, which both follow and cut across geologic structures. Local changes in channel gradient and geometry occur where the channel crosses a more resistant bedrock unit, but the longitudinal profile as a whole is concave. Coarse sediment is introduced via tributary channels and landslides. The basin has high values of discharge per unit area. Channel geometry, bed grain-size, velocity, and discharge were surveyed for 40 short (50-200 m-long) channel reaches throughout the basin to examine how downstream hydraulic geometry relations and other channel characteristics (i) compare to those from mountain drainages in temperate regions, and (ii) reflect site-specific variables versus variables such as drainage area and discharge that change progressively downstream. Downstream hydraulic geometry exponents are 0.36 for hydraulic radius, 0.43 for channel top-width, and 0.24 for mean velocity. These values are similar to the average values for rivers worldwide, despite the inclusion of step-pool, pool-riffle, and bedrock gorge reaches in the data set. The presence of strong downstream hydraulic geometry trends indicates that hydraulic driving forces sufficiently exceed resisting forces to override specific lithologic influences on channel width and depth when averaged across sub-basin to basin scales. Poor correlations between grain size and drainage area, discharge, or reach gradient and between reach gradient and drainage area or discharge suggest that landslides and bedrock lithology locally control grain size and reach gradient.

Key words: Panama; Río Chagres; river hydraulic geometry

R. S. Harmon (ed.), The Río Chagres, Panama, 169-188.

1. INTRODUCTION

Few investigators have examined river networks in mountainous tropical environments. The tropical networks might be expected to share several characteristics present in some mountain networks of temperate regions (Wohl, 2000), such as steep gradients and a segmented longitudinal profile, as expressed in knickpoints, the absence of strong linear relations between downstream hydraulic geometry variables and discharge, or abrupt changes in valley morphology.

Tropical mountain networks might also be expected to contain resistant channel boundaries dominated by bedrock and very coarse clasts; coarse sediment supplied directly from hillslopes; an abundant supply of large woody debris (LWD); minimal flood plain development; a seasonally variable hydroclimatic regime; high boundary roughness and highly turbulent flow; and stochastic bed load movement as a result of high entrainment thresholds.

Tropical river networks might differ from those in other mountainous regions because of the absence of past or contemporary glaciation. River dynamics in tropical mountainous regions might also differ because of high rates of rock weathering and LWD decay; high rates of discharge per unit drainage araea generated in portions of the tropical basins or across the entire basin by monsoonal or cyclonic precipitation; and the larger transport capacities associated with more frequent heavy precipitation across the basin. These differences might produce channels with less downstream segmentation because of the lack of glacial influence and less pronounced variability in bedrock resistance.

Tropical rivers might also be more dynamic in terms of local channel adjustment, on timescales of a year to a few decades, because of the frequent high discharges and associated high values of velocity, shear stress, and stream power, as well as an absence of stable LWD. If these inferences are correct, tropical mountain rivers might better approximate the downstream hydraulic geometry relations for fully alluvial rivers than mountain river networks in drier regions, because the tropical rivers would be more capable of adjusting channel form to discharge.

Published studies of downstream hydraulic geometry along mountain rivers are relatively few. Such studies include the work of Caine and Mool (1981) in the Middle Hills of Nepal, where hydraulic geometry relations were similar to those reported from other regions of the world (Park, 1977). Studies from the Canadian Rockies (Ponton, 1972) and the Colorado Rockies (Phillips and Harlin, 1984) demonstrated that channel characteristics did not follow the expected downstream hydraulic geometry trends because of either gradient changes related to glaciation or substantial

changes in alluvial substrate. Molnar and Ramirez (2002), using data published by McKerchar *et al.* (1998) and Ibbitt *et al.* (1998) for two mountain rivers in New Zealand, found consistent downstream trends in channel width, but weaker and less consistent downstream trends in hydraulic radius and velocity.

None of these previous studies focused on the downstream trends of mountain river channels in tropical environments. In this paper, field data from the upper Río Chagres in Panama are used to examine how downstream hydraulic geometry relations and other channel characteristics (i) compare to those from mountain drainages in temperate regions, and (ii) reflect site-specific variables versus variables such as drainage area and discharge that change progressively in a downstream direction.

2. FIELD AREA

The entire Río Chagres watershed drains 3340 km^2 in central PanamaThe 1934 creation of Madden Dam and Lago Alhajuela divided the watershed into upper and lower catchments, known as the Gatun basin and Alhajuela basin, respectively. Alhajuela is drained by three major river networks: the Río Pequeni, Río Boqueron, and upper Río Chagres, which collectively provide nearly half the water supply of the entire Río Chagres watershed. The upper Río Chagres drains 414 km^2 of this steep, mountainous terrain (Fig. 1), where hillslopes exceed 45° in over 90% of the sub-basin (Larsen, 1984; Robinson, 1985). The 60 km-long upper Río Chagres descends approximately 850 m from its headwaters to Lago Alhajuela, which currently serves as its effective base level.

The majority of the upper Río Chagres basin lies within Parque Nacional Chagres, although 30% of the land is in private ownership. Human land use is primarily cultivation that is restricted to these private land holdings, and road and trail access is minimal. The majority of the land surface is covered by intact primary tropical and seasonally tropical rainforest. Trees can attain a height of 30 m and a diameter of 2.2 m (R. Condit, Smithsonian Tropical Research Institute, pers. comm., 2003).

Preliminary geologic mapping (Wörner *et al.,* 2005, this volume) indicates that the bedrock geology underlying the upper Río Chagres basin comprises a series of strongly faulted and variably altered intrusive, volcanic, and volcaniclastic lithologies outcropping discontinuously along the channels of the upper Río Chagres. They subdivided the bedrock into four general types: (i) coarse-grained igneous rocks ranging in composition from gabbro to granite, (ii) mafic to intermediate composition volcanic rocks

erupted as submarine lava flows, (iii) volcaniclastic rocks that derive from the submarine eruption and fragmentation of lavas, and (iv) andesite dikes which crosscut all other lithologies. The age of these rocks is difficult to assess without absolute age dating, but related sediments are of lower Tertiary age. At the sub-basin to basin scale of tens to hundreds of square kilometers, bedrock structural characteristics appear to influence regional drainage net development in that the NE-SW trend of the major channels coincides with regional fault and dike patterns, as denoted from a 10 m-resolution digital elevation model (DEM) of the basin (H. Mitasova, pers. comm., 2002). The movement along these faults is mostly, but not exclusively, near vertical and probably represents strike-slip displacement during bending of the Central American isthmus (R. Harmon, pers. comm., 2002).

Figure 1. Location map of the upper Río Chagres drainage basin, Panama. The channel

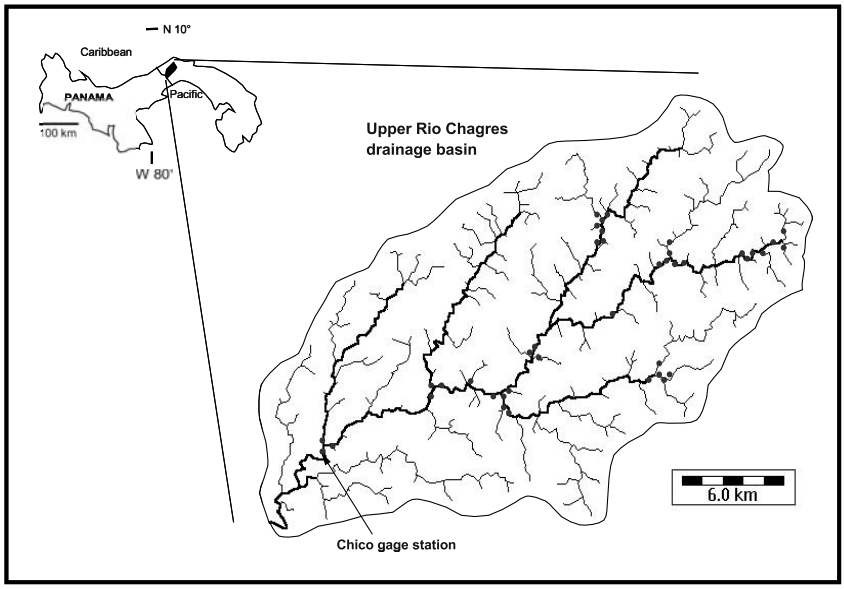

network is derived from the 10 m digital elevation map of the region. Lighter dots indicate the 40 study reaches.

Mean annual precipitation at the headwaters of the upper Río Chagres has not been measured, but recorded data at Lago Alhajuela indicate a mean annual precipitation of 2590 mm during 1914-1995. Some 90% of this rain falls during May-December (Houseal, 1999). Preliminary soils investigations in the drainage basin suggest that overland flow dominates hillslopes during the dry season. Soil water repellency causes a disproportionate increase in runoff during the first few storms after the dry season. Subsurface flow dominates hillslopes during the wet season, with

positive soil water pressures leading to non-Darcian flow through pipes and macropores (Harrison *et al.,* 2005, Chapter 7 and Hendrickx *et al.,* 2005, Chapter 8).

Discharge in the upper Río Chagres basin has been measured at the Chico gage (Fig. 1) since 1933. Discharge typically varies between 10-20 m^3/s during the dry season and over 1000 m^3/s during the monsoon season. Mean annual peak flow is 1049 m^3/s, and the flood of record was 3780 m^3/s in November 1966.

Dense canopy cover along even the largest channels prevents the derivation of an accurate longitudinal profile from the 10 m-resolution DEM of the upper Río Chagres basin. However, the general DEM-derived profile and our field observations suggest that the river has a concave longitudinal profile with some knickpoints up to 10 m high in the headwaters, and one smaller knickpoint 3 m high midway down the basin.

3. METHODS

An initial aerial reconnaissance of the basin was conducted via helicopter in order to select appropriate channel reaches for surveying. Site selection was based on both spatial importance in the context of the research objectives and accessibility. Forty short channel reaches (50-200 m long) were designated throughout the upper Río Chagres basin river network. At each reach, a geographic position was obtained using a Trimble Pro XRS global positioning unit. Channel geometry was surveyed, including gradients for channel-bed, water-surface, and high-flow marks. Gradients for some channel reaches were estimated from DEM coverage of the basin and are likely less accurate than those gradients surveyed directly. Reaches with DEM-based estimates are indicated in Table 1.

Channel width, depth, paleostage indicators, and bed form wavelength and amplitude were also surveyed using either a total station or a hand level, metric tape, and stadia rod. Bed form wavelength is defined as the average downstream distance between equivalent points (riffle crest to riffle crest, for example), and bed form amplitude is defined as the average elevation difference between the step lip and the base of the step for step-pool channels, and the average residual pool depth for pool-riffle channels. Low-flow velocity was measured at the time of field work using a 1-D Marsh-McBirney electromagnetic current meter and. bed grain-size distribution measured using a random walk (Wolman, 1954). At bedrock outcrops along the channel, rock-mass strength was measured below the high-flow mark (Selby, 1980).

Data analysis focused on calculating bankfull hydraulic variables for each study reach. In this context, bankfull flow represents the mean annual high flow, defined in the field based on both the interface between vegetative growth parallel to streamflow and growth normal to channel flow and the presence of fluvially deposited wood and debris. Bankfull discharge was calculated using the surveyed channel geometry and field-estimated Manning's *n* value for high flow based on visually-assessed boundary roughness. The *n* value was constrained by measured low-flow velocity and calculated discharge at the time of the survey. Cross-sectionally averaged values of hydraulic variables during bankfull flow were calculated as:

$$\text{bed shear stress, } \tau = \gamma R S \quad (1)$$

$$\text{stream power per unit area, } \omega = \tau v \quad (2)$$

$$\text{total stream power, } \Omega = \gamma Q S \quad (3)$$

$$\text{Darcy-Weisbach friction factor, } f = (8gRS)/v^2 \quad (4)$$

where γ is the specific weight of water (9800 N/m^2), R is hydraulic radius in m, S is streambed gradient in m/m, v is mean velocity in m/s, Q is discharge in m^3/s, and g is gravitational acceleration (9.8 m/s^2).

Critical shear stress for mobilizing the D_{84} grain size at each study reach was calculated using Komar's (1987) equation:

$$\tau_c = 0.045(\rho_s - \rho)\, g\, D_{50}^{0.6}\, D_{84}^{0.4} \quad (5)$$

where ρ_s is sediment density (2.65 g/cm^3), ρ is water density (1 g/cm^3), and τ_c is in dynes/cm^2.

4. RESULTS

4.1 Observed Channel Characteristics

Helicopter flights across the upper Río Chagres drainage basin permitted observation of vegetated abandoned meanders that occur approximately 5-30 m above the active channel. These relict channels indicate that the sinuous upper Río Chagres is migrating laterally as it incises, despite its narrow, confined valley geometry.

The helicopter flights and the ground-based field work also revealed many vegetated and recent landslide scars. From the soil profiles exposed along the hillslopes where landsliding has occurred, landslides apparently have introduced a full range of clay- to boulder-size sediment into the channels. The lack of fine sediment deposits in the channels at or

immediately downstream from the landslides suggest that flows are competent to transport clay- to gravel-size sediment downstream quickly after a landslide. Some of the landslides were associated with cobble-boulder deposits immediately downstream, but these seldom formed a deposit noticeably larger than other steps or riffles present upstream from the landslides, again suggesting highly competent flows in the channel.

Very little large woody debris (LWD) was observed along the channels in the upper Río Chagres basin, despite the density of mature forest in the basin. A few recently deposited logs were present in headwater areas, but not in the middle and lower portions of the upper Río Chagres. Where LWD was observed, it occurred mostly in depositional zones along channel margins and did not apparently serve the geomorphic roles commonly described for LWD in temperate-zone mountain rivers, such as creating sediment storage zones, stabilizing channel banks, or providing nucleation sites for bars or islands. The absence of LWD in and along the channel network is probably primariy a result of the extremely high decay rate of wood in Panama; logs of some tree species decay within 6 months, and even the most persistent woods decay within 20 years (R. Stallard, USGS, pers. comm., 2002). The high values of velocity and stream power present throughout the upper Río Chagres network probably also help to mobilize and physically break down LWD.

Numerous discontinuous bedrock outcrops along the channel bed and banks suggest that bedrock is present at shallow depths below an alluvial veneer throughout the channel network. At the cross-sectional to reach scale of tens to hundreds of square meters, bedrock lithology and joint geometry are consistently associated with characteristic channel width/depth ratios, gradients, and bend angles. Wide, low gradient channels having minimal exposed bedrock during low flows are associated with granites, microdiorites, and altered volcanic andesitic and volcaniclastic lithologies. Granites are also associated with abundant grus (sand-gravel size sediment) and large, rounded boulders (Fig. 2). Narrow, incised, higher gradient channel reaches with continuous bedrock exposure and sharper bends are associated with gabbros and diorites (Fig. 3). Individual channel reaches of tens to hundreds of meters in length both follow and cut across joints and faults.

Figure 2. View upstream in a study reach where the pool-riffle channel is formed in granite.

Figure 3. View downstream in a study reach where the channel forms a bedrock gorge in a mafic substrate.

Surveyed reaches included three basic channel types: step-pool (Fig. 4), pool-riffle (Fig. 2) and bedrock gorge (continuous bedrock exposure, generally step-pool or pool-rapid bedforms; Fig. 3). Steps and pools occurred along channels with smaller drainage areas, very coarse sediment, and high gradients. Pools and riffles occurred at a range of drainage areas, but had smaller clasts and lower gradients. Bedrock gorges had a range of

drainage areas, grain sizes, and gradients. Although the larger step-forming clasts in some of the step-pool channels appeared to be mobilized infrequently, most of the channel-bed clasts were imbricated but not tightly packed, suggesting more frequent mobility.

Figure 4. View upstream in a study reach where the step-pool tributary channel is formed in granitic substrate.

4.2 Channel Characteristics

The summary of the cross-sectionally averaged characteristics at the 40 study reaches (Table 1) indicates a wide range in the values of most variables. Field-estimated bankfull discharge has a strong log-linear correlation with drainage area (Fig. 5). Downstream hydraulic geometry exponents for bankfull hydraulic radius (Fig. 6a), bankfull channel top width (Fig. 6b), and bankfull mean velocity (Fig. 6c) were calculated using the reach data. These values, 0.36 for radius, 0.43 for width, and 0.24 for velocity, are similar to the average values for rivers worldwide (Park, 1977). Discharge has a strongly log-linear relation with both hydraulic radius and channel top width, although some outliers exist. These outliers do not consistently represent alluvial or bedrock channels, small or large drainage areas, or any one of the three primary channel types (step-pool, pool-riffle, or bedrock gorge). The relation between discharge and velocity is more variable (Fig. 6c), and again outliers exhibit no consistent characteristics.

Table 1. Listing of variable values by study reach for the upper Río Chagres basin, Panama.

Area	S	Q	D_{50}	D_{84}	T	T_c	ω
21.2	.0344	397	18	32	573	170	3785
22.3	.0069	431	11	23.5	183	112	737
36.6	.0050	148	30	38.5	98	249	220
37.5	.0109	374	24	35	256	209	1198
60.6	.0109	909	19	33	278	178	1812
60.8	.0015	87	14	24	29	130	36
75.9	.0092	857	18.5	30	306	168	1660
10.8	.0125	47	16.5	26.5	80	150	168
15.0	.0132	323	14	19	272	119	1282
15.5	.0080	97	16	23.5	73	140	205
20.6	.0138	390	30	52.5	298	282	1481
0.5	.0340	22	21	42	267	208	848
20.0	.0340	431	18	40	733	186	4574
2.5	.0174	93	14	24	256	130	1106
13.0	.0166	216	40	64	277	362	1271
32.7	.0094	318	33	45.5	211	282	865
47.8	.0040	423	20	35	74	188	237
1.0	.0267	46	11	22.5	314	110	1159
48.7	.0040	216	30	92.5	63	353	136
1.1	.0670	14	35	63.5	394	333	1036
29.3	.0146	206	24	39	272	219	1261
29.6	.0083	131	21	34	114	191	325
12.8	.0143	228	18	36	280	178	1329
6.1	.0133	48	13	27.5	143	132	439
6.3	.0835	159	21	36	1227	196	9293
92.8	.0068	221	20.5	36	127	193	402
3.6	.0253	10	15	25.5	174	139	436
88.3	.0309	241	10.5	19	363	100	1802
175.8	.0110	2620	20	38	356	194	2070
171.7	.0271	1063	21	33.5	744	190	6085
2.9	.0360	36	20	55.5	353	226	1340
4.4	.0821	66	48	102.5	805	488	3844
269.0	.0178	1525	30	46	436	267	3537
1.6	.0727	48	21	43.5	285	211	834
49.4	.0102	344	15	25.5	210	139	870
280.3	.0125	1586	26	36.5	429	224	2765
329.8	.0100	683	8.5	16	186	82	942
41.8	.0099	216	8	13	204	73	832
364.0	.0004	1058	13	20.5	24	117	53
407.0	.0014	1231	11	16	80	96	242

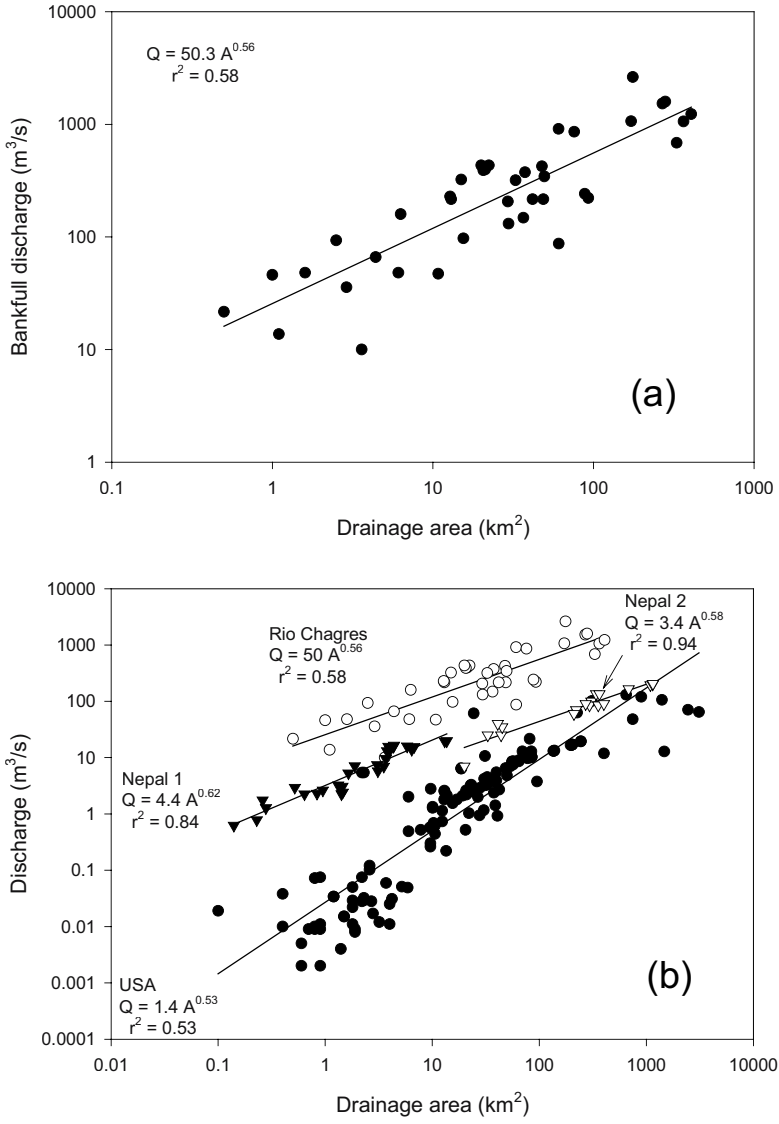

Figure 5. (a) Regression of drainage area and bankfull discharge estimated from high-flow indicators at study sites throughout the upper drainage basin. (b) Comparison of discharge-drainage area relations for the Río Chagres and for mountain drainage basins elsewhere in the world. "Nepal 1" is the Middle Himalaya, "Nepal 2" is the upper Himalaya, "USA" includes data from Colorado, Wyoming, Montana, Washington, and Alaska (Data sources: Caine and Mool, 1982; Curran and Wohl, 2003; MacFarlane and Wohl, 2003; E. Wohl, unpublished data.)

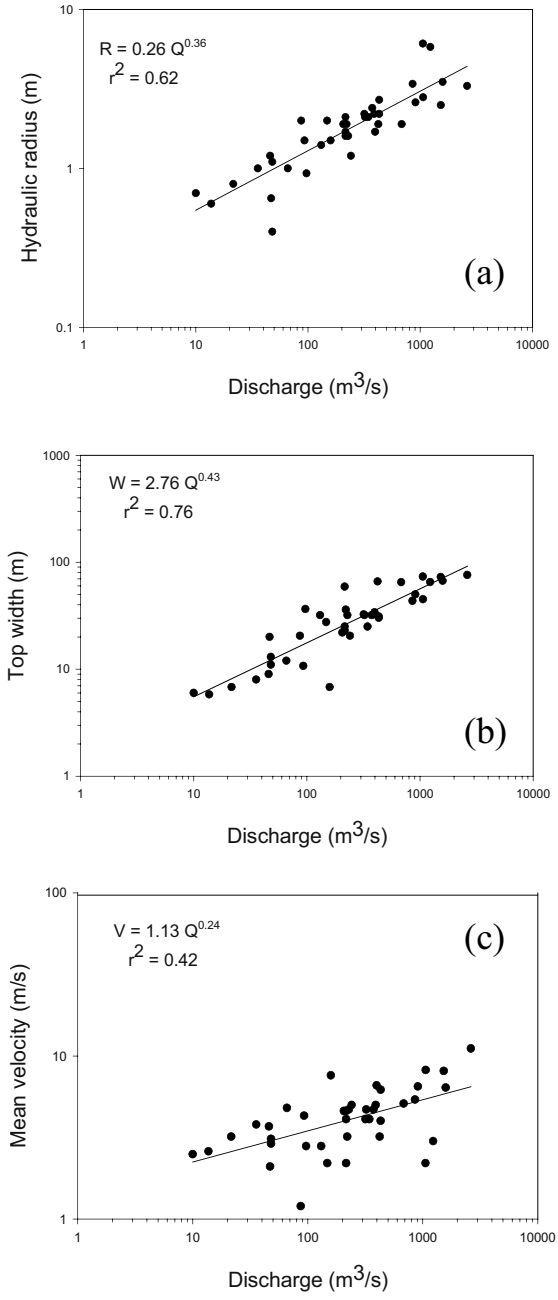

Figure 6. Downstream hydraulic geometry relations. (a) hydraulic radius, (b) channel top width, and (c) mean velocity.

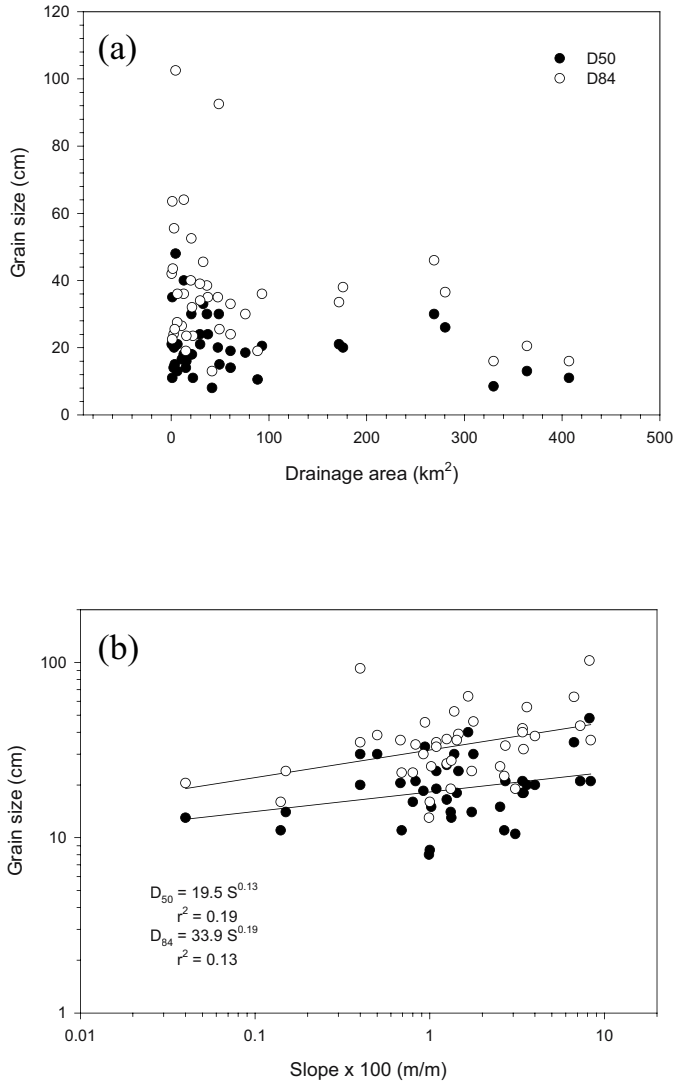

Figure 7. Grain size at each study reach, represented by D50 and D84, versus (a) drainage area and (b) reach gradient.

Using D_{50} and D_{84} as indicators, grain size at a reach correlates poorly with bankfull discharge, drainage area (Fig. 7a) and reach gradient (Fig. 7b). Reach gradient also correlates poorly with discharge and drainage area (Fig. 8). Critical shear stress for D_{84}, as calculated using equation 5, is greater than

bankfull shear stress at more than half of the study reaches (28 out of 40; Fig. 9). This suggests that the coarsest clasts throughout the channel network are generally mobilized on approximately an annual basis.

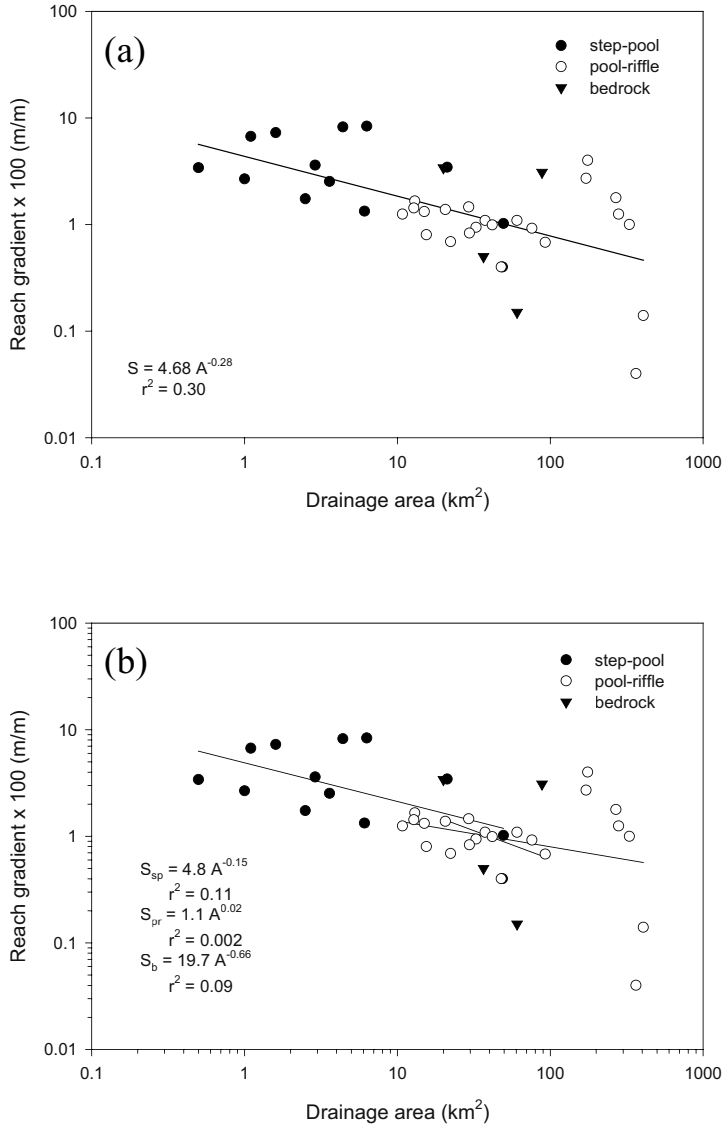

Figure 8. Reach gradient versus drainage area, plotted with (a) a single regression line and (b) a regression line for each channel type.

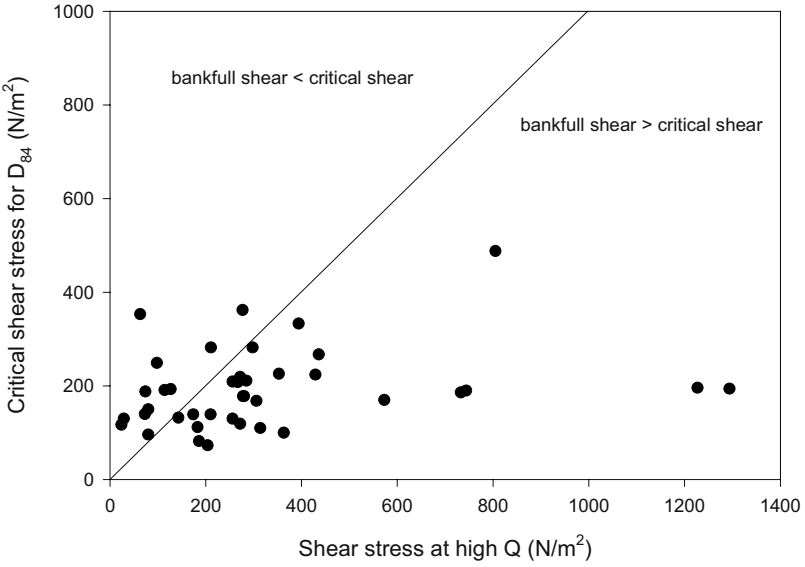

Figure 9. Estimated bed shear stress during bankfull flow versus critical shear stress for the D_{84} grain size at each study reach, estimated using Komar (1987).

Both stream power per unit area (Fig. 10a) and total stream power (Fig. 10b) peak approximately halfway down the drainage basin. Searches for correlations between potential control variables and the response variables of bed form wavelength and amplitude and Darcy-Weisbach friction factor revealed that friction factor correlates with hydraulic radius (Fig. 11) and bed form wavelength correlates with reach gradient (Fig. 12). However, the wavelength-slope correlation reflects the presence of both step-pool and pool-riffle channels in the data set. Bed form wavelength does not correlate with reach gradient within either the step-pool or pool-riffle subset. The spacing of pools in the pool-riffle channels averages 3.5 times bankfull channel width (range 1.1 to 8), which is within the range of spacing values found for temperate rivers (Keller and Melhorn, 1978). Along the step-pool channels, the ratio of step amplitude/ wavelength/ reach gradient fell between 1 and 3, similar to the values found for channels in temperate regions (MacFarlane and Wohl, 2003). The ratio of step amplitude to step wavelength also approximated 1.5 times the reach gradient, the condition described by Abrahams *et al.* (1995) as creating maximum flow resistance and greatest channel stability for step-pool channels.

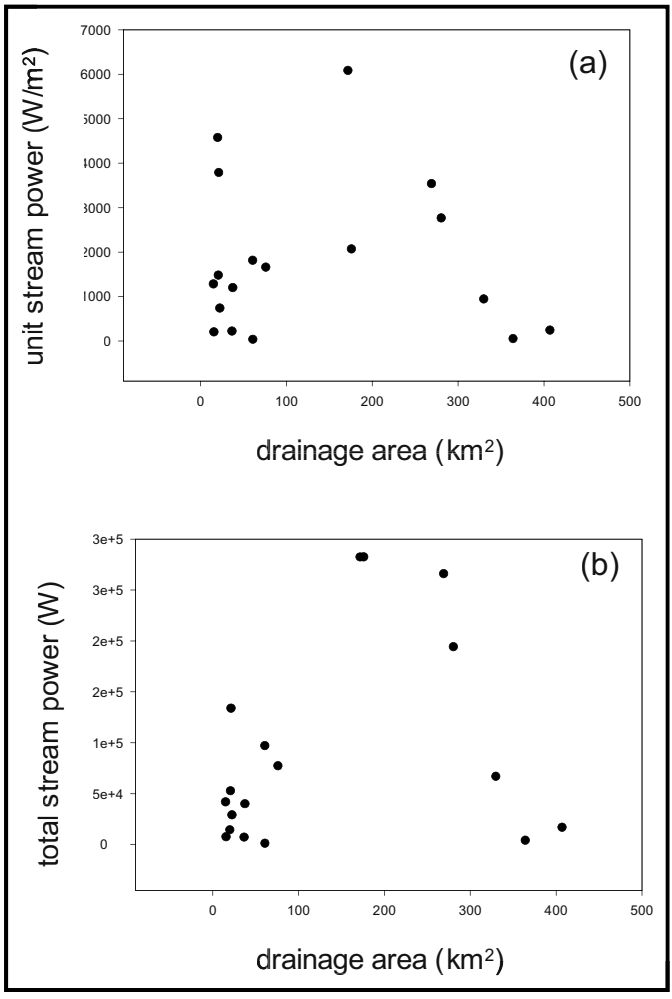

Figure 10. Downstream distribution of (a) unit stream power and (b) total stream power.

5. DISCUSSION AND CONCLUSIONS

Specific lithologies often correspond to distinctive channel geometries throughout the basin. However, the similarity between the upper Río Chagres hydraulic geometry exponents and the average values for rivers worldwide, as well as the strong log-linear correlations for hydraulic radius and channel width with respect to discharge, imply that hydraulic driving

forces sufficiently exceed substrate resistance to erosion to override specific lithologic influences on channel width and depth at sub-basin to basin scales. This may result from the combination of (i) high rates of rock weathering in the humid tropical climate of the upper Río Chagres basin; (ii) the limited along-channel exposure of any particular lithology; and (iii) the very high values of discharge (Fig. 5b), velocity, and stream power relative to drainage area, and hence the large hydraulic driving forces, of the upper Río Chagres. Local influences appear to strongly influence some channel characteristics, however. The lack of correlation between grain size and either reach gradient, discharge, or drainage area suggests that local influences in the form of landslides and bedrock lithology complicate these relationships.

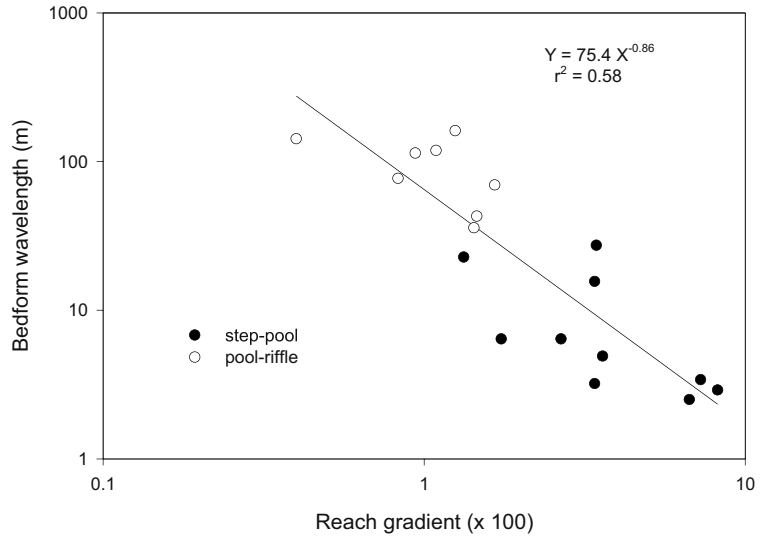

Figure 11. Regression relation between bankfull hydraulic radius and bankfull Darcy-Weisbach friction factor.

The other reach-scale channel characteristics considered generally fall within the range of values from rivers in temperate regions. Reach-scale bed gradients for step-pool and pool-riffle reaches, for example, are very similar to those for temperate mountain rivers as cited in Montgomery and Buffington (1997). Knighton's (1999) empirical and theoretical study of downstream trends in stream power suggested that total stream power peaks at an intermediate distance between a river's headwaters and mouth, whereas stream power per unit area peaks closer to the headwaters. Both measures of stream power peak at an intermediate distance along the upper Río Chagres, but too few studies of this type exist for temperate-region rivers to allow a

detailed comparison. The wavelength and amplitude of bed forms along the upper Río Chagres channels correspond to those described for temperate mountain rivers, as do the bankfull values of Darcy-Weisbach friction factor and the correlation between friction factor and bankfull hydraulic radius (Curran and Wohl, 2003; MacFarlane and Wohl, 2003; E. Wohl, unpublished data).

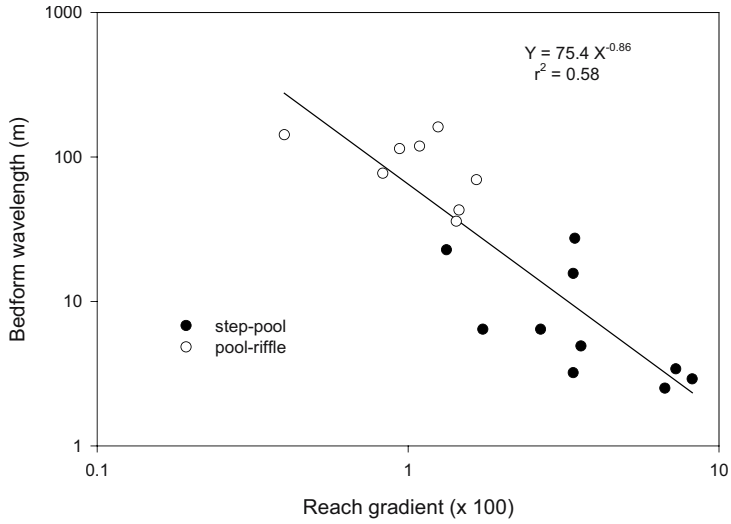

Figure 12. Plot of bed form wavelength for step-pool and pool-riffle channels versus reach gradient. Bed form wavelength was not measured at all study reaches (n = 18). This plot only includes sites for which reach gradient was measured (not those sites for which reach gradient was estimated from the 10-m DEM).

Returning to the potential differences between rivers draining mountainous catchments in tropical and temperate environments, data from the upper Río Chagres suggest that this tropical river has less downstream segmentation than many temperate mountain rivers. Downstream segmentation, expressed via the presence of large knickpoints, the absence of strong linear relations between downstream hydraulic geometry variables and discharge, or abrupt changes in valley morphology, is largely absent along the upper Río Chagres. The relatively consistent downstream trends in width and depth relative to discharge along the upper Río Chagres may reflect the combination of rapid rates of rock weathering and high values of unit discharge, velocity, and stream power. In this context, Caine and Mool's (1981) data from Nepal, which also display good downstream hydraulic geometry relations, plot closest to the upper Río Chagres data in terms of

unit discharge (Fig.5). The combination of rapid weathering and high unit discharge along the Río Chagres facilitates the adjustment of channel reaches to relatively consistent downstream trends, despite the abundance of bedrock of differing lithologies. Calculations of critical shear stress and observations of the lack of LWD and the lack of tightly packed streambed substrate suggest that the upper Río Chagres is also subject to more frequent flood-related bed mob ility and disturbance than many mountain rivers in drier temperate regions.

In summary, the upper Río Chagres results provide a starting point for characterizing the downstream hydraulic geometry relations of rivers in tropical mountain environments. More extensive downstream hydraulic geometry data are needed from a variety of mountain river networks to fully explore the inferences presented here that mountain rivers in tropical environments, despite local influences on grain size and gradient, may better approximate average downstream hydraulic geometry relations for fully alluvial rivers than do mountain river networks in drier regions.

ACKNOWLEDGEMENTS

This research was funded by grant DAAD 19-00-1-0474 from the US Army Research Office. The 2002 field work, organized by the Tropical Regions Test Center (US Army Yuma Proving Ground). S. Howe, A. Alveo, R. Stallard, and A. Iglesias provided critical field assistance; and L. deWong and the staff at IEASA (Investigacion y Evaluacion Ambiental, S.A.) kept the field work going with vital logistical support. I thank them all.

REFERENCES

Abrahams, AD, Li, G, and Atkinson, JF, 1995, Step-pool streams: adjustment to maximum flow resistance: Water Resour. Res., 31: 2593-2602.

Caine, N and Mool, PK, 1981, Channel geometry and flow estimates for two small mountain streams in the Middle Hills, Nepal: Mt. Res. Dev., 1: 231-243.

Curran, JH and Wohl, EE, 2003, Large woody debris and flow resistance in step-pool channels, Cascade Range, Washington: Geomorph., 51: 141-157.

Harrison, JBJ and Hendrickx, JMH, Vega, D, and Calvo, LE, 2005, Character and Spatial Variability of Soils in Two Small First Order Drainage Basins, Upper Río Chagres Watershed, Panama: in *The Río Chagres: A Multidisciplinary Perspective of a Tropical River Basin* (RS Harmon, ed.), Kluwer Acad./Plenum Pub., New York, NY: 97-112.

Hendrickx, JMH, Vega, D, Harrison, JBJ, Calvo, LE, Arias, P, and Miller, TW, 2005, Soil Hydrology along Steep Hillslopes in the Río Chagres Watershed: in *The Río Chagres: A*

Multidisciplinary Perspective of a Tropical River Basin (RS Harmon, ed.), Kluwer Acad./Plenum Pub., New York, NY: 113-138.

Houseal, B, 1999, Plan de manejo y desarrollo del parque nacional Soberania: in *Protecting Watershed Areas - Case of the Panama Canal* (MS Ashton, JL O'Hara and R Hauff, eds.), Food Products Press, New York, NY.

Ibbitt, RP, McKerchar, AI, and Duncan, MJ, 1998, Taieri river data to test channel network and river basin heterogeneity concepts: Water Resour. Res., 34: 2085-2088.

Keller, EA and Melhorn, WN, 1978, Rhythmic spacing and origin of pools and riffles: Geol. Soc. Am. Bull., 89: 723-730.

Knighton, AD, 1999, Downstream variation in stream power: Geomorph., 29: 293-306.

Komar, PD, 1987, Selective gravel entrainment and the empirical evaluation of flow competence: Sedimentol., 34: 1165-1176.

Larsen, CL, 1984, Controlling erosion and sedimentation in the Panama Canal watershed: Water Int.: 161-164.

MacFarlane, WA and Wohl, EE, 2003, The influence of step composition on step geometry and flow resistance in step-pool streams of the Washington Cascades: Water Resour. Res., 39: ESG 3-1 to 3-13.

McKerchar, AI, Ibbitt, RP, Brown, SLR, and Duncan, MJ, 1998, Data for Ashley river to test channel network and river basin heterogeneity concepts: Water Resour. Res., 34: 139-142.

Molnar, P and Ramirez, JA, 2002, On downstream hydraulic geometry and optimal energy expenditure: case study of the Ashley and Taieri Rivers: Jour. Hydrol., 259: 105-115.

Montgomery, DR and Buffington, JM, 1997, Channel-reach morphology in mountain drainage basins: Geol. Soc. Am. Bull., 109: 596-611.

Park, CC, 1977, World-wide variations in hydraulic geometry exponents of stream channels: an analysis and some observations: Jour. Hydrol., 33: 133-146.

Phillips, PJ and Harlin, JM, 1984, Spatial dependency of hydraulic geometry exponents in a subalpine stream: Jour. Hydrol., 71: 277-283.

Ponton, JR, 1972, Hydraulic Geometry in the Green and Birkenhead Basins, British Columbia: in *Mountain Geomorphology: Geomorphological Processes in the Canadian Cordillera* (HO Slaymaker and HJ McPherson, eds.), Tantalus Research Ltd., Vancouver, Canada: 151-160.

Robinson, FH, 1985, A Report on the Panama Canal Rain Forest: Meteorol. Hydrol. Branch, Eng. Div., Panama Canal Commission, Balboa Heights. Panama: 70p.

Selby, MJ, 1980, A rock mass strength classification for geomorphic purposes: with tests from Antarctica and New Zealand: Zeitsch. Geomorph., 24: 31-51.

Wohl, E, 2000, *Mountain Rivers*: Am Geophys. Union Press, Washington, DC.

Wolman, MG, 1954, A method of sampling coarse river-bed material: EOS, Trans. Am. Geophys. Union, 35: 951-956.

**Wörner, G, Harmon, RS, Hartmann, G, and Simon, K, 2005, Igneous Geology and Geochemistry of the Upper Río Chagres Basin: in *The Río Chagres: A Multidisciplinary Perspective of a Tropical River Basin* (RS Harmon, ed.), Kluwer Acad./Plenum Pub., New York, NY:

Chapter 12

BEDROCK CHANNEL INCISION ALONG THE UPPER RÍO CHAGRES BASIN, PANAMA

Ellen Wohl[1] and Gregory Springer[2]
[1]Colorado State University, [2]Ohio University

Abstract: Examination of various types of bedrock channel segments throughout the upper Río Chagres network indicates the influences of lithology, rock-mass strength, jointing, and resistance to weathering on channel geometry. Bedrock channel segments throughout the upper Río the Chagres basin take the form of step-pool sequences, pool-riffle sequences, and knickpoints and gorges. Mafic lithologies in the catchment have the greatest rock-mass strength and the longest exposures along the active channel, and are more likely to exert a strong local control on channel geometry. The longest continuous exposure of resistant rocks in the middle and lower portions of the upper Río Chagres occurs in the Dos Cascadas reach, where upstream migration of two knickpoints has created a gorge. Surface textures (*e.g.*, the presence of potholes) and erosion mechanisms of individual rock units in the Dos Cascadas reach correlate strongly with fracture spacing and rock hardness.

Key words: Panama; Río Chagres; bedrock channels; river knickpoints; lithologic effects

1. CHARACTERISTICS OF BEDROCK CHANNELS

Bedrock channels occur where at least half of the river bed and banks are exposed bedrock, or are covered by an alluvial veneer that is largely mobilized during high flows, such that underlying bedrock geometry strongly influences flow hydraulics and sediment movement (Tinkler and Wohl, 1998). The presence of bedrock at the surface or at very shallow depth indicates a lack of sediment supply relative to the transport capacity of the river, a situation more likely to be present in high-relief environments such as mountainous catchments. Even rivers in mountainous regions are unlikely to have continuous bedrock exposure along their entire length, however; alternating alluvial and bedrock channel segments are more

R. S. Harmon (ed.), The Río Chagres, Panama, 189-209.

commonly present. The location of bedrock segments can reflect a local limitation to sediment supply, localized tectonic uplift, or the presence at the surface of bedrock units relatively resistant to weathering and erosion (Tinkler and Wohl, 1998).

The bed and banks of bedrock channel segments have much higher cohesion and resistance to erosion than alluvial segments. Where bedrock and alluvial channel segments alternate downstream, the bedrock segments can thus create local base levels that limit the adjustment of upstream alluvial segments. The importance of weathering during periods of low flow in weakening bedrock channel boundaries remains unclear (Hancock and Small, in press). Most bedrock channel erosion likely occurs during periods of high flow through a combination of abrasion, quarrying, and cavitation (Wohl, 1998). Heterogeneities in the rock surface produced by bedding planes, joints, or crystal boundaries initiate flow separation that leads to differential erosion through abrasion. The differential erosion further enlarges the heterogeneity, creating a self-enhancing feedback that produces sculpted forms such as grooves and potholes (Wohl, 1993; Tinkler and Wohl, 1998; Wohl, 1998; Springer and Wohl, 2002). In densely bedded or jointed rocks, quarrying of detached blocks through hydraulic lift forces provides a very effective mechanism of erosion (Hancock *et al.,* 1998). Deep flows with high velocities can induce cavitation that effectively erodes cohesive boundaries (Wohl, 1998).

Bedrock channel segments are likely to have a higher gradient, a lower width/depth ratio, and coarser-grained alluvial deposits than fully alluvial reaches (Tinkler and Wohl, 1998). Bedrock channel forms include anastomosing, meandering, undulating walls, pool-riffle, step-pool, inner channel, and knickpoints (Wohl, 1998). These different forms reflect the balance between hydraulic driving forces and substrate resistance, as expressed through varying mechanisms of erosion. As with alluvial channels, the morphology of a bedrock channel segment thus provides insight into the forces and processes acting on that segment.

Knickpoints and associated gorges are much more common along bedrock channel segments than along alluvial segments. A knickpoint is a step-like discontinuity in the longitudinal profile of a river. Unlike bed-steps, which commonly maintain their longitudinal position over time, knickpoints are likely to migrate headward at varying rates (Wohl, 2000a). A knickpoint may be created when base level fall, or uplift of the drainage basin, increases channel gradient and the river's incisional capability so that a knickpoint originating at the river mouth erodes upstream (Seidl and Dietrich, 1992). A knickpoint may also result from an increase in the ratio of water/sediment discharge (Wohl, 2000a), or from the exposure of particularly resistant

material in the river bed (Miller, 1991). The steep face of a knickpoint may be maintained during headward erosion in bedded or jointed substrates (Holland and Pickup, 1976; Bishop and Goldrick, 1992; Wohl *et al.,* 1994; Pyrce, 1995), but is likely to become less pronounced with time in massive, homogeneous substrate (Gardner, 1983; Stein and Julien, 1993). A knickpoint created by the presence of aresistant substrate will either disappear or become a more gradually steepened knickzone once the river has incised an inner channel through the resistant unit (Biedenharn, 1989). Jointed or bedded, resistant rocks and an unstable base level history are thus probably necessary for knickpoints to be maintained over any but very short time periods (Tanaka *et al.,* 1993; Seidl *et al*., 1994).

Knickpoints represent sites of great concentration of energy dissipation along a river (Young, 1985). Reported rates of knickpoint migration range from 2 to 100 cm/kyr (Tinkler and Wohl, 1998; Wohl, 1999), and can be two orders of magnitude greater than erosion rates elsewhere along a river (Seidl *et al.,* 1997). The presence of knickpoints along a river can indicate that other forms of channel incision cannot keep pace with uplift, resulting in steepening of the channel longitudinal profile until a knickpoint is formed and incision occurs fairly rapidly. Thus, the formation and headward retreat of a knickpoint can determine the extent to which a bedrock channel segment is serving as a local base level limiting incision along upstream alluvial segments.

Headward retreat of a knickpoint or knickzone through a resistant substrate unit can leave behind a deep, narrow gorge. The maintenance of a deep, narrow channel cross section following knickpoint recession both reflects the erosional resistance of the channel boundaries, and maximizes the shear stress and stream power per unit area for a given discharge and channel gradient (Baker, 1988; Wohl, 1992, 1998, 2000a; Wohl and Ikeda, 1997).

This chapter describes the characteristics of bedrock channel segments along the upper Río Chagres, with a focus on the morphology, forces, and processes of the Dos Cascadas reach of the main channel. Two prominent knickpoints and a gorge occur in the Dos Cascadas reach.

2. METHODS

Several field and analytical methods were used to examine the relations among bedrock channel form and process along the upper Río Chagres. Cross-sectional and longitudinal channel geometry was surveyed as described in Wohl (2005, this volume). Coarse-clast deposition within each

channel segment was characterized by measuring the intermediate diameter of clasts selected using a random-walk method (Wolman, 1954). Rock-mass strength was characterized using the index developed by Selby (1980), which includes joint geometry, relative weathering, groundwater seepage, and bedrock compressive strength as measured with a Schmidt hammer. Also utilized in this analysis were bedrock channel segments studied during the 2002 field season (Wohl, 2005, this volume), to which was added a detailed characterization of the channel segment around Dos Cascadas, where two prominent knickpoints occur (Fig. 1). Each of the bedrock channel segments measured during 2002 included one surveyed cross section and one measurement of rock-mass strength. For the Dos Cascadas segment, several cross sections were surveyed in order to use step-backwater modeling to estimate high-flow hydraulics, and rock-mass strength was measured at 29 sites along the channel in order to characterize lateral and longitudinal variability. Some portions of the Dos Cascadas channel segment have well-developed sculpted forms of potholes and grooves (Fig. 2), whereas other portions lack sculpted features. Joint density measurements were made in two sculpted and two unsculpted sections of bedrock. At each site, spacing was measured between 175 consecutive joints along a transect roughly parallel to the channel trend.

Step-backwater modeling utilized the 1-D model *HEC-RAS* (USACE, 1998). In this steady-flow model, the channel is characterized by surveyed cross-sections, with information provided about distance and elevation change between cross-sections in order to specify longitudinal gradient. The 1-D energy equation is coupled with an equation specifying head loss between successive cross sections. The most important adjustable parameter in this equation is the roughness coefficient, which is visually estimated (Miller and Cluer, 1998). The model predicts longitudinal water-surface profile for a specified discharge, and estimated discharge can of interest matches high-water marks surveyed in the field (O'Connor and Webb, 1988). The model also calculates user-specified hydraulics variables such as velocity, shear stress, or stream power – either as cross-section averages or as averages pertaining to a specific portion of the cross-section (Miller and Cluer, 1998). Because the 1-D *HEC-RAS* model does not adequately address the highly developed flow separation and turbulence likely to be present in very deep, narrow cross sections, a flow-modeling reach was surveyed in the upper portion of Dos Cascadas, above the upstream knickpoint. No attempt was made to model flow in the constricted inner channel that is present downstream from the first knickpoint.

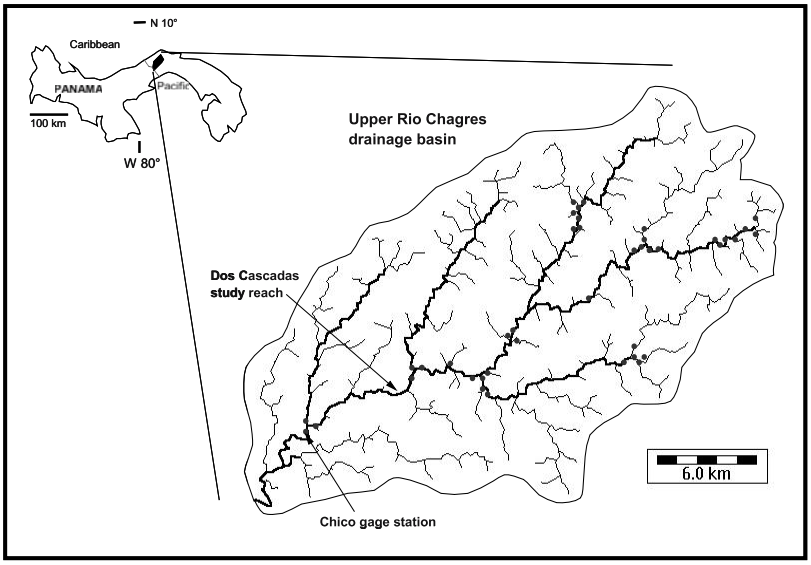

Figure 1. Location map of the upper Río Chagres drainage basin, Panama. Channel network is derived from the 10-m digital elevation map of the region. Lighter dots indicate the 40 river reaches studied in 2002.

Figure 2. Sculpted forms on river left at Dos Cascadas (upstream knickpoint at left of photograph). Sixty-meter tape and pair of legs provide a scale.

3. BEDROCK CHANNEL SEGMENTS ALONG THE UPPER RÍO CHAGRES

The upper Río Chagres basin drains 414 km^2 of steep, mountainous terrain. The channel of the main river descends approximately 850 m from its headwaters to Lago Alhajuela, which currently serves as its effective base level. Mean annual precipitation at the headwaters of the upper Río Chagres basin has not been measured, but recorded data for Lago Alhajuela, at the basin outlet, indicate a mean annual precipitation of 2590 mm during 1914-1995. Ninety percent of this rain falls during May-December wet season (Houseal, 1999). Discharge in the upper basin has been gaged at the Chico station (Fig. 1) since 1933. Discharge typically varies between 10-20 m^3/sec during the dry season and over 1000 m^3/sec during the monsoon season. Mean annual peak flow is 1049 m^3/sec, and the flood of record was 3780 m^3/sec was recorded in November 1966.

Preliminary geologic mapping (Wörner *et al*., 2005, Chapter 5) indicates that the bedrock geology underlying the upper Río Chagres basin comprises a series of strongly faulted and variably altered intrusive, volcanic, and volcaniclastic lithologies that outcrop discontinuously along the channels of the upper Río Chagres. Four general bedrock types were recognized: (i) coarse-grained igneous rocks ranging in composition from gabbro to granite, (ii) mafic to intermediate composition volcanic rocks erupted as submarine lava flows, (iii) volcaniclastic rocks derived from the submarine eruption and fragmentation of lavas, and (iv) andesite dikes which crosscut all other lithologies. The age of these rocks is difficult to assess without absolute age dating, but related sediments are of lower Tertiary age.

As in many mountainous drainage basins, bedrock and alluvial channel segments alternate throughout the upperRío Chagres catchment. Step-pool and pool-riffle sequences constitute the most commonly found types of channel morphology. Step-pool sequences consist of vertical steps formed of bedrock or coarse clasts with a plunge pool at the base of each step (Wohl, 2000a). Throughout the upper Río Chagres basin, step-pool sequences are most common at channel gradients of 0.010-0.082 (Wohl, 2005, this volume). Pool-riffle sequences consist of alternating topographic depressions (pools) and topographic rises (riffles) in the channel bed (Wohl, 2000a). Pools and riffles most commonly occur throughout the Río basin in alluvium at channel gradients of 0.004-0.018, but are also occasionally formed in bedrock (Wohl, 2005, this volume).

Channels throughout the upper Río Chagres catchment tend to display typical downstream hydraulic geometry relationships such that channel width, flow depth, and velocity increase proportional to discharge; $w = Q^{0.4}$,

$d = Q^{0.4}$, and $v = Q^{0.2}$, respectively (Wohl, 2005, this volume). However, the relationships among discharge, channel dimensions, and flow hydraulics include variability introduced by site-specific factors such as bedrock outcrops.

The influence that a bedrock outcrop exerts on channel geometry appears to depend on both the extent of the outcrop and the lithology. Outcrops limited to a downstream exposure of a few meters may locally constrict the channel width, or induce flow separation that creates localized scour in the channel bed. For example, most of the channel segments within the upper Río Chagres catchment are sinuous, and bedrock outcrops less than 10 m in downstream length commonly occur along the outside of meander bends in association with a well-developed pool. Abandoned meanders 5-30 m above the presently active channel provide evidence that meanders migrate laterally as they incise. This indicates that the presence of bedrock does not 'fix' a meander bend in place, although the bedrock probably influences the geometry of the bend. Where bedrock is exposed for more than approximately 10 m along the channel boundaries, that segment of channel is likely to have a slightly steeper gradient, lower width/depth ratio, and coarser-grained alluvial veneer than an alluvial channel segment located at a similar position in the drainage basin. For example, six bedrock and alluvial channel segments with comparable drainage areas had average values as follows: $S_b = 0.032$, $S_a = 0.011$, $w/d_b = 13.2$, $w/d_a = 17.5$, $D_{84b} = 32$ cm, $D_{84a} = 28$ cm, where subscript *b* denotes bedrock channel segments and subscript *a* denotes alluvial channel segments.

The various lithologic types present along the channels within the upper Río Chagres basin likely differ in their resistance to both weathering and processes of fluvial erosion such as abrasion and quarrying. Bedrock exposures greater than a few meters in length along the channel are almost entirely mafic lithologies such as andesite dikes. This presumably reflects the greater resistance of these units to weathering and fluvial erosion. A comparison of rock-mass strength for felsic versus mafic lithologies supports this interpretation (Fig. 3).

Knickpoints are widespread in the uppermost reaches of the upper Río Chagres basin (S. Howe, pers. comm., 2003), as expected for channel segments with small drainage areas and low values of stream power that presumably cannot keep pace with base level fall (Merritts and Vincent, 1989). Substantial knickpoints are also present along the upper portion of the Río Chagres upstream from its confluence with the Río Chagrecito, and in the Dos Cascadas segment of the main channel of the upper Río Chagres between the its confluences with the Río Limpio and the Río Chico (Fig. 1). Each of these knickpoints is formed in a mafic lithology that is strongly

jointed. Headward retreat of the two knickpoints at Dos Cascadas has produced a long gorge downstream from the knickpoints.

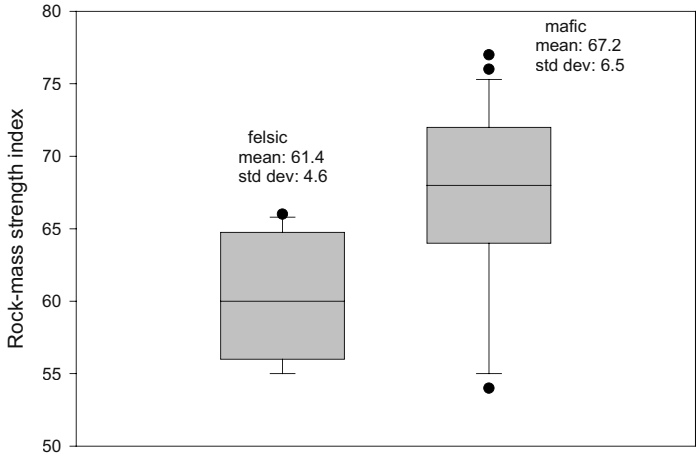

Figure 3. Comparison of rock-mass strength values for felsic and mafic lithologies exposed along the channels of the Río Chagres drainage basin. Note that the sample size is much greater for the mafic lithologies. The mean values for felsic and mafic lithologies are significantly different at $\alpha = 0.05$.

4. THE DOS CASCADAS SEGMENT

4.1 Substrate Characteristics and Resistance

The two knickpoints that form Dos Cascadas represent the most substantial profile discontinuity along the upper Río Chagres downstream from its confluence with the Río Chagrecito. The lithologic units in which the knickpoints and gorge are formed also represent the longest continuous exposure of bedrock present along the mainstem of the upper Río Chagres. The channel upstream from the knickpoints has a pool-rapid sequence with coarse-grained alternate bars (D_{50} = 145 mm, D_{84} = 245 mm) and bedrock outcrops in the active channel. Four cross-sections were surveyed upstream from two substantial rapids above Dos Cascadas (Fig. 4). Although the channel reach examined did not include the rapids, average channel gradient was still fairly high at 0.0023 m/m. Using high-water marks in the form of vegetation changes and fluvial debris, channel top width during high flow was estimated as approximately 46 m, and average depth as 2 m.

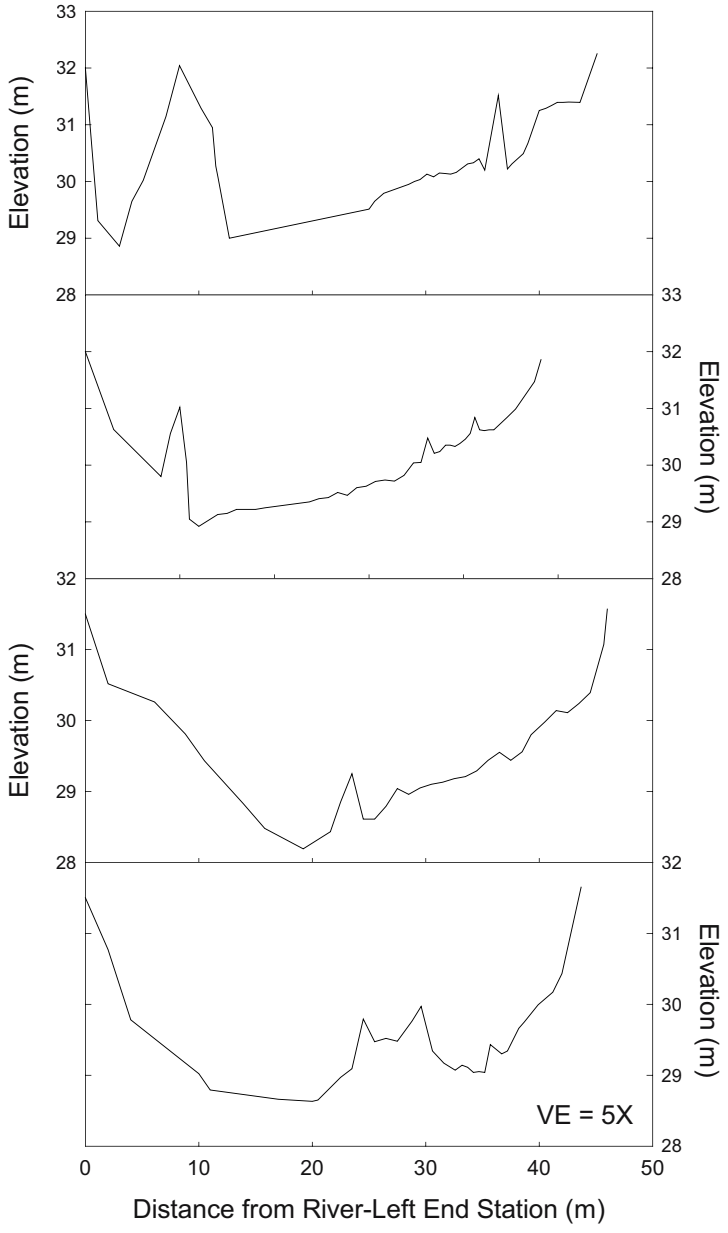

Figure 4. Cross-sections surveyed in the upper reach at Dos Cascadas on the Río Chagres. The uppermost cross-section is the upstream-most cross-section and vice versa. Note the relatively low relief of channel surfaces

A second reach was surveyed that included one cross-section approximately 50 m upstream from the first knickpoint, a second cross-section at the knickpoint lip, and a third cross section approximately 100 m downstream from the knickpoint lip, and well upstream from the second knickpoint (Fig. 5). The gradient approaching the knickpoint lip is 0.005. Top width was estimated during high flow as 40 m, and average depth as 5 m. In the gorge downstream from the knickpoint lip, high-flow top width decreases to 28 m and average depth is 4.2 m, suggesting very rapid and presumably turbulent flow along the gorge. The first knickpoint had a water-surface drop of 1.6 m during the low-flow conditions at the time of the survey (13 March 2005), but the high-water marks suggest that the water-surface drop would be negligible during high-flow conditions. Gradient in the gorge downstream from the first knickpoint is 0.004.

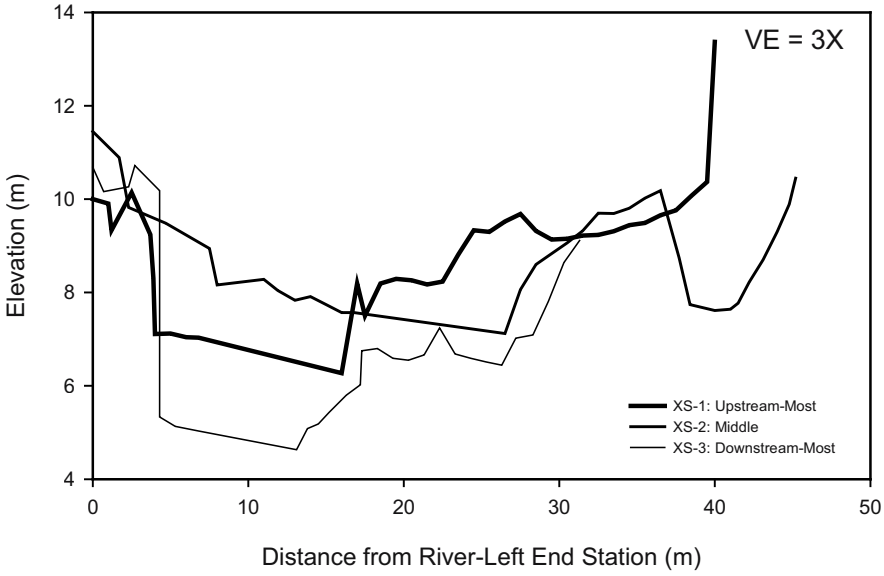

Figure 5. Cross-sections surveyed in the lower reach at Dos Cascadas on the upper Río Chagres. The cross-sections are superimposed to show the change in elevation surfaces and shape as a function of position relative to the knickpoint, which is located a few meters downstream of cross-section 2 (XS-2).

The lip of the upstream knickpoint is composed of andesite. Meter-thick andesite dikes and volcanoclastics lie below (downstream). Surface textures and erosion mechanisms of individual rock units are controlled by fracture-

spacings and, apparently, rock hardness. For instance, well-developed sculpted forms cover the surfaces of a chloritized andesite beneath the lip-forming andesite (Fig. 2). The rock hardness of the sculpted andesite is 50 ± 5 (n = 30). The remaining beds in the knickpoint score between 54 and 59, with mean scores statistically distinguishable from the sculpted bed for $\alpha = 0.01$. Joint spacing along sculpted portions of bedrock near the upper knickpoint is significantly larger (α = 0.05) than joint spacing along un-sculpted portions (Fig. 6). The two unsculpted sites do not differ significantly from one another, but the two sculpted sites are different at α = 0.05. The right bank sites (boxes 1 and 3, reading Fig. 6 from left to right) have more widely spaced joints than the left bank sites. The association of sculpted forms with the softest lithology present in the reach is, therefore, reflective of wider joint spacing in sculpted bed(s); jointing plays an important role in determining meso-scale erosion patterns in the vicinity of the upper knickpoint.

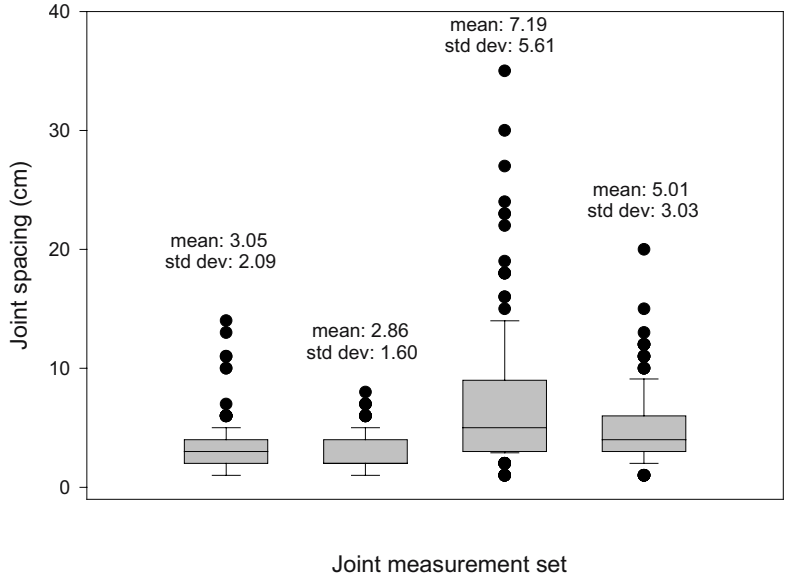

Figure 6. Joint spacing along unsculpted and sculpted portions of the channel boundaries downstream from the upper knickpoint at Dos Cascadas.

The influence of jointing is most important among rocks of similar composition. Based on rock-mass strength measurements taken throughout the upper Río Chagres drainage in 2002, mafic lithologies have a higher

average rock-mass strength than felsic lithologies (Fig. 3). Average rock-mass strength measured along the gorge downstream from the upper knickpoint at Dos Cascadas is intermediate in value, but rock hardnesses of felsic rocks are significantly lower than adjacent rocks. The overall resistances of individual felsic units are also lower, as measured by Selby scores (Fig. 7). The erosivity contrast is expressed in the vicinity of the upper knickpoint by the presence of alcoves excavated into felsic rocks along the channel margins. As discussed previously, exposures of felsic rocks are less common than mafic rocks in the watershed and bedrock outcrops in the channel are most commonly andesites and mafic rocks. Locally, exposure of felsic rocks reflects dynamic, cross-strike incision near the knickpoint, which is actively maintaining exposures of all local stratigraphic units.

Rock properties within the vicinity of the upper knickpoint are most varied downstream from the knickpoint. Passage of the upper knickpoint has produced an inner channel whose overall relief, as measured from flat surfaces on either bank, is greater than that upstream of the knickpoint (Figs. 4 and 5). Relief is as little as 2 m above the knickpoint (Fig. 5). Additional accommodation space is created in the form of an inner channel downstream during upstream translation of the knickpoint. The result is an increase in relief and longitudinal exposures of both felsic and mafic rocks.

As a result, whereas contrasts between felsic and mafic rocks are expressed as variations in the presence and length of exposures in the low relief channel upstream of the knickpoint, erosivity contrasts between the rock types are expressed as large-scale horizontal and vertical undulations of channel surfaces. Less resistant felsic rock units have been eroded to form the negative relief structures and the comparatively more resistant mafic rock units form the positive relief surfaces. Figure 7 indicates that the increased access to felsic rocks is associated with large variations in rock hardness and Selby scores over the short distances that represent typical unit thickness (meter-scale). Contrasts in resistance are highlighted by coefficients of variation (*CV*), which are sample standard deviations divided by means. Values of *CV* are plotted in Figure 7 for rock hardness values. Larger values indicate wider variations in rock hardness for a given unit. It is inferred that greater variations in rock hardness within a unit are associated with greater erosivity because weak areas are preferentially eroded, which aids erosion of more resistant portions of the unit. Rock units with greater values of *CV* are more fractured or weathered at Dos Cascadas. These units typically have negative relief in comparison to units with low *CV* values.

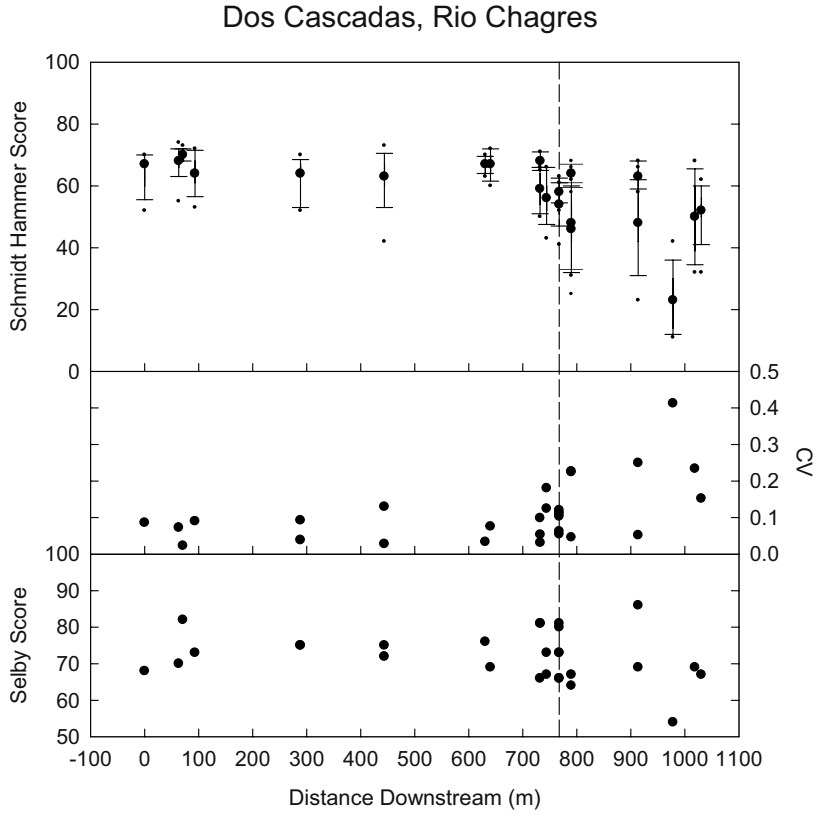

Figure 7. Longitudinal distribution of select variables associated with substrate resistance in both of the reaches examined at Dos Cascadas. The 0 x-position is the location of the upstream-most cross section used in the hydraulic models. The vertical dashed line represents the position of the upstream knickpoint. The better exposure of felsic rocks downstream of the knickpoint partially explains the large change in the variability of all three y-axis variables. The felsic rocks are less resistant (e.g., hard) and typically yield greater variations in Schmidt hammer scores because of fracturing and weathering.

Flow in the reach containing the first (upstream) knickpoint is against the bedrock dip, which probably increases substrate resistance (Wohl, 2000b). However, the river crosses the rock units obliquely, with individual units trending downstream from outcrops on the river-right bank (Fig. 8). The effect of this geometric arrangement is that hydraulic forces acting upon blocks on the river-right bank can slide or accelerate blocks in the downstream direction and into the channel. In contrast, hydraulic forces acting on the river-left bank accelerate blocks into the bank. The effect of this dichotomy is that blocks are more readily detached from the river-right

bank. As a result, there are many alcoves and vertical undulations where blocks have been removed from the river-right bank and slide into the mainstem channel (Fig. 9). In contrast, the river-left bank is partially cliff-lined and variations in surface relief are step-like with comparatively flat surfaces bounded by sharp discontinuities. This asymmetry (Fig. 9b) is also present at the downstream knickpoint. The general failure of blocks to slide into the channel on the river-left bank translates to longer residence times of large blocks, which must be removed by corrasion and comparatively small-scale block detachment or wholesale cliff collapse as a result of gradual undercutting. Such asymmetry in erosivity may aid inner channel development at Dos Cascadas by favoring greater transverse and vertical persistence of river-left bank surfaces during channel incision in the form of in-channel cliffs.

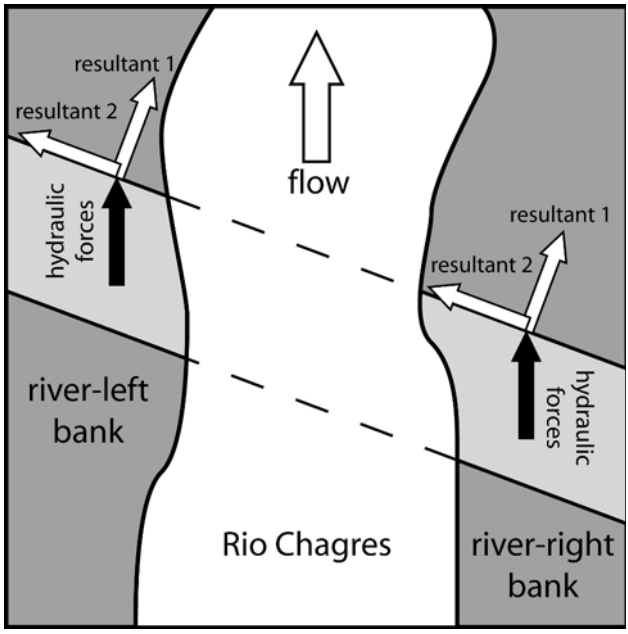

Figure 8. Schematic illustration of how the orientation of inclined strata to the direction of flow influences the alignment of acceleration vectors created by hydraulic phenomena. Acceleration of blocks on the upstream portion of an outcrop, which is river-right in this diagram, will have a resultant vector that is oriented toward the channel and is, hence, favorable for displacement (e.g., sliding) of blocks into the channel. In contrast, blocks on the downstream outcrop will be accelerated into the channel bank and will therefore be less likely to be quarried.

Figure 9a. Upstream view of river-right just below first knickpoint. A person is standing in embayment for scale.

Figure 9b. Upstream view below first knickpoint. Note oblique passage of rock units across the river and differences in channel topography between river-left (foreground) and river-right (across the river in this view).

4.2 Hydraulics

The forces associated with erosion in bedrock streams can be roughly approximated via in-channel velocities and select hydraulic-related variables. To this end, flood hydraulics were modeled for the upstream reach using the four cross-sections obtained from the channel survey (Fig. 5) and the 1-D, step-backwater program *HEC-RAS* (USAHEC, 1998). The cross-sections are spread along a longitudinal distance of 250 m. Additional cross-sections were interpolated between the surveyed cross-sections so as to improve model stability. A model discharge of 680 m^3/sec was used for all model runs. The discharge is an approximated value obtained from fieldwork conducted in a nearby reach in 2002. Values of Manning's *n* were estimated and two model runs were made using values of $n = 0.035$ and $n = 0.045$.

Table 1. Selected streamflow variables from a reach 400-800 m upstream of Dos Cascadas

Discharge (m^3/s)	*n*	Maximum Depth (m)	Top Width (m)	u (m/s)	Froude No.	Ω (W)	ω (W/m^2)	T (N/m^2)
680	0.035	5.3	45	4.1	0.7	580	13	140
680	0.045	5.7	45	3.6	0.6	630	14	170

Model results (Table 1) are consistent with the presence of a bedrock channel. Velocities, stream powers, and shear stresses are large compared to lowland alluvial channels (Wohl, 2000a). The average velocity is ~4 m/sec for both values of *n*. These velocities are sufficient to transport large clasts, even in the absence of intense vortices and highly variable water surfaces associated with standing and breaking waves, which are likely to be present given the high Froude numbers. Reported Froude numbers are width-averaged values (Table 1). Actual Froude numbers near the thalweg are likely to be higher. This places constraints on the ability to interpret the results of the model runs because the limited data available require flow to be modelled as uniform and steady. Nonetheless, the results clearly support the conclusion that the model discharge is associated with large erosion potentials. Additional evidence comes from the values of stream power and shear stress calculated for the reach (Table 1). Stream power is large compared to lowland and alluvial streams, although unit stream power is unexpectedly small for calculated velocities and shear stresses. The low value of unit stream power is explained by the dependence of the variable on discharge, which is comparatively small for the channel width. The shear

stress values are very large and can be interpreted to mean that the stream is readily capable of transporting large clasts and of detaching blocks of bedrock. Evidence of this is seen in the coarse cobble bars observed within and near the reach and by the fact that the channel is in large part bedrock-lined (*i.e.*, supply limited).

4.3 Substrate Erosion and Sediment Transport

The grain sizes observed in the active channel (D_{50} = 145 mm, D_{84} = 245 mm) attest to the ability of the stream to transport coarse sediments, although large boulders were not observed. Drag and lift forces acting on clasts are proportional to velocity and the square of the effective diameter of the particle (D) and the square of velocity (Hancock *et al.*, 1998). The large velocities and shear stresses are therefore important with respect to channel erosion and morphology because they simultaneously preclude occlusion of the bed by sediment and serve to accelerate abrasive and percussive tools (larger clasts). Percussion marks score the edges of some bedrock faces. However, the majority of surfaces within a few vertical meters of the low-water surface show evidence of abrasion by suspended sediment or small clasts. Low-lying surfaces are smooth compared to higher surfaces, although not polished. Polishing is only displayed in sculpted forms, which include: isolated potholes; longitudinally asymmetrical, flow-aligned, meter-high outcrops that resemble roche moutonees with downstream faces partially hollowed out by sculpted forms; wavy undulations on channel walls that resemble lateral potholes; and flutes. Sand banks and meter-thick slackwater deposits composed of sand are found in the gorge. The high velocities suggest that sand, a potentially potent agent of erosion, is probably transported as suspended load. This interpretation is supported by the presence of slackwater deposits several meters above bed surfaces exposed during the dry season. The overall importance of sculpted forms in long-term erosion of this reach of the upper Río Chagres is difficult to assess without monitoring of annual changes in bed surfaces, but the effects of abrasion are pervasive and we saw few displaced blocks attributable to nearby bed surfaces. The lack of obviously coincident detached blocks and concavities could reflect the ability of the upper Río Chagres to rapidly transport quarried blocks away from their source.

The effects of quarrying are most obvious on the river-right bank in the vicinity of the upper knickpoint at Dos Cascadas. Comparatively weak strata are preferentially eroded to form alcoves and strike-oriented depressions. A prominent strike-oriented depression lies to the river-right of the waterfall that is the upper knickpoint. The depression is carved into felsite and

descends from the river-right channel margin to a short drop-off into the dry-season water-surface within the inner channel. The depression apparently acts as an overflow feature during moderate flows. The corresponding outcrop on the river-right bank does not display a depression, in agreement with the expectation that quarrying of blocks is probably eased on the river-right bank by the favorable orientation of acceleration vectors (Fig. 8).

5. DISCUSSION AND CONCLUSIONS

Bedrock properties including lithology, jointing, dip, and resistance to weathering clearly play an important role in controlling the distribution and geometry of bedrock channel segments within the upper Río Chagres basin. Bedrock outcrops a few meters in length along the active channel may locally constrict the channel or induce flow separation and streambed scour. Scour associated with bedrock outcrops along the channel banks is particularly common in meander bends. Bedrock exposures greater than approximately 10 m along the active channel are likely to create channel reaches with slightly steeper gradient, lower width/depth ratio, and coarser-grained alluvial veneer than adjacent alluvial channel segments. These longer bedrock outcrops are likely to be present in mafic lithologies, which have greater values of rock-mass strength than felsic lithologies.

The Dos Cascadas reach, which represents the most substantial profile discontinuity and the longest continuous bedrock exposure in the middle and lower reaches of the upper Río Chagres, is formed predominantly in mafic lithologies. The two knickpoints in this reach are formed in andesite. The surface textures and erosion mechanisms of individual rock units at the knickpoints and in the gorge downstream from the first knickpoint correlate strongly with fracture spacing and rock hardness. Sculpted portions of the channel are formed in softer rocks with more widely spaced joints. Felsic rock units, which tend to be more fully excavated along the river banks, have larger coefficients of variation in rock-mass strength. Local dip also appears to control channel geometry in the gorge; rocks on river-right strike into the channel and are more excavated than equivalent rock units on river-left.

The presence of the gorge downstream from the first knickpoint suggests that this knickpoint has been maintained through time as it has migrated upstream. The formation of the knickpoint and gorge presumably result from the presence of an extensive outcrop of resistant mafic rocks. These rocks are present for at least several hundred meters upstream from the first knickpoint, suggesting that the knickpoint will also be maintained as it migrates headward through this portion of the Río Chagres. The existence of

two knickpoints only a few hundred meters apart along the channel suggests that the rate of migration of the upstream knickpoint is not keeping pace with downstream profile lowering, causing a second knickpoint to form and migrate upstream. These knickpoints together form a local baselevel for the upstream portion of the basin and limit the rate at which the upper basin can respond to changes in ultimate baselevel.

ACKNOWLEDGEMENTS

The bulk of the field work described in this paper was conducted during a visit to the upper Río Chagres in March 2005, although we also draw on data from the 2002 field season. We thank Susan Howe and Aquilino Alveo for field assistance in 2002 and LuisYen for field assistance in 2005. During both field seasons, Russell Harmon and the staff of IEASA in Panama provided invaluable assistance with logistics. Russell Harmon and Gerhard Wörner provided the information on the geological field mapping and bedrock lithologic data. This research was funded under grant DAAD 19-00-1-0474 from the US Army Research Office.

REFERENCES

Baker, VR, 1988, Flood erosion, in *Flood Geomorphology* (VR Baker, RC Kochel and PC Patton, eds.), John Wiley, New York, NY: 81-95.

Biedenharn, DS, 1989, Knickpoint migration characteristics in the loess hills of North Mississippi, USA: in US-China Sedimentation Symposium.

Bishop, P and Goldrick, G, 1992, Morphology, processes and evolution of two waterfalls near Cowra, New South Wales: Australian Geogr., 23: 116-121.

Gardner, TW, 1983, Experimental study of knickpoint and longitudinal profile evolution in cohesive, homogeneous material. Geol. Soc. Amer. Bull., 94: 664-672.

Hancock, GS and Small, EE, 2005, The coupling of weathering and rock erosion in streams. Jour. Geophys. Res. Earth Surfaces, in press.

Hancock, GS, Anderson, RS, and Whipple, KX, 1998, Beyond power: bedrock river incision process and form: in *Rivers Over Rock: Fluvial Processes in Bedrock Channels* (KJ Tinkler and EE Wohl, eds.), Amer. Geophys. Union Press, Washington, DC: 35-60.

Holland, WN and Pickup, G, 1976, Flume study of knickpoint development in stratified sediment: Geol. Soc. Amer. Bull., 87: 76-82.

Houseal, B, 1999, Plan de manejo y desarrollo del parque nacional Soberania. USAID/INRENARE, Panama City, Panama, in *Protecting Watershed Areas. Case of the Panama Canal* (MS Ashton, JL O'Hara and R Hauff, eds.), Food Products Press, New York: 4.

Merritts, DJ and Vincent, KR, 1989, Geomorphic response of coastal streams to low, intermediate, and high rates of uplift, Mendocino triple junction region, northern Californina: Geol. Soc. Amer. Bull., 100: 1373-1388.

Miller, AJ and Cluer, BL, 1998, Modeling considerations for simulation of flow in bedrock channels: in *Rivers Over Rock: Fluvial Processes in Bedrock Channels* (KJ Tinkler and EE Wohl, eds.). Amer. Geophys.Union Press, Washington, DC: 61-104.

Miller, JR 1991, The influence of bedrock geology on knickpoint development and channel-bed degradation along downcutting streams in south-central Indiana: Jour. Geol., 99: 591-605.

O'Connor, JE and Webb, RH, 1988, Hydraulic modeling for paleoflood analysis: in *Flood Geomorphology* (VR Baker, RC Kochel and PC Patton, eds.), John Wiley and Sons, New York, NY: 393-402.

Pyrce, RS, 1995, A Field Investigation of Planimetric Knickpoint Morphology from Rock-Bed Sections of Niagara Escarpment Fluvial Systems: MA Thesis, Wilfrid Laurier Univ., Canada.

Seidl, MA and Dietrich, WE, 1992, The problem of channel erosion into bedrock: Catena, Supplement, 23: 101-124.

Seidl, MA, Dietrich, WE, and Kirchner, JW, 1994, Longitudinal profile development into bedrock: an analysis of Hawaiian channels: Jour. Geol., 102: 457-474.

Seidl, MA, Finkel, RC, Caffee, MW, Hudson, GB, and Dietrich, WE, 1997, Cosmogenic isotope analyses applied to river longitudinal profile evolution: problems and interpretations: Earth Surface Proc. Landforms, 22: 195-209.

Selby, MJ, 1980. A rock mass strength classification for geomorphic purposes: with tests from Antarctica and New Zealand: Zeitschr. Geomorph., 24: 31-51.

Springer, GS and Wohl, EE, 2002. Empirical and theoretical investigations of sculpted forms in Buckeye Creek Cave, West Virginia: Jour. Geol., 110: 469-481.

Stein, OR and Julien, PY, 1993, Criterion delineating the mode of headcut migration. Jour. Hydraul. Eng., 119: 37-50.

Tanaka, Y, Onda, Y, and Agata, Y, 1993, Effect of rock properties on the longitudinal profiles of river beds: comparison of the mountain rivers in granite and Paleozoic sedimentary rock basins: Geogr. Rev. Japan, 66A: 203-216.

Tinkler, K and Wohl, EE, 1998, A primer on bedrock channels, in *Rivers Over Rock: Fluvial Processes in Bedrock Channels* (KJ Tinkler and EE Wohl, eds.), Amer. Geophys. Union Press, Washington, DC: 1-18.

US Army Corps of Engineers, 1998, HEC-RAS River Analysis System: Hydraulic Reference Manual. USACE Hydrologic Engineering Center,, Davis, CA.

Wohl, EE, 1992, Bedrock benches and boulder bars: floods in the Burdekin Gorge of Australia: Geol. Soc. Amer. Bull., 104: 770-778.

Wohl, EE, 1993, Bedrock channel incision along Piccaninny Creek, Australia: Journ. Geology, 101: 749-761.

Wohl, EE, 1998, Bedrock channel morphology in relation to erosional processes, in *Rivers Over Rock: Fluvial Processes in Bedrock Channels* (KJ Tinkler and EE Wohl, eds.), Amer. Geophys. Union Press, Washington, DC: 133-151.

Wohl, EE, 1999, Incised bedrock channels, in *Incised River Channels* (SE Darby and A Simon, eds.), John Wiley and Sons, Chichester, UK: 187-218.

Wohl, EE, 2000a, *Mountain Rivers*, Amer. Geophys. Union Press, Washington, DC:, 320p.

Wohl, EE, 2000b, Substrate influences on step-pool sequences in the Christopher Creek drainage, Arizona: Jour. Geol., 108: 121-129.

Wohl, EE, 2005, Downstream hydraulic geometry along a tropical mountain river: in *The Río Chagres: A Multidisciplinary Profile of a Tropical Watershed* (RS Harmon, ed.), (RS Harmon, ed.), Kluwer Acad./Plenum Pub., New York, NY: 169-188.

Wohl, EE, Greenbaum, N, Schick, AP, and Baker, VR, 1994, Controls on bedrock channel incision along Nahal Paran, Israel: Earth Surface Proc. Landforms, 19: 1-13.

Wohl, E and Ikeda, H, 1997. Experimental simulation of channel incision into a cohesive substrate at varying gradients: Geology, 25: 295-298.

Wolman, MG, 1954, A method of sampling coarse river-bed material: EOS, Trans. Amer. Geophys. Union, 35: 951-956.

Worner, G, Harmon RS, Hartmann, G, and Simon, K, 2005, Igneous geology and geochemistry of the upper Río Chagres basin: in *The Río Chagres: A Multidisciplinary Profile of a Tropical Watershed* (RS Harmon, ed.), Kluwer Acad./Plenum Pub., New York, NY: 65-82.

Young, RW, 1985, Waterfalls: form and process: Zeitschr. Geomorph., 55: 81-95.

Chapter 13

USING TRMM TO EXPLORE RAINFALL VARIABILITY IN THE UPPER RÍO CHAGRES CATCHMENT, PANAMA

Ryan G. Knox, Fred L. Ogden and Tufa Dinku
University of Connecticut

Abstract: The upper Río Chagres basin is a significant source of water for operation of the Panama Canal, producing a disproportionate share of the total runoff to the canal and also serving as the source of metropolitan drinking water for Panama City and Colon. To better understand the distribution of rainfall in the upper Río Chagres watershed, a study was performed using rainfall observations from both ground- and space-based platforms in a geo-spatial statistical framework. The ground-based data are from two rain gages with long-term records and five additional gages installed in 1998. Given the significant topographic relief, and the sparsely distributed network of rain gages, it is likely that the spatial variability of rainfall is not accurately measured by this rain gage network. This paper asks two questions: Does a significant relationship exist between precipitation and elevation? Can the fraction of total catchment's rainfall coverage for storm events be determined? Three methods are to answer these questions ussing TRMM (Tropical Rainfall Measurement Mission) data products. The TRMM satellite provides 4 km^2 resolution PR (Precipitation Radar) and much coarser TMI (TRMM Microwave Imager) observations multiple times per day. The instruments observe swath widths of 220 and 758 km respectively. Full basin coverage of a spatially distributed rain field observation is possible at PR resolution, allowing for determination of the areal extent of rain. Moreover, TRMM data can be used to develop a statistical model of the spatial variability of rainfall in an effort to make basin average estimates. Thirdly, available TRMM rainfall estimates are used directly, in validation of rain gage data.

Key words: Panama; Río Chagres; climatology; rainfall monitoring; potential evaporation; TRMM

R. S. Harmon (ed.), The Río Chagres, Panama, 211-226.

1. INTRODUCTION AND BACKGROUND

For the purposes of modeling and studying catchment runoff phenomena, hydrologists are often confronted with assessing the spatial variability of precipitation. There are various practical reasons for performing such analysis, especially in areas where water balance is carefully scrutinized. The general interest is to explore the basin scale spatial variability of rainfall intensity estimates and test for a general precipitation relationship to orography.

The upper Río Chagres basin, situated north of the Panama Canal on the Isthmus of Panama, has many attractive features for study. As a primary contributor of water to the Panama Canal and its operations, there are long-term data sets for the region. Data are available from telemetered rain gage stations situated in and around the upper Río Chagres catchment, provided by the Autoridad del Canal de Panama (ACP). While most records are available continuously since early 2000, data exist as far back as the late 1970s for two of the gages. The upper Río Chagres basin covers 414 km^2 with elevation range of roughly 180 to 1000 meters. There are steep mountainous slopes in most of the catchment. Furthermore, at the Isthmus scale, Espinosa (1998) indicates the region is characterized by seasonal climatic conditions with frequent heavy rainfall.

The first motivation for this study arose from parallel efforts by Niedzialek and Ogden (2005, this volume). In considering topography, local climatic conditions of heavy rainfall and steep climatological gradients, significant and quantifiable spatial trends in rainfall may exist. Therefore, the use of data from the TRMM (Tropical Rainfall Measurement Mission) satellite are investigated to discern any spatial patterns and trends in precipitation across the upper Río Chagres watershed. If a statistical relationship between rain rate and elevation can be detected, then it should be possible to develop a generalized functional relationship between elevation and mean rainfall. Also of interest are other discernable forms of spatial variability in mean rainfall

2. METHODOLOGY

Data were utilized from seven active ACP rain gages. These gages each have continuous data records dating back to the spring of 2000. Figure 1 shows rain gage locations in and around the upper Río Chagres basin featured on a digital elevation map.

To process the rain gage data, rainfall tips were summed over daily time intervals to record total rainfall depth, the sums were conditional on the event that all gages received rain on a given day. Daily measurements presented much noise. To reduce this data, conditioned daily totals were summed at monthly resolution. Monthly accumulations were normalized by the average of the field during that month. Figure 2 shows normalized monthly rainfall accumulations for the rain gages versus elevation. The null hypothesis for the study was that relative rainfall accumulation is not dependant on elevation with statistical significance. A linear regression was fit to the data assuming relative rain accumulation and elevation are the dependant and independent variables, respectively, and an F statistic used as an objective function. This compares the divergence of gage means from the field average to the amount of variability expected at each gage. In this case, a small F statistic (F = 0.8525) and weak slope are reported. This indicates that the rainfall accumulation change is insignificant at different elevations compared to the amount of internal variance.

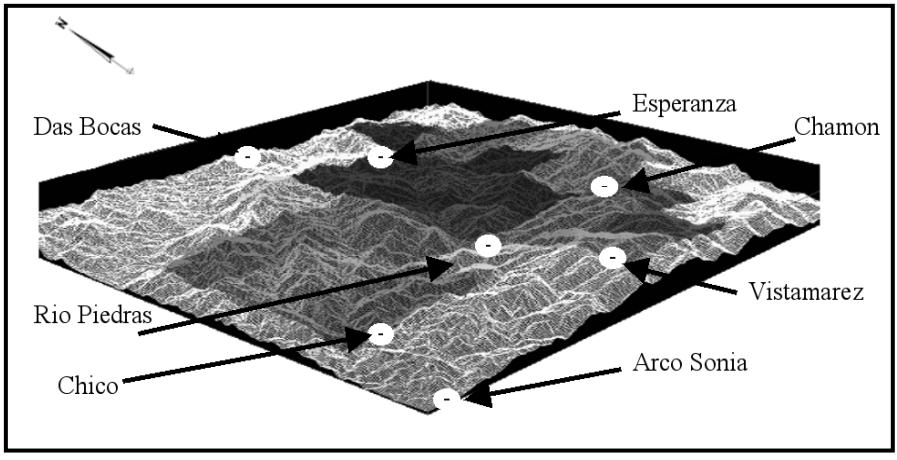

Figure 1. Digital elevation map of the upper Río Chagres watershed illustrating the spatial layout of rain gages across the basin

Espinosa (1998), in a climatological report, depicts the relative monthly wind directional intensities for the town of Cristobal on the northern Atlantic coast of Panama. The mean wind direction is significantly biased towards the north and northeast in the dry season and moderately biased towards the north in the wet season. Considering that the upper Río Chagres basin may be subject to such climatological influences like moist airflows from the

north, this analysis tested for the presence of relative precipitation to location relationships. Normalized monthly rainfall versus latitude is plotted in Figure 3, rather than elevation as in Figure 2. The plan view orientation of the gages in Figure 1 can be referenced to the latitudinal distribution shown. Again, a regression fit was again applied to the data. This case shows a more pronounced slope and robust F-statistic (F = 106.6) compared to those cases showing generalized elevation effects.

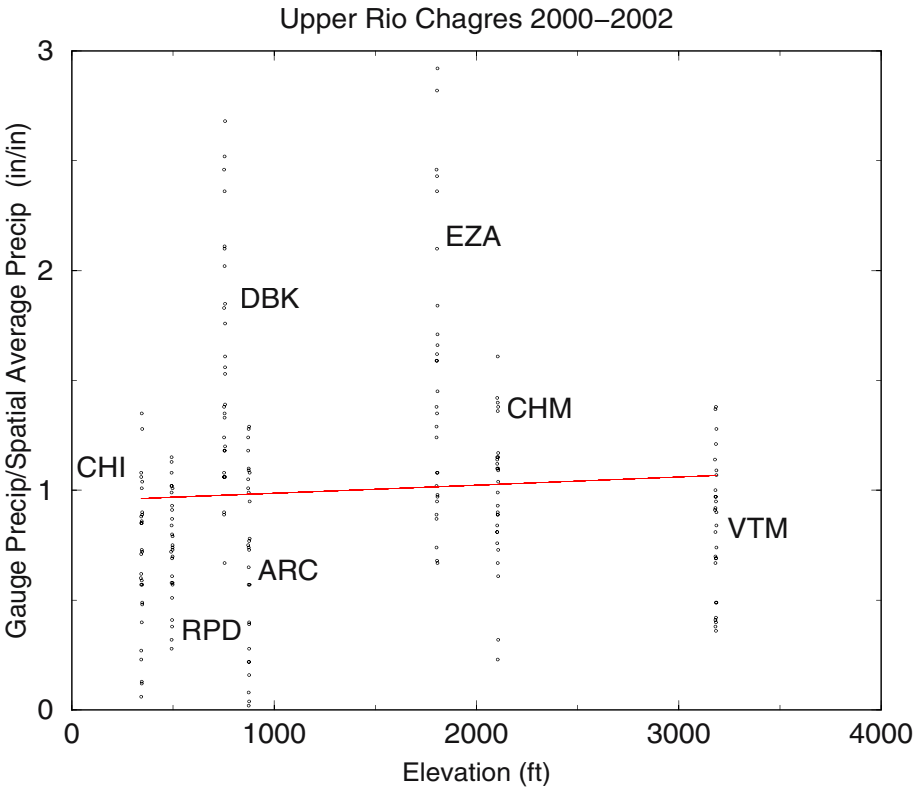

Figure 2. Normalized monthly rain accumulations as seen by recorded by the local rain gages plotted on respective elevation. Data record is from spring 2000 through 2002.

Comparing Figures 2 and 3, it is apparent that there is a strong N-S gradient in rainfall, with rainfall being highest at gages in the north, and lowest in the south. This feature points to added complexity in addition to elevation, given the poor relationship displayed in Figure 2. However, it is impossible to continue much further inference about the spatial structure of the rainfall from the given rain gage network.

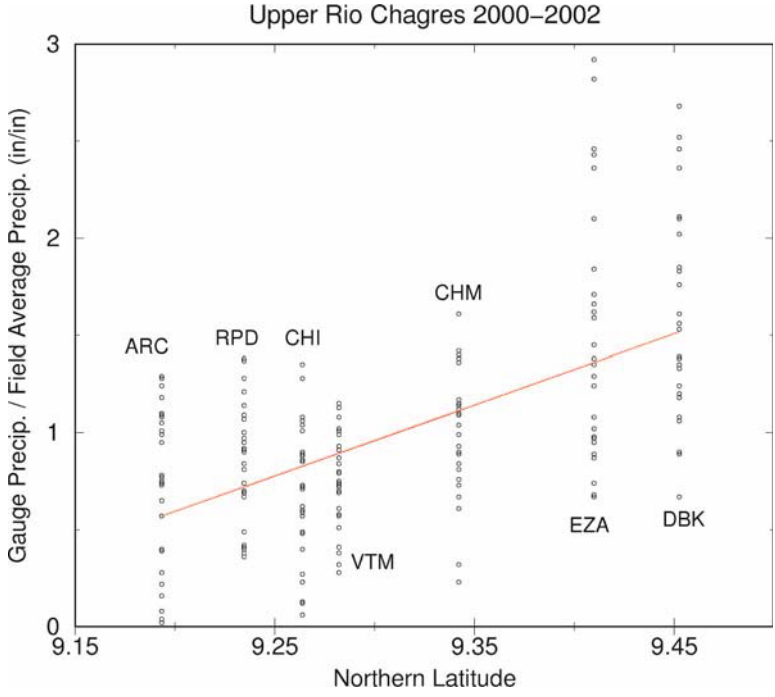

The TRMM (Tropical Rainfall Measurement Mission) satellite is a joint project between the US National Aeronautics and Space Administration (NASA) and the National Space Development Agency of Japan (NASDA). TRMM has a 35^{o} orbital inclination, which restricts the satellite to the tropics and sub-tropics. The TRMM satellite is a current leading technology available for space-based remote sensing precipitation estimation. The platform hosts several instruments including a Lightning Image Sensor, a Cloud-Earth Radiant Energy System and a Visible Infrared Scanner. This work targeted the use two instruments; the TRMM Microwave Imager along with the Precipitation Radar. The spatial resolution of the TMI is approximately 5x7 km^2 at highest frequency channels up to 63x37 km^2 at low frequency. Interested that TMI swath widths offer more overpasses of the basin on average, it was observed that the resolution was too coarse at most channels to portray spatial variability at the spatial scale of interest For this reason, use of the TMI data was not considered. Follow-up studies could use the highest frequency TMI band (*e.g.,* 85 GHz) for rainfall estimation. A value study on resolution and overpass frequency is being considered.

TRMM Precipitation Radar (PR) products have better resolution of approximately 4-5 km depending on orbit height, and the off-nadir look angle. This resolution allows rainfall over the basin to be discretized into a 28-cell grid, which is acceptable to portray spatial variability of rainfall. 2A25 data provide instantaneous rainfall products of 3-D rain fields derived from active Precipitation Radar reflectivity. The 2A25 rainfall data are based on a Z-R conversion and attenuation correction algorithm. Iguchi and Menghini (1994) explain the technique as a hybrid of Hitschfeld-Bordan and surface reference methods used to produce vertical reflectivity profiles. Rainfall intensities are distributed horizontally and vertically. The vertical precipitation profile comprises 80 swath height elevations at 250 m apart reaching a ceiling of 20 km. The data files available in HDF format contain individual orbital swaths (earth overpasses) of rain rates, location, scan time and various supplementary data. TRMM 2A25 rainfall data were acquired compliments of the NASA Goddard Space Flight Center DAAC web server. Figure 4 shows the UTM projection view of typical PR swaths of the region, the overpass swath width of approximately 214 km can be seen by the straight lines. Grey-scale contours indicate precipitation seen by the TRMM overlaid on the Panamanian coastline. The Panama Canal and eastern contributing basins are featured in the figure.

The first steps taken in processing TRMM data consisted of performing a spatial search on TRMM 2A25 looking for all available events within the central Panama area of interest (8.58^{o}N latitude, 80.72^{o}W longitude to 9.5^{o}N latitude, 79.17^{o}W longitude). A mask identifying the 28 grid centers covering the upper Río Chagres basin was merged with a second algorithm to geo-locate those nearest PR pixels defining TRMM data. Nearest PR pixels within a 5x5 km^2 box surrounding stationary grid cells were averaged and assigned to the surface grid cells. PR precipitation swaths are non-stationary in their location and require geo-referencing per each event. No-rain events and orbitals without complete basin coverage were discarded. All available overpasses of 2A25 PR data were selected from 1999-2002 and were applied to the algorithms. A total of 506 overpasses were retrieved over the box enclosing the upper Río Chagres basin that met our conditioning criteria, 100 orbits were found to have rainfall in at least one of the 28 bins over the upper Río Chagres for that overflight.

The effect of ground clutter on data quality was considered. The 2A25 data separate surface clutter ranges from clutter free ranges by observing complimenting PR 1C21 outputs, however surface clutter can, on occasion, be unavoidably misinterpreted as rain echoes, especially in mountainous regions (TRMM, 1999). As previously noted, there is an approximate 1000m height differential between high mountain peaks within the upper Río Chagres watershed and sea level. Moreover, the geometry of the TRMM

satellites travel and declination angle results in radar reflectivity bins that are not horizontal far from the nadir. The tipped bins can extend to a maximum of 500 meters from edge to center swath height**.** To avoid complications and potential clutter, we elected to use minimum bin height of 1750 meters, to positively avoid ground clutter. The TRMM 2A25 product returns a specified signal for bad or cluttered data, which was filtered during data processing. In the event that any of the 2A25 grid cells above the charges basin returned this clutter signal, that event was omitted entirely. It was found that at higher elevations, there were much fewer occasions where clutter was present in captured rainfall events.

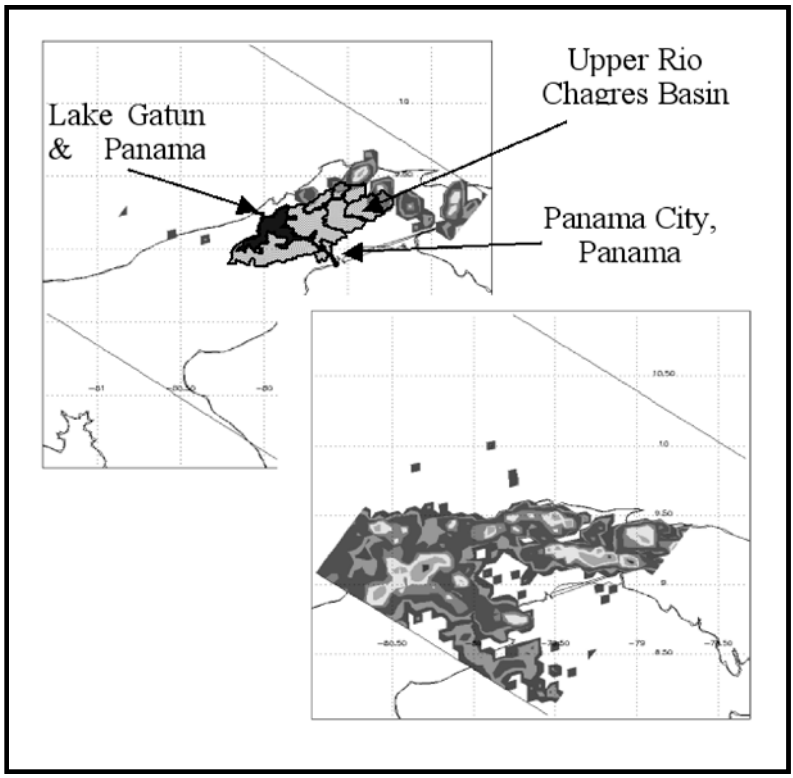

Figure 4. Sample images of precipitation as viewed by TRMM orbital swaths. The upper panel features the catchment boundaries and reference locations. Precipitation is contoured in grey scale by variable intensity in the lower panel.

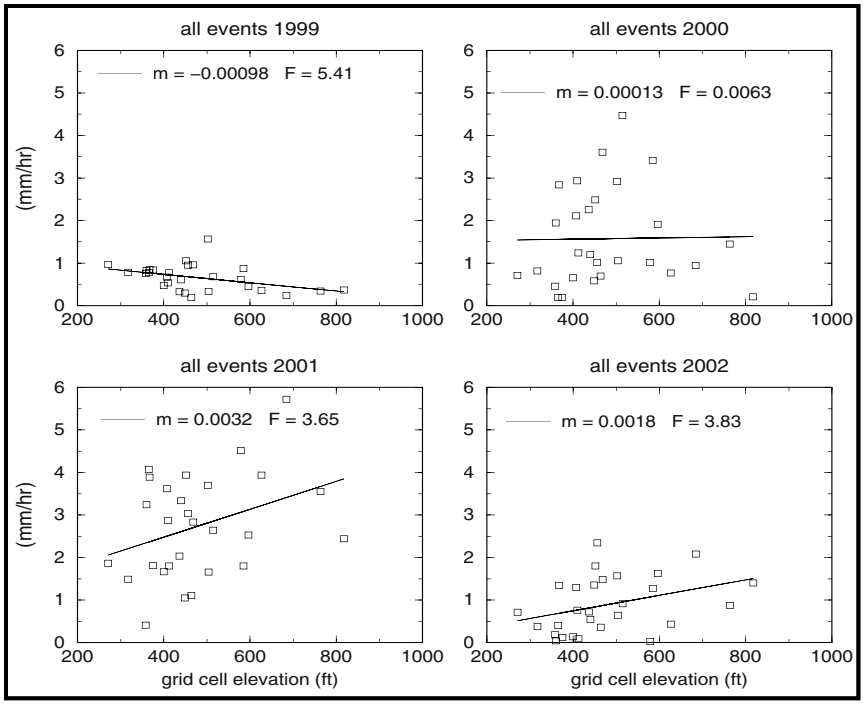

Figure 5. Mean TRMM precipitation intensity estimates of grid cells in the upper Río Chagres basin. Comparison of yearly means. Cell values are plotted against average topographic elevation.

The initial objective of the TRMM data analysis was to test the hypothesis that there may be a generalized orographic effect. Of the 100 positive rain events, various yearly time frames and seasons were further grouped for analysis. Captured rain events by the TRMM PR were cycled for each year of the study, rainfall intensities on each of the cells were averaged over their respective time interval. Figure 5 compares the yearly mean rainfall (mm/hr) estimated at 2000 meters to the individual elevation of the cell. Cell center elevations were determined by averaging the nearest grid cells. The elevation data was retrieved from a 90 m digital elevation model.

Mean PR rain intensities over a four-year period at bin heights of 2000 and 1750 meters are compared in Figure 6. Likewise for each elevation, wet season only data were compared to full years for the time span of 1999-2002. The wet season was selected as including all events from July through January.

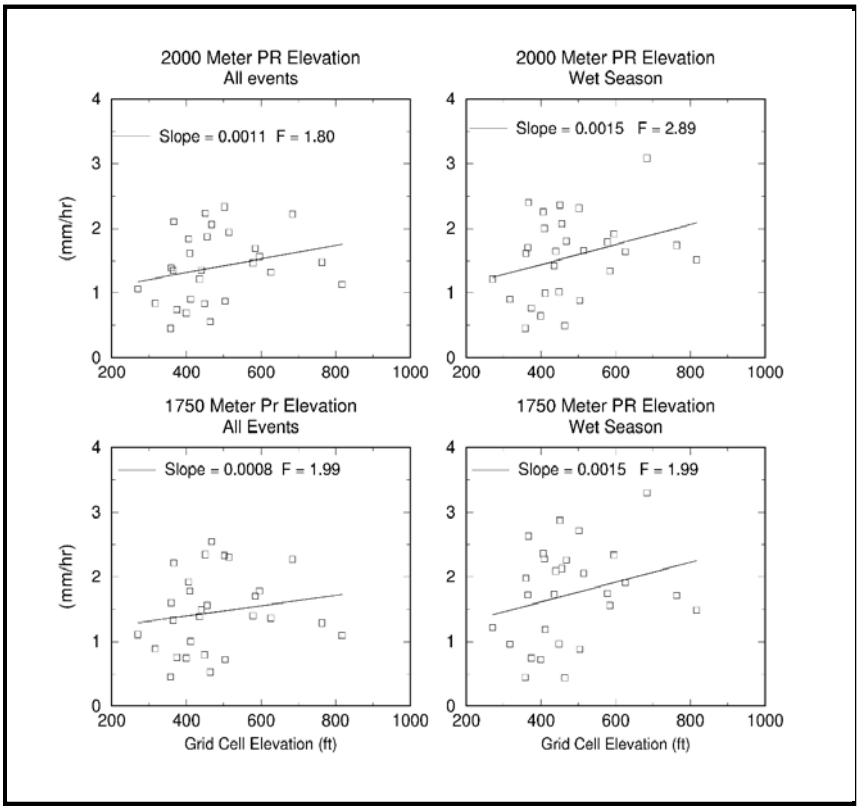

Figure 6. Mean TRMM precipitation intensity estimates of grid cells in upper Río Chagres basin. Dual comparison of 1750 and 2000 m swath height estimates coupled with wet season only and yearly data. Cell values are plotted against average topographic elevation.

Recalling that the rain gages reported a positive and more robust linear regression of rain accumulation with increased latitude than that of purely generalized orography, a similar approach was taken with TRMM data. TRMM rainfall estimates for each grid cell were normalized by the spatial mean and plotted against their individual latitudes. A slight trend was noticed and it can be interpreted from the linear regression in Figure 7 that the gross difference in mean rain at latitudinal extremes was 24%. However, the powerful multidimensionality of the TRMM spatial estimates is shadowed. Furthermore, the statistics are not as significant as those latitudinal effects present in the rain gages.

GRASS open-source GIS software was used to display areal projections of TRMM rainfall accumulations on 4x4 km^2 grids over the upper Río

Chagres watershed. Figures 8 and 9, show the two dimensional relative rainfall intensity. Rainfall for each grid cell was accumulated over the course of TRMM observations. Each cell was then normalized by the spatial mean accumulation, therefore making a mean relative rainfall accumulation of 1. Values have been scaled by 1000 for mapping purposes. Higher rainfall accumulation is characterized by darker shades but more directly the fraction.

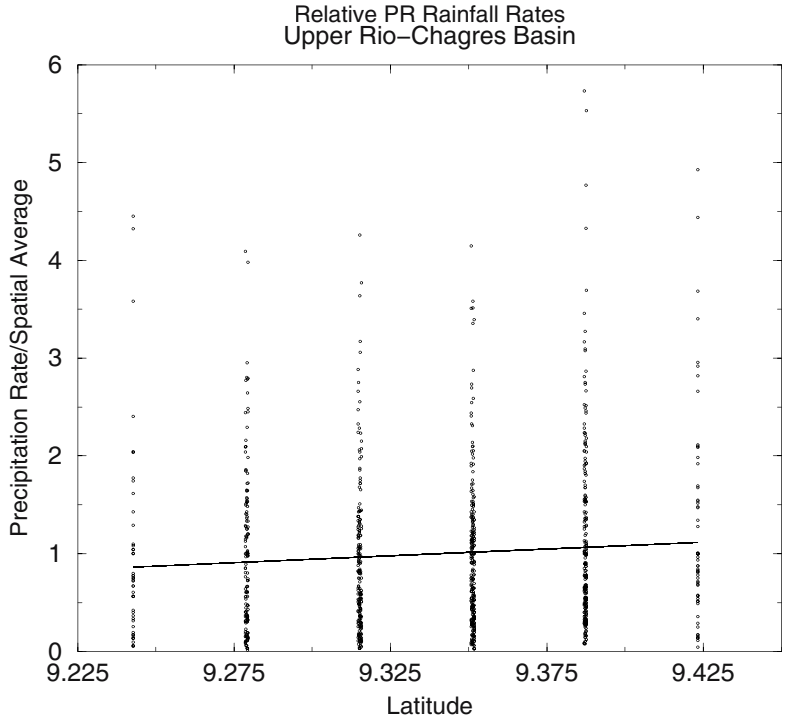

Figure 7. Spatially normalized TRMM precipitation estimates at variable latitude. Data taken from season observations 1999-2002.

Note that the relative rainfall accumulations shown in Figure 9 are summations of random samples from a continuous space-time series of rainfall. The probability was calculated that TRMM observed rainfall in each grid cell out of the total one hundred events with positive rainfall inside the basin. All events that contributed to deriving the relative spatial rainfall accumulation field were summed to total positively recorded events per grid. Figure 10 shows the percentage of times rain was captured by TRMM for each grid cell.

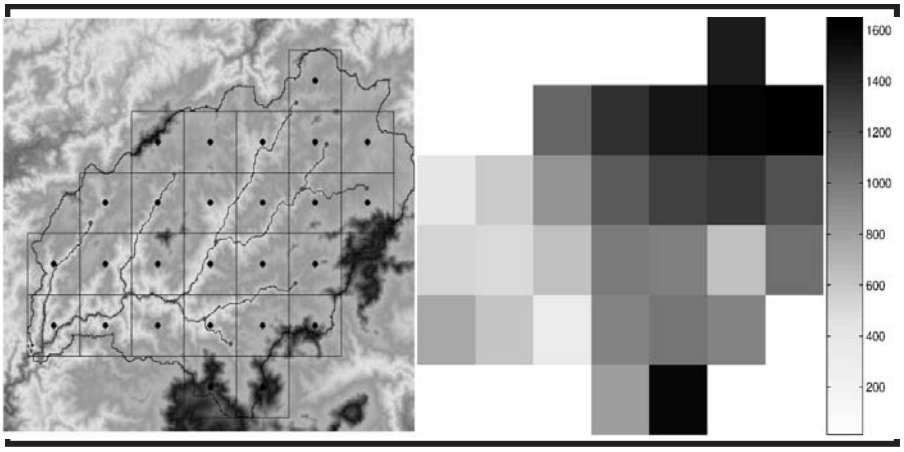

Figure 8. (left) and *Figure 9* (right). Stationary TRMM pixel locations are overlaid on a digital elevation model in the left panel. The right panel refers to the same location in space, and portrays the relative mean rainfall accumulation for the period of TRMM observations. Values portrayed as integers, fractional amounts can be achieved by scaling down by 1000.

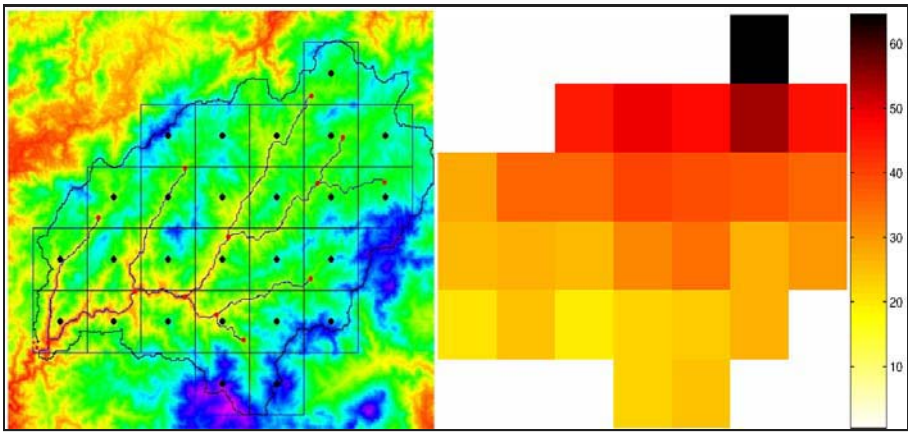

Figure 10 (left) and *Figure 11* (right). Stationary TRMM pixel locations are featured with total counts of rain events per each grid cell over the total period of observation. The right panel refers to the same location in space, and portrays the relative mean rainfall accumulation for the period of TRMM observations. Values portrayed as integers, fractional amounts can be achieved by scaling down by 1000.

3. DISCUSSION AND ANALYSIS

In this analysis effort, a weighting scheme was needed to describe the spatial variability of rain for input to hydrologic models. The null hypothesis was set that rain rate could not be related as a function of orography. If negated, there is potential that rain rates could be described by an elevation function. A functional relation (P-E) could be used to assign weights for hydrologic model inputs. It was decided to consider the rain events over the continuous record from 2000 through 2002 as a random process, and compare monthly precipitation values to their respective elevations to ascertain if a robust linear relationship could be found indicating that generally more precipitation occurs at higher elevation? The obvious variance in the rain gage data as described by Figure 2, as well as the near-zero slope and small F statistic do not statistically support the presence of a general and linear orographic effect through the data.

It should be noted that, at some locations such as the Dos Bocas and Esperanza gages, there is significantly higher relative monthly rainfall. These locations can be cited as places of relatively high North latitude, not elevation. If a generalized relationship did exist, it would be expected that rain gauges at the highest elevations, such as Chamon and especially Vista Mares, to have much larger rainfall accumulations. This is not the case. The highest recorded precipitation was present in those gauges farther north. The data in Figure 3 indicate that there is a much stronger general linear relationship between normalized monthly rainfalls as a function of latitude. The TRMM latitudinal rainfall intensity data shown in Figure 7 indicates that the trend is positive with respect to latitude, however the relationship is weak. It can be concluded, for instance, that the mean rainfall observed over Dos Bocas is separated from mean rainfall at Chico. This only implies a non-homogenous spatial rainfall probability irrespective of gradient. A generalized spatial gradient as sought with TRMM analysis may still exist.

According to rain gage record, a weak positive trend is observed in mean precipitation as a function of elevation, conditional upon rainfall over a 4-year time span. Additionally in Figure 5, those TRMM data for 2002 were the first observed and hinted that there may be some general P-E relation. Further assessment indicated that this tendency was not consistent in 2001, 2000, and 1999. This was especially apparent in 1999. Representing a year of drought, 1999 may be characteristic of abnormal seasonal weather conditions. However, these graphs show little to no indication of a P-E relation of statistical significance for the upper Río Chagres watershed.

Figure 6, compared elevation swaths and returned relatively similar results, as did the wet season. Changing observation criteria had little effect on uncovering a more robust relationship. This was consistent with the

results forwarded by the rain-gauge data, affirming that a generalized P-E relationship does not exist.

The TRMM PR makes approximately 1.1 overflights per day, on average, at the latitude of the region of interest. It is critical to realize that one should not regard the 2A25 estimates as having the ability to infer a temporal statistic, random observations at roughly daily time scales can not support this. Instead, the observations must be viewed purely as a 100 random events within the 4-year time domain. However, TRMM PR estimates can be used to identify mean climatological difference in space, over the appropriate time and space scales. The working spatial scale is quite small for this study, and does not allow for spatial averaging which can eliminate noise. However, given 100 overflights during rain, it is possible to make qualitative assessments and distinctive observations of the rainfall variability within the basin. This assumption is dependant on the fact that TRMM overpasses are not diurnally biased in time. The probability of occurrence for rainfall events on a sub-daily scale may not be consistent with the probability of TRMM capture.

Considering that the hourly overflight probability of the TRMM satellite is distributed uniformly across the day, the probability of capturing a rain event by the TRMM radar would theoretically match the distribution of actual rain occurrence. Figure 12 shows the probability of TRMM and gage based rain occurrence taken from five local gages over the 1999-2002 TRMM overflight time domain as a function of hour of the day (local Panama time). Figure 12 illustrates that the peak probability of capturing rain match, and there is some agreement that TRMM probability of capture is commensurate with the rainfall occurrence probability derived from the gage data

Based on this observation it is inferred from the mean rainfall intensity maps and the latitude effect of rain gauges displayed in Figure 3, that the headwaters of the basin are receiving generally more rainfall than the outlet. This is a qualitative observation that in the northeast part of the watershed we notice generally higher rainfalls.

It was observed that Esperanza and Dos Bocas had higher rain averages than did the Vista Mares and Chamon gages. Similarly, we can see the TRMM data estimates higher rainfall over the Esperanza gage and less over the Chamon and Vista Mares as well. If, for instance, moisture flows from the Caribbean Sea, the precipitation recorded by a rain gage or observed by TRMM may be effected by topography. Figure 13 gives a three dimensional representation of the landscape of the upper Rio Charges basin. A color grid much like those portrayed in figures 9 and 10 represents relative rainfall

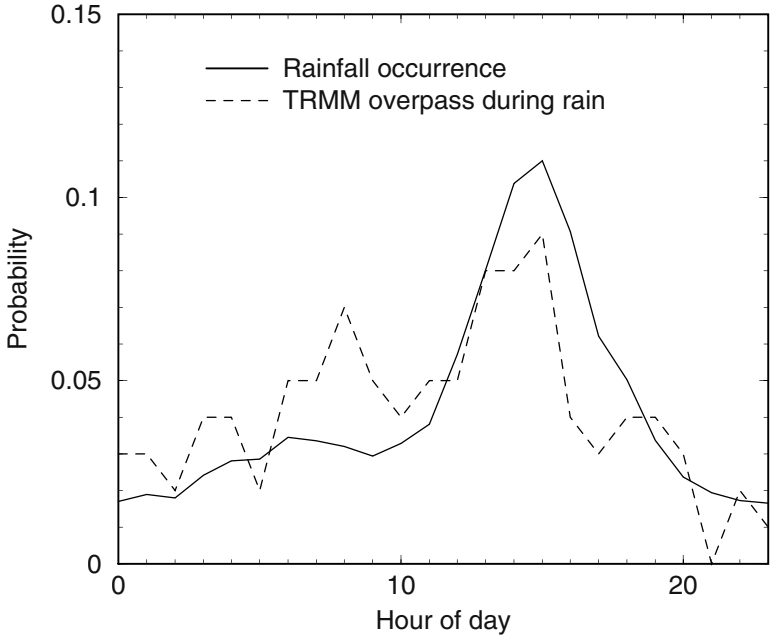

Figure 12. Diurnal probability mass curves of TRMM and rain gage capture of rainfall events. Observations were taken over the joint parameter space January 2000 through December 2002.

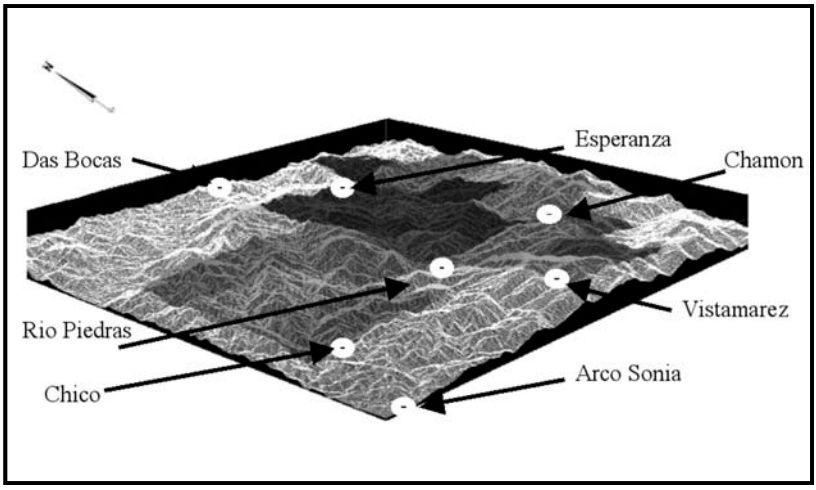

Figure 13. A 3-D relief image of the upper Río Chagres drainage basin, showing rain gages, overlaid with mean precipitation intensity from TRMM PR observations. Intensities are shown by grey scale intensity.

intensity, which is essentially the relative rainfall accumulation map scaled by the relative frequency of events per cell. The locations of the gauges are highlighted as well. The Vista Mares gage is situated on the south side of a ridge, yet is located at a relatively high elevation. Moisture flowing from the north could possibly create a rain shadow effect on southern aspects of ridges. The adjoining cell on the ridge, which is also the highest elevation, will receive the highest rainfall in the basin, while the cell over the Vista Mares gage does not. Furthermore, the Esperanza gage is located on the northern side of the ridge while the Dos Bocas gage is situated closest to the Caribbean coast.

4. CONCLUSIONS

The results of this analysis of rain gage and TRMM data indicate that there is no general P-E relation in the upper Río Chagres catchment. There appears to be a trend of decreasing rainfall from the NE to SW part of the basin. In summary, it is noted that defining spatial climatologic gradients using TRMM is for the most part inadequate at our current time and space scales and as well when used at exceedingly high swath elevations in the presence of signal noise. Qualitative observation can be made that the headwater region of the watershed receives generally more rainfall than other parts of the catchment.

One of the attractive features of using space-based platforms is that remote locations of the globe can be accessed. Getting a first look at particular basins of interest with TRMM data products could yield very useful information on how to optimally site rage gages in a basin.

Our analysis of TRMM data needs further study. It is planned to make use of local radar estimates to evaluate quantitative comparisons of rainfall estimates based on both rain gage and TRMM observations of rainfall.

ACKNOWLEDGEMENTS

This work was funded by the U.S. Army Research Office, Terrestrial Sciences Program, Grant DAAD19-01-1-0629. We appreciate the help of Jon Zahner, M.S. Candidate at the University of Connecticut. TRMM data were provided by NASA/NASDA TRMM, DAAC. We appreciate receiving data from Michael Hart and Carlos Vargas of the Panama Canal Authority.

REFERENCES

Espinosa, JA, 1998, Veranillo De San Juan within the Panama Canal Watershed: Meteorological and Hydrographic Branch, Engineering Division Panama Canal Commission. Balboa Heights, Panama.

Iguchi, T and Meneghini, R, 1994, Intercomparison of single frequency methods for retrieving a vertical rain profile from airborne or spaceborn data: Jour. Atm. Oceanic Tech., 11: 1507-1516.

Niedzialek, JM and Ogden, FL , 2003, Runoff Production in the Río Chagres Catchment, Panama, proc. Intl. Scientific Symp., The Río Chagres: A Multidisciplinary Profile of a Tropical Watershed, Abstract Volume, 24-26 Feb., Gamboa Panama.

TRMM Precipitation Radar Team. 1999, Tropical Rainfall Measuring Mission Precipitation Radar Algorithm: Instruction Manual. (1.0) National Space Development Agency of Japan (NASDA) and National Aeronautics and Space Administration (NASA)

Chapter 14

TREE SPECIES COMPOSITION AND BETA DIVERSITY IN THE UPPER RÍO CHAGRES BASIN, PANAMA

Rolando Pérez[1], Salomón Aguilar[2], Agustín Somoza[2], Richard Condit[1], Israel Tejada[2], Clara Camargo[1], and Suzanne Lao[1]
[1]Smithsonian Tropical Research Institute, [2]Autoridad Nacional del Medioambiente de Panama

Abstract: Tree species composition at two sites in the upper Río Chagres basin of central Panama was evaluated using rapid inventory methods. At each site, two 40x40 m quadrats were demarcated, and each was thoroughly searched for tree and shrub species. The 40x40 m quadrats had a mean of 155 species each, and the four pooled had 285 species; 29 other species were noted along trails near the survey plots. These inventories were compared to 81 others within the Panama Canal Watershed, and forest composition and diversity was evaluated relative to mean dry season duration. The upper Río Chagres sites have high rainfall and are rich in tree species relative to most of the area; the only area with higher diversity is the Santa Rita Ridge, along the Caribbean coast, which is even wetter. Many tree species are restricted to these wet areas of central Panama, not occurring in drier areas of the Pacific slope or central Panama.

Key words: Panama, Panama Canal Watershed; upper Río Chagres basin; rain forest; tree species; β-diversity

1. INTRODUCTION

1.1 Forest Tree β-Diversity, Central Panama

Central Panama has high β-diversity of forest trees. In ecological jargon, this means that species turnover from site to site is high (Condit *et al*., 2002).

R. S. Harmon (ed.), The Río Chagres, Panama, 227-235.

Individual sites in the area, however, have only moderate diversity by tropical forest standards. For instance, a single hectare of forest on Barro Colorado Island in the Panama Canal has about 90 tree species (Leigh, 1999). By contrast, sites in Amazonia and Southeast Asia can have three times this number (Phillips *et al*., 1994). But, Panama's total diversity is as high as anywhere in the world (Barthlott *et al*., 1996), because high β-diversity makes up for middling local diversity.

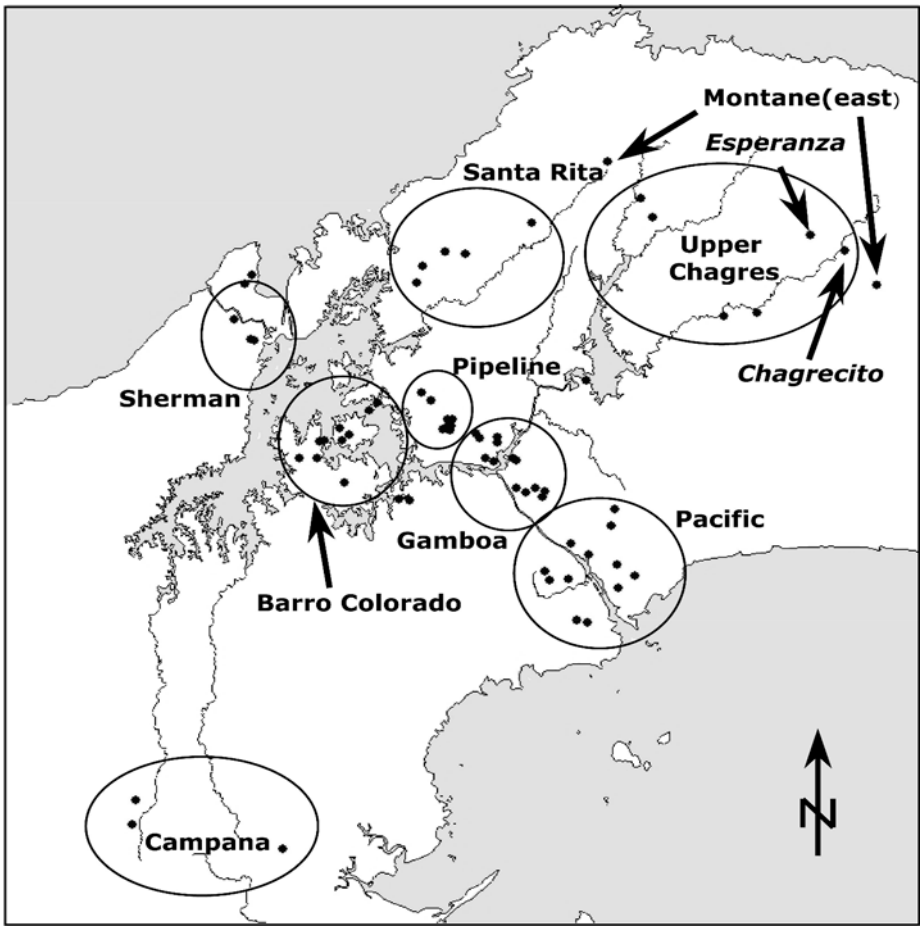

Figure 1. Tree inventories and regions of the Panama Canal Watershed. Inventory sites are denoted solid points; these sites are grouped into regions as indicated by ovals. The new inventories carried out as part of the 2002 field program are the upper Río Chagres sites are labelled 'Esperanza' and 'Chagrecito'.

High species turnover in central Panama is at least partly due to the climatic gradient across the Isthmus (Pyke *et al*., 2001; Condit *et al*., 2002). The Pacific slope is relatively dry, whereas the Caribbean coast is wet. High ridges along the Caribbean coast are especially wet. Tree species composition changes markedly from dry to wet zones. However, most of our studies to date (Pyke *et al*., 2001; Condit *et al*., 2002) have been restricted to the corridor of forest immediately adjacent to the Panama Canal. East of this corridor lies a much larger block of forest - along the Santa Rita Ridge near the Caribbean coast, and in the upper Río Chagres basin (Fig. 1). Both areas are wet, relative to the Canal corridor, but neither has been studied in any detail. In particular, the upper Río Chagres region, which has no roads, is heavily forested, and is of difficult access. As a result, current knowledge of tree species on the Santa Rita Ridge and in the upper Río Chagres regions is sparse. Because the climate in these two regions is much wetter than the rest of the Panama Canal Watershed, it is likely that many unusual and previously unknown species are present there.

1.2 Precipitation Patterns in Central Panama

All of central Panama has a distinct dry season, typically lasting from late December until late April. This dry season is crucial to the forest: some species are deciduous during the dry season, and fruit production in many species is synchronized with the dry season. Many species are stressed at by water shortage the end of the dry season (Leigh *et al.,* 1990, Engelbrecht *et al*., 2002). This is most evident during unusually long dry seasons, such as in 1983, when many trees wilted and died (Condit *et al*., 1995; Leigh, 1999).

We have been examining the degree to which tree species ranges are limited by the length of the annual dry period. Of particular interest is whether species able to tolerate long drought occur widely compared to drought-sensitive species, which are restricted to the wet slopes of the Caribbean coatsal region of the country. To estimate the intensity of the dry season, precipitation data from the Autoridad del Canal de Panama (ACP) was used. The period during which evapotranspiration exceeds rainfall at 40 different sites was determined from smoothed weekly curves rainfall of and evapotranspiration, (see details in Condit *et al*., 2000, 2005). The longest dry season occurs near Panama City on the Pacific coast, averaging 149 days. At the other extreme, the dry season is 90-110 days long on the Santa Rita Ridge and in the northern parts of the upper Río Chagres basin (Fig. 1).

A linear regression was fit of dry season length on latitude, longitude, and elevation, and this model used to model to interpolate to each tree-inventory site (Pyke *et al*.; 2001). The simple, linear model is crude and

preliminary, and precipitation data are scanty from the upper Río Chagres area, but for now it is the best available interpolation method. With advancements presented in this volume (Georgakakos *et al*., 2005, Chapter 23; Hendrickx *et al.,* 2005, Chapter 8; Knox *et al.,*2005, Chapter 13), it is hoped to eventually generate more precise estimates of annual dry-season length at all inventory sites.

2. TREE INVENTORIES

Data has been assembled on the tree species present at 87 sites in the vicinity of the Panama Canal Watershed, using three different inventory methods. One method was the census plot, in which every individual tree was measured and mapped, including three large plots of 4, 6, and 50 ha (Condit *et al.,* 2005) and 46 small plots of 0.32 ha or 1 ha (Pyke *et al.,* 2001; Condit *et al*., 2002). In most plots, trees ≥1 cm dbh (*i.e.,* diameter at breast height) were counted, but in nine, only trees ≥10 cm dbh were included (Pyke *et al.,* 2001). The second technique, called the 'quick plot' method: all species in square plots of either 0.16 ha (40x40 m) or 1 ha (100x100 m) are recorded. In 'quick plots', an area is demarcated precisely and searched exhaustively for species, but individuals are neither marked nor counted. In the final type of inventory, or 'transect' approach, tree species are recorded along trails covering <1 km, with no attempt to cover any specific area and withput attempting to be exhaustive. A total of 24 transects have now completed. Figure 1 shows the location of all sites, both plots and inventories (some inventory sites are so close together that they appear as single points on the map).

During February and March, 2002, six of these inventories were completed in the upper Río Chagres basin, as part of a program of scientific fieldwork organized by US Army Research Office. The upper Río Chagres region is protected within the Chagres National Park by Panama's Autoridad Nacional del Medioambiente, (ANAM) and includes more than 150,000 ha of near-pristine old-growth forest (Ibáñez *et al*., 2002). The entire region is devoid of roads, and the eastern section contains no human settlements (Condit *et al*., 2001; Ibáñez *et al*., 2002). Previously, four forest plots had been established in the upper Río Chagres basin (Fig. 1), but no plots were located in the most remote northeastern section.

Two new sites were visited in 2002 (Fig. 1). The first was situated in the upper portion Río Esperanza drainage, which is a major sub-basin of the upper Río Chagres basin.The second site is a location adjacent to the confluence of the upper Río Chagres, and Río Chagrecito. Forests near both sites were tall, old-growth forest that was free of any visible human

disturbance. Two plot locations were chosen at each site for detailed tree inventory, largely based on convenience: the plots were within 1 km of the fieldwork campsites, far enough above the rivers to avoid floodplain or recent fluvial depositions, and on ridge crests and upper slopes to avoid steep gullies. Beyond this, no attempt was made to select specific features of the forest and, as far as could be ascertained during the short time in the field, the plots were representative of overall diversity and structure of the surrounding forest.

At each site, two quick plots of 40x40 m square (0.16 ha) were completed, for a total of four inventories. Each plot was marked with orange flagging at approximately 5 m intervals, and each 5x40 m rectangle was walked systematically. Every tree larger than 1 cm in stem diameter within the plot was checked, and it is considered that very close to all the species present in each plot were located. In addition, tree species were recorded along the trails between campsite and plots, matching the transect method of species inventory.

Any tree species that could not be immediately identified in the field, based on prior experience throughout central Panama, was collected, whether flowering or not. In addition, nearly all flowering or fruiting specimens were collected (except for very familiar, widespread species). If necessary, a slingshot was used to collect on tall trees. Specimens were folded in newspapers for the return trip to Panama City, then dried and eventually compared with herbarium specimens at the Smithsonian Tropical Research Institute and the National Herbarium at the University of Panama.

Lists were assembled of every species encountered in each of the 40x40 m plots and along the transects. These were compared with species lists from the 81 other inventory sites in the Panama Canal Watershed. The complete species list is given at the web site: http://ctfs.si.edu.

For a broad assessment of species' ranges relative to dry season, the 87 inventories were divided into three climatic regions: (i) Caribbean and montane wet, (ii) intermediate, and (iii) Pacific dry. The wet region included the upper Río Chagres, Santa Rita, Campaña, and Montane East sites (Fig. 1), where the estimate of dry-season duration was 94-130 days with a mean of 118 days). The dry region included Gamboa, the Pacific sites, and a single transect at the Madden Dam (Fig. 1); where the dry season estimate is 129-147 days, with a mean of 138 days. The intermediate region included all remaining sites, where the dry season lasted 116-135 days, with a mean of 127 days.

3. TREE SPECIES DIVERSITY IN THE UPPER RÍO CHAGRES BASIN

The four 40x40 m plots at the Río Esperanza and Río Chagrecito sites included a mean of 155 tree species ≥1 cm in stem diameter (Tables 1 and 2). An average of 174 species was recorded in one full plot and one quick plot on the Santa Rita ridge. No other region in the Canal watershed averaged 100 species per 40x40 m quadrat (Table 1). The four plots at the Río Esperanza and Río Chagrecito sites included a total of 285 species, when their species lists were pooled. In addition, 29 more species were recorded on the transects, bringing the total number to 314. Of these 314 species, 50 of them had never before been encountered elsewhere in the Panama Canal Watershed.

Table 1. Species diversity in different regions of the Panama Canal Watershed, per 4 0x40 m inventory plot. Data from both full plots and quick plots are combined, with the number of each plot type indicated.

Site	Species	Full Plots	Quick Plots
Santa Rita	174.0	1	1
Upper Chagres	155.0	0	4
Pipeline	99.7	10	0
Sherman	94.9	34	0
Barro Colorado	92.6	35	0
Laguna	87.5	2	0
Gamboa	70.7	6	6
Pacific	56.7	22	3

4. RANGES OF UPPER RÍO CHAGRES TREE SPECIES ACROSS THE PANAMA CANAL WATERSHED

Besides the inventories undertaken at Río Esperanza and Río Chagrecito sites, four additional tree census plots previously had been completed with in of the upper Río Chagres region (Pyke *et al*. 2001). Two of these were immediately adjacent to the Río Chagres, downstream from its confluence with the Río Esperanza (Fig. 1). The other two were at sites located between the Río Boquerón and Río Pequení, north of Lago Alajuela (Fig. 1). Species lists from those plots were pooled with the list of 314 species recorded at the

Río Esperanza and Río Chagrecito sites. This produced a total list of 435 tree species for the upper Río Chagres region.

Table 2. UTM coordinates and elevation (ASL) of the four upper Río Chagres inventory plots, based on GPS. Coordinates refer to the corner of each quadrat furthest to the southwest.

Site	UTM east	UTM north	Elevation
Chagrecito-1	684333.3	1034639.5	309 m
Chagrecito-2	684397.0	1035202.5	413 m
Esperanza-1	680538.4	1036732.7	306 m
Esperanza-2	680113.2	1036889.2	286 m

Of the regions designated in Figure 1, Santa Rita is the locale most similar to the upper Río Chagres area in terms of its tree species composition. The pooled list for five Santa Rita sites included 408 tree species, 228 of which were also found in the upper Río Chagres basin. Altogether, Santa Rita and the upper Río Chagres inventories included 615 tree species. Adding two plots at elevation >600 m, but immediately adjacent to the upper Río Chagres region (referred to as Montane East in Fig. 1), this pooled list reached 698 tree species.

In 67 inventory sites along the Panama Canal (all but Santa Rita, Upper Chagres, Montane East, and Campaña; Fig. 5-1) there were 667 tree species. Only 291 of these species were also recorded in the Santa Rita, Upper Río Chagres, and Montane East regions.

At all 87 inventory and plot sites throughout the Panama Canal Watershed, 1162 tree species were recorded. The largest number of these were restricted to the wet region (Table 3). The next largest number of species were widespread, occurring from the driest to the wettest regions. Only 101 species were restricted to the driest zone.

5. CONCLUSIONS

The biggest break in tree species composition in the Panama Canal Watershed region occurs between the Santa Rita region and the forests in the vicinity of the Panama Canal. The wettest zone – which includes the Santa Rita Ridge along the Caribbean coast, the upper Río Chagres region, and montane sites in the far east and far west of the watershed - carries the highest number of species in the area, and most of these are restricted to the

wet zone. In contrast, the dry zone carries fewer species and has few restricted species.

The region of the upper Río Chagres basin in the far east of the Panama Canal Watershed area remains poorly explored botanically. It is expected, in the future, that more species will be uncovered there that are currently not known from central Panama. Further exploration of the region is clearly warranted.

Table 3. Number of tree species with various geographic ranges in Central Panama. The three regions – wet, intermediate, and dry – are defined in the methods. These ranges refer only to local occurrence; most species occur widely throughout the neotropics.

Species Range in the Panama Canal Watershed	# Species	% of Total Species
Widespread	198	17.0
Wet forest only	495	42.3
Wet-intermediate	113	9.7
Intermediate only	114	9.8
Dry-intermediate	131	11.3
Dry side only	101	8.7
Wet and dry, not intermediate	10	0.9
TOTAL	1162	100

ACKNOWLEDGEMENTS

The 2002 fieldwork in the upper Río Chagres basin was facilitated by the Tropical Regions Test Center (US Army Yuma Proving Ground), and we thank the organizers and the entire camp crew for their support. The Smithsonian Tropical Research Institute provided herbarium support and miscellaneous funding. The University of Panama offered access to the National Herbarium on the campus.

REFERENCES

Barthlott, W, Lauer, W, and Placke, A, 1996, Global distribution of species diversity in vascular plants: towards a world map of phytodiversity: Erdkunde, 50, 317-327.

Condit, R, Aguilar, S, Hernández, A, Pérez, R, Lao, S, Angehr, G, Hubbell, SP, and Foster, RB, 2005, Tropical forest dynamics across a rainfall gradient and the impact of an El Niño dry season: Jour. Tropical Ecol., in press.

Condit, R, Hubbell, SP, and Foster, RB, 1995, Mortality rates of 205 neotropical tree and shrub species and the impact of a severe drought: Ecol. Monogr., 65: 419-439.

Condit, R, Hubbell, S., and Foster, RB, 1996, Changes in a tropical forest with a shifting climate: results from a 50 ha permanent census plot in Panama: Jour. Tropical Ecol., 12: 231-256.

Condit, R, Pitman, N, Leigh, EG, Chave, J, Terborgh, J, Foster, RB, Núñez, PV, Aguilar, S, Valencia, R, Villa, G, Muller-Landau, H, Losos, E, and Hubbell, SP, 2002, Beta-diversity in tropical forest trees: Science, 295: 666-669.

Condit, R, Robinson, WD, Ibáñez, R, Aguilar, S, Sanjur, A, Martínez, R, Stallard, R, García, T, Angehr, G, Petit, L, Wright, SJ, Robinson, TR, and Heckadon, S, 2001, Maintaining the canal while conserving biodiversity around it: A challenge for economic development in Panama in the 21st century: Bioscience, 51: 135-144.

Condit, R, Watts, K, Bohlman, SA, Pérez, R, Hubbell, SP, and Foster, RB, 2000, Quantifying the deciduousness of tropical forest canopies under varying climates: Jour. Veg. Sci., 11: 649-658.

Engelbrecht, BMJ, Wright, SJ, and De Steven, D, 2002, Survival and ecophysiology of tree seedlings during El Niño drought in a tropical moist forest in Panama: Jour. Tropical Ecol., 18: 569-579.

Georgakakos, KP and Sperfslage, JA, 2005, Operational Rainfall and Flow Forecasting for the Panama Canal Watershed: in *The Río Chagres: A Multidisciplinary Perspective of a Tropical River Basin* (RS Harmon, ed.), Kluwer Acad./Plenum Pub., New York, NY: 323-333.

Hendrickx, JMH, Bastiaanssen, WGM, Noordman, EJM, Hong, S-H, and Calvo, L, 2005, Estimation of Regional Actual Evapotranspiration in the Panama Canal Watershed using *SEBAL*: in *The Río Chagres: A Multidisciplinary Perspective of a Tropical River Basin* (RS Harmon, ed.), Kluwer Acad./Plenum Pub., New York, NY: 313-321.

Ibáñez, R, Condit, R, Angehr, G, Aguilar, S, Garcia, T, Martínez, R, Sanjur, A, Stallard, R, Wright, SJ, Rand, AS, and Heckadon, S, 2002, An ecosystem report on the Panama Canal: monitoring the status of the forest communities and the watershed: Env. Mon. Assess., 80: 65-95.

Knox, RG Ogden, FL and Dinku, T, 2005, Using TRMM to explorerRainfall variability in the upper Río Chagres catchment, Panama: in *The Río Chagres: A Multidisciplinary Perspective of a Tropical River Basin* (RS Harmon, ed.), Kluwer Acad./Plenum Pub., New York, NY: 211-226.

Leigh, EGJ, Windsor, DM, Rand, AS, and Foster, RB, 1990, The impact of the "El Niño" drought of 1982-83 on a Panamanian semideciduous forest: in *Global Ecological Consequences of the 1982-83 El Niño-Southern Oscillation* (PW Glynn, ed.), Elsevier, Amsterdam, The Netherlands: 473-486

Leigh, EG, Jr., 1999, *Tropical Forest Ecology: A View from Barro Colorado Island*: Oxford Univ. Press, Oxfoed, UK.

Phillips, OL, Hall, P, Gentry, AH, and Vásquez, R., 1994, Dynamics and species richness of tropical rain forests: Proc. Nat. Acad. Sci., 91: 2805-2809.

Pyke, CR, Condit, R, Aguilar, S, and Lao, S, 2001, Floristic composition across a climatic gradient in a neotropical lowland forest: Jour. Veg. Sci., 12: 553-566.

Chapter 15

A NOTE ON AMPHIBIANS AND REPTILES IN THE UPPER RÍO CHAGRES BASIN, PANAMA

Roberta Ibáñez D.[1,2]
[1]*Smithsonian Tropical Research Institute and* [2]*Universidad de Panama*

Abstract: Twenty-nine amphibians and six reptiles were recorded at a site in the upper Río Chagres basin at the confluence of the Río Chagrecito with the upper Río Chagres. Most of them are assumed to be the common species, partly due to the brief time and search effort spent at the site. The amphibians and reptiles found at this site are also present in nearby sites, such as Las Pavas stream and along the Piedras-Pacora ridge. This survey provides information on the herpetofauna present in a virtually unexplored area of the upper Río Chagres basin. The treefrog *Hyla boans* was not previously known from the upper Río Chagres region.

Key words: Panama; Río Chagres; herpetofauna; amphibians; reptiles

1. INTRODUCTION

The upper Río Chagres basin, including the Río Chagres and the Río Pequení, was explored biologically during the 1910-1912 "Smithsonian Biological Survey of the Panama Canal Zone" (Heckadon-Moreno, 1998). Although no herpetologist participated in this survey, a few amphibian and reptile specimens were collected by the researchers (Schmidt, 1933).

Dunn and Bailey (1939) compiled a list of 37 species of snakes recorded from ridges of the Río Chagres watershed, mainly based on the collection of specimens made during the surveys to map the area in the period 1927-1936. During the 1992-1993 study entitled "Estudio de las Alternativas al Canal de Panama", an inventory of amphibians and reptiles was undertaken in San Juan de Pequení and Tranquilla (Ibáñez *et al.,* 1995a). This study recorded 60 species of amphibians and reptiles in San Juan de Pequení and 43 species

R. S. Harmon (ed.), The Río Chagres, Panama, 237-242.

in Tranquilla, including a new frog species of the genus *Atelopus* (Ibáñez *et al.,* 1995b).

The herpetofauna of the Piedras-Pacora ridge, in the upper Río Chagres basin, is one of the best known in the region. Ibáñez *et al.* (1994) published a list of 60 amphibians and 71 reptiles that were observed along this mountain ridge. An effort to expand the knowledge of the amphibians and reptiles of the upper Río Chagres watershed was undertaken during the dry season of 1997, as part of the project "Monitoreo en la Cuenca del Canal de Panama" (PMCC). During this effort, the amphibians and reptiles were sampled at four sites of difficult access: Cerro Bruja, Cerro Brewster, the Las Pavas stream, and the Río Pequení-Río San Miguel confluence, where additional species were found that had not been previously recorded in the region (PMCC, 1999). This paper reports on the amphibians and reptiles recorded during a short visit in February 2002 to a site at the upper Río Chagres-Río Chagrecito confluence in a virtually unexplored region of Panama.

2. METHODOLOGY

This herpetological survey was undertaken as part of a fieldwork program organized during February-March 2002 by US Army Research Office. The upper Río Chagres basin lies within a region of more than 150,000 ha of near-pristine old-growth forest in the Chagres National Park and is protected by Panama's Autoridad Nacional del Ambiente - AMAM (Ibáñez *et al*., 2002). The study site was located at the confluence of the upper Río Chagres and its tributary the Río Chagrecito at 9°21'29.67" N latitude and 79°19'23.13" W longitude (see Fig.1 of Kinner *et al.,*2005, Chapter 6). Except for the field campsite, which had been cleared a few days before the field visit, the vegetation the vegetation at the site was mature tropical moist forest. The adjacent reach of the upper Río Chagres had a low water level, and its margins consisted of the exposed rocky riverbed.

A generalized search for amphibians and reptiles was undertaken at this site by a pair of researchers on March 12-13, 2002, following the procedure described by Ibáñez *et al.* (1995a). The elevation range surveyed at the site was 290-475 m above sea level. This search was conducted during a single 24-hr period, *i.e.,* during both day and night, by walking the area and inspecting suitable locations, in order to detect the maximum possible number of species. The diurnal search effort amounted to 9.54 person-hrs, the nocturnal search effort to 4.76 person-hrs (total 14.3 person-hrs). The search was limited primarily to terrestrial habitats and small forest streams. Only the shallow edges of the large rivers, the upper Río Chagres and Río

Table 1. List of amphibian species observed at the Río Chagres-Río Chagrecito confluence, upper Río Chagres basin, Panama.

taxon	# of individuals	relative abundance (%)
CLASS AMPHIBIA (29 species)		
ANURA (29)		
Bufonidae (3)		
Bufo coniferus	1	0.6
B. haematiticus	95	53.1
B. marinus	6	3.4
Centrolenidae (1)		
Cochranella albomaculata	2	1.1
Dendrobatidae (6)		
Colostethus flotator	5	2.8
C. inguinalis	-	-
C. pratti	-	-
C. talamancae	1	0.6
Dendrobates auratus	1	0.6
D. minutus	3	1.7
Hylidae (5)		
Agalychnis callidryas	-	-
Gastrotheca cornuta	-	-
Hyla boans	-	-
Smilisca phaeota	-	-
S. sila	5	2.8
Leptodactylidae (14)		
Eleutherodactylus opimus	2	1.1
E. bufoniformis	1	0.6
E. cerasinus	3	1.7
E. crassidigitus	4	2.2
E. cruentus	3	1.7
E. diastema	-	-
E. fitzingeri	6	3.4
E. gollmeri	8	4.5
E. ridens	3	1.7
E. talamancae	3	1.7
*E. quidditus**	5	2.8
Leptodactylus pentadactylus	-	-

* Includes two species similar in appearance that have different advertisement calls, both present at the site.

Chagrecito, were inspected. Some species were not visually observed, but detected by their vocalizations (*i.e.,* advertisement calls). A few others were opportunistically seen and/or heard at times when no active search was being performed. The number of individuals refers only to juveniles and adults, not to tadpoles.

Table 2. List of reptile species observed at the Río Chagres-Río Chagrecito confluence, upper Río Chagres basin, Panama.

Taxon	# Individuals	Relative Abundance (%)
CLASS REPTILIA (6 species)		
LACERTILIA (6)		
Iguanidae (5)		
Anolis humilis	2	1.1
A. limifrons	4	2.2
A. poecilopus	2	1.1
Basiliscus basiliscus	6	3.4
Corytophanes cristatus	1	0.6
Teiidae (1)		
Ameiva festiva	7	3.9

3. RESULTS AND DISCUSSION

Twenty-nine amphibians and six reptiles were recorded during the site survey (Tables 1 and 2). Most of the species found are probably common at this site, given the limited time that was available for the search effort. A relatively high number of anurans were found, despite the low search effort and the timing of that effort (dry season). This suggests that a higher number of anuran species may be present in the site. Moreover, anuran communities of the greater Panama Canal Watershed are known to be more diverse at moderate elevations (Condit *et al.,* 2001; Ibáñez *et al.,* 2002), such as the elevation range sampled in the area of the Río Chagres-Río Chagrecito confluence.

A few species of reptiles, but no snakes, were recorded. For the reptiles, a more detailed and prolonged sampling effort is required to adequately determine the species present in the area, particularly in the case of snakes (Myers and Rand, 1969). The treefrog, *Hyla boans,* constitutes a species not previously recorded in the upper Río Chagres basin, despite its extremely wide distribution range in Panama (Duellman, 2001). Some individuals of

this species were heard calling, and many schools of tadpoles were observed along the edges of the upper Río Chagres. The relatively high proportion of individuals of *Bufo haematiticus* (Table 1) was due to the numerous juveniles observed along the margins and banks of the river.

The herpetofauna observed at Río Chagres-Río Chagrecito confluence area is also present in nearby sites, such as Las Pavas stream (a tributary of the upper Río Chagres) and along the more intensively and thoroughly surveyed Piedras-Pacora ridge to the southeast. At the Las Pavas stream site at 130-300 m elevation, 29 species of amphibians and 18 species of reptiles were observed during a 9-10 day survey conducted during the 1997 dry season (PMCC, 1999). An equal number of anuran species were recorded at the upper Río Chagres-Río Chagrecito confluence and Río Chagres-Las Pavas confluence, with 71% of species observed present in both sites.

The diversity and abundance of frogs of the genus *Eleutherodactylus* present at the Río Chagres-Río Chagrecito confluence may be partly related to the well-preserved condition of its forest. In addition, the variety of frogs associated with streams, found at this site, points to a healthy anuran community.

ACKNOWLEDGEMENTS

The fieldwork was funded by the Tropical Regions Test Center (US Army Yuma Proving Ground) and the organizers and the entire camp crew are thanked for their support. Thanks are also extended to A. Almanza for assistance in the field and laboratory.

REFERENCES

Condit, R, Robinson, WD, Ibáñez, R, Aguilar, S, Sanjur, A, Martínez, R, Stallard, RF, García, T, Angehr, GR, Petit, L, Wright, SJ, Robinson, TR, and Heckadon, S, 2001, The status of the Panama Canal Watershed and its biodiversity at the beginning of the 21st century: BioScience, 51: 389-398.

Duellman, WE, 2001, The hylid frogs of Middle America: SSAR Contrib. Herpetol., 18: 1-1180.

Dunn, ER, and Bailey, JR, 1939, Snakes from the uplands of the Canal Zone and of Darien: Bull. Mus. Comp. Zool., 86: 1-22.

Heckadon-Moreno, S, 1998, *Naturalistas del Istmo de Panama*: Editorial Santillana, Panama.

Ibáñez, R, Arosemena, FA, Solís, FA, and Jaramillo, CA, 1994, Anfibios y reptiles de la Serranía Piedras-Pacora, Parque Nacional Chagres: Scientia (Panama), 9: 17-31.

Ibáñez, R, Condit, R, Angehr, GR, Aguilar, S, García, T, Martínez, R, Sanjur, A, Stallard, RF, Wright, SJ, Rand, AS, and Heckadon, S, 2002, An ecosystem report on the Panama

Canal: monitoring the status of the forest communities and the watershed: Env. Monitor. Assess., 80: 65-95.

Ibáñez, R, Jaramillo, CA, Arrunátegui, M. Fuenmayor, Q, and Solís, FA, 1995a, II. Inventario biológico del Canal de Panama. Estudio Herpetológico: Scientia (Panama), Número Especial, 2: 107-159.

Ibáñez, R, Jaramillo, CA, and Solís, FA, 1995b, Una especie nueva de *Atelopus* (Amphibia: Bufonidae) de Panama: Carib. Jour. Sci., 31: 57-64.

Kinner, D, Mitasova, H, Stallard, RF, Harmon, RS, and Toma, L, 2005, GIS Database and Stream Network Analysis for the Upper Río Chagres Basin, Panama: in *The Río Chagres: A Multidisciplinary Perspective of a Tropical River Basin* (RS Harmon, ed.), Kluwer Acad./Plenum Pub., New York, NY: 83-96.

Myers, CW, and Rand, AS, 1969, Checklist of amphibians and reptiles of Barro Colorado Island, Panama, with comments on faunal change and sampling: Smithsonian Contrib. Zool., 10: 1-11.

PMCC, 1999, *Proyecto de Monitoreo de la Cuenca del Canal, Informe Final, Junio 1999*, USAID-STRI-ANAM, Panama City, Panama.

Schmidt, KP, 1933, Amphibians and Reptiles Collected by the Smithsonian Biological Survey of the Panama Canal Zone: Smithsonian Misc. Coll., 89: 1-20.

Part III: The Regional Perspective

Chapter 16

HIGH SPATIAL AND SPECTRAL RESOLUTION REMOTE SENSING OF PANAMA CANAL ZONE WATERSHED FORESTS:

An Applied Example Mapping Tropical Tree Species

Stephanie Bohlman[1,3] and David Lashlee[2]

[1]University of Washington, [2]Yuma Proving Ground, [3]Current Affiliation: Smithsonian Tropical Research Institute

Abstract: High spatial resolution airborne and satellite sensors have been used with varying degrees of success to measure deciduousness, canopy structure, and light interception, and to identify tree species in the Panama Canal Watershed. Results reported to date indicate that remotely sensed data have a high degree of accuracy in measuring deciduousness and leaf density in the upper canopy, but less accuracy than in temperate systems in measuring canopy light interception for semi-deciduous lowland tropical forests in the canal watershed. Of particular relevance to evergreen forests like the upper Río Chagres basin, this work examines whether high spectral resolution data, like that collected by the HYDICE system, can separate canopy species based on hyperspectral signatures in the 0.4 to 2.5-µm wavelength region. If a few well-selected spectral bands could accurately differentiate species, tropical canopies in remote and rugged terrain could be mapped using relatively simple, but optimized sensor systems.

Key words: Panama Canal Watershed; remote sensing; HYDICE; tree species mapping

1. INTRODUCTION

Remote sensing of the world's forests has become increasingly important for various ecological applications, including inputs to biogeochemical cycling models and tracking land use changes (Field *et al.,* 1995; Achard *et al.,* 2002). An important advantage of using remote sensing over point field studies is that it can provide continuous data on ecosystem variables that cannot readily be collected from the ground, and this approach can be used

R. S. Harmon (ed.), The Río Chagres, Panama, 245-258.

to monitor these parameters through time. Most uses of remote sensing have been global or regional in extent, covering areas of 100's to 1,000's of kilometers, but remote sensing holds great promise also for augmenting finer, large-scale studies; for example, focusing on individual watersheds. Remote sensing can assist in watershed studies in two ways, by (i) placing the watershed within the context of the wider array of vegetation types across the landscape and (ii) providing canopy information, which can be difficult to study from the ground in remote areas. For obtaining biophysical information of tropical watersheds, high-resolution images (with pixel sizes of 5 m or less) are more appropriate than coarse resolution data (with pixel sizes from 10 m to 1 km) because the higher resolution better matches the spatial information and the scale of the field studies.

When verifying remote sensing interpretations, it is important to link environmental data to specific image pixels, which is easily accomplished using high-resolution data, since they have a similar spatial scale as the field measurements. In this way, intense ecological studies paired with high-resolution images provide an important way to test the interpretations that are made routinely on coarser scale data. For the past five years, we have been using remote sensing images with high spatial and spectral resolution to study the ecology of lowland tropical forests within the Panama Canal Watershed. This paper presents some results on the type of information that can be gained from these data in tropical forests, focusing on mapping individual tree crowns of different species.

The high species diversity and inaccessibility of many tropical forests make it exceedingly difficult to map distributions of tree species from the ground. Studies of landscape species diversity are almost always based on a series of small plots 1 ha or less in size (Condit *et al.;* 2002; Perez *et al.;* 2005, this volume). Remote sensing, which can cover large extents with continuous coverage, offers potential of increasing our understanding of species distributions. Remote sensing has been used successfully to discriminate different tropical forest 'ecotypes' (Weishampel *et al.,* 1998; Tuomisto *et al.,* 1995; Adams *et al.,* 1995) but, until recently, spatial resolutions of available sensors were too poor to reliably discriminate individual crowns or species. However, there are some airborne sensors now available that have sufficiently high spectral and spatial resolutions to detect individual crowns. A fundamental question then becomes whether or not tropical tree pecies have sufficient spectral differences to be distinguished by remote sensing techniques. Previous studies in temperate forests (Gougeon *et al.,* 1999; Key *et al.,* 2001) suggest that different species are discernable, but this has not yet been investigated in species-rich tropical forests.

There are numerous characteristics of tree crowns that potentially could generate spectral differences among species. Spectra of individual tree

crowns result primarily from the reflectance, absorption, and transmission properties of leaves and wood, the arrangement of the leaves and wood in the crown, and the shape of the crown, which creates shading and shadowing (Adams *et al.,* 1995). Lianas and epiphytes present in the crown may have different spectral properties than the host tree. Furthermore, spectra of individual leaves can vary with age, water content, chemical composition or epiphyll cover (Guasman 1985; Roberts *et al.,* 1998; Yoder *et al,.* 1995). Even if individual species are not separable, groups of species with common functional characteristics, like deciduous trees, can potentially be mapped from remotely sensed images. In a highly diverse forest, it is impossible to distinguish all species with current sensor technology. However, it may be possible to map either common species or species that exhibit distinct spectral signatures at certain periods of the year that make them distinguishable from the 'matrix' of other species.

This study focuses on testing the statistical separability of species in a small number of broad wavelength ranges derived from hyperspectral images. The interest is in determining if a small number of wavelength bands, which could be incorporated into future sensors, can accurately map common species as a precursor to more detailed analyses using the full dimensionality of hyperspectral data.

2. METHODS

2.1 The Study Site

The Parque Natural Metropolitano – Metropolian National Park - (8°56'N latitude, 9°33'W longitude) is located within the city limits of Panama City on the Pacific side of the Isthmus of Panama. It has a strong dry season from January to April. The average annual rainfall is 1850 mm with 90% on average falling in the wet season from June to November. During the dry season, part of the forest is deciduous (Fig. 1).

2.2 Image Data Collection

During the dry season in March 1998, the airborne Hyperspectral Digital Imagery Collection Experiment (HYDICE) sensor collected images of various locations across the Panama Canal Watershed. These images have a spatial resolution of 1 m to 3.5 m and contain 210 1.0-μm wide wavelength bands in the range 0.4-2.5 μm. In this study, we are using 1-m resolution

images of the Parque Metropolitano. During the flight, four wooden (painted) and four canvas calibration panels were placed in a clearing within 100 m of the crane to calibrate the images from radiance to apparent spectral reflectance using the 'Empirical Line Method'. Average radiance values of each panel were extracted from the image and used to develop regression equations between image radiance and reflectance for each panel measured in the field during the HYDICE mission using a portable ASD FieldSpec spectrometer (Analytical Spectral Devices, 1995; note: The use of trade, product or firm names is for descriptive purposes only and does not imply endorsement by the US Government). The slope and intercept (gain and offset) of the regression equations were applied to each pixel in the image.

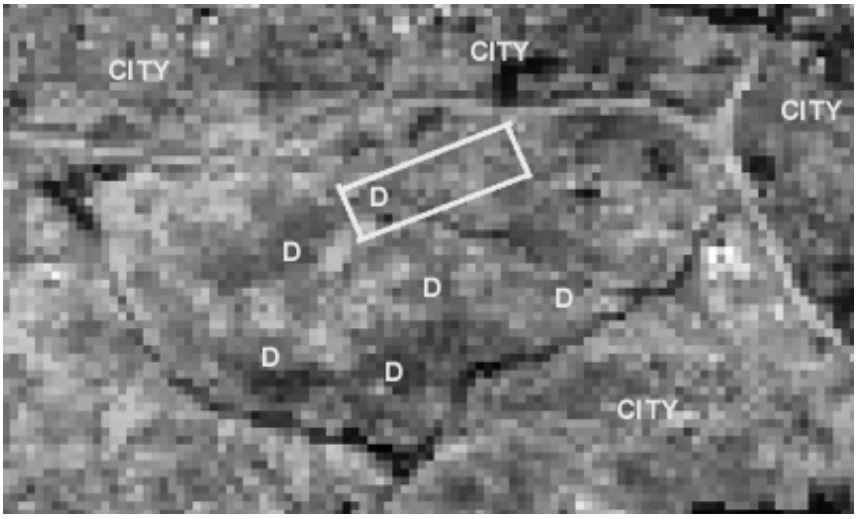

Figure 1. Grayscale rendition of color a LANDSAT TM image of Parque Natural Metropolitano, Panama City, Panama from the dry season in April 1998. The original color figure is provided on the CD accompanying this volume. The letter "D" in the figure indicates patches of forest that are highly deciduous. The rectangular box indicates the area shown in Figure 2.

In 1991, the Smithsonian Tropical Research Institute erected a 50-m tall construction crane in the park for accessing and studying the forest canopy. The dominant species at Parque Metropolitano are *Anacardium exelsum* and *Luehea seemanii* (Fig. 2). There are many species that lose their leaves for the entire dry season, including *Bursera simarouba*, *Cavanillesia platanifolia*, *Calycophyllum candidissimum*, *Guazuma ulmifolia*, *Pseudobombax septenatum*, and *Spondias mombin*. Numerous studies of canopy physiology and ecology have been conducted on the tree crowns at the crane site (*e.g.,* Mulkey *et al.,* 1996; Meinzer *et al.,* 1997).

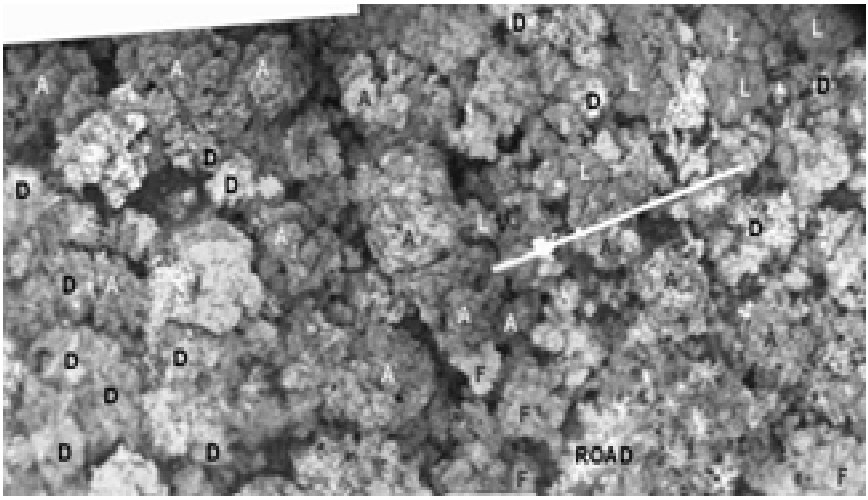

Figure 2. Grayscale rendition of the high-resolution multispectral color image of the area immediately adjacent to the canopy crane in the Parque Natural Metropolitano, Panama City, Panama. The original color figure is provided on the CD accompanying this volume. The pixel resolution is 0.2 m, 4 times greater than that for HYDICE images. The white line is the arm of the crane and letters indicate different species or types of tree crowns: "A" = Anacardium exelsum, "L" = Luehea seemanii "F" = Ficus insipida and "D" = deciduous tree crowns.

2.3 Ground Data Collection

Individual tree crowns were located on the ground by taking a three-band color composite of the images in the field. Crowns on the ground were matched with those in the images using landmarks and visual inspection. The many man-made features, such as roads and buildings, visible in the images allowed navigation to individual crowns. Once a crown was co-located in the image and on the ground, it was identified to species. Percent liana coverage of the upper surface of the canopy was estimated by visual inspection using binoculars. Overall, 266 crowns from 25 species were identified.

2.4 Data Analysis

For the initial data analysis described in this paper, species with six or more crowns with no liana coverage and no part of their crown over a road or grassy area were selected for study. The species that fit this description were *Anacardium exelsum*, *Luehea seemanii*, *Ficus insipida*, and *Phoebe*

cinnamomifolia. *Anacardium* and *Luehea* also had six or more crowns with liana coverage ≥50%, which were used to test the impact of high liana load on reflectance patterns. All deciduous crowns were considered together, as previous experience has shown that individual deciduous species are not separable. The deciduous species used were *Bursera simarouba*, *Cavanillesia platanifolia*, *Calycophyllum candidissimum*, *Guazuma ulmifolia*, *Pseudobombax septenatum*, and *Spondias mombin*. Reflectance data were extracted from the images by drawing polygons of 10-100 pixels over individual crowns. All image processing was done with the Environment for Visualization of Images (ENVI) software package (Research Systems Inc., Boulder, CO, USA).

Differences between species pairs were compared on a band-by-band basis using statistical 2-tailed 't'-tests. Bands in the major water absorption wavelengths (1.33-1.5 μm and 1.7-2.04 μm) and at the beginning and end of the sensor wavelength range (<450 μm and >2.27 μm) were excluded due to system noise. Therefore, only 129 bands were analyzed. All possible pair combinations (23), including high and low liana density for *Anacardium*, *Luehea,* and deciduous trees, were compared. Significant differences between species pairs at the 0.05 significance level were found to be similar in distinct wavelength ranges. Thus, the data were further reduced from 129 bands to 8 bands with similar relationships between species pairs (Table 1).

Table 1. Wavelength ranges used in HYDICE analysis, including the physiological properties that most strongly influence each range.

Spectral Region	Wavelength Range (μm)	Physiological Driver
Blue	0.451 – 0.519	Chlorophyll
Green	0.524 – 0.572	Leaf material
Red	0.579 – 0.675	Chlorophyll
NIR1	0.684 – 0.909	Leaf material
NIR2	0.923 – 1.10	Water content
NIR3	1.11 – 1.33	Leaf material
MIR1	1.50 – 1.91	Water content
MIR2	2.04 – 2.27	Water content

3. RESULTS

The most easily separable groups of species using the March 1998 HYDICE images are deciduous versus non-deciduous species. Deciduous species (combined as a group) differed from each non-deciduous species in most bands – blue, red, NIR1, NIR2, NIR3 and MIR2 (for acronym definitions, see Table 1), but not in the green or MIR1 bands (Table 2, Figs. 3 and 4). Among the non-deciduous species, *Luehea*'s spectral signature was the most distinct. *Luehea* varied from *Anacardium*, *Ficus* and *Phoebe* in blue, red, NIR3, MIR1 and MIR2 bands (Table 2, Figs. 3 and 4). *Ficus* and *Phoebe* are spectrally similar to *Anacardium*. *Phoebe* and *Anacardium* do not have any significantly different bands. *Ficus* and *Anacardium* contrasted only in the blue region. However, *Ficus* is separable from *Phoebe* in all the visible bands – blue, green and red, as well as MIR2.

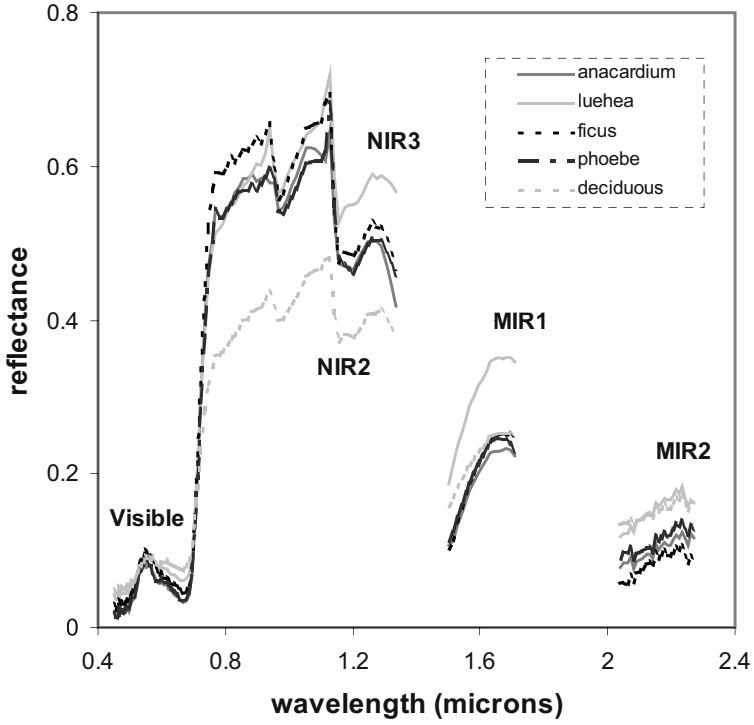

Figure 3. Average percent reflectance for deciduous species combined and four non-deciduous species at the Parque Natural Metropolitano, Panama City, Panama. The original color figure is provided in Appendix II on the CD accompanying this volume.

Table 2. Significant differences between pairs of species (or deciduous species combined) for different broad spectral regions from the HYDICE data for Parque Natural Metropolitano, Panama City, Panama. Differences were determined using 't'-tests. A difference at the 0.05 significance level is indicated by a "+".The letter designations are: B = blue, R =red, and G = green.

Species 1		**Species 2**		**Wavelength Region**							
Species	Liana load	Species	Liana load	B	G	R	NIR1	NIR2	NIR3	MIR 1	MIR 2
Anacardium	high	*Anacardium*	none	-	-	-	-	-	-	-	-
Luehea	high	*Luehea*	none	-	-	-	-	+	+	+	-
deciduous	high	Deciduous	none	-	+	+	-	-	-	-	+
Anacardium	none	*Luehea*	none	+	-	+	-	-	+	+	+
Anacardium	none	*Ficus*	none	+	-	-	-	-	-	-	-
Anacardium	none	*Phoebe*	none	-	-	-	-	-	-	-	-
Anacardium	none	Deciduous	none	+	-	+	+	+	+	-	+
Luehea	none	*Ficus*	none	+	-	+	-	-	+	+	+
Luehea	none	*Phoebe*	none	+	-	+	-	-	+	+	+
Luehea	none	Deciduous	none	+	-	+	+	+	+	-	+
Ficus	none	*Phoebe*	none	+	+	+	-	-	-	-	+
Ficus	none	Deciduous	none	+	-	+	+	+	+	-	+
Phoebe	none	Deciduous	none	+	-	+	+	+	+	-	+
Anacardium	high	*Luehea*	none	+	-	-	-	-	+	-	-
Anacardium	high	*Ficus*	none	+	-	-	-	-	-	-	-
Anacardium	high	*Phoebe*	none	-	-	-	-	-	-	-	+
Anacardium	high	Deciduous	none	+	-	+	+	+	+	-	-
Anacardium	high	Deciduous	high	-	+	-	+	+	+	+	+
Luehea	high	*Anacardium*	none	+	-	+	-	-	-	+	+
Luehea	high	*Ficus*	none	-	-	+	+	-	-	+	+
Luehea	high	*Phoebe*	none	+	-	+	-	-	-	+	-
Luehea	high	Deciduous	none	-	-	-	+	+	+	+	+
Anacardium	high	Deciduous	none	+	-	+	-	-	+	+	+

For *Luehea*, *Anacardium* and the deciduous species, there were few consistent trends in how high liana coverage affected reflectance. For all three species, high liana coverage decreased reflectance in NIR1 and NIR2, but the difference was only statistically significant for *Luehea* (Table 2, Fig. 5). Low and high liana coverage canopies of *Luehea* also contrasted in NIR3

and MIR1. For *Anacardium*, there were no significant differences in reflectance between trees with and without lianas in any band. However, deciduous trees with and without lianas differed in the green, red and MIR2 bands. For *Anacardium*, high liana loads did not change its separability from the other species. High liana loads only changed the separability of *Luehea* in NIR3. Overall, the most useful bands for separation were blue, red, NIR3, and MIR2, while the green band was the least useful.

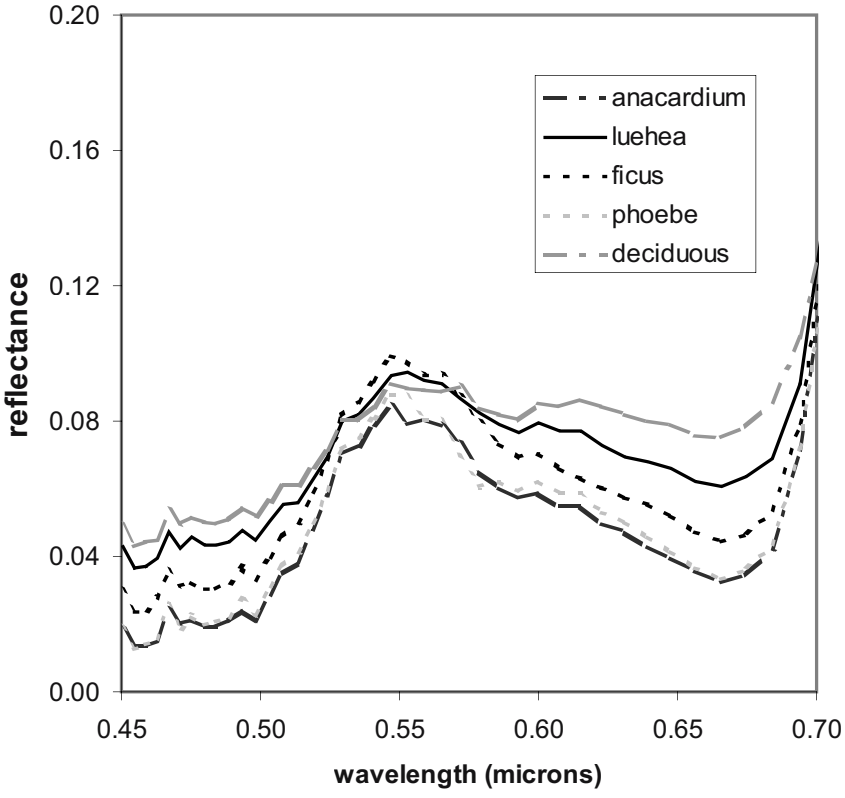

Figure 4. Average percent reflectance in the visible bands for combined deciduous species and four non-deciduous species at Parque Natural Metropolitano, Panama City, Panama. The original color figure is provided on the CD accompanying this volume.

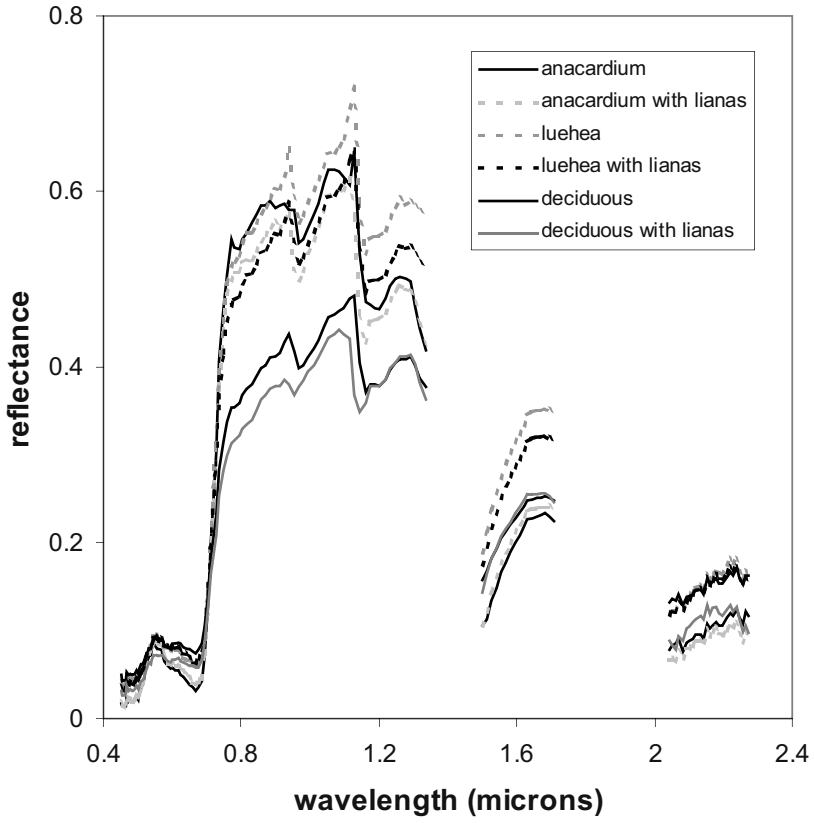

Figure 5. Average percent reflectance in the visible bands for crowns with and without lianas at Parque Natural Metropolitano, Panama City, Panama. Crowns with lianas have 50% liana coverage. The original color figure is provided on the CD accompanying this volume.

4. DISCUSSION

4.1 Deciduous Versus Non-Deciduous

The greatest contrast in reflectance throughout the visible and infrared portions of the spectrum is between deciduous and non-deciduous species (Figs. 1 and 2). Using HYDICE data, non-deciduous species differed from deciduous species in all bands except green and MIR1. Spectral differences between deciduous and non-deciduous species are due to the amount of wood exposed at the canopy surface in deciduous crowns. Wood and leaves have distinct spectral signatures throughout the visible-infrared portions of

the electromagnetic spectrum. Deciduous spectra look like a mixture of wood and leaves whereas fully leaved tree spectra look more like that of a stack of leaves.

Spectral differences between trees with and without leaves are apparent in multiple spectral bands and at many spatial scales. Thus, two well-placed spectral bands may be sufficient to distinguish fully leaved versus deciduous crowns. In a separate study at the Parque Metropolitano canopy crane, it was observed that the Normalized Difference Vegetation Index, or NDVI (a ratio of the red and NIR1 bands) has a strong correlation with the percent deciduousness of overstory trees through time (Bohlman, 2005). Furthermore, we found that even in images with reduced spatial and spectral resolution in which individual crowns cannot be resolved, the percentage of deciduous versus non-deciduous trees can be mapped. Using LANDSATt Thematic Mapper data, which has a 30-m pixel size (Fig. 1), a strong correlation was observed between deciduousness predicted by a spectral mixture model applied to the satellite image and percent of deciduous trees measured on the ground (Bohlman, 2005). Mapping deciduous versus non-deciduous trees on the landscape is important for modeling forest function because leaf density is an important determinant of both carbon and water cycling.

4.2 Deciduous Versus Non-Deciduous

Spectral differences among species within the deciduous or non-deciduous groups are much smaller than between the two groups. Previous work examining deciduous species indicates that they are not spectrally separable (Bohlman, 2005), and no attempt was made to separate them in this study. The non-deciduous species had varying levels of separability in the dry season. The species *Luehea* was the most spectrally distinct, which may be due to several physiological characteristics it displays in the dry season. *Luehea* has reduced leaf density in the dry season, which may allow more wood in the canopy to be exposed. The *Luehea* leaves that are held in the canopy in the dry season are physiologically distinct from *Luehea* leaves in the wet season (Kitajima *et al.,* 1997). *Luehea* leaves have a distinctly brown color in the dry season but are green in the wet season. Dry season leaves are adapted to take advantage of the high light conditions in the dry season (Graham *et al.,* 2003).

The other non-deciduous species studied, *Anacardium*, *Ficus*, and *Phoebe,* were not easily separable using the broad band analysis in this study. *Anacardium* and *Phoebe* have no significant differences in any band and *Anacardium* and *Ficus* were only separable in the blue band. Although

these three species have high leaf density in the dry season, their canopy structures are different. The species *Anacardium* and *Phoebe* have deeper canopies without distinct layers, whereas *Ficus* has several distinct mono-layers of leaves.

4.3 Liana Loads

High liana loads had surprisingly little effect on the spectral signatures and separability of species. Lianas had the greatest effect on the deciduous trees and *Luehea*, which have decreased leaf density in the dry season. There was no significant effect of liana load on *Anacardium*, which has high leaf density in the dry season. Despite the spectral differences for deciduous trees and *Luehea* between crowns with no lianas and high liana density, these species were still separable from the other species in the study.

5. FUTURE ANALYSES

Other analysis techniques should increase the separability of *Anacardium*, *Ficus* and *Phoebe*. Future analyses that will be applied to the data include narrow band comparisons, band ratios, and first derivative analysis, which shows the changes between spectral areas, shape indices and principle components analysis (Cochrane, 2000). However, band-by-band comparison is important in the context of developing a simple multi-band imaging system that is more cost effective than hyperspectral sensors such as HYDICE. All species pairs with statistically significant differences had at least one significant difference in a visible color band - blue, green or red. Therefore, traditional color aerial photography could be useful in separating some species, such as *Luehea* in the dry season. However, for most species pairs, multiple differences in both visible and infrared bands would allow these species to have greater separability using a visible-infrared imaging systems rather than color photography alone.

Time of year and the phenological pattern of a species are important considerations in determining if species are separable. Targeting a species when it has low leaf density, senescent leaves, flower or fruits, may make it more separable from the species matrix in which the species occurs. For example, *Luehea* has low leaf density and distinctly colored brown leaves in the dry season. In the wet season, *Luehea*, like nearly all other species at the site, has high leaf density and green-colored leaves. Thus, *Luehea* may not be spectrally separable in the wet season.

ACKNOWLEDGEMENTS

Ideas to use HYDICE for species identification were developed in collaboration with M. Clark of the University of California, Santa Barbara. Support for S. Bohlman was provided by a Mellon Research Exploration Award in Tropical Biology from the Smithsonian Tropical Research Institute. V. Morrill, YPG Conservation Program Manager, provided a technical review of the paper, which. also has been reviewed by the US Army for Operational Security and approved for public release; distribution is unlimited.

REFERENCES

Achard, F, Eva, HD, Stibig, H-J, Mayaux, P, Gallego, J, Richards, T, and Malingreau, J-P, 2002, Determination of deforestation rates of the world's humid tropical forests: Science 297: 999-1002.

Adams, JB, Sabol, DE, Kapos, V, Filho, RA, Roberts, DA, Smith, MO, and Gillespie, AR, 1995, Classification of multispectral images based on fraction of endmembers: Applications to land-cover change in the Brazilian Amazon: Rem. Sens. Env. 52: 137-154.

Analytical Spectral Devices, 1995, Technical Guide: Analytical Spectral Devices, Inc., Boulder, CO.

Bohlman, SA, 2005, The Relationship Between Canopy Structure, Light Dynamics and Deciduousness in a Seasonal Tropical Forest in Panama: A Multiple Scale Study Using Remote Sensing and Allometry: PhD Dissertation, Univ. Washington, Seattle, WA.

Condit , R, Pitman, N, Leigh, E, Chave, J, Terborgh, J, Foster, RB, Nunez, P, Aguilar, S, Valencia, R, Villa, G, Losos, E, Muller-Landau, H, and Hubbell, SP, 2002. Beta diversity in tropical forest trees: Science, 295: 666-669.

Cochrane, MA, 2000, Using vegetation indices variability for species level classification of hyperspectral data: Int. Jour. Rem. Sens., 21: 2075-2087.

Field, CB, Randerson, JT, and Malmstrom, CM, 1995, Global net primary production: combining ecology and remote sensing: Rem. Sens. Environ., 51: 74-88.

Gausman, HW, 1985, Plant Leaf Optical Properties in Visible and Near-Infrared Light: unpubl. report, Texas Tech Univ., Lubbock, TX: 78p.

Graham, EA, Mulkey, SS, Kitajima, K, Phillips, NG, and Wright, SJ, 2003, Cloud cover limits net CO_2 uptake and growth of a rainforest tree during tropical rainy seasons: Proc. Nat. Acad. Sci. 100: 572-576.

Gougeon, FA, Leckie, DG, Paradine, D, and Scott, I, 1999, Individual Tree Crown Species Recognition: The Nahmint Study. in *International Forum on Automated Interpretation of High Resolution Digital Imagery for Forestry* (DA Hill and DG Leckie, eds.), Canadian Forest Service, Victoria, BC.

Key, T, Warner, TA, McGraw, JB, and Fajvan, MA. 2001, A comparison of multispectral and multitemporal information in high spatial resolution imagery for classification of individual tree species in a temperate hardwood forest: Rem. Sens. Env., 75: 100-112.

Kitajima, K, Mulkey, SS and Wright, SJ, 1997b, Seasonal leaf phenotypes in the canopy of a tropical dry forest: Photosynthetic characteristics and associated traits: Oceologia. 109: 490-498.

Meinzer, FC, Andrade, JL, Goldstein, G, Holbrook, NM, Cavelier, J and Jackson, P, 1997, Control of transpiration from the upper canopy of a tropical forest: the role of stomatal, boundary layer and hydraulic architecture components: Plant Cell Env., 20: 1242-1252.

Mulkey, SS, Kitajima, K, and Wright, SJ, 1996, Plant physiological ecology of tropical forest canopies: Trends Ecol. Evol., 11: 408-412.

Pérez, R, Aguilar, S, Somoza, A, Condit, R, Tejada, I, Camargo, C, and Lao, S, 2005, Tree Species Composition and Diversity, Upper Chagres River Basin, Panama: in *The Río Chagres: A Multidisciplinary Perspective of a Tropical River Basin* (RS Harmon, ed.), Kluwer Acad./Plenum Pub., New York, NY: 227-135.

Roberts, DA, Nelson, BW, Adams, JB, and Palmer, F, 1998, Spectral changes with leaf aging in Amazon caatinga: Trees, 12: 315-325.

Tuomisto, H, Ruokolainen, K, Kalliola, R, Linna, A, Danjoy, W, and Rodriguez, Z, 1995, Dissecting Amazonian biodiversity: Science, 269: 63-66.

Weishampel, JF, Sloan, JH, Boutet, JC and Godin, JR, 1998, Mesoscale changes in textural pattern of 'intact' Peruvian rainforests (1970s-1980s): Int. Jour. Rem. Sens., 19: 1007-1014.

Yoder, BJ and Pettigrew-Crosby, RE, 1995, Predicting nitrogen and chlorophyll content and concentrations from reflectance spectra (400-2500 nm) at leaf and canopy scales: Rem. Sens. Env., 53: 199-211.

Chapter 17

BIOGEOGRAPHIC HISTORY AND THE HIGH BETA-DIVERSITY OF RAINFOREST TREES IN PANAMA

Christopher W. Dick, Richard Condit, and Eldridge Bermingham
Smithsonian Tropical Research Institute

Abstract: In a recent study examining the degree to which tree species composition differs among rainforest sites (*i.e.,* β-diversity), Condit *et al.* (2002) found that plots in the Panama Canal Watershed separated by 50 km were more highly differentiated than plots in western Amazonia separated by nearly 1400 km. The high β-diversity of trees in Panama was attributed to sharp environmental gradients between the Atlantic and Pacific coasts. However, the pattern may also result from Panama's history as a land bridge over which floras from Central America and South America mixed during the Great American Biotic Interchange (GABI) roughly 3 million years ago. Under this scenario, it would be expected that wetter Panamanian forests would contain more trees of South American origin, whereas drier Panamanian forests would have more trees of Mesoamerican origin due to the historical prevalence of dry habitats in Mesoamerica. This idea was tested by quantifying the geographic distributions of 714 tree species found in three sites in the Panama Canal Watershed, which represent a gradient in annual rainfall. Nearly identical proportions of geographic representation of trees among the three sites, with species distributions of *ca.* 15% Mesoamerican, 17% South American, 9% Panama endemic, and 59% widespread. These data do not support the biotic interchange hypothesis. However, this analysis found that 433 of the 714 tree species (61%) have a cross-Andean distribution, which suggests that these tree species may be sufficiently old to have participated in the GABI.

Key words: Panama; rain forest; tree species; biotic interchange; β-diversity; biogeography

1. INTRODUCTION

In species-rich tropical rainforests, most ecological studies are performed within forest inventory plots of ≤50 ha, which have yielded huge numbers of tree species and, thus, high levels of α-diversity (Condit *et al.,* 2000).

R. S. Harmon (ed.), The Río Chagres, Panama, 259-269.

Networks of small inventory plots have also been able shed light on patterns of β-diversity (change in species composition between sites) of Neotropical rainforest trees. In a comparison of forest inventory plots from Panama and the western Amazon, Condit *et al.* (2002) observed that β-diversity was higher along a 50 km latitudinal transect in Panama than between the widely scattered Amazonian sites. Rainfall gradients are steeper and soils more variable in Panama, and local adaptations may result in high β-diversity (Ruokolainen *et al.,* 2002). However, Panama is also a contact zone for floras that originated in North and South America, so biogeographic history may also explain landscape patterns of species diversity. In order to understand how these forests communities were assembled, one must consider the geographic origins of their constituent species.

1.1 History of Rain Forests in North and South America

The rainforests of Amazonia have experienced a relatively stable and moist climate since the mid-Tertiary time, and its flora may be largely autochthonous (Hooghiemstra and van der Hammen, 1998). Mesoamerica, on the other hand, was a refuge for the broadly distributed North American rainforest flora that persisted through the greenhouse climates of the Paleocene (*ca.* 65-55 Ma) and Eocene (*ca.* 54-35 Ma) time (Morley, 2000). Following a period of drying during the Oligocene (*ca.* 35-24 Ma), North American rainforests receded into Mesoamerica, and the core Mesoamerican forests were dry and seasonal, with wetter forests clinging to narrow strips of coastline (Morley, 2000).

The floras of Central and South America have had two major opportunities for floristic interchange since South America separated from Africa during mid Cretaceous time (*ca.* 96 Ma). In the late Paleocene (*ca.* 54 Ma), the eastward migrating Proto-Antillean archipelago (see Harmon, 2005b, Chapter 4) permitted some rainforest plants to island hop between North and South America (Raven and Axelrod, 1974; Gentry, 1982). This may explain some taxonomic affinities between South America and the Eocene flora (*ca.* 54 Ma) of the southeast United States (*e.g.,* Herendeen and Dilcher, 1990). South America remained an island continent for roughly 50 million years, until the consolidation and uplift of Panama about 3 million yeas ago (Coates and Obando, 1996) provided the first continuous land bridge between North and South America. The Panama land bridge allowed two independently evolved biotas to mix, producing the phenomenon designated by Simpson (1940) as the‘Great American Biotic Interchange’ (GABI). Although studies of the interchange usually consider migrations between Central and South America, the islands that formed the pre-

Isthmian archipelago (Harmon, 2005, this volume) may have harbored its own endemic floras and faunas, much as the West Indies do today. Excavations of mid-Miocene (*ca.* 18 Ma) fossils from the Gatun Fm. in central Panama provide evidence of rainforest vegetation and large grazing animals, such as horses and rhinoceroses (Whitmore and Stewart, 1965).

1.2 Weedy Amazonian Trees

The exchange of plant taxa between North and South America could have greatly enriched the floristic diversity of both continents. Gentry (1982) has suggested, however, that the exchange was disproportional. North America contributed many of the montane taxa (>2000 m) found in the Andes, a few of which have descended into the lowland forests (<1000 m), whereas the great majority of lowland plant taxa crossed the landbridge from South America. Gentry (1982) suggested that lowland Mesoamerican forests are comprised largely of widespread Amazonian species, with few representatives of the original North American lowland flora. Gentry's conclusion was based on extensive observations and field collections in the northern South America and in the Panama Canal Watershed area, but it finds only limited support in a study by Croat and Busey (1975) of the geographic distributions of the known tree species of Barro Colorado Island (BCI), which were 13% endemic to Panama, 17% widespread endemic between Costa Rica, Panama, and Colombia, 13% South American (extending as far north as Costa Rica), and 45% widespread (Table 1).

Table 1. Geographic affinities of the Barro Colorado Island, Panama flora (modified from Table 1 of Croat and Busey, 1975). Included are trees, lianas, and epiphytes. N refers to the number of species per life form. PE = Panama endemic; WE = wide endemic and refers to a range that includes Costa Rica and/or Colombia; CA = Central America and refers to a range that extends from Mexico to Colombia; SA = South America and refers to a distribution that extends as far north as Costa Rica; W = Widespread and applies to species that occur in most of the Neotropical countries and extend occasionally to the West Indies.

life form	N	PE	WE	CA	SA	W
Tree	53	15%	17%	9%	13%	45%
Liana	103	11%	11%	16%	16%	46%
Epiphyte	147	12%	8%	15%	7%	55%

The years following Croat and Busey (1975) brought a surge of information on the taxonomy and species distribution of Panamanian trees, due to (i) the intensive forest inventories in Panama initiated in the 1980's (Hubbell and Foster, 1983; Pyke *et al.*, 2001), and (ii) the electronic

cataloguing of herbarium collections, from which species ranges may be quickly tabulated. Whereas Croat and Busey (1975) were able to consider 53 tree species on Barro Colorado Island (BCI), we now have information about 983 tree species in the Panama Canal Watershed (Condit *et al.,* 2001).

2. OBJECTIVES

This study had two primary objectives. The first was to expand upon the analysis of Croat and Busey (1975) and address the observation by Gentry (1982) about the geographic distributions of rain forest tree communities. Under Gentry's hypothesis, the tree species in Panama should have widespread distributions between Central and South America, with the broadest geographic coverage in South America or the Amazon basin. However, if the flora represents a mixture of floral elements from Central and South America, one would expect to find a comparable number of species with primarily Mesoamerican and primarily South American geographic distributions. This question was addressed through reference to the geographic distributions of Panamanian trees obtained from the TROPICOS-VAST database of the St. Louis Botanical Garden, the Flora Neotropica monograph series, and the checklist of the Flora of Panama (D'Arcy, 1987).

The second objective of the study was to examine the hypothesis that high β-diversity in Panamanian trees derives in part from the mixing of independently derived floras during the Great American Biotic Interchange, first suggested by Dick *et al.* (2003). Under this hypothesis, it would be expected that the seasonal forests of the Panama Canal Watershed would contain more species with Central American distributions, whereas the wetter forests of the watershed should contain species with geographic affinities to South America, since Mesoamerican forests were highly seasonal compared to Amazonian forests prior to the biotic interchange. Our approach assumes that geographic distributions reflect dispersal from areas of origins (Willis, 1922), and that many of the tree species under consideration in fact participated in the biotic interchange.

3. MATERIALS AND METHODS

3.1 Study Species and Sites

Our analysis considered 714 tree species found in the Center for Tropical Forest Sciences (CTFS) inventory plots in the Panama Canal Watershed. The species are classified into 327 genera and 40 families, and are all angiosperms, with the exception of the conifer *Podocarpus oleifolius* (Podocarpaceae).

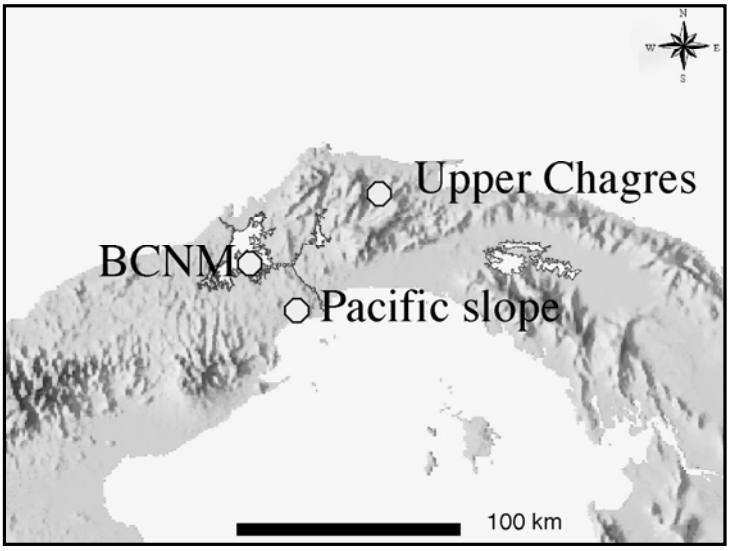

Figure 1. Locations of the 3 study sites along the N-S gradient of central Panama.

Table 2. Three Central Panamanian sites considered in this study, number of tree species (N) and annual rainfall (drawn from Pyke et al. (2001).

site	N	annual rainfall
Upper Chagres	337	3500 mm
Barro Colorado	275	2637 mm
Pacific	358	1800 mm

The geographic distribution was compared of species from three tree communities located along a climatic gradient in the Panama Canal Watershed (Fig. 1; Table 2). The information on rainfall and geological substrate is drawn from Pyke *et al.* (2001). The upper Río Chagres area (327

species) is the wettest and most northern location. It is situated close to the Atlantic coast in an area where soils have developed over pre-Tertiary basaltic bedrock (see Wörner *et al.*, 2005, Chapter 5). The Barro Colorado National Monument (BCNM; 275 species) falls in the center of the north-south climatic gradient and contains several geological substrates, including Oligocene limestone and sandstone and Miocene basalt. The Pacific lowland sites (358 species) contain the most seasonal forests and lie on a bedrock of pre-Tertiary basalts. Because of seasonality and an intense dry season along the Pacific side of Panama, it was expected that the Pacific lowland forests would contain the greatest number of Mesoamerican-derived species.

3.2 Geographic Range Data

The geographic ranges of the Panamanian trees was evaluated through reference to the TROPICOS-VAST database of the Missouri Botanical Garden (www.mobot.org). TROPICOS provides collection information on 1,634,040 specimens housed at the Missouri Botanical Garden, with links to the collections database of the New York Botanical Garden. Additional range information was obtained from Flora Neotropica, which provided information for about 10% of the species in this study. For each species, presence or absence was determined in all of the Neotropical countries that contain rainforest: Mexico, Belize, El Salvador, Guatemala, Honduras, Costa Rica, Panama, Colombia, Ecuador, Peru, Bolivia, Paraguay, Argentina, Brazil, French Guiana, Surinam, Guyana, and Venezuela. Determinations were made whether populations were found east and/or west of the northern Andean cordilleras for species with a southern limit in Colombia or Ecuador.

Table 3. Nine fine-scale geographic range designations (column 1) and four broad range categories (column 2) applied the presence/absence data in each Neotropical country for the 714 tree species of the Panama Canal Watershed.

Geographic Range	Geographic Center
1. Panama to north of Costa Rica	Mesoamerica
2. Endemic to Panama	Panama
3. Panama and Costa Rica only	Panama
4. Panama, Costa Rica and Colombia	Panama
5. Colombia to north of Costa Rica	Mesoamerica
6. Panama and Colombia only	Panama
7. Panama to beyond Colombia	South America
8. Costa Rica to S. America beyond Colombia	South America
9. North of Costa Rica to beyond Colombia	Widespread

3.3 Range Classifications

Nine non-overlapping geographic range categories were defined based on the country presence/absence data (Table 6-3). These nine distributions were lumped into four broad categories, based on the approximate center of geographic distribution: (i) The 'Mesoamerica' center of distribution included Mesoamerican countries that lie north of the Nicaragua/Costa Rica border, with a southern range limit of Panama or Colombia; (ii) The 'Panama' center included species endemic to Panama or extending to Costa Rica or Colombia; (iii) 'South America' species occurred in the Amazon basin and did not occur north of Costa Rica; (iv) 'Widespread' species are those ranging north of Costa Rica, and extending east of the Colombian Andes. It is not possible to infer a continental origin of the widespread species.

4. RESULTS

Table 4 lists the geographic distributions of Panamanian tree communities as percentages. Widespread species made the largest percentage in all sites and ranged from 47% (336 species) in the Panama Canal Watershed area as a whole to 63% of species in the upper Río Chagres area. The proportion of Mesoamerican species ranged from 16% to 13% (upper Río Chagres), and is comparable to the proportion of South American trees, which ranged from 21% in the greater Panama Canal Watershed to 16% in the upper Río Chagres. The proportion of endemics ranged from 16% in the entire area to 8% in the upper Río Chagres area. Sites within Panama did not have a notably different geographic composition of their tree floras, although the Panama Canal Watershed region as a whole contained fewer widespread species and more endmic species (12%) have been collected in the Caribbean islands, which suggests the potential for water dispersal, and/or anthropogenic introductions.

Table 4. Geographic affinities of Panamanian rainforest tree species from three study sites. The number of tree species documented in the inventory plots in the entire Panama Canal area is provided in the second row. The geographic designations are described in Table 3.

Site	N	*Mesoamerica*	*Panama*	*South America*	*Widespread*
Canal area	714	16%	16%	21%	47%
Chagres	337	13%	8%	16%	63%
BCNM	275	15%	10%	17%	57%
Pacific	356	16%	9%	17%	58%

5. DISCUSSION

Despite the limited tree species pool available for their study (n = 53), Croat and Busey (1975) found similar proportions of widespread and South American tree species (Table 3). By contrast, Croat and Busey (1975) listed over twice the proportion of Panama-centered species observed in this study. This discrepancy may be explained by the greater geographic coverage of botanical collecting since the early 1970's, which has expanded our knowledge of species' ranges. Many of the Croat and Busey (1975) endemics would probably now be placed in the Mesoamerica or South America geographic categories.

The results of this study indicates that Gentry (1982) was partly correct in his appraisal of Central America as a colonization front for widespread Amazonian species. Approximately 63% of the tree species of the Canal watershed also occur in Amazonia. However, our study indicates that only 21% of the widespread species are primarily Amazonian in distribution. The other 47% are so widely distributed that, without information about their broader phylogenetic relationships, it would be impossible to infer a North or South American origin.

It is notable that 433 species cross over the Andes. This suggests that these species originated prior to the formation of the Panama isthmus, since the Andes has provided a strong dispersal barrier for lowland rainforest plants since its major emergence and uplift during late Miocene to early Pliocene (*ca.* 11-3.6 Ma) time (Lundberg *et al.,* 1998) (The dispersed islands of proto-Panama coalesced slightly later at about *ca.* 3 Ma (Coates and Obando, 1996)). Raven (1999) noted that approximately 30% of the lowland flora in Ecuador (1,431 species) occur on both slopes of the Andes, implying ages of several million years for those species. Molecular clock analyses of DNA sequences from the cross-Andean tree populations lend support to an Andean vicariance hypothesis (Dick *et al.,* 2003; C. Dick, unpublished data), although some species-rich and cross-Andean tree groups, such as the *Inga*, have probably diversified much more recently (Richardson *et al.,* 2001) and therefore have successfully dispersed across the northern Andes.

Of the various categories of geographic distribution, only the endemic taxa varied proportionally among the three sites. The upper Río Chagres area, for example, contained only half (8%) the proportion of endemics represented in the Panama Canal Watershed as a whole (16%). The higher level of endemism in the overall flora suggests that our study sites do not encompass areas with unique habitats and specialized floras. The unanticipated broad geographic distribution of most species in the Panamanian tree community is positive news for conservation, as it suggests that the loss of local populations will not produce global extinctions.

However, although endemics represent a small proportion of the species that were examined, their absolute numbers are high (n = 114). Endemic species, along with those that haven't yet received taxonomic descriptions, may be globally threatened by the extirpation of populations in the Panama Canal Watershed as it faces growing threats from development and urbanization (Condit *et al.,* 2001).

In conclusion, the distribution data do not provide strong support for a historical explanation for Panama's high β-diversity. It was expected that the Pacific site species would exhibit a geographic affinity with Mesoamerica and the upper Río Chagres species would show a high floristic affinity with Amazonia. Our approach did not permit that distinction to be made, however, because so many species are widespread and can probably persist at low population densities in suboptimal habitats. Studies that consider the relative abundances of tree species in relation to their geographic distribution – rather than simple presence or absence – may yet reveal a biogeographic signature in the distribution of tree species in central Panama.

ACKNOWLEDGEMENTS

We would like to thank R. Harmon for organizing the Chagres Scientific Symposium that produced this volume. The Panama tree inventories were coordinated under the auspices of the Center for Tropical Forest Sciences (CTFS) of the Smithsonian Tropical Research Institute (STRI) and were funded in large part by the US Agency for International Development (US AID) and Panama's Autoridad Nacional del Medio Ambiente (ANAM). We also acknowledge the botanical and database expertise behind the Panama data, in particular, R. Pérez, S. Aguilar and S. Lao. We thank M. Correa for important discussions, and Catalina Perdomo for help in determining the cross-Andean distribution of Colombian and Ecuadorian tree species.

REFERENCES

Coates, AG and Obando, JA, 1996, The Geologic Evolution of the Central American Isthmus: in *Evolution and Environment in Tropical America* (JBC Jackson, AF Budd, and AG Coates, eds.), Univ. Chicago Press, Chicago, IL: 21-56.

Condit, R, Ashton, PS, Baker, P, Bunyavejchewin, S, Gunatilleke, S, Gunatilleke, N, Hubbell, SP, Foster, RB, Itoh, A, LaFrankie, JV, Lee, HS, Losos, E, Manokaran, N, Sukumar, R, and Yamakura, T, 2000, Spatial patterns in the distribution of tropical tree species: Science, 288: 1414-1418.

Condit, R, Pitman, NCA, Leigh, EG, Chave, J, Terborgh, J, Foster, RB, Nuñez, P, Aguilar, S, Valencia, R, Villa, G, Muller-Landau, HC, Losos, E, and Hubbell, SP, 2002, Beta-Diversity in tropical forest trees: Science 295: 666-669.

Condit, R, Robinson, D, Ibañez, R, Aguilar, S, Sanjur, A, Martinez, R, Stallard, RF, García, T, Angehr, G, Petit, L, Wright, SJ, Robinson, T, and Heckadon, S, 2001, The status of the Panama Canal Watershed and its biodiversity at the beginning of the 21st Century: BioScience, 51: 389-400.

Croat, TB, and Busey, P, 1975, Geographic affinities of the Barro Colorado Island flora: Brittonia, 27: 127-135.

D'Arcy, WG, 1987, Flora of Panama: Checklist and Index, Part 1: The Introduction and Checklist: Missouri Botanical Garden, St. Louis, MO.

Dick, CW, Abdul-Salim, K, and Bermingham, E, 2003, Molecular systematics reveals cryptic tertiary diversification of a widespread tropical rainforest tree: Am. Nat., 162: 691-703.

Gentry, A, 1982, Neotropical floristic diversity: phytogeographical connections between Central and South America - Pleistocene climatic fluctuations or an accident of Andean Orogeny?: Annals Missouri Bot. Garden, 69: 557-593.

Harmon, RS, 2005b, The Geological Development of Panama: in *The Río Chagres: A Multidisciplinary Perspective of a Tropical River Basin* (RS Harmon, ed.), Kluwer Acad./Plenum Pub., New York, NY: 45-62.

Herendeen, PS, and Dilcher, DL, 1990, Fossil mimosoid legumes from the Eocene and Oligocene of southeastern North America: Rev. Palaeobot. Palynol., 62: 339-362.

Hooghiemstra, H, and van der Hammen, T, 1998, Neogene and Quaternary development of the neotropical rain forest - the forest refugia hypothesis, and a literature overview: Earth Sci. Rev., 44: 147-183.

Hubbell, SP, and Foster, RB, 1983, Diversity of Canopy Trees in a Neotropical Forest and Implications for Conservation: in *Tropical Rain Forest: Ecology and Management* (AC Chadwick, ed.), Blackwell Sci. Pub., Oxford, UK.

Lundberg, JG, Marshall, LG, Guerrero, J, Horton, B, Malabarba, MC, and Wesselingh, F, 1998, The Stage for Neotropical Fish Diversification- A History of Tropical South American Rivers: in *Phylogeny and Classification of Neotropical Fishes*, (LR Malabarba, RE Reis, RP Vari, SM Lucena & CAS Lucena, eds.), Edipucrs, Porto Alegre: 13-48.

Morley, RJ, 2000, *Origin and Evolution of Tropical Rain Forest*s: John Wiley & Sons Ltd, West Sussex, UK.

Pitman, NCA, Terborgh, J, Silman, MR, Núñez, PV, Neill, DA, Cerón, CR, Palacios, W., and Aulestia, M, 2001, Dominance and distribution of tree species in upper Amazonian terra firme forests: Ecology, 82: 2101-2117.

Pyke, CR, Condit, R, Aguilar, S, and Lao, S, 2001, Floristic composition across a climatic gradient in a neotropical lowland forest: Jour. Veg. Sci., 12: 553-556.

Raven, PH, 1999, Forward: in *Catalogue of the Vascular Plants of Ecuador* (PM Jørgensen and S León-Yánez, eds.): Missouri Botanical Garden, Saint Louis, USA: vi-viii.

Raven, PH, and Axelrod, DI, 1974, Angiosperm biogeography and past continental movements: Ann. Missouri Botanical Garden, 61: 539-673.

Richardson, JE, Pennington, RT, Pennington, TD, and Hollingsworth, PM, 2001, Rapid diversification of a species-rich genus of neotropical rain forest trees. Science, 293: 2242-2245.

Ruokolainen, K, Tuomisto, H, Chave, J, Muller-Landau, HC, Condit, R, Pitman, NCA, Terborgh, J, Hubbell, SP, Leigh, EG, Duivenvoorden, JF, Svenning, J-C, and Wright., SJ, 2002, Beta diversity in tropical forests. Science, 297: 1439-1440.

Simpson, GG, 1940, Mammals and land bridges: Jour. Wash. Acad. Sci., 30: 137-163.

Whitmore, FC, and Stewart, RH, 1965, Miocene Mammals and Central American seaways: Science, 148: 180-185.

Willis, J., 1922, *Age and Area*: Cambridge Univ. Press, Cambridge, UK.

Chapter 18

WORLD HOLDINGS OF AVIAN TISSUES FROM PANAMA:

With Notes on a Collection from the Upper Río Chagres, 2002

Sievert Rohwer and Robert C. Faucett
University of Washington Burke Museum

Abstract: The avifauna of Panama may be better documented than that of any other country in Central America. Museum expeditions over the past 100 years have yielded a wealth of traditional specimens and an excellent understanding of bird distribution and occurrence across the country. Unfortunately, most of these expeditions were mounted in the first half of the century well before the importance of preserving tissue samples had been realised. Consequently, the world holdings of avian tissue from Panama are grossly inadequate. A compilation of the world holdings of avian tissue from Panama is presented which illustrates the need for continued general collecting throughout Panama. Recent contributions made during a recent field visit to the upper Río Chagres basin in 2002 are listed and guidance provided about where future collecting is needed.

Key words: Panama; Río Chagres; avifauna

1. INTRODUCTION

Over 900 species of birds have been recorded from the Republic of Panama and roughly a third of these probably occur in the upper Río Chagres drainage basin (see Fig. 1 of Chapter 1). The University of Washington Burke Museum collected birds at two localities in the upper Río Chagres basin in late February to mid-March of 2002 as part of a much larger investigation of the geohydrology and biota of this region. In a 3-week survey, just over 200 specimens of 72 species of birds were collected and about 40 additional species observed. With such a short time in the field, there seemed little to be gained by reporting exclusively on the specimens collected at the two localities examined. Instead, this report summarizes world holdings of avian tissues samples from the Republic of Panama,

R. S. Harmon (ed.), The Río Chagres, Panama, 271—280.

including the new specimens collected during the upper Río Chagres basin field work, hoping that this summary will help guide future avian collecting in Panama.

With the revolution in sequencing technology of the last 20 years, genetic studies of variation across geography have become the preferred tool for investigations of relationships among populations and of the history of populations. For example, DNA sequences from different geographic regions might be reciprocally monophyletic, suggesting a history of isolation and helping identify cryptic species. Further, coalescence analyses reveal population increases and the magnitude and direction of gene flow (Hewitt, 1966; Templeton, 1988; Emerson et al., 2001). This new field, collectively known as phylogeography (Avise, 2000), is becoming an important tool in conservation biology. Gene sequence data is much more effective than morphological measurements at quantifying population differentiation and at identifying lineages that could represent undescribed species or the incipient differentiation of new species. Because the preservation of tissue samples for research in genetics began less than 25 years ago, only a relatively small fraction of the world's fauna is represented by even single tissue samples in museum collections throughout the world.

General collecting is the most effective way to generate the samples needed for future phylogeographic analyses. Ideally, a region or country would be covered with a grid of localities from which at least 3-5 individuals of common birds had been sampled. These would provide a basis for preliminary investigations that might then lead to more intensive sampling of individual species in regions of genetic transition or possible isolation. It is fundamentally important to recognize that comparative phylogeographic studies of the birds of a country or large region cannot be pursued efficiently if collecting takes place on a species-by-species basis. Instead, localities must be collected generally if the basic genetic resources required for phylogeography analyses of multiple species are to be generated in a timely and economical fashion. Fortunately, this has been the approach to avian collecting in Panama. Here we review the world's holdings of avian tissues from Panama and summarize the geographic distribution of the localities from which these tissues were collected.

2. SUMMARY AND ANALYSIS OF AVIAN TISSUES FROM PANAMA

By consulting with colleagues and by reviewing museums web-sites for institutions with significant tissue collections, it was determined that only four museums held significant numbers of tissues from Panama, the National

Museum of Natural History (NMNH), the Louisiana State University Museum of Natural Science (LSU), the Academy of Natural Sciences of Philadelphia (ANSP), and the University of Washington Burke Museum (UWBM). Curators at each of these institutions kindly supplied us with electronic lists of their tissue samples from Panama along with locality records. These were combined into a single list using the nomenclature of Parker *et al.* (1996) to resolve differences in species names among institutions. The full list of holdings for these four institutions is presented in Appendix 1.

The total number of tissue specimens from Panama was 3,874, making it one of the best sampled countries for its size in the world. Nonetheless, there were a remarkable number of gaps in the sampling. For example, 915 species of birds have been recorded from the Republic of Panama, yet no tissue sample from Panama exists for 45% of these species (Fig. 1); another 24% of Panamanian birds are represented by just 1-3 tissues from Panama (Fig. 1). Only 25% of Panama birds are represented by five or more tissue specimens, and three of the 28 species represented by samples of more than 20 individuals have already been the subject of detailed phylogeographic studies (Brumfield *et al.,* 2001; Gonzalez *et al*., unpub. manuscript)

To explore differences among species in the number of tissue samples available from Panama, the overview provided in Figure 8-1 was subdivided according to the information on residency status and abundance provided by Parker *et al.* (1996). Birds that breed in Panama are much better represented in collections than either regular non-breeders or vagrants (Fig. 2).

Just 37% of the breeding species of Panama are unrepresented in collections and 223 of these species (32%) are represented by 5 or more tissue samples. In contrast, more than 70% of regular non-breeders and more than 85% of vagrants are not represented by tissue samples collected in Panama. The high percentage for vagrants is not surprising because these species are rarely encountered.

The very high percentage of regular non-breeders that are not represented in tissue collection is disturbing. Many of these Panamanian birds are migrants that breed in North America. For migrants, genetic and stable isotope analyses are becoming increasingly useful in establishing connectivity between wintering and breeding populations (Marra *et al.,* 1998; Hobson 1999). Thus, tissue samples from these Panamanian birds could be of great value in determining whether future population declines (or increases) were due to habitat changes in those parts of their breeding range that produce the populations wintering in Panama or, instead, were due to habitat changes in Panama. For this reason, institutions collecting in Panama should be encouraged to collect migrants, in addition to the tropical resident species that normally are impetus for mounting expeditions.

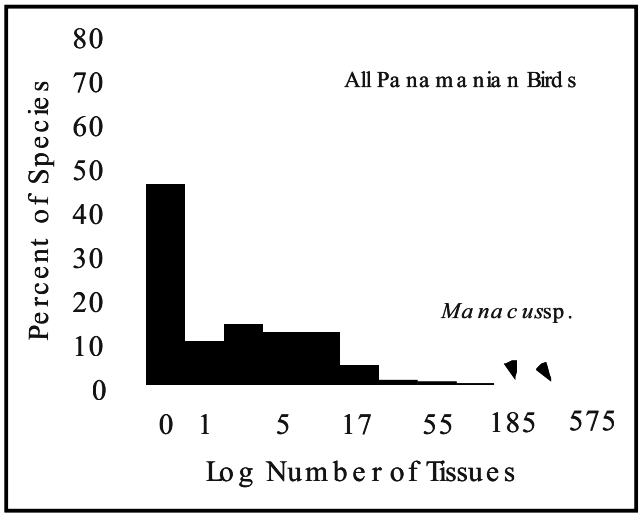

Figure 1. Percent of bird species occurring in Panama plotted by the number of tissue samples available from Panama. The horizontal axis is plotted on a log scale because only a few of these species are represented in the world's collections by large numbers of tissues from Panama.

The summary of avian tissue holdings from Panama was also subdivided by the relative abundance categories provided in Parker *et al.* (1996). In this analysis we collapsed the designations 'Common' and 'Fairly Common' into 'Common' and used the primary designation for species with intermediate status (*i.e.,* 'Uncommon/Fairly Common'as 'Uncommon'). Not surprisingly, Common species are much better represented in the world's tissue collections than 'Uncommon' and 'Rare' species; yet, more than 41% of Neotropical birds that are considered 'Common' are not represented by even a single sample in the world's tissue collections from Panama (Fig. 3)!

Species that are 'Common' and that also breed in Panama hold the most potential for phylogeographic studies for two reasons. First, 'Common' breeders tend to be resident species that may be prone to population differentiation and even the formation of cryptic species because they generally have low dispersal. Further, the very fact that these species are 'Common' makes feasible assembling the samples required for phylogeographic studies. For this summary, the species collected in Panama were partitioned into a combined category of 'Common Breeders' (from Parker *et al.,* 1996), which represent the union of the top two graphs in Figures 2 and 3. This yielded 506 species and the distribution of tissue sampling shown in Figure 4.

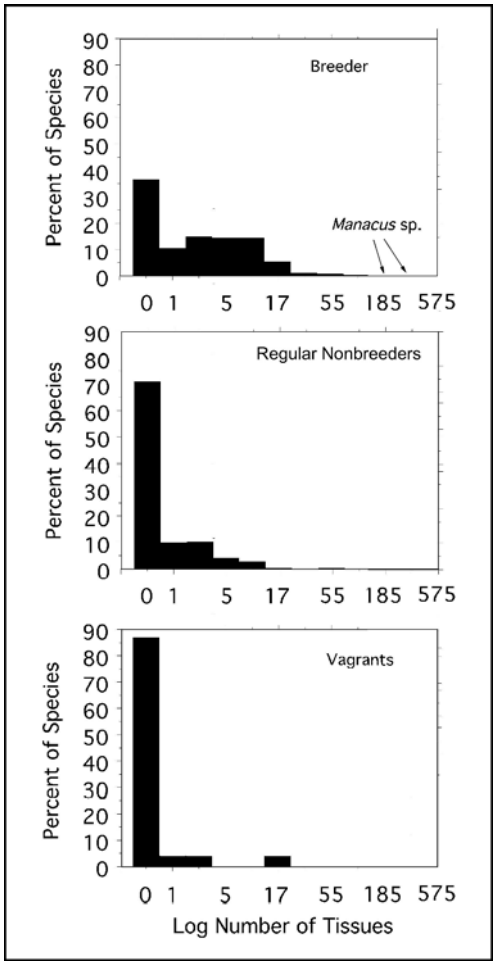

Figure 2. Percent of bird species occurring in Panama plotted by the number of tissue samples available from Panama. In this histogram the Panamanian avifauna was subdivided into breeders, regular non-breeders and vagrants, following Parker *et al.* (1996). The horizontal axis is plotted on a log scale because only a few of these species are represented in the world's collections by large numbers of tissues from Panama.

Not surprisingly, the percent of species that are not represented by even a single tissue sample drops still further in this summary to 33%. Nonetheless, it was surprising that just 23 of the 506 common breeding birds of Panama (less than 5%) were represented by 20 or more tissue samples from Panama. In most cases no one would attempt even a preliminary study of phylogeography without having at least 20 individual samples for a species, and without these samples being distributed across localities in different regions.

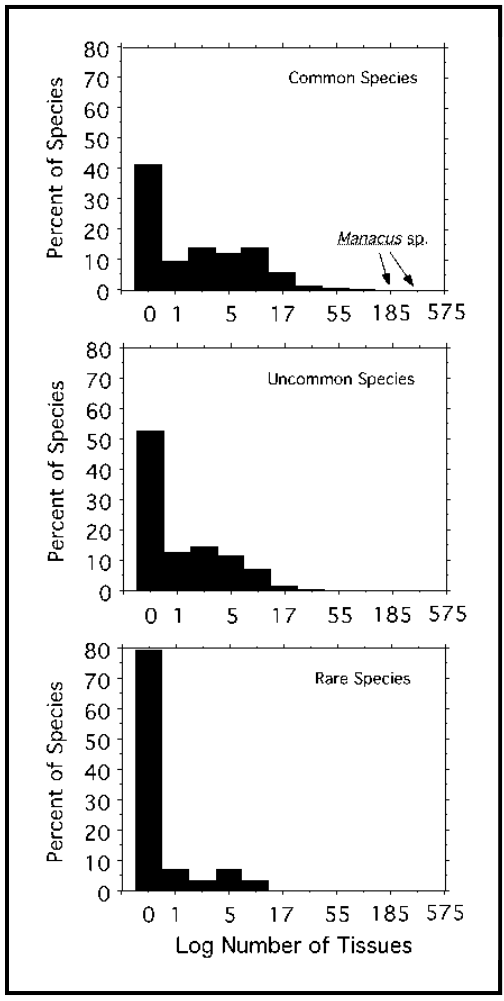

Figure 3. Percent of bird species in Panama plotted by the number of tissue samples available from the country. In this histogram the Panamanian avifauna was subdivided into common species, uncommon species and rare species, following Parker *et al.* (1996). The horizontal axis is plotted on a log scale because only a few of these species are represented in the world's collections by large numbers of tissues from Panama.

For a country the size of Panama, publishable phylogeographic analyses would typically include more than 50 specimens; yet only 6 of the 506 common breeding birds of Panama are represented by such large samples, and three of these species have been the subject of detailed studies with associated targeted collecting (Brumfield *et al.,* 2001; Gonzalez *et al.,* unpub. manuscript).

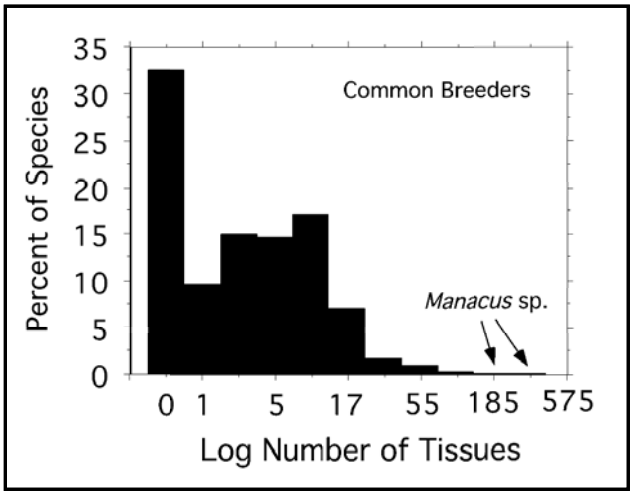

Figure 4. Percent of the Panamanian avifauna that consists of common breeders (following Parker *et al.,* 1996), plotted by the number of tissue samples available from Panama. This is the subset of Panamanian species for which phylogeographic studies should be most valuable. The X-axis is plotted on a log scale because only a few of these species are represented in the world's collections by large numbers of tissues from Panama.

3. GEOGRAPHIC DISTRIBUTION OF TISSUE SAMPLES FROM PANAMA

Phylogeographic studies are no better than the distribution of the sampling. Thus, the major sampling localities for tissue collections are plotted on the map of Panama presented in Figure 5. To reduce clutter and emphasize the regional distribution of samples, localities separated by less than 25 km have been combined and those combined sample localities from which less than 20 specimens were available have been eliminated. In general, sampling in Panama has been concentrated in four regions, Bocas del Toro, the Azuero Peninsula, the Panama Canal Zone region and the Darien. Large areas of Panama are unrepresented by even single localities from which more than 20 avian tissues have been collected, including the Pearl Islands, much of the Caribbean and Pacific coasts, and the interior of Veraguas. It is hoped is that this map will provide a useful guide to future areas that need to be targeted for general collecting.

4. THE UPPER RÍO CHAGRES COLLECTION

In the 12 days of field work in the upper Río Chagres–Río Chagrecito confluence at 9˚21' N latitude and 79˚19'W longitude, (ii) and at a site just below the confluence of the Río Esperanza with the upper Río Chages at 9˚23'N latitude and 79˚21'W longitude (see Fig. 1 of Chapter 6) These sites are referenced on the map in Figure 5 by their sample sizes of 102 and 113 specimens, respectively. The primary value of these collections is that they expanded the geographic coverage of collections in the region of the Canal Zone. Among the 215 specimens we collected were significant additions to the world's tissue holdings from Panama; first, second, or third specimens were added for 16 species (Table 1), and additional samples were added for 23 species previously represented by just 4-9 specimens from Panama (Table 1). Several of the additions we made to the holdings from Panama may be accounted for by the fact that our camps were located on reaches along the upper Río Chagres, which formed a break in the surrounding forest that allowed us to collect several species that are difficult to collect from the forest floor. For example, 9 specimens of *Neochelidon tibialisa*, a swallow that normally forages over rivers and streams, by collecting them as they passed over the Río Chagres region.

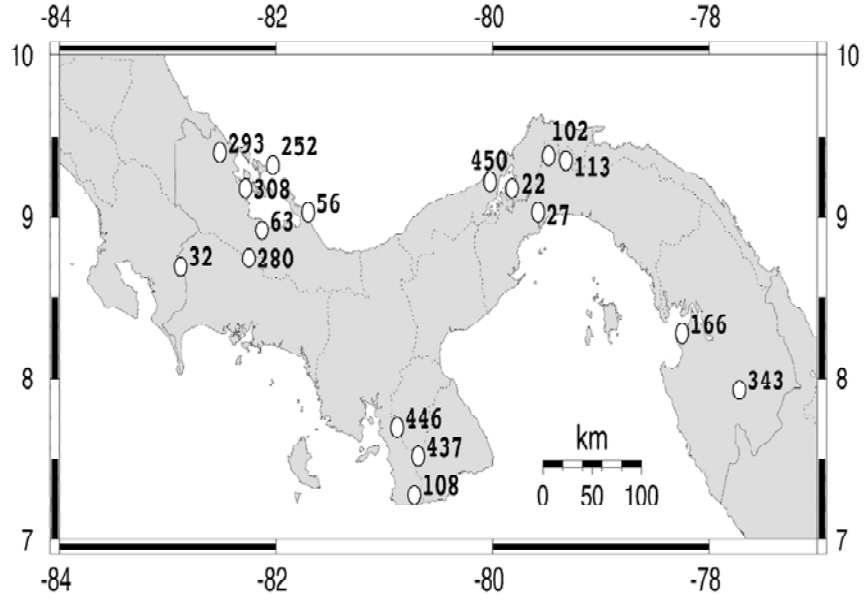

Figure 5. Distribution of Panamanian localities for which over 20 avian tissue samples are available in the world's museums. Numbers adjacent to each locality represent the numbers of tissues available from each of these places.

Similarly, the caprimulgid, *Lurocalis semitorquatus* is a nocturnal forest bird, which is rare in collections, but which was able to collected over a sandbar in the upper Río Chagres (Table 1). More generally, most of the significant additions we made to the world's tissue holdings from Panama were birds that are uncommonly encountered; as shown in Figure 3, these species are poorly represented in the world's tissue collections.

Four other species collected during the upper Río Chagres fieldwork are worth noting. The rare humid forest woodpecker, *Campephilus heamatogaster*, represents the first tissue specimen for Panama from outside Darien province. This may be the most northerly tissue held for the species, which ranges from western Panama to eastern Peru and comprises two subspecies (*C. h. heamatogaster* and *C. h. splendens*). The quail, *Rynchortx cinctus*, is very poorly represented in tissue collections and infrequently encountered; the specimens collected in the upper Río Chagres drainage probably represent the most northerly tissue samples in the world. The dove, Geo*trygon veraguensis*, is also noteworthy because the specimen may represent the first tissue sample from anywhere in the world.

ACKNOWLEDGEMENTS

Thanks are extended to the following individuals and institutions for providing electronic lists of their tissue holdings from Panama: F. Sheldon, R. Brumfield and D. Dittman at the Louisiana State University Museum of Natural Science; M. Braun, C. Huddleson and S. Olsen at the U.S. National Museum of Natural History; and, L. Joseph and N. Rice at the Philadelphia Academy of Natural Sciences. E. Bermingham of the Smithsonian Tropical Research Institute arranged our participation on the Chagres field program, encouraged this report, and provided a copy of unpublished work on Bay Wrens. V. Rohwer, S. Birks and K. Davis helped RF with the Chagres fieldwork. Logistical support for the field work was provided by the Tropical Regions Test Center (U.S. Army Yuma Proving Ground).

REFERENCES

Avise, JC, 2000, *Phylogeography*: Harvard Univ. Press, Cambridge, MA.

Brumfield, RT, Jernigan, RW, Mcdonald, DB, and Braun, MJ, 2001, Evolutionary implications of divergent clines in an avian (*Manacus*: Aves) hybrid zone, Evolution, 55: 2070–2087.

Emerson, BC, Paradis, E, Thebaud, C, 2001, Revealing the demographic histories of species using DNA sequences: Trends Ecol. Evol., 16:707-716.

González, MA, Eberhard, JR, Lovette, IJ, Olson SL, and Bermingham, E, 2003, Mitochondrial DNA phylogeography of the Bay Wren (*Thryothorus nigricapillus*) complex: unpublished manuscript.

Hewitt, GM, 1996, Some genetic consequences of ice ages, and their role in divergence and speciation: Biol. Jour. Linnean Soc., 58:247-276.

Hobson, KA, 1999. Tracing origins and migration of wildlife using stable isotopes: A review: Oecologia, 120: 314-326.

Marra, PP, Hobson, KA, and Holmes, RT, 1998, Linking winter and summer events in a migratory bird using stable carbon isotopes. Science, 282: 1884-1886.

Parke, TA III, Stotz, DF, Fitzpatrick, JW, 1996, Ecological and Distributional Databases for Neotropical Birds: in *Neotropical Birds: Ecology and Conservation* (DF Stotz, TA Parker III, JW Fitzpatrick, and DK Moskovtz, eds.), Univ. Chicago Press, Chicago, IL: 1-479.

Templeton, A, Routman, RE, and Phillips, C, 1995, Separating population structure from population history: A cladistic analysis of the geographical distribution of mitochondrial DNA haplotypes in tiger salamander, *Ambystoma tigrinum*: Genetics, 140: 767-782.

Chapter 19

ESTIMATION OF LANDSLIDE IMPORTANCE IN HILLSLOPE EROSION WITHIN THE PANAMA CANAL WATERSHED

Robert F. Stallard[1] and David A. Kinner[1,2]
[1]*US Geological Survey,* [2]*University of Colorado*

Abstract: This paper presents an approach for assessing the regional importance of landslides based on conventional daily-discharge and daily-sediment data from sub-basins within the Panama Canal Watershed. In many wet mountainous regions, sediment yields are controlled by both surficial erosion and deep, landslide erosion. Landslides require that rainfall (and by inference runoff) exceed a threshold. Runoff can be used to derive a parameter termed 'landslide days', with a suitable correction factor, to account for evapotranspiration, infiltration, and rainfall patchiness. The approach developed then uses runoff as the driver for a simple surficial-erosion model and landslide days as the driver for a landslide model. In a case study of the Panama Canal Watershed, this model describes spatial and temporal patterns of annual yields with a high degree of efficacy, demonstrating that simple daily data can be used to determine whether a river basin, such as the upper Río Charges basin, might be undergoing substantial landslide-related erosion.

Key words: Panama; Panama Canal Watershed; Río Charges; landslide erosion; erosion modeling

1. INTRODUCTION

Landslides represent an energetic mass-wasting process that erodes substantial quantities of solids in a short time. Typical prerequisites for landslides are steep slopes and either bedrock that is structurally unstable (relatively non-cohesive, sheared, or fractured) or, in the case of stable bedrock, degraded through chemical or physical weathering. The specific subject of this paper are soil-derived landslides, often referred to as 'soil avalanches.' which encompass a range of phenomena such as simple block

R. S. Harmon (ed.), The Río Chagres, Panama, 281-295.

slides and debris flows. Soil landslides are often associated with outbreaks that are triggered by events, such as large amounts of intense precipitation, typically exceeding some regional slide-inducing threshold (Starkel, 1972; Caine, 1980; Larsen and Torres-Sánchez, 1989; Scatena and Larsen, 1991; Larsen and Simon, 1993; Montgomery and Dietrich, 1994; Montgomery *et al*., 2000; Reid, 1998; Crosta, 1998), or earthquakes (Simonett, 1967; Garwood *et al.*, 1979; Keefer, 1984, 2000).

Human activities, notably deforestation (Larsen and Santiago Roman, 2001; Larsen and Torres-Sánchez, 1998; Montgomery *et al.,* 2000) and road building (Larsen and Parks, 1997; Wemple, *et al*., 2001) increase the rate and frequency of soil avalanching. In turn, soil-avalanche outbreaks and associated debris flows are responsible for major loss of human life and property such as recently happened in Central America during Hurricane Mitch in 1998 (Molnia and Hallam, 1999) or in coastal Venezuela during the intense and prolonged rains of December, 1999 (Larsen *et al.,* 2001).

Retrospective studies of the sort that have taken place in the aftermath of deadly landslides triggered by intense rains, while extremely interesting post-mortems, do not represent a way of assessing landslide risk in regions that have not been hit by a severe storm in recorded memory. Other procedures, using relatively common types of hydrologic data and topographic maps need to form the basis of assessing whether a region is landslide-prone. One such approach is demonstrated here using data from the Panama Canal Watershed.

2. LANDSLIDE ESTIMATION WITH MULTI-YEAR DAILY SEDIMENT LOADS

The economic role of the Panama Canal in global commerce is well known, and because of its importance, the Panama Canal Watershed is particularly data rich, having been hydrologically-monitored, mapped, and variously characterized for more than a century.

The former Río Chagres basin (see Fig. 3 of Harmon, 2005a, this volume), which forms the majority of the Panama Canal Watershed, consists of upland in the northeast and southwest, with an extensive lowland in between. Half of the Panama Canal runs through Gatún Lake formed by flooding the lower course of the old Río Chagres (Fig. 1). The northeastern uplands drain a deeply exhumed oceanic volcanic terrain consisting of granites, microdiorites, and altered volcanic andesitic and volcaniclastic lithologies that have been intruded by gabbros and diorites (see Wörner *et al.,* 2005, this volume), veneered by thin soils (see Harrison *et al.,* 2005, this volume). The southwestern uplands are comprised of mostly younger

volcanic rocks. The lowlands form a trough filled with marine and terrestrial sediments and some eruptive volcanic rocks. The best tropical forest cover is in upper portions of the Chagres National Park in the northeast and in Soberania National Park and the Barro Colorado Nature Monument along the Panama Canal (Condit, *et al,.* 2001; Ibáñez *et al.,* 2002). Elsewhere, land cover is a mosaic of pasture, second growth, forest patches, urbanizations, and roads. Hillslopes in both the lowlands and uplands are generally steep and straight and the river network demonstrates strong lithologic control, all features of a landscape undergoing weathering-limited (supply-limited) erosion (Stallard, 1995b). The Isthmus of Panama has a strong north-south (Caribbean-Pacific) rainfall gradient, with in excess of 3,000 mm in the north to about 1,500 in the south. More rain falls in uplands than the lowlands due to orographic effects.

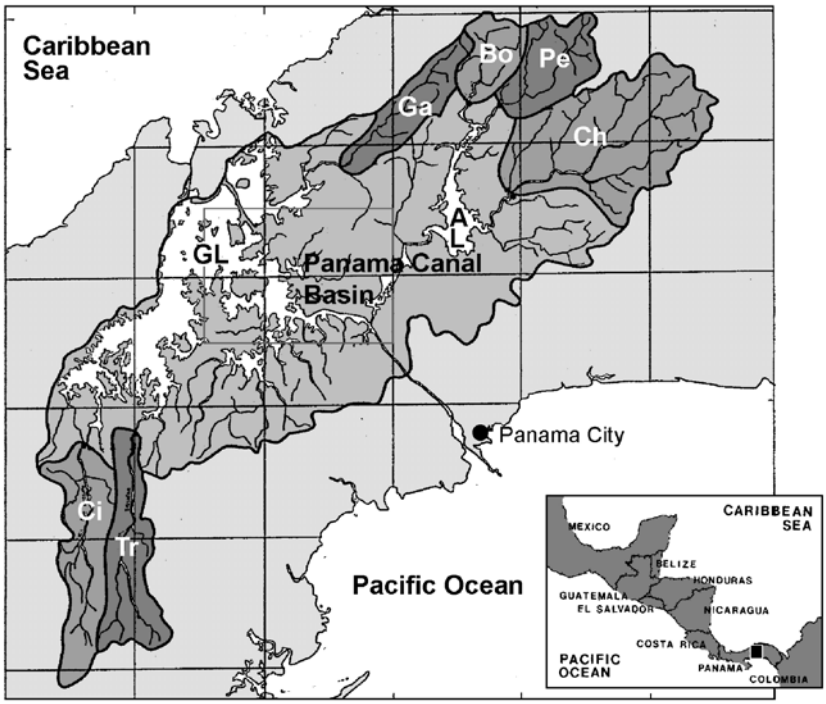

Figure 1. Location map for the case-study basins within the greater Panama Canal Watershed. Letter codes in black letters: AL = Lago Alhajuela, GL = Gatún Lake. Letter codes in white letters: Bo = Río Boquerón, Ch = upper Río Chagres, Ci = Río Ciri Grande, Ga = Río Gatún, Pe = Río Pequení, Tr = Río Trinidad.

Table 1. Basin properties and results of the hybrid surface erosion - landslide erosion model for major sub-basins of the Panama Canal Watershed

	Upper Río Chagres at Chico Gage	Río Boquerón at Peluca Gage	Río Pequení at Candelaria Gage	Río Gatún at Ciento Gage	Río Trinidad at El Chorro Gage	Río Cirí Grande at Cañones
Basin Properties[1]:						
Area (km^2)	414	91	135	117	174	186
Land Cover						
Forest	98.0	83.9 %	94.6 %	62.5 %	18.2 %	20.2 %
Second Growth	1.0	4.9 %	1.9 %	9.7 %	29.7 %	35.6 %
Cleared Land	1.0	11.2 %	3.4 %	27.5 %	50.9 %	42.5 %
Bare Soil	0.0	0.0 %	0.1 %	0.3 %	1.2 %	1.7 %
Population (1996)	145	455	180	2,303	3,110	3,000
Mean Slopes	29E	21E	25E	20E	13E	15E
Runoff (mm yr^{-1})	2579	2975	3491	1882	1157	1552
Landslide Days	5	48	30	6	0	3
Measured Yield (Mg/km/yr)	289	887	658	305	112	195
Equilibrium Yield (Mg/km/yr)	126	136	149	107	86	98
Mean Concentration (mg/L)	112	298	189	162	97	126
Equilibrium Concentration	49	46	43	57	74	63
Measured Equilibrium	2.3	6.5	4.4	2.8	1.3	2.0
Model: Surficial Erosion Plus Landslide Erosion: Yield = a▪(runoff)^b+c▪(landslide days with factoR =						
F	0.85	0.85	0.85	0.85	0.85	0.85
a	4.54▪	1.26▪1	$8.20 \cdot 10^2$	$1.59 \cdot 10^5$	7.86▪1	2.35▪1
b	1.1	1.0	1.0	2.2	2.0	1.8
C (Mg/km/slide day)	98.8	158.7	182.7	71.8	0.0	200.5
Degrees of Freedom	11	11	11	5	5	5
Correlation Coefficient	0.80	0.979	0.965	0.831	0.972	0.994
Surficial Erosion (Mg/km/yr)	258	411	316	261	112	135
Slide Erosion (Mg/km/yr)	31	476	342	43	0	60
Slide/Total Erosion (%)	11%	54%	52%	14%	0%	31%
1. Basin properties from PMCC (1999)						

The Panama Canal Watershed is subject to wet-season rains (April to December), and water storage is very carefully controlled at the end of the wet season to maximize water in storage within the two lakes of the Panama Canal - Gatún Lake and Lago Alhajuela- while using water in excess of this maximum for electric power generation during the wet season. Accordingly, this study uses data that has been collected for the operation of the Panama Canal (Fig. 1, Table 1) by the Autoridad del Canal de Panama

(ACP), formerly the Panama Canal Commission (PCC) and its predecessor the Panama Canal Company. These data were originally summarized by Stallard (1999) in PMCC (1999). A wide variety of hydrologic data has been collected. The longest data sets, some predating the construction of the Panama Canal, include rainfall, river discharge, and pan evaporation. Daily measurements of sediment in three rivers of the watershed - upper Río Chagres, Río Boquerón, and Río Pequení, - commenced in 1981 in response to concerns about loss of storage capacity in Lago Alhajuela, the dry-season water-supply lake for operation of the Panama Canal (Wadsworth, 1978; Larson, 1979; Robinson, 1985; Alvarado, 1985). In 1987, these measurements were expanded to include the other major gaging sites (Río Gatún, Río Trinidad, and Río Ciri Grande).

The ACP sediment-discharge data set is notable from the perspective of tropical rivers, where very few sites have such long-term daily sediment measurements. The procedures were largely adapted from the sediment sampling and processing techniques of the US Geological Survey (Guy, 1969; Guy and Norman, 1970). The methodologies have remained fixed for the entire duration of the data set (J. Tutzauer and L. Alvarado, ACP, pers.comm.); thus, trends that may be evident should not have been caused by changes in procedures.

Intra-annual variation is enormous, so water discharge and sediment discharge were totaled for each year of record. Because rains stop in December, calendar years and water years coincide. A helicopter-based examination of the watershed by Robinson (1985), and helicopter overflights and numerous site visits from 1996 to 2002, indicate that most channels have boulder beds with very little fine particle component and almost no developed floodplains, thus little storage of fine sediment is anticipated from one water year to the next. Accordingly, these totals (Figs. 2, 3). were divided by basin area to get runoff (mm/ yr) and sediment yield ($kg/km^{-2}/yr$). Sediment yield equates to 'denudation rate' or 'basin-averaged erosion rate,' rather than a 'local erosion rates.' The runoff pattern reflects the rainfall gradient, with the northern-most mountainous rivers (upper Río Chagres, Río Boquerón, and Río Pequení) having the most rain, and the more southerly and less elevated rivers (Río Gatún, Río Trinidad, and Río Ciri Grande) having the least.

For reference, Table 1 includes a model equilibrium sediment yield for chemical weathering of younger igneous and metamorphic terrains (Stallard, 1995a, b). Softer bedrock, such as many types of sedimentary rock, will naturally poduce higher rates of physical erosion than this equilibrium model predicts. All six rivers have sediment yields that are above the equilibrium model (Table 1). Assuming that the model is reasonable within a factor of 2

to 3, only the Río Boquerón and Río Pequení have yields that are substantially above the model predictions. Deforestation appears to be the most likely mechanism that would enhance sediment yields. According to Condit *et al.* (2001) and Ibáñez *et al.* (2002), as well as the characterization of the watersheds by Robinson (1985), only the upper Río Chagres basin is minimally affected by human activities. The sediment yield of the Río Boquerón basin is 3-times that of the upper Río Chagres basin, and the yield of the Río Pequení basin is over 2-times that of the upper Río Chagres basin.

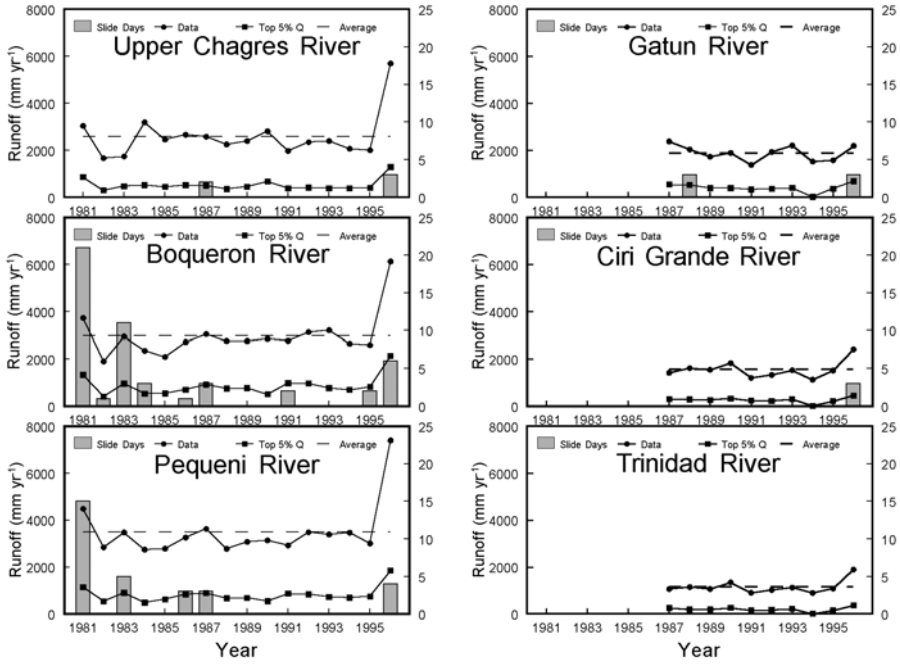

Figure 2. Illustration of the inter-annual variations in selected hydrologic properties for the sub-basins of the case-study within the Panama Canal Watershed. Landslide days were calculated as described in the text. The top 5% of flow is the total runoff for the 18 days each year with the greatest runoff. Neither the annual runoff nor the top 5% of days correlate well with the annual sediment yield presented in Figure 3. The average runoff is for the period of record used in this graph.

Sediment yields reflect contributions from both shallow surface erosion and deep landslide erosion. Surficial erosion includes sediment transport by raindrop splash, sheet wash, rill formation, and gullying. Although some gullying can be quite deep, most deep erosion is by landsliding. These physical-erosion processes operate in both natural and developed settings, but typically with greater intensities in the latter, when examined on human time scales.

Sediment yields generally declined from 1981 through 1995 (Fig. 3, but these declines are not matched by decreases in runoff (Fig. 2). The year 1996 was especially wet, among the wettest on record for each river. Sediment yields increased, but although the highest sediment yields of record would be expected if surficial erosion were the primary source of sediment, yields on the upper Río Chagres, Río Boquerón, and Río Pequení for 1996 are similar to or less than in 1981, the next wettest year.

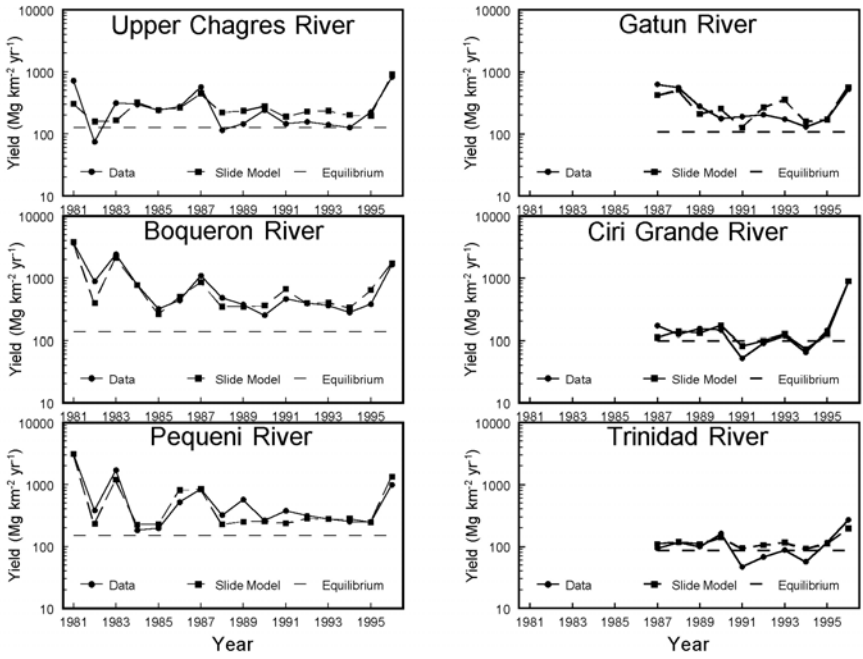

Figure 3. Annual sediment yield for the major rivers of the Panama Canal Watershed. The 'model' dash line is the sediment yield that might be expected for equilibrium erosion from a young mountainous terrain with the average runoff for the respective river basin over the period of record from Stallard (1995b).

3. MODELS AND MODELING APPROACHES

To model these data, a dual-mechanism sediment source (surficial erosion and landslides) was assumed. Surficial erosion is described using a simple and rather conventional formulation that relates annual sediment yield, Y (year), to annual runoff, R (year):

$$Y(\text{year}) = a \cdot R(\text{year})^{b}, \quad (1)$$

where a and b are regression coefficients. Landslides require a threshold amount of rainfall to be triggered. For tropical settings with the island-arc geology of Puerto Rico or Panama, the threshold amount of rainfall is described by the equation (Larsen and Simon, 1993):

$$P = 91.46 \cdot T^{0.18}, \quad (2)$$

where P is rainfall in mm and T is duration of rainfall in hours. For storms with a duration of 24, 48, and 72 hours, the threshold rainfall is 162, 184, and 197 mm, respectively, or roughly 200 mm.

Although there are numerous rain gages within the Panama Canal Watershed, the coverage is still inadequate to map daily precipitation and estimate the number of days per year in which landslides could be triggered. Therefore, instead of precipitation, this analysis used daily runoff data, R, calculated from the daily discharge data.

$$R = P \cdot A^{-1}, \quad (3)$$

where A is basin area. Each day of the year is characterized. A particular day is defined as a landslide day if:

$$R\ (24, 48, 72\ \text{hr}) > F@91.46 \cdot D^{0.18}\ (D = 24, 48, 72\ \text{hr}), \quad (4)$$

where F is an empirical factor between 0 and 1 that adjusts the threshold for two factors that reduce runoff relative to local rainfall – (i) evapotranspiration and (ii) infiltration. If F is 1, then it is assumed that runoff faithfully tracks rainfall. Rainfall patchiness, where parts of a watershed will be over the threshold, and other parts below the threshold, would tend to increase F. When rainfall is patchy, the largest rivers may have landslide-producing storms in a portion of their basins without producing a cumulative amount of runoff that exceeds the slide threshold. Accordingly, values of $F > 1$ were tested. For each river, and for each year of the data set, the number of landslide days, as defined by the above equation, were totaled and assigned this total per year to landslide days per year, N (year).

Thus, the final form of the surface-erosion, landslide-erosion model is:

$$Y(\text{year}) = a \cdot R(\text{year})^{b} + c \cdot N(\text{year}). \quad (5)$$

There are four adjustable parameters in this 'Surface Erosion-Landslide Erosion' model. The landslide threshold adjustment parameter, *F,* is assumed to be the same for all of the watersheds, and is optimized iteratively. The optimum value was 0.85, which indicates, in essence, that it can be assumed that $R = 0.85 \cdot P$ for large storms. The remaining coefficients were estimated iteratively using a non-linear regression procedure. For each river, the coefficients and 'quality-of-fit' information are given in Table (1). This model tracks inter-annual variations rather well (Fig. 4). The fraction of total physical erosion that can be attributed to landslides ranges from none for the Río Trinidad to more than 50% for the Río Boquerón and Río Pequení.

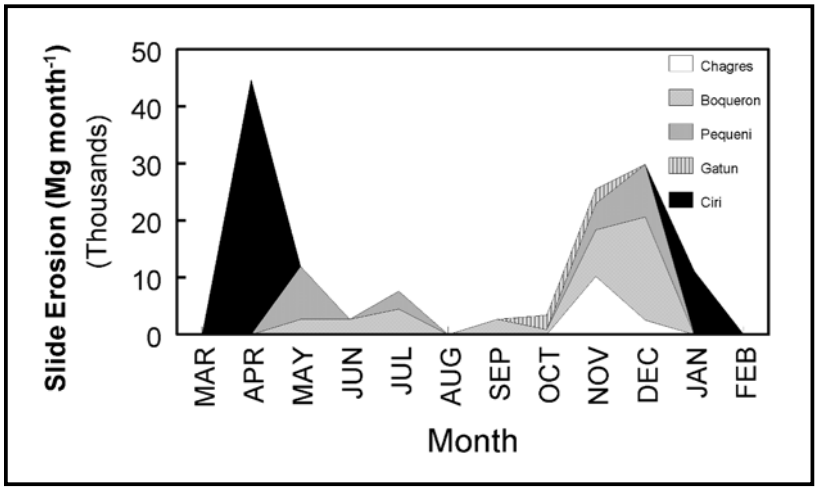

Figure 4. Monthly landslide yield for all of the case-study rivers. This was obtained by retabulating landslide days for the entire record for each river on a monthly basis.

The lesser sediment yields for 1996, as compared to 1981, despite the greater runoff of 1996, can be attributed to fewer landslide days in 1996. For rivers with many landslide days, the exponent, *b*, was low, near 1, while for rivers with few landslide days, the exponent was significantly greater. This difference may in part be due to an unresolvable cross-correlation between annual runoff and landslide days. Such a cross-correlation could be statistical or physical. For example the rate of surficial erosion on landslide scars could increase surficial erosion following slides (Larsen, *et al*., 1998).

When re-tabulated on a monthly basis for the period of record, the distribution of landslide days throughout the year is distinctly bimodal (Fig. 4). The dry season typically runs from January through April. The wet

season starts in May, often has a less stormy period in August, then peaks in November/December. No slide occurred in February, March, and August. On the east side of the Panama Canal, most of the slide days occur in the late wet season, whereas in the west (Río Ciri Grande), most of the landslides occur during the early wet season.

It might be argued that 'landslide days' could instead be 'channel-bank erosion days' or 'channel-bed erosion days', or possibly, 'freshly plowed farm-field days'. These options cannot be rigorously ruled out, but several aspects of the rivers examined suggest that these alternatives are unlikely. First, if the highest flows are considered as an indicator of channel mobilization, no effect is seen. In Figure 2, the total runoff for the 18 highest-runoff days per year (top 5%) was calculated. When these values are included in the regression equation, instead of 'landslide days', the quality of fit is significantly lower, because this parameter is too highly correlated with annual runoff. This indicates that phenomena that relate to extremely high flows are adequately embedded in the surficial-erosion term in Equation 5.

Second, regarding agricultural effects, within the Panama Canal Watershed, there is little mechanical agriculture, and land typically is cleared by burning. Within burned areas, smaller plots are tilled. Areal and satellite photography (Condit *et al.,* 2001) indicates that 1-5% of deforested land is cropland. Land preparation happens during the dry season. The driest sub-basins are also most agricultural (Río Ciri Grande and Río Trinidad in Table 1). These do not show exceptional sediment yields, indicating that direct agricultural effects do not dominate.

4. MODELING THE HUMAN OVERPRINT

The Panama Canal BWatershed is home for more than 100,000 people (Condit *et al.,* 2001), and, therefore, it is necessary to ask whether this may have skewed the results of this study. Human activities appear to have an effect in the amount of landslide erosion. Of the mountainous subbasins having landslides (upper Río Chagres, Río Boquerón, Río Pequení, and Río Ciri Grande), only the upper Río Chagres is mostly forested (Table 1), and the mass of sediment generated in the upper Río Chagres basin per landslide day, c, is about half that of the other, deforested watersheds.

Table 2. Comparison of estimated landslide frequency on forested and developed landscapes within the central Panama Canal Watershed.

	In Park Lands[1] (44%of land area)	Developed Lands (56% of land area)
Slope Class		
Slope <12	52.34	56.27
Slope >12	47.66	43.73
Aspect		
Facing Aspect (North)[2]	22.88	24.00
Lee Aspect (South)	24.51	23.41
Normal Aspect (East and West)	52.61	52.59
Land Cover		
Forest	93.98	50.29
Agriculture	5.71	47.80
Roads and Houses[3]	0.16	0.99
Urban Areas	0.15	0.92
Landslide Frequency (slides/km^2/yr)[4]	0.84	1.76
[1]Park lands refer to Soberania National Park and the Barro Colorado Nature Monument, both areas of limited development. For maps of boundaries, human populations, and land cover, refer to Condit *et al.* (2001).		
[2]North aspects face most storms in central Panama		
[3]All features were given a 10 m buffer		
[4]Landslide frequency was computed using combinations of the above parameters and the model of Larsen and Torres-Sanchez (1998) developed for the Blanco region of Puerto Rico.		

To assess the effect of deforestation and road building on sediment yields from soil avalanching, the empirical landslide erosion model developed for the Río Blanco basin in Puerto Rico by Larsen and Torres-Sanchez (1998) was applied to the central Panama Canal Watershed (central rectangle in Fig. 1). This region includes a wide range of land cover and land use, ranging from intact forests in Soberania National Park and the Barro Colorado Nature Monument to a mix of pasture, second growth, and urbanization. Although the model was developed in a region with hurricanes and frontal rainstorms, it is expected that the similarity in annual precipitation, bedrock type, and temperature make it relatively applicable to Panama. Topographic parameters–slope, aspect–were derived from a 1:25,000-scale, 10 m digital elevation map of the six 7.5 minute quadrangles surrounding Barro Colorado Island (PMCC, 1999). Because of the lack of mountainous areas in central Panama, only the parts of the Río Blanco basin model applicable to elevations <400 m were used. Land use was derived from LANDSAT

imagery of the region (PMCC, 1999), and approximate locations of roads and rural dwellings were digitized from the original topographic maps and given 10 m buffers following the procedure of Larsen and Torres-Sanchez (1998).

The model results (Table 2) indicate that landslide frequency doubles outside of the protected confines of the nature preserves, due largely to the increase in agriculture (48% outside of the parks) and the greater number of roads. The aspect and slope class variables are remarkably similar in both locations, leaving land-use as the major factor in increasing landslide frequency. Despite the application to Panama of an empirical model developed for Puerto Rico, the estimate of 1 landslide per km^2 per yr seems entirely reasonable for the forested portions of the central Panama Canal Watershed. The factor-of-two difference between forested and non-forested settings is in general agreement with the results of the previous landslide-day model.

5. CONCLUSIONS

Because of the erosional significance of landslides and their importance as a hazard, global assessment of landslide-affected landscapes is important. Accordingly, an approach is proposed based on conventional daily-discharge and daily-sediment data, demonstrating that these data can be used to determine whether a river basin might be undergoing substantial landslide-related erosion. In such settings, sediment yields are controlled both by surficial erosion and deep, landslide erosion. Landslides require that rainfall (and by inference runoff) exceed a threshold. With a suitable correction factor, to account for evapotranspiration, infiltration, and rainfall patchiness, runoff can be used to derive a parameter we call landslide days. The model then uses runoff as the driver for a surficial erosion model and landslide days as the driver for a landslide model. In the example here, the Panama Canal Watershed, this model describes spacial and temporal patterns of annual yields with a high degree of efficacy.

Within the Panama Canal Watershed, the tributaries with the least runoff have few or no landslide days, and despite being deforested, they do not have an especially excessive sediment yields. In contrast, the tributaries with greater runoff and many landslide days had higher sediment yields, including one with intact forests, the upper Río Chagres. It is anticipated that if this approach is used worldwide that the transition to landslide-driven erosion would be 800 mm to 1000 mm. The transition would be lower in basins subjected to intense storms such as hurricanes.

Before concluding, it is important to note that the effects of landslides on people in the Panama Canal Watershed can be significant. The landscape erosion model identifies landslide-prone regions and times of the year. Such information can and should be used in risk assessments as the human population in the tropics continue to grow and as people move into more unstable areas.

ACKNOWLEDGEMENTS

Portions of the work described in this chapter were funded by the US Geological Survey, US Agency for International Development, and the Smithsonian Tropical Research Institute. Data and initial modeling are presented in Panama Canal Watershed Monitoring Project (1999).

REFERENCES

Alvarado K, 1995, La sedimentación del lago Alhajuela: in *Agonía De La Naturaleza*, (S Heckadon Moreno, and J Espinosa González, eds.), Instituto de Investigación Agropecuaria de Panama and Smithsonian Tropical Research Institute, Balboa, Panama: 103-123.

Caine, N, 1980, The rainfall intensity-duration control of shallow landslides and debris flows: Geogr. Annal.: 62A: 23-27.

Condit, R, Robinson, WD, Ibáñez R, Aguilar, S, Sanjur RA, Martínez, R, Stallard, RF, García, T, Angehr, GR, Petit, L, Wright, SJ, Robinson, TR, and Heckadon Moreno, S, 2001, The status of the Panama Canal Watershed and its biodiversity at the beginning of the 21st Century: Bioscience, 51: 389-398.

Crosta, G, 1998, Regionalization of rainfall thresholds: an aid to landslide hazard evaluation: Env. Geol., 35:, 131-145.

Garwood, NC, Janos, DP, and Brokaw, NVL, 1979, Earthquake-caused landslides: A major disturbance to tropical forests: Science, 205: 997-999.

Guy, HP, 1969, *Laboratory Theory and Methods for Sediment Analysis*: US Geol. Surv. Tech. Water-Resour. Inv., Book 3, Chapter C2.

Guy, HP, and Norman, VW, 1970, *Field Methods for Measurement of Fluvial Sediment*, US Geol. Surv. Tech. Water-Resour. Inv., Book 3, Chapter C2.

Harmon, RS, 2005, An Introduxtion to the Panama Canal Watershed: in *The Río Chagres: A Multidisciplinary Perspective of a Tropical River Basin* (RS Harmon, ed.), Kluwer Acad./Plenum Pub., New York, NY: 19-28.

Harrison, JBJ, Hendricks, JMH, Vega, D, Calvo-Gobbetti, LE, 2005, Soils of the Upper Río Chagres basin: in *The Río Chagres: A Multidisciplinary Perspective of a Tropical River Basin* (RS Harmon, ed.), Kluwer Acad./Plenum Pub., New York, NY: 97-112.

Ibáñez D., R, Condit, R, Angehr, GR, Aguilar, S, García, T, Martínez, R, Sanjur, A, Stallard, RF, Wright, SJ, Rand, AS, and Heckadon Moreno, S, 2002, An ecosystem report on the Panama Canal: Monitoring the status of the forest communities and the watershed: Env. Mon. Assess., 80: 65-95.

Keefer, DK, 1984, Landslides Caused by Earthquakes: Geol. Soc. Amer. Bull., 95: 406-421.

Keefer, DK, 2000, Statistical analysis of an earthquake-induced landslide distribution - the 1989 Loma Prieta, California event: Eng. Geol., 58: 231-249.

Larsen, MC, and Parks, JE, 1997, How wide is a road? The association of roads and mass-wasting in a forested montane environment: Earth Surf. Proc. Landf., 22: 835-848.

Larsen, MC, and Santiago Roman,A, 2001, Mass wasting and sediment storage in a small montane watershed: An extreme case of anthropogenic disturbance in the humid tropics: in *Geomorphic Processes and Riverine Habitat, 2001*, *American Geophysical Union Monographs*, (JM Dorava, F Fitzpatrick, BB Palcsak, and DR Montgomery, eds.), Amer. Geophys. Union, Washington, D.C.

Larsen, MC, and Simon, A, 1993, A rainfall intensity-duration threshold for landslides in a humid-tropical environment, Puerto Rico: Geogr. Annal., 75A: 13-23.

Larsen, MC, and Torres-Sánchez, AJ, 1992, Landslides triggered by Hurricane Hugo in eastern Puerto Rico, September 1989: Carib. Jour. Sci., 28: 113-125.

Larsen, MC, and Torres-Sánchez, AJ, 1998, The frequency and distribution of recent landslides in three montane tropical regions of Puerto Rico: Geomorph., 24: 309-331.

Larsen, MC, and Torres-Sánchez, AJ, and Concepción, IM, 1998, Slopewash, surface runoff, and fine-litter transport in forest and landslide scars in humid-tropical steeplands, Luquillo Experimental Forest, Puerto Rico: Earth Surf. Proc. Landf., 24: 481-502.

Larsen, MC, Vasquez Conde, MT, and Clark, RA, 2001, Landslide hazards associated with flash-floods, with examples from the December, 1999 disaster in Venezuela: in *Coping With Flash Floods*, *NATO ASI Series C: Mathematical and Physical Sciences* (E Gruntfest and J Handmer, eds.), Kluwer, Acad. Pub., Dordrecht, Holland: 259-275.

Larson, C, 1979, Erosion and sediment yield as affected by land use and slope in the Panama Canal Watershed: Proc. III World Cong. Water Resour., Int. Water Resour. Assoc., Mexico City, Mexico, Part III, 1086-1095.

Molnia, BF and Hallam, CA, 1999, *Open Skies Aerial Photography of Selected Areas in Central America Affected by Hurricane Mitch*, US Geol. Surv. Circ. 1181.

Montgomery, DR, and Dietrich, WE, 1994, A physically based model for the topographic control on shallow landsliding: Water Resour. Res., 30: 1153-1171.

Montgomery, DR, Schmidt, KM, Greenberg, HM, and Dietrich, WE, 2000, Forest clearing and regional landsliding: Geology, 28: 311-314.

Panama Canal Watershed Monitoring Project, 1999, *Report of the Panama Canal Watershed Monitoring Project*, 8 volumes, 21 CD-ROMS.

Reid, LM, 1998, Calculation of average landslide frequency using climatic records: Water Resour. Res., 34: 869-877.

Robinson, FH, 1985, *A Report on the Panama Canal Rain Forest:* Meteorol. Hydrograph. Branch, Eng. Div., Panama Canal Commission, Balboa Heights, Panama.

Scatena, FN, and Larsen, MC, 1991, Physical aspects of Hurricane Hugo in Puerto Rico: Biotropica, 23: 317-323.

Simonett, DS, 1967, Landslide distribution and earthquakes in the Bewani and Torricelli Mountains, New Guinea: A statistical analysis: in *Landform Studies From Australia and New Guinea* (JN Jennings, and JA Mabbutt, eds.), Australian National Univ. Press, Canberra, Australia: 64-84.

Stallard, RF, 1995, Relating chemical and physical erosion: in *Chemical Weathering Rates of Silicate Minerals*, (AF White, and SL Brantley, eds.), Rev. Mineral., 31: 543-564.

Stallard, RF, 1995, Tectonic, environmental, and human aspects of weathering and erosion: A global review using a steady-state perspective: Ann. Rev. Earth Planet. Sci. , 12: 11-39.

Stallard, RF, 1999, ed., Erosion and the effects of deforestation in the Panama Banal Basin: in *Report of the Panama Canal Watershed Monitoring Project*, Panama Canal Watershed Monitoring Project. Chapter II.8.

Starkel, L, 1972, The role of catastrophic rainfall in the shaping of the relief of the lower Himalaya (Darjeeling Hills): Geogr. Polonica, 21: 103-147.

Tutzauer, JR, 1990, *Madden Reservoir Sedimentation, 1984-1986*, Meteorol. Hydrograph, Branch, Eng. Div., Panama Canal Commission, Balboa Heights, Republic of Panama.

Wadsworth, FH, 1978, Deforestation - Death to the Panama Canal: *Proc. U.S. Strategy Conference on Tropical Deforestation,* US Dept. State and US Agency Int. Dev., Washington, D.C., 22-24.

Wemple, BC, Swanson, FJ, Jones, JA, 2001. Forest roads and geomorphic process interactions, Cascade Range, Oregon: Earth Surf. Proc. Landf., 26: 191-204.

Wörner, G, Harmon, RS, Hartmann, G, and Simon, K, 2005, Igneous Geology and Geochemistry of the Upper Río Chagres Basin: in *The Río Chagres: A Multidisciplinary Perspective of a Tropical River Basin* (RS Harmon, ed.), Kluwer Acad./Plenum Pub., New York, NY: 65-82.

Chapter 20

LONG-TERM SEDIMENT GENERATION RATES FOR THE UPPER RÍO CHAGRES BASIN:
Evidence from Cosmogenic ^{10}Be

Kyle K. Nichols[1], Paul R. Bierman[2], Robert Finkel[3], and Jennifer Larsen[2]
[1]Skidmore College, [2]University of Vermont, [3]Lawrence Livermore National Laboratory

Abstract: In situ-produced cosmogenic ^{10}Be was measured in 17 sediment samples to estimate the rate and distribution of sediment generation in the upper Río Chagres basin over the last 10 to 20 kyr. Results indicate that the upper Río Chagres basin is generating sediment uniformly. Nuclide activities suggest basin-wide sediment generation rates of 143 and 354 tons/km/yr (avg. = 234 ± 74 tons/km/yr; n = 7) for small tributary basins and 248 to 281 tons/km/yr (avg. = 267 ± 97 tons/km/yr; n = 3) for large tributary basins. The weighted average of all tributaries is 269 ± 63 tons/km/yr; n = 10). A sample collected upstream of Lago Alhajuela suggests that the entire basin is exporting sediment at a rate of 275 ± 62 tons/km/yr. These cosmogenic nuclide measurements all suggest that the upper Río Chagres basin (when considered on scales <5 km^2 to >350 km^2) is generating sediment at ~270 tons/km/yr. This long-term (1 -20 kyr) sediment generation rate that is equivalent to the estimate derived from suspended sediment yield measured below the upper Río Chagres- Rió Chico confluence from 1981-96 (289 tons tons/km/yr). Such similarity implies that decadal and millennial sediment yields are similar. Thus, short-term sediment yields and long-term sediment generations are in balance, implying steady landscape behavior over time. The background sediment yield suggests that it would take ~3,600 years to completely fill Lago Alhajuela, the reservoir for the Panama Canal. Taking into account the present day 2- to 3-fold increase in sediment yields for adjacent human-impacted Rió Boquerón and Rió Pequení basins, the filling time is reduced to ~2,000 years. However, it would only take between 250 to 600 years to reduce the reservoir capacity (69% of maximum) enough to drain the entire reservoir for precipitation conditions similar to the 1982 *El Niño* event. Such models highlight the importance of proper watershed management in order to reduce the sedimentation of Lago Alhajuela.

Key words: Panama; Río Chagres; cosmogenic isotopes; erosion; sedimentation; sediment yield

R. S. Harmon (ed.), The Río Chagres, Panama, 297-313.

1. INTRODUCTION

Lago Alhajuela, an artificial dammed lake at the outlet of the upper Río Chagres basin, provides up to 40% of the water necessary to operate the Panama Canal (Larsen and Albertin, 1984). Even though the storage capacity of the lake is vital to the operation of the canal and thus, the global economy, little is known about the rate and processes of sediment production in tributary drainage basins. Transportation of this sediment into Lago Alhajuela is steadily reducing its water storage capacity.

Little is understood about the geomorphology and hydrology of the upper Río Chagres basin and its headwater areas because the watershed is thickly vegetated and there are no established transportation routes (Fig.1). The Panamanian government protects the basin from development as the Chagres Nnational Park. Therefore, human disturbance within the basin is minimal compared to adjacent lands and recent disturbances are mostly confined to the lower elevations and to the Rió Piedras tributary in the southern portion of the watershed.

Total relief across the 466 km^2 upper Río Chagres basin is *ca.* 800 m. The basin is dominated by steep hillslopes (Fig. 2). Aerial and ground observations suggest that sediment is delivered to the channels both through biologically driven soil creep and by landslides. Field observations show that the rivers flow on bedrock throughout much of the basin, suggesting little sediment storage (Fig. 3). However, in the upper reaches of the Río Chagres, Rió Esperanza, and Rió Chagricito rivers, local areas have up to 2 m of boulders and alluvium overlain by floodplain deposits. Once sediment is delivered from the hillslopes to the channel, it is quickly transported out of the drainage basin as suggested by the extensive reaches of bedrock-floored channels and small aerial extent of sediment storage (Fig. 3).

Little is known about the geology of the inaccessible upstream most reaches of the upper Río Chagres basin. Available geologic information (Coates and Obando, 1996; Harmon, 2005, this volume) and maps and recent field study (Wörner *et al*., 2005; this volume) suggest that the basin is a patchwork of igneous lithologies (including basalts, gabbros and granites) that have been accreted to the Central American landbridge. The mean annual precipitation for the Lago Alhajuela watershed is 2840 mm per year (Larson and Albertin, 1984). Most precipitation falls from mid-April to mid-December; January through March are the dry months.

The climate of central Panama over the past 14,000 years, inferred from analysis of sediment cores from two lakes ~200 km east of the Río Chagres basin, changed from drier to wetter near the Pleistocene–Holocene climatic transition ~10,000 years ago (Bush *et al.,* 1992). Additional dry periods (~3800 to 3700 yr BP, ~3400 to 2500 yr BP, and ~1900 yr BP to the present)

may have occurred in central Panama during the Holocene as suggested by evidence from two swamps in the Darien province east of the Río Chagres watershed (Bush and Colinvaux, 1994). Although much of central Panama may have experienced limited fluctuations in climate over the past 10,000 years, dated sediment cores from lakes west of the upper Río Chagres basin suggest that sedimentation rates have remained constant except for a slight increase in the sedimentation rate between 7,500 to 5,000 years ago (Bush *et al.,* 1992).

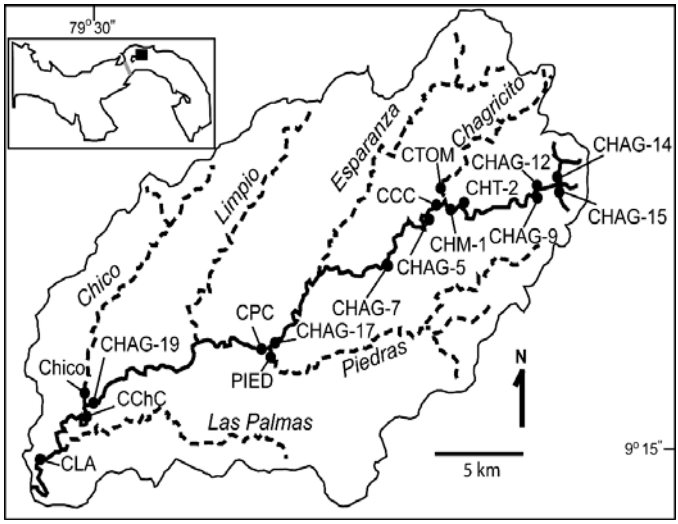

Figure 1. Upper Río Chagres basin. Solid black line represents the course of the upper Río Chagres. Dashed lines represent major tributaries; tributary names are in italics. Sample locations are shown by black dots. Small lines connect sample locations to sample names. Inset box shows Panama with gray line representing the Panama Canal and the black box representing the location of the upper Chagres basin.

At present, Lago Alhajuela ensures continued operation of the canal during the dry season and during years of drought. However, in recent decades there has been concern that the water storage capacity of Lago Alhajuela is decreasing due to the accumulation of sediment in the lake, the source of which is the surrounding watersheds (Wadsworth, 1978, Larsen, 1979; Larsen and Albertin, 1984). Others worry that future decreases in runoff (perhaps driven by human-induced climate change or by land use) might be more important than sedimentation (Condit *et al.,* 2001). In any case, decreased water storage in Lago Alhajuela due to either sedimentation or decreased runoff from the watershed could hinder canal operation.

Figure 2. Aerial photograph of the upper Río Chagres basin. Note complete and dense tropical rain forest cover and signs of significant landsliding.

Figure 3. Aerial photograph in the of the upper Río Chagres basin showing dense vegetation extending all the way to channel margins. The channel bottom in this reach near CHAG-7, like much of the river, is dominated by exposed bedrock.

This paper presents cosmogenic nuclide data, gathered from 17 fluvial sediment samples collected in several of the largest drainage basins of the upper Río Chagres watershed that feed Lago Alhajuela. These nuclide data and interpretative models are used to estimate the long-term, baseline (natural) rates of sediment generation, which, because sediment storage in the basins is minimal, is interpreted as sediment yields and compare directly to suspended sediment data collected for the upper Río Chagres basin since 1981.

2. METHODS

A total of 17 fluvial sediment samples were collected (Fig. 1). and analyzed for cosmogenic ^{10}Be in the 250 μm to 850 μm grain size fraction. Seven samples are used to calculate sediment generation rates in small, steep headwater tributaries (≤ 5 km^2). At the confluence of three major tributaries (the Rió Chagricito, Rió Piedras, and Rió Chico), one sample was collected from the main stem of the upper Río Chagres, one sample from the tributary (to determine the sediment generation rates of large sub-basins), and one sample of the mixed sediment > 200 m downstream of the confluence (to determine the sediment mixing efficiency of the upper Río Chagres). A sample collected on the first sand bar upstream of Lago Alhajuela is used to determine the average sediment yield of the entire upper Río Chagres watershed.

All samples were sieved, etched in one HCl bath, etched in four HF and HNO_3 baths, and the remaining heavy minerals separated by density in order to isolate 30-40 g of pure quartz (Kohl and Nishiizumi, 1992). A beryllium carrier (250 μg) was added and Be was purified using chromatographic techniques. The ^{10}Be/^{9}Be ratios were determined at Lawrence Livermore National Laboratory using accelerator mass spectrometry. All sample ratios were corrected using two procedural blanks that were prepared and measured at the same time as each batch of six samples.

Basin-scale sediment generation rates were calculated using the sea-level, high latitude nuclide production rate estimates (5.2 atoms g^{-1} y^{-1}) from Bierman *et al.* (1996) and the established interpretive model described in Brown et al., (1995), Granger *et al.,* (1996), and Bierman and Steig (1996). Since there is no consensus that Lal's (1991) approach for scaling altitude and latitude is flawed (Desilets *et al.,* 2001; Dunai, 2001; Dunai, 2000), his calculations were used. However, the overall muon contribution to the production rate is only a few percent, is within the production rate error, and is insignificant to the overall conclusions of the paper thus, the calculations

presented here were made for neutrons only. Basin average sediment production rates were calculated using a weighted average production rate based on 120 m bins of basin hypsometry. Equivalent rock lowering rates were calculated using an average density of 2.7 g cm^{-3}.

3. RESULTS

Analyses of ^{10}Be in upper Río Chagres basin sediment quantifies the long-term rates of sediment generation and, by inference, sediment yield within the watershed (Table 1). The nuclide based sediment generation rates are similar for small tributary basins, large tributary basins, and for the entire upper Río Chagres basin.

Table 1. ^{10}Be nuclide data for samples collected from the upper Río Chagres basin.

Sample	Northing	Easting	Basin Area (km^2)	^{10}Be Activity (10^5 atoms/g)	Sediment Generation ($tons/km^2/y^r$)	Inferred Bedrock Erosion Rate (mm/kyr)
CCC	683856	1035085	61	3.00 ± 0.17	254 ± 46	94 ± 17
CChC	664177	1024708	409	2.22 ± 0.15	324 ± 73	120 ± 27
CHAG-5	683828	1034712	<1	2.86 ± 0.15	248 ± 54	92 ± 20
CHAG-7	690811	1035999	1	4.55 ± 0.45	143 ± 32	53 ± 12
CHAG-9	689469	1035341	4	2.55 ± 0.15	270 ± 59	100 ± 22
CHAG-12	689832	1035755	1	3.78 ± 0.22	211 ± 46	78 ± 17
CHAG-14	690786	1035986	5	5.22 ± 0.28	149 ± 32	55 ± 12
CHAG-15	690786	1035986	4	2.95 ± 0.17	262 ± 57	97 ± 21
CHAG-17	674379	1027651	178	3.21 ± 0.21	227 ± 51	84 ± 19
CHAG-19	664043	1024825	367	2.79 ± 0.23	259 ± 59	96 ± 22
Chico	663969	1025076	42	2.41 ± 0.22	273 ± 62	101 ± 23
CHM-1	684345	1034940	38	3.71 ± 0.18	208 ± 54	77 ± 20
CHT-2	684551	1034226	<1	2.10 ± 0.15	354 ± 78	131 ± 29
CLA	661366	1022074	466	2.56 ± 0.16	275 ± 62	102 ± 23
CPC	674158	1027592	274	2.76 ± 0.17	270 ± 59	100 ± 22
CTOM	684284	1035285	24	3.04 ± 0.18	248 ± 78	92 ± 29
PIED	674386	1027396	96	2.72 ± 0.15	281 ± 62	104 ± 23

Northing and Easting are in UTM coordinates and NAD 27 Canal Zone grid. Sediment generation and erosion rates are calculated using sea level, >60° ^{10}Be production rates of 5.2 atoms/g/yr (Bierman *et al*., 1996) scaled using only neutrons (Lal, 1991). ^{10}Be activity error is only analytic. Sediment generation and erosion rate uncertainties are fully propagated and include a 10% (1σ) uncertainty in nuclide production rates as well as uncertainty in rock density, carrier addition, and nuclide attenuation.

Table 2. ^{10}Be nuclide based erosion rates and sediment yields for suite of samples collected near the confluences of three major tributary systems of the upper Río Chagres basin.

Tributary System	Sample	Basin Area (km^2)	Sediment Generation (tons/km^2/yr)	Inferred Bedrock Erosion Rate (mm/kyr)
Rió Chagricito				
Main stem Río Chagres	CHM-1	38	208 ± 54	77 ± 20
Rió Chagricito	CTOM	24	248 ± 78	92 ± 29
Below confluence	CCC	61	254 ± 46	94 ± 17
Rió Piedras				
Main stem Río Chagres	CHAG-17	178	227 ± 51	84 ± 19
Rió Piedras	PIED	96	281 ± 62	104 ± 20
Below confluence	CPC	274	270 ± 59	100 ± 22
Rió Chico				
Main stem Río Chagres	CHAG-19	367	259 ± 59	96 ± 22
Rió Chico	Chico	42	273 ± 62	101 ± 23
Below confluence	CChC	409	324 ± 73	120 ± 27

Table 3. ^{10}Be-based and weighted average sediment yields and bedrock inferred erosion rates of small and large tributaries within the upper Río Chagres basin without upstream samples compared to the ^{10}Be-based sediment yield and erosion rate of sample CLA.

Tributary System	Sample	Basin Area (km^2)	Sediment Generation (tons/ km/yr)	Bedrock Inferred Erosion Rate (m/ kyr)
Headwater	CHAG-5	<1	248 ± 54	92 ± 20
Headwater	CHAG-7	1	143 ± 32	53 ± 12
Headwater	CHAG-9	4	270 ± 59	100 ± 22
Headwater	CHAG-12	1	211 ± 46	78 ± 17
Headwater	CHAG-14	5	149 ± 32	55 ± 12
Headwater	CHAG-15	4	262 ± 57	97 ± 21
Headwater	CHT-2	<1	354 ± 78	131 ± 29
Chagricito	CTOM	24	248 ± 78	92 ± 29
Piedras	PIED	96	281 ± 62	104 ± 23
Chico	Chico	42	273 ± 62	101 ± 23
Area Weighted Average			*269 ± 63*	100 ± 23
Entire Basin	**CLA**	**466**	**275 ± 62**	**102 ± 23**

The ^{10}Be activity of small (≤ 5 km^2) tributary basin samples ranges from 2.10 to 5.22 x 10^5 atoms/g (Table 1). These activities are consistent with sediment generation rates of 354 ± 78 to 149 ± 32 ton/km^2/yr, the equivalent of average basin-wide rock erosion rates of 131 ± 29 to 55 ± 12 mm/kyr.

Each set of three sediment samples collected both upstream and downstream of the confluences of three major tributaries have sediment generation rates (208 ± 54 to 324 ± 87 ton/km^2/yr) and thus, bedrock erosion rates that are within one standard deviation of each other (77 ± 20 to 120 ± 27 mm/kyr; Table 2). The sample collected closest to Lago Alhajuela (CLA) has an intermediate ^{10}Be activity and a basin-wide sediment generation rate that is statistically equal to the weighted average of the tributary basins lacking upstream samples (Table 3).

4. DISCUSSION

Cosmogenic nuclide analyses provide the first estimates of long-term sediment generation and bedrock erosion rates in the Panamanian highlands. Inferred bedrock erosion rates range from 53 to 131 mm/kyr and average about 100 mm/kyr. The ^{10}Be-based estimates are strictly applicable only to quartz-bearing lithologies (Bierman and Steig, 1996). At the local-scale in the upper Río Chagres basin, the distribution of quartz-bearing lithologies is poorly known (Wörner *et al.,* this issue). Recent fieldwork shows that granite is concentrated in the headwaters of the upper Chagres, Chagricitio, Piedras, and Esparanza rivers. The other basins, while quartz poor, still yield enough quartz to measure ^{10}Be. Although our samples estimate sediment generation for the quartz-bearing lithologies, mafic rocks likely erode at different rates over small spatial- and short temporal-scales. However, since there is no significant topographic relief between different lithologies within each basin, we assume that the entire basin is eroding at the ^{10}Be-based rates over the effective time-scale of ^{10}Be production in this rapidly eroding landscape (~10 – 20 kyr).

It is important to consider how different sediment delivery processes affect the results of models used to interpret ^{10}Be activities in terms of sediment generation rates. The two dominant sediment delivery processes in the greater Panama Canal Watershed area (see Fig 1. of Georgakakos and Sperfslage, 2005, this volume) are biologically driven soil creep and shallow landsliding (Stallard, 1999). Biologically driven soil creep effectively mixes sediment to a depth determined by how far down animals burrow and root systems penetrate, perhaps up to 1 m depth in this landscape. Such well-mixed soil profiles are attributed to surface processes (Nichols *et al.,* 2002) and/or bioturbation (Heimsath *et al.,* 2002; Perg *et al.,* 2003; Phillips *et al.,*

1998). Biogenic mixing does not require continuous activity over tens of thousands of years; recent and rapid mixing of soil also homogenizes the nuclide activity at depth. These biologic processes, which are very active in the upper Río Chagres watershed, should result in a well-mixed soil profile (up to 1 m deep) in which nuclide activity does not change.

Landslides in the upper Río Chagres basin are more common in the few areas that have been disturbed by human activity (Stallard, 1999; Larsen and Torres-Sánchez, 1998) such as the Rió Piedras tributary and down stream of the Rió Piedras-upper Río Chagres confluence where there is subsistence farming. Removing vegetation from hillslopes increases the frequency of landsliding. Field observations suggest that most of the landslides are relatively small and shallow (1 to 2 m depth). Such shallow landsliding does not affect the ^{10}Be-based sediment generation rates as indicated by the similar calculated sediment generation rates in the impacted Rió Piedras basin and the other undisturbed basins (Table 1).

The small basins (≤ 5 km^2) appear to generate sediment, and thus erode, at a variety of different rates, a common observation (Matmon *et al*., 2003; Bierman *et al*., 2001b). However, the range of sediment yields (and inferred erosion rates) becomes smaller as basin area increases, reflecting the mixing of sediment in the fluvial system (Fig. 4). The sediment generation rate of basins 5 km^2 or smaller is 234 ± 74 tons/km/yr. The variation in erosion rates for the small basins is most likely due a range of different slopes within the small basins (Matmon *et al.,* 2003) and the spatial and temporal variability in sediment flux from deep (>2 m) landslides. Temporarily high sediment fluxes from deep landslides would cause ^{10}Be measurements to overestimate the sediment yield. In contrast to the range of sediment generation rates in small basins, the larger basins (>20 km^2) have more consistent sediment generation rates. The average sediment generation rate for the large basins is 267 ± 17 tons/km/yr.

The average sediment generation rate of the entire basin is represented by sample CLA just upstream of the upper Río Chagres-Lago Alhajuela confluence (Fig. 1). The average basin-wide sediment generation rates suggested by sample CLA is 275 ± 62 tons/km/yr. This value is similar to the weighted average of all other basins without upstream samples, 269 ± 63 tons/km/yr (Table 3). Such consistency, between sediment yield estimates for small headwater basins and large tributary basins suggests that the Río Chagres mixes sediment well, that there is no significant long-term sediment storage and/or evacuation (*c.f.,* Clapp et al., 2002) within the basin, and that the entire basin is eroding at a similar rate.

The nuclide-based bedrock erosion rates of tropical Panama are comparable to nuclide-based bedrock erosion rates of other high runoff and

rainfall locales. Nuclide-based erosion rates in the granitic Icacos River basin (4000 mm runoff annually) in Puerto Rico is ~43 mm/kyr (Brown *et al.*, 1995). Although the Icacos basin denudation rate is near the low end of the upper Río Chagres basin erosion rates, the Icacos basin is only 3.26 km^2. Some small headwater basins in the upper Río Chagres basin also have similarly low erosion rates (Table 3). Another locale with similar erosion rates is the arkosic sandstone in the Drift Creek basin (180 km^2) in Oregon (USA). Drift Creek receives >2000 mm of rainfall annually and has a ^{10}Be-based erosion rate between 120 and 135 mm/kyr (Bierman *et al.*, 2001a). The long-term erosion rates in Drift Creek are similar to the long-term erosion rates in the upper Río Chagres basin.

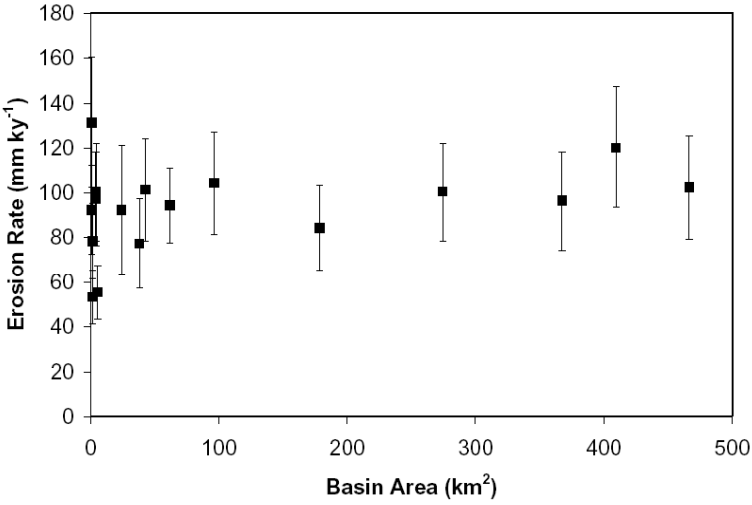

Figure 4. ^{10}Be-based erosion rates for each sub-basin in the upper Río Chagres watershed. Black squares represent model erosion rates. Bars represent uncertainty propagating both analytical error and 10% uncertainty in production rates.

Suspended sediment data have been collected since 1981 at the Chico gage station, which is located about a kilometer downstream of sample site CChC (Fig. 1). The available data (up to 1996) indicate that the average, contemporary sediment yield from the upper Río Chagres watershed is 289 ± 56 tons/km^{-2}/yr (Stallard, 1999); equivalent to an erosion rate of 107 ± 21 mm/kyr. The present-day sediment yield averaged over 16 years is consistent with the sediment yield of sample CLA averaged over millennia by ^{10}Be (275 ± 65 tons/km^{-2}/yr), suggesting that further basin management will not reduce the sediment yield.

4.1 Geologic Implications

The similarity between long and short-term sediment yields is striking. Perhaps, such similarity reflects the stability of climate in the region over at least the past 10,000 years (Bush and Colinvaux, 1994; Bush *et al.,* 1992), the lack of significant anthropogenic disturbance, minimal potential for sediment storage in the basin, and a thick forest cover that stabilizes many slopes. In any case, present-day sediment generation processes in the upper Río Chagres basin are probably representative of long-term sediment generation processes.

Previous research comparing present-day and ^{10}Be-based sediment generation rates demonstrate that sediment generation rates are similar at some sites, while at other sites they differ. In tectonically active areas or in densely populated regions, ^{10}Be-based sediment generation estimates exceed present-day measured sediment yields (Bierman *et al.,* 2001b; Schaller *et al.,* 2001). Such results imply that large, sediment transport events are missed by short-term sediment monitoring. For example, in Idaho, up to 84 years of suspended sediment yield data underestimates ^{10}Be data due to infrequent, and unsampled, large sediment transport events caused by either large storms or wide spread forest fires (Kirchner *et al.,* 2001). Such discrepancies may be less likely in tropical climates, such as Panama, that receive more homogeneous precipitation and less frequent widespread forest fires. Some other studies find that sediment yields exceed ^{10}Be-based sediment generation rates (Clapp *et al.,* 2000, 2001; Brown *et al.,* 1995) suggesting that sediment stored in the basin is being mined. Other studies find that sediment generation rates measured by both methods are similar (Matmon *et al.*, 2003; Granger *et al.,* 1996; Nott and Roberts, 1996), suggesting constant average erosion rates over time.

The ^{10}Be estimate of sediment yield, and thus mountain erosion, are representative over the 10^4 to 10^5-year time scale. Extrapolation to the longer time scales of landscape evolution (*ca.* 10^7 years) in Panama is uncertain. Furthermore, since there were several island chains in the Panama region, one cannot be sure when the rocks of the upper Río Chagres basin were exposed sub-aerially or what the paleotopography was before and soon after the closing of the Central American Landbridge some 3.5 My ago (Coates *et al.,* 1992). If uplift and exposure of Chagres region rocks is assumed at 3.5 Ma, then erosion rates were likely lower when relief was small, increased significantly during mountain uplift and basin formation, and then decreased to the measured long-term rates to maintain the present topography.

4.2 Modeling of Lago Alhajuela Storage Capacity

By using the ^{10}Be-based background sediment yield estimates, assuming a thick forest cover, and no anthropogenic disturbance, natural filling rate of the reservoir feeding the Panama Canal can be estimated. The original working capacity of the reservoir was 612 million cubic meters (Larson and Albertin, 1984). Using ^{10}Be-based average sediment generation rates of the Chagres basin (275 tons/km^{-2}/yr) for the entire 979 km^2 Lago Alhajuela watershed, and a sediment density in the reservoir of 1.6 g/cm^3, it would take on the order of 3,600 years for Lago Alhajuela to fill with sediment. However, two smaller basins to the north of the upper Río Chagres basin, Rió Boquerón (91 km^2) and Rió Pequení (131 km^2), have 16-year sediment yields that are 2-3 times higher than the 16-year Chagres sediment yield (Stallard, 1999). The higher sediment yields from the Rió Boquerón and Rió Pequení basins are most likely due to clearing of the forest cover from <20% the watersheds (Larson and Albertin, 1984). Correcting for the 2- to 3-fold higher current sediment yields of the Rió Pequení and the Rió Boquerón basins by assuming an average 2.5-fold higher sediment yield for the disturbed areas outside of the upper Río Chagres watershed, the reservoir filling time decreases to *ca.* 2,000 years. These estimates are for full sedimentation of the reservoir, not for when the reservoir would cease to provide adequate water for canal operation. The ^{10}Be-based estimates of reservoir filling are far shorter than earlier estimates of full sedimentation of the reservoir that ranged from *ca.* 5,000 years (from data collected in 1900) to 11,200 years (from data collected from 1929 to 1931; Adams, 1947).

To understand the importance of the water storage capacity of Lago Alhajuela, consider the following possible scenario. Presently, it takes an average of 191,000 m^3 of water to transport each ship through the Panama Canal, 40% of which is provided from Lago Alhajuela (Condit *et al.,* 2001; Larson and Albertin, 1984). On average, 37 ships pass through the canal per day (Larson and Albertin, 1984). At these rates, and based on the distribution of runoff throughout the year (Espinosa *et al.,* 1997), there is adequate runoff from the Lago Alhajuela basin to operate the canal at full capacity from May through December. The dry period from January through

Table 4. (overleaf) Water storage in Lago Alhajuela based upon &5% or normal precipitation and 69% of maximum capacity.

Month	Observed runoff (mm/d)	Adjusted runoff (mm/d)	Monthly runoff (m)	Monthly runoff volume (10^7 m^3)	Volume water used for ships (10^7 m^3)	Runoff available after canal use (10^7 m^3)	Water in Lago Alhajuela (10^7 m^3)
Jan	2.41	1.81	0.06	5.49	12.0	-6.56	35.7
Feb	1.05	0.79	0.02	2.16	10.9	-8.72	26.9
Mar	0.67	0.50	0.02	1.53	12.0	-10.50	16.4
Apr	1.65	1.24	0.04	3.63	11.7	-8.03	8.4
May	3.28	2.46	0.08	7.47	12.0	-4.58	3.8
Jun	4.33	3.25	0.10	9.54	11.7	-2.12	1.7
Jul	4.48	3.36	0.10	10.2	12.0	-1.85	*-0.2*
Aug	5.3	3.98	0.12	12.1	12.0	0.01	*-0.2*
Sep	5.38	4.04	0.12	11.9	11.7	0.19	0.0
Oct	6.91	5.18	0.16	15.7	12.0	3.68	3.7
Nov	8.3	6.23	0.19	18.3	11.7	6.62	10.3
Dec	4.93	3.70	0.11	11.2	12.0	-0.83	42.2

Observed runoff from Espinosa *et al.* (1997). Adjusted runoff based on 25% decrease in precipitation similar to 1982 *El Niño* event. Monthly runoff volume is based on Lago Alhajuela watershed area of 979 km^2. Water used by ships is based on 191,000 m^3 per ship, 37 ships per day (Condit *et al.*, 2001), and a sliding percentage of water need from Lago Alhajuela. At current runoff values, Lago Alhajuela supplies 40% of canal water. At 75% of current runoff, Lago Alhajuela would supply 55% of canal water (100%-(60%*75%)).

April, by contrast, does not provide adequate runoff and, therefore, storage of water in Lago Alhajuela is critical to canal operation. At lower precipitation rates and, therefore, runoff rates, the storage capacity of the reservoir becomes of paramount importance.

A likely scenario that includes 75% of normal precipitation (the value of the 1982 *El Niño* event; Condit *et al*., 2001) and a reduction in reservoir volume to 69% of capacity would completely drain the reservoir in July and August (Table 4), stopping ship traffic. Such a situation of reduction in reservoir volume from sediment accumulation could take only 500 to 600 years. These calculations are conservative because Lago Alhajuela is also used for hydroelectric generation and as a water supply. Furthermore, land use could alter the runoff by decreasing dry period runoff (Condit *et al*., 2001; Stallard, 1999) and thus, increase the importance of maximum storage capacity.

Recent data from the 1983 Madden Lake (previous name of Lago Alhajuela) Hydrographic Survey calculated that the reservoir capacity already was reduced by 5% over a period of ~50 years, more than three fold faster than the ^{10}Be-based estimates (Alvardo, 1985). At such sedimentation rates, the reduction to 69% capacity could take only an additional 250 years. From these estimates, it is evident that further reduction in reservoir capacity, from sedimentation combined with either successive dry years or from a change in climate to less precipitation (Espinosa *et al.,* 1997), would have significant effects on the canal operation and on the economy of Panama and possibly the world. Such filling of the reservoir, however, could be countered by expensive dredging to regain storage capacity. Thus, it is apparent that proper watershed management in the Lago Alhajuela basin is necessary to maintain sufficient water storage capacity.

This analysis does not predict when shipping would first be affected. In fact, during the *El Niño* year of 1997 - 1998, ships transiting the Panama Canal had to carry less cargo in order to transit the canal during low water (Espinosa, 2003). The analysis presented here is meant to highlight the importance of understanding background sediment yield rates to better predict the effective lifetime of reservoirs.

5. CONCLUSIONS

This paper provides the first ^{10}Be-based sediment generation rates for tropical Panama based upon the analysis of 17 sediment samples from the upper Río Chagres basin. This watershed is generating sediment at an average rate of 275 tons/ km/yr, the equivalent of rock erosion at *ca.* 100 mm/kyr. The ^{10}Be-based sediment yields are consistent with suspended

sediment data collected since 1981. Due to little land disturbance and no significant climate change, the upper Río Chagres basin is eroding uniformly suggesting that the basin is steadily losing mass over the 10 to 20 kyr time frame. Adjacent basins, heavily impacted by agriculture, have significantly higher contemporary sediment yields and are thus, no longer exhibiting steady landscape behavior.

The water storage capacity of Lago Alhajuela is important to the operation of the Panama Canal. Lowered average annual precipitation combined with a modest additional loss of storage capacity could significantly affect the number of ships that can be conveyed through the canal. It is apparent that more intensive land use within the Lago Alhajuela watershed (and the accompanying increase in sediment yield) could have adverse effects on storage capacity and thus, on the economy of Panama and possibly the world.

ACKNOWLEDGEMENTS

Travel and analyses for research was funded by DEPSCoR grant #DAAD199910143 and by STIR grant DAAD 19-02-1-0436. The data were collected during the 2001 Río Chagres Expedition funded by the U.S. Army Tropical Research Center, the Yuma Proving Ground and the U.S. Army Research Office. R. Harmon, R. Stallard, E. Wohl, and S. Howe helped in sample collection. B. Copans purified the quartz. An anonymous reviewer provided helpful comments on an earlier version of the manuscript. A special thank you to S. Howe who spent countless pre-excursion hours arranging the logistics to make sure all went smoothly.

REFERENCES

Adams, HW, 1947, *Data on Sediment Transportation and Deposition in the Canal Zone:* Dept. Operation. Maint., and Spec. Eng. Div., Panama Canal Commission, Balboa Heights, Panama.

Alvardo, L.A. 1985. *Sedimentation in Madden Reservoir*: Meteorol. Hydrog. Branch, Eng. Div., and Eng. Const. Bureau, Panama Canal Commission, Balboa Heights, Panama.

Bierman, P, Clapp, E, Nichols, K, Gillespie, A, and Caffee, M, 2001a, Using cosmogenic nuclide measurements in sediments to understand background rates of erosion and sediment transport: in *Landscape Erosion and evolution Modeling,* (RS Harmon and WW. Doe, eds.), Kluwer Acad./Plenum Pub., New York, NY: 89-116.

Bierman, P, Pavich, M, Gellis, A, Larsen, J, Cassell, E, and Caffee, M, 2001b, Erosion of the Rio Puerco basin, New Mexico – First cosmogenic analysis of sediments from the drainage network of a large watershed: (abs) Geol. Soc. Am. Abs. Prog., 33: A-314.

Bierman, PR, Larsen, P, Clapp, E, and Clark, DH, 1996, Refining estimates of ^{10}Be and ^{26}Al production rates: Radiocarbon, 38: 149

Bierman, PR, and Steig, E, 1996, Estimating rates of denudation and sediment transport using cosmogenic isotope abundances in sediment: Earth Surf. Proc. Landf., 21: 125-139.

Brown, E, Stallard, RF, Larsen, MC, Raisbeck, GM, and Yiou, R, 1995, Denudation rates determined from the accumulation of in situ-produced ^{10}Be in the Luquillo Experimental Forest, Puerto Rico: Earth Planet. Sci. Lett., 129: 193-202.

Bush, MB and Colinvaux, PA, 1994, Tropical forest disturbance: Paleoecological records from Darien, Panama: Ecology, 75: 1761-1768.

Bush, MB, Poperno, DR, Colinvaux, PA, DeOliveira, PE, Krissek, LA, Miller, MC, and Rowe, WE, 1992, A 14,300-yr paleoecological profile of a lowland tropical lake in Panama: Ecol. Monogr., 62: 251-275.

Clapp, EM, Bierman, PR, Nichols, KK, Pavich, M, and Caffee, M, 2001, Rates of sediment supply to arroyos from upland erosion determined using in situ produced cosmogenic ^{10}Be and ^{26}Al: Quat. Res., 55: 235-245.

Clapp, EM, Bierman, PR, Schick, AP, Lekach, J, Enzel, Y, and Caffee, M, 2000, Sediment yield exceeds sediment production in arid region drainage basins: Geology, 28: 995-998.

Clapp, EM, Bierman, PR, Caffee, MW, 2002, Using ^{10}Be and ^{26}Al to determine sediment generation rates and identify sediment source areas in an arid region drainage basin: Geomorph., 45: 89-104.

Coates, AJ, Jackson, JBC, Collins, LS, Cronin, TM, Dowsett, HJ, Bybell, LM, Jung, P, and Obando, JA, 1992, Closure of the Isthmus of Panama: The near-shore marine record of Costa Rica and western Panama: Geol. Soc. Amer. Bull., 104: 814–828.

Condit, R, Robinson, WD, Ibáñez, R, Aguilar, S, Sanjur A, Martínez, R, Stallard, RF, García, T, Angehr, G, Petit, L, Wright, SJ, Robinson, TR, and Heckadon, S, 2001, The status of the Panama Canal watershed and its biodiversity at the beginning of the 21st century: BioScience, 51: 389-398.

Desilets, D, Zreda, M, and Lifton, NA, 2001, Comment on 'Scaling factors for production rates of in situ produced cosmogenic nuclides: a critical reevaluation' by TJ Dunai: Earth Planet. Sci. Lett., 188: 283-287.

Dunai, TJ, 2000, Scaling factors for production rates of in situ produced cosmogenic nuclides: a critical reevaluation: Earth Planet. Sci. Lett., 176: 157-169.

Dunai, TJ, 2001, Reply to comment on 'Scaling factors for production rates of in situ produced cosmogenic nuclides: a critical reevaluation: Earth Planet. Sci. Lett., 188: 289-298.

Espinosa, JA, 2003, The Climatology of Panama: in *International Scientific Symposium, The Rio Chagres: A Multidisciplinary Profile of a Tropical Watershed*: Gamboa, Panama.

Espinosa, D, Méndez, A, Madrid, I, and Rivera, R, 1997, Assessment of climate change impacts on the water resources of Panama: the case of the La Villa, Chiriquí, and Chagres river basins: Climate Change, 9: 131-137.

Georgakakos, KP and Sperfslage, JA, 2005, this volume, operational rainfall and flow Forecasting for the Panama Canal Watershed: in *The Río Chagres: A Multidisciplinary Perspective of a Tropical River Basin* (RS Harmon, ed.), Kluwer Acad./Plenum Pub., New York, NY: 323-333.

Granger, DE, Kirchner, JW, and Finkel, R, 1996. Spatially averaged long-term erosion rates measured from in-situ produced cosmogenic nuclides in alluvial sediment: Jour. Geol., 104: 249-257.

Harmon, R.S. this volume. The Geologic Development of Panama: in *The Río Chagres: A Multidisciplinary Perspective of a Tropical River Basin* (RS Harmon, ed.), Kluwer Acad./Plenum Pub., New York, NY: 45-62.

Heimsath, AM, Chappell, J, Spooner, NA, and Questiaux, DG, 2002, Creeping soil: Geology, 30: 111–114.

Kirchner, JW, Finkel, RC, Riebe, CS, Granger, DE, Clayton, JL, King, JG, and Megahan, WF, 2001. Mountain erosion over 10 yr, 10 ky, and 10 my time scales: Geology, 29: 591-594

Kohl, CP, and Nishiizumi, K, 1992, Chemical isolation of quartz for measurement of *in-situ*-produced cosmogenic nuclides: Geochim, Cosmochim. Acta, 56: 3583-3587.

Lal, D, 1991, Cosmic ray labeling of erosion surfaces: In-situ production rates and erosion models: Earth Planet. Sci. Lett., 104: 424-439.

Larsen, MC, and Torres-Sánchez, AJ, 1998, The Frequency and distribution of recent landslide in three montane tropical regions of Puerto Rico: Geomorph., 24: 309-331.

Larson, C, 1979, Erosion and sediment yield as affected by land use and slope in the Panama Canal watershed: Proc. III World Cong.Water. Resour., Int. Water Resour. Assoc., Mexico City, Mexico, Part III, 1086-1095.

Larson, CL and Albertin, W, 1984, Controlling erosion and sedimentation in the Panama Canal watershed: Water Intern., 9: 161-164.

Matmon, A, Bierman, PR, Larsen, J, Southworth, S, Pavich, M, and Caffee, M, 2003, Temporally and spatially uniform rates of erosion in the southern Appalachian Great Smoky Mountains: Geology, 31: 155–158.

Nichols, KK, Bierman, PR, Hooke, RL, Clapp, EM, and Caffee, M, 2002, Quantifying sediment transport on desert piedmonts using ^{10}Be and ^{26}Al: Geomorph., 45: 105-126.

Nott, J, and Roberts, R, 1996, Time and process rates over the past 100 my; A case for dramatically increased landscape denudation rates during the late Quaternary in northern Australia: Geology, 24: 883-888.

Perg, LA, Anderson, RS, and Finkel, RC, 2001, Use of a new ^{10}Be and ^{26}Al inventory method to date marine terraces, Santa Cruz, California, USA: Geology, 29: 879-882.

Phillips, WM, McDonald, EV, Reneau, SL, Poths, J, 1998, Dating soils and alluvium with cosmogenic ^{21}Ne depth profiles; case studies from the Pajarito Plateau, New Mexico, USA: Earth Planet. Sci. Lett., 160: 209-223.

Schaller, M, von Blanckenburg, F, Hovius, N, and Kubik, PW, 2001, Large-scale erosion rates from in situ-produced cosmogenic nuclides in European river sediments: Earth Planet. Sci. Lett., 188: 441-458.

Stallard, RF, ed., 1999. Erosion and the effects of deforestation the Panama Canal basin: in *Report of the Panama Canal Watershed Monitoring Project* (Panama Canal Watershed Monitor. Proj.: Chap. II.8.

Wadsworth, FH, 1978, Deforestation: death to the Panama Canal: in Proc. US Strat. Conf. on Tropical Deforestation, US Dept. State and US Agency. Inter. Devel., Washington DC: 22-24.

Wörner, G, Harmon, RS, Hartmann, G, and Simon, K, 2005, Igneous geology and geochemistry of the upper Río Chagres basin: in *The Río Chagres: A Multidisciplinary Perspective of a Tropical River Basin* (RS Harmon, ed.), Kluwer Acad./Plenum Pub., New York, NY: 65-82.

Chapter 21

ESTIMATION OF REGIONAL ACTUAL EVAPOTRANSPIRATION IN THE PANAMA CANAL WATERSHED

Jan M.H. Hendrickx[1], Wim G.M. Bastiaanssen[2], Edwin J.M. Noordman[2], Sung-Ho Hong[1], and Lucas E. Calvo-Gobbetti[3]
[1]New Mexico Tech, [2]WaterWatch, [3]Universidad Tecnológica de Panama

Abstract: The upper Río Chagres basin is a part of the Panama Canal Watershed. The least known water balance component of this watershed is evapotranspiration. Measurements of actual evapotranspiration rates on the ground are difficult and expensive. The objective of this study is to demonstrate a new inexpensive method for determination of regional evapotranspiration in the watershed. The method uses LANDSAT satellite images that are analyzed using the Surface Energy Balance Algorithms for Land (*SEBAL*). We use an image from March 27, 2000, for estimation of the distribution of the regional actual evapotranspiration in the Panama Canal Watershed and surrounding areas.

Key words: Panama Canal Watershed; evapotranspiration; *SEBAL* ; remote sensing

1. INTRODUCTION

The upper Río Chagres basin is a part of the greater Panama Canal Watershed (see Georgakakos and Sperfslage, 2005, this volume, Fig. 1). The least known water balance component of this watershed is evapotranspiration. Measurements of actual evapotranspiration rates on the ground are difficult, expensive,and therefore not usually included in operational water budget analyses. The objective of this study is to demonstrate a new and inexpensive method for determination of regional actual evapotranspiration across a watershed. The method uses LANDSAT satellite images that are analyzed using the Surface Energy Balance Algorithms for Land (*SEBAL*). As an example of the *SEBAL* potential, a LANDSAT image for Panama from 27 March 2000 is used to estimate the

R. S. Harmon (ed.), The Río Chagres, Panama, 315-323.

distribution of the regional actual evapotranspiration (ET) in the Panama Canal Watershed and surrounding areas.

2. SURFACE ENERGY BALANCE ALGORITHM FOR LAND (*SEBAL*)

2.1 Remote Sensing for Evapotranspiration

Remote sensing methods use surface reflectances and the radiometric surface temperature from satellite spectral measurements to estimate ET from local to regional scales. First, surface parameters such as albedo, surface temperature, and vegetation indices are derived for each image pixel. Next, these surface parameters, together with field data, are used to solve the energy balance and ET is taken as the residual term. Following partly Kustas and Norman (1996), four different groups of remote sensing methods are recognized: (i) statistical methods, (ii) numerical simulation models, (iii) land use maps combined with traditional ET equations, and (iv) physically-based analytical approaches. The statistical methods relate the difference between satellite observed surface temperature and air temperature to ET (*e.g.,* Jackson *et al.,* 1977; Nieuwenhuis *et al.,* 1985; Seguin and Itier, 1983). These approaches require few input data, but often assume all meteorological variables but surface temperature spatially constant. This limits their application to homogeneous regions. Numerical models solve the equations of the energy and mass flow processes in the soil-vegetation-atmosphere system (*e.g.,* Camillo *et al.,* 1983; Carlson *et al.,* 1994; Sellers *et al.*, 1992) and require many input variables describing soil and vegetation properties. Since such detailed data sets are rarely available on regional scales, these models are less suitable for many satellite remote sensing hydrology studies. Current methods to compute ET over the irrigated and riparian areas of river valleys and rangelands in the western United States use remote sensing and GIS tools to create land use maps. This information, together with standard meteorological measurements, becomes input into traditional ET equations. These procedures are often cumbersome, slow, and expensive to implement and can have large uncertainty.

Physically based analytical methods evaluate the components of the energy balance and generally determine the ET rate as the residual:

$$R_n + G + H = \lambda E \tag{1}$$

where R_n is the net incoming radiation flux density (W/m^2), G is the ground heat flux density (W/m^2), H is the sensible heat flux density (W/m^2), and λE is the latent heat flux density (W/m^2), which is the ET rate. The parameter λ in Equation (1) is the latent heat of vaporization of water (J/kg) and E is the vapor flux density (kg/m^2/s). In many remote sensing evaporation algorithms evaporation E includes not only bare soil evaporation but also canopy transpiration. This notation is followed in this paper.

The main challenge in the energy balance is to determine the partitioning of the available energy ($R_n - G$) into λE and H. The net radiation R_n is estimated from the remotely sensed surface albedo, surface temperature, and solar radiation calculated from standard astronomical formulae (Iqbal, 1983). The ground heat flux G is determined through semi-empirical relationships with R_n, surface albedo, surface temperature, and vegetation index. The most critical factor in the physically based remote sensing algorithms is to solve the equation for the sensible heat:

$$H = \rho_a c_p \frac{T_{aero} - T_a}{r_{ah}} \tag{2}$$

where ρ_a is the density of air (kg/m^3), c_p is the specific heat of air (J/kg/K), r_{ah} is the aerodynamic resistance to heat transfer (s/m), T_{aero} is the surface aerodynamic temperature, and T_a is the air temperature either measured at a standard screen height or the potential temperature in the mixed layer (Brutsaert *et al.,* 1993). The aerodynamic resistance to heat transfer is affected by windspeed, atmospheric stability, and surface roughness (Brutsaert, 1982). The simplicity of Equation (2) is quite deceptive since T_{aero} cannot be measured by remote sensing. Remote sensing techniques measure the radiometric surface temperature T_{rad},which is not the same as the aerodynamic temperature. The two temperatures usually differ by 1 to 5°C. Unfortunately, a small uncertainty of 1°C in $T_{aero} - T_a$ can result in a 50 W/m^2 uncertainty in H (Campbell and Norman, 1998). Although many investigators have tried to solve this problem by adjusting r_{ah} or using an additional resistance term, no generally applicable method has been developed yet (Kustas and Norman, 1996). Therefore, Campbell and Norman (1998) conclude that a practical method for using satellite surface temperature measurements should have at least three qualities: (i) accommodate the difference between aerodynamic temperature and radiometric temperature, (ii) not require a measurement of near-surface air temperature, and (iii) rely more on differences of surface temperature over

time or space rather than absolute surface temperatures to minimize the influence of atmospheric corrections and uncertainties in surface emissivity.

2.2 The Surface Energy Balance Algorithm for Land (*SEBAL*) Method

SEBAL is a practical method that meets the three requirements formulated by Campbell and Norman (1998). It overcomes the problem of inferring the aerodynamic temperature from the radiometric temperature and the need for near-surface air temperature measurements by directly estimating the temperature difference between a T_1 and a T_2 taken at two arbitrary levels z_1 and z_2 without explicitly solving the absolute temperature at a given height. The temperature difference for a dry surface without evaporation is obtained from the inversion of the sensible heat transfer equation with latent heat flux λE=0 so that H=R_n-G (Bastiaanssen *et al.,* 1998a):

$$T_1 - T_2 = \Delta T_a = \frac{H\, r_{ah}}{\rho_a\, c_p}. \tag{3}$$

For a wet surface all available energy R_n-G is used for evaporation λE so that H=0 and ΔT_a=0. Field observations have indicated that land surfaces with a high ΔT_a are associated with high radiometric temperatures and those with a low ΔT_a with low radiometric temperatures. For example, in New Mexico and Idaho, moist irrigated fields have a much lower ΔT_a than dry rangelands. Field measurements in Egypt and Niger (Bastiaanssen *et al.,* 1998b), China (Wang *et al.,* 1998), USA (Franks and Beven, 1997), and Kenya (Farah, 2001) have shown that the relationship between T_{rad} and ΔT_a is linear, such that:

$$\Delta T_a = c_1\, T_{rad} - c_2 \tag{4}$$

where c_1 and $_2$ are the linear regression coefficients valid for one particular moment (the time and date the image is taken) and landscape. By using the minimum and maximum values of ΔT_a as calculated for the coldest and warmest pixel(s), the extremes of H are used to find the regression coefficients c_1 and c_2 which will prevent outliers of H-fluxes. Thus, the empirical Equation (4) meets the third quality stated by Campbell and Norman (1998) that one should rely on differences of the radiometric surface temperature over space rather than absolute surface temperatures, to minimize the influence of atmospheric corrections and uncertainties in surface emissivity.

Equation (3) has two unknowns: ΔT_a and the aerodynamic resistance to heat transfer r_{ah}, which is affected by wind speed, atmospheric stability, and surface roughness (Brutsaert, 1982). Several algorithms take a few field measurements of wind speed and consider these as spatially constant over representative parts of the landscape (*e.g.,* Hall *et al.,* 1992; Kalman and Jupp, 1990; Rosema, 1990). This assumption is only valid for uniform homogeneous surfaces. For heterogeneous landscapes a wind speed near the ground surface is required for each pixel. One way to overcome this problem is to consider the wind speed spatially constant at a height of 200 m above ground level. This is a reasonable assumption since at this height the wind speed is not affected by local surface heterogeneities. The wind speed at this height is obtained by an upward extrapolation of one wind speed measurement at 2 or 10 m to 200 m using a logarithmic wind profile. The wind speed at each pixel is obtained by a downward extrapolation using the surface roughness, which is determined for each pixel using an empirical relationship between surface momentum roughness z_{0m} and the Normalized Difference Vegetation Index (NDVI) or the Soil Adjusted Vegetation Index - SAVI (Huette, 1988). The end result of all these calculations is the determination of a r_{ah} and ΔT_a for each pixel which allows us to find the sensible heat flux for each pixel. After inserting R_n, G, and H into Equation (1) the latent heat flux λE or ET rate is derived for each pixel.

Is *SEBAL* 'old technology'? *SEBAL* has the three qualities that Campbell and Norman (1998) deem necessary for a practical method that uses satellite surface temperature measurements for determination of consumptive water use. At first sight *SEBAL* is quite similar to other ET methods that use T_{rad} and ΔT but with one significant difference. *SEBAL* uses an internal auto-calibration process that eliminates the need for actual measurements of T_{rad} and/or ΔT as well as for atmospheric corrections. *SEBAL* is automatically calibrated for biases through the regression calibration of Equation (4), which is based on a cold and warm pixel. Thus, the surface temperature T_{rad} is used as a distribution parameter for partition of the sensible and latent heat flux. ΔT_a floats above the land surface as it is indexed to T_{rad}, through calibration Equation (4), but it does not require actual measurements on the ground or atmospheric corrections.

2.3 Daily Actual Evapotranspiration

SEBAL yields an estimate of the instantaneous ET (mm/hour) at the time of the LandSat overpass around 11:00 am. This hourly ET rate needs to be extrapolated to the daily ET. The extrapolation is done using the evaporative fraction (*i.e.,* the ratio of latent heat over the sum of latent and sensible heat)

that has been shown to be approximately constant during the day. Therefore, multiplication of the evaporative fraction determined from *SEBAL* with the total daily available energy yields the daily evapotranspiration rate.

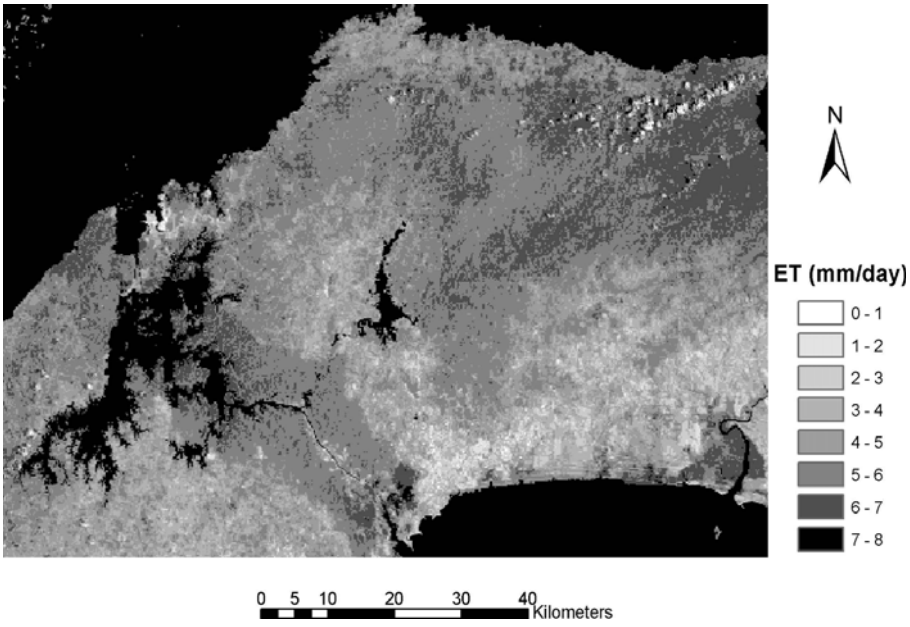

Figure 1. Daily actual evapotranspiration rates on 27 March 2000, in the Panama Canal Watershed and surrounding areas derived from *SEBAL* .

2.4 *SEBAL* Applications

SEBAL has only recently been validated (Bastiaanssen *et al.,* 1998a,b, 2002; Bastiaanssen, 2000) and appears rather insensitive for errors in parameters such as NDVI and atmospheric disturbances (Hendrickx *et al.,* 2002). *SEBAL* has matched latent heat flux measurements on the ground very well in Spain, Italy, Turkey, Pakistan, India, Sri Lanka, Egypt, Niger, and China (Bastiaanssen *et al.,* 1998a,b; Bastiaanssen and Bos, 1999; Bastiaanssen, 1995, 2000), Idaho (Allen *et al.,* 2001), and more recently New Mexico (Hendrickx,, web site: www.sahra.arizona.edu/research/TA2) and yields robust estimates of consumptive water use in large irrigated areas. Previous applications in the humid tropics of Sri Lanka and Kenya (Farah, 2001) confirm its potential for the Panama Canal Watershed.

3. THE APPLICATION OF *SEBAL* IN THE PANAMA CANAL WATERSHED

SEBAL has been applied to a LANDSAT image of 27 March 2000, which covers the entire Panama Canal Watershed, for determination of the regional actual evapotranspiration in the central Panama. The watershed includes lakes, tropical forests, agricultural lands, and bare soils. The evaporation rates vary from as high as 7 mm/day in the lakes to as low as 1 mm/day in urban areas. There is a striking difference between the undisturbed natural forest areas along the Canal and inside the upper Río Chagres watershed, with evaporation rates around 6 to 4 mm/day, and those of cleared lands used for agriculture, which exhibit rates around 4 to 2 mm/day. The deep-rooted trees have still access to sufficient root zone soil moisture to maintain a relatively high transpiration rate while the shallow rooted agricultural crops are suffering from water shortage at the end of the dry season.

The actual evapotranspiration rates derived from *SEBAL* seem quite reasonable. However, more study is needed to verify the energy components determined from remote sensing imagery using *SEBAL* with those measured on the ground with eddy covariance systems and scintillometers. After validation in the field, *SEBAL* holds promise to estimate evapotranspiration rates in the Panama Canal Watershed for a fraction of the costs needed for the installation of a watershed wide network of eddy covariance systems.

ACKNOWLEDGEMENTS

We appreciate the support for this research received from the Army Research Office, US Yuma Proving Ground Tropic Regions Test Center, New Mexico Tech, and the Universidad Tecnológica de Panama.

REFERENCES

Allen, RG, Bastiaanssen, WBM, Tasumi, M, and Morse, A., 2001, Evapotranspiration on the watershed scale using the *SEBAL* model and LandSat Images: Paper #01-2224, ASAE, Ann. Int. Meeting, Sacramento, CA.

Bastiaanssen, WGM, 1995, Regionalization of surface flux densities and moisture indicators in composite terrain: Ph.D. Thesis, Wageningen Agricultural Univ. (also appeared as Report 109, DLO Winand Staring Centre), Wageningen, The Netherlands: 273p.

Bastiaanssen, WGM, Menenti, M, Feddes, RA, and Holtslag, AAM, 1998a, A remote sensing surface energy balance algorithm for land (*SEBAL*), Part 1, Formulation: Jour. Hydrol., 212-213:198–212.

Bastiaanssen, WGM, Pelgrum, H, Wang, J, Ma, Y, Moreno, JF. Roerink, GJ, Roebeling, RA, and van der Wal, T., 1998b, A remote sensing surface energy balance algorithm for land (*SEBAL*), Part 2, Validation: Jour. Hydrol., 212–213:213–229.

Bastiaanssen, WGM and Bos, MG, 1999, Irrigation performance indicators based on remotely sensed data: a review of literature: Irrigat. Drain. Sys., 13:291-311.

Bastiaanssen, WGM, Ahmad, MD, and Chemin, Y, 2002, Satellite surveillance of evaporative depletion across the Indus Basin: Water Resour. Res., 38: 1273-1281.

Bastiaanssen, WGM, 2000, *SEBAL* -based sensible and latent heat fluxes in the irrigated Gediz Basin, Turkey: Jour. Hydrol., 229: 87-100.

Brutsaert, W, 1982, *Evaporation into the Atmosphere:* Reidel Pub., Dordrecht, The Netherlands.

Brutsaert, W, Hsu, AY, and Schmugge, TJ, 1993,. Parameterization of surface heat fluxes above a forest with satellite thermal sensing and boundary layer soundings: Jour. Appl. Meteorol., 32: 909–917.

Camillo, PJ, Gurney, RJ, and Schmugge, TJ, 1983m, A soil and atmospheric boundary layer model for evapotranspiration and soil moisture studies: Water Resour. Res., 19: 371–380.

Campbell, GS and Norman, JM, 1998, *An Introduction to Environmental Biophysics:* Springer-Verlag, New York, NY.

Carlson, TN, Gillies, RR, and Perry, EM, 1994, A method to make use of thermal infrared temperature and NDVI measurements to infer soil water content and fractional vegetation cover: Remote Sens. Rev. 52: 45–59.

Farah, HO, 2001, Estimation of Regional Evaporation Under Different Weather Conditions from Satellite and Meteorological Data. A Case Study in the Naivasha Basin, Kenya: Doctoral Thesis Wageningen Univ.

Franks, SW and Beven, KJ, 1997, Estimation of evapotranspiration at the landscape scale: a fuzzy disaggregation approach: Water Resour. Res., 33: 2929–2938.

Georgakakos, KP and Sperfslage, JA, 2005, Operational Rainfall and Flow Forecasting for the Panama Canal Watershed: in *The Río Chagres: A Multidisciplinary Perspective of a Tropical River Basin* (RS Harmon, ed.), Kluwer Acad./Plenum Pub., New York, NY: 323-333.

Hall, FG, Huemmrich, KF, Goetz, SJ, Sellers, PJ, and Nickeson, JE. 1992, Satellite remote sensing of the surface energy balance: success, failures and unresolved issues in FIFE: Jour. Geophys. Res., 97: 19,061–19,090.

Hendrickx, JMH, Hong, S-H, Miller, T, Small, E, Neville, P, Cleverly, J, and Bastiaanssen, WGM, 2002, Actual ET rates derived by *SEBAL* in the Middle Rio Grande Valley: (abs) Am. Geophys. Union Annual Meeting, San Francisco.

Huette, AR, 1988, Soil-adjusted vegetation index (SAVI): Remote Sens. Env.. 25: 89-105.

Iqbal, M, 1983, *An Introduction to Solar Radiation:* Academic Press, Toronto, Canada.

Jackson, RD, Reginato, RJ, and Idso, SB, 1977, Wheat canopy temperature: a practical tool for evaluating water requirements: Water Resour. Res., 13: 651-656.

Kalman, JD and Jupp, DLB, 1990, Estimating evaporation from pasture using infrared thermography: evaluation of a one-layer resistance model: Agr. Forest Meteorol., 51: 223–246.

Kustas, WP and Norman, JM, 1996, Use of remote sensing for evapotranspiration monitoring over land surfaces: Hydrol. Sci. Jour., 41: 495–515.

Nieuwenhuis, GJ., Schmidt, EA, and Thunnissen, HAM, 1985, Estimation of regional evapotranspiration of arable crops from thermal infrared images: Int. Jour. Remote Sens., 6: 1319–1334.

Rosema, A, 1990, Comparison of meteosat-based rainfall and evapotranspiration mapping of Sahel region: Remote Sens. Env., 46: 27–44.

Seguin, B and Itier, B, 1983, Using midday surface temperature to estimate daily evaporation from satellite thermal IR data: Int. Jour. Remote Sens., 4: 371–383.

Sellers, PJ. Heiser, MD, and Hall, FG, 1992, Relationship between surface conductance and spectral vegetation indices at intermediate ($100m^2$–$15km^2$) length scales: Jour. Geophys. Res. 97: 19033–19059.

Wang, J, Bastiaanssen, WGM, Ma, Y, and Pelgrum, H, 1998, Aggregation of land surface parameters in the oasis-desert systems of Northwest China: Hydrol. Proc., 12: 2133–2147.

Chapter 22

OPERATIONAL RAINFALL AND FLOW FORECASTING FOR THE PANAMA CANAL WATERSHED

Konstantine P. Georgakakos and Jason A. Sperfslage
Hydrologic Research Center

Abstract: An integrated hydrometeorological system was designed for the utilization of data from various sensors in the 3300 km^2 Panama Canal Watershed for the purpose of producing real-time, spatially distributed, mean areal rainfall estimates, and rainfall and flow forecasts. These forecasts are used by the Panama Canal Authority for water management. The system ingests raw data from a 10 cm weather radar, automated rain gauges and surface meteorological stations, streamflow gauges, radiosonde upper air profilers, and analysis and forecast fields from the operational 80 km Eta numerical weather prediction model of the US National Weather Service State estimators utilize all available data for cloud, soil and channel model state updating and rainfall and flow forecast variance generation. Merged radar and rain gage fields are produced in real time and are used to compute mean areal precipitation for each sub-catchment in the watershed. Results of real time operation for the years 2000 and 2001 show useful system forecasts during severe storm periods.

Key words: Panama; Panama Canal; hydrometeorological modeling; weather radar; rainfall-runoff; flow forecasting

1. INTRODUCTION

In 1998, as part of a science cooperation and technology transfer effort, the Hydrologic Research Center (HRC) and collaborators designed and implemented at the Panama Canal Authority (Autoridad del Canal de Panama, ACP) a prototype system for the real-time rainfall estimation and forecasting over a number of small sub-catchments of the 3,300-km^2 mountainous Panama Canal Watershed (PCW) in Panama (Fig. 1). The system (called *PANMAP*) uses as input *Eta* model forecasts (on an 80 km

R. S. Harmon (ed.), The Río Chagres, Panama, 325-335.

grid) and observations from surface hydrometeorological stations, upper air radiosondes, and a 10 cm weather radar, to produce mean areal precipitation estimates and forecasts within the PCW on scales of 90-735 km^2 with a maximum 12-hr lead time and with hourly resolution. The system design combines embedded cloud models and state estimators for data assimilation and uncertainty estimation (Georgakakos *et al.,* 1999).

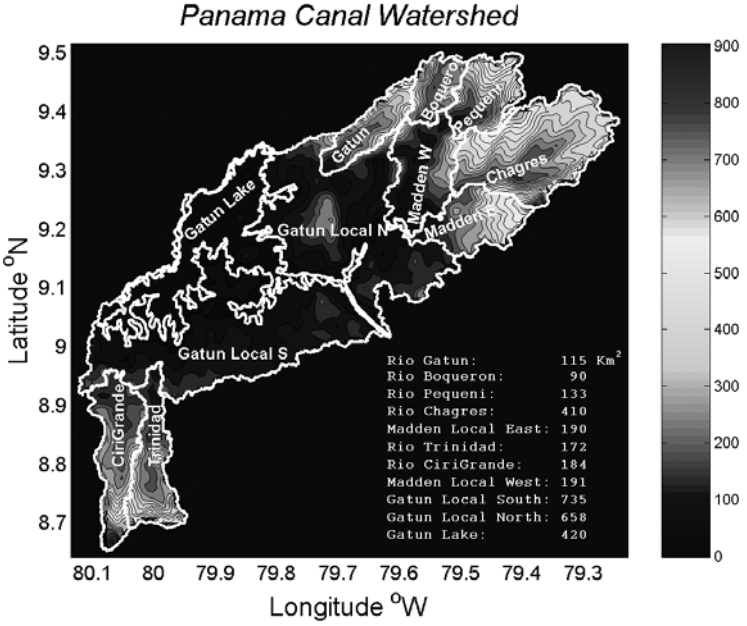

Figure 1. The Panama Canal Watershed showing terrain elevation (1 km DTM) and sub-catchments.

The rainfall forecasts and associated forecast variance are input to operational hydrologic models, implemented for each PCW sub-catchment within the framework of the *US National Weather Service River Forecast System* (*NWS-RFS*). The hydrologic model (*SS-SAC*; Sperfslage and Georgakakos, 1996) combines an adaptation of the Sacramento soil moisture accounting model with a robust state estimator for real-time updating from flow observations and forecast variance generation. In addition to the forecasts produced, the system also produces real-time estimates of mean areal rainfall for each of the sub-catchments of the PCW on the basis of merging radar and rain gauge data with an adaptive procedure for real-time radar-rainfall bias reduction. The ACP has been using the system operationally since October 1998. This paper outlines design features of the

system and presents results from an evaluation of system performance using the operational data for the wet part of the years 2000 and 2001.

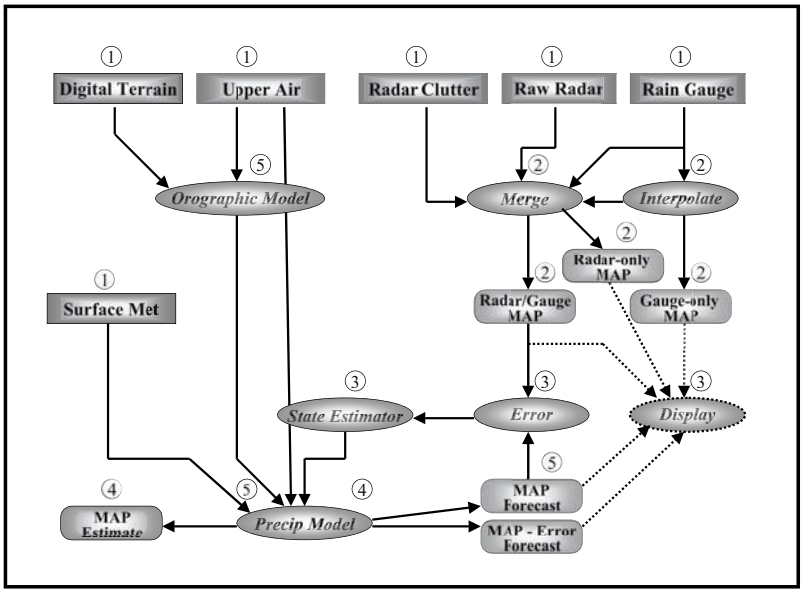

Figure 2. PANMAP system components and links.

2. INTEGRATED SYSTEM DESIGN

PANMAP is a prototype operational mean areal rainfall estimation and forecast system with a full uncertainty package. The main system components and links are shown schematically in Figure 2. The mean areal rainfall estimation component, designed and implemented in collaboration with University of Iowa researchers (see Georgakakos *et al.,* 1999), quality controls the radar reflectivity data, accounting for ground clutter and anomalous propagation, develops real time estimates of the radar-rainfall bias adjustment factor, merges hourly estimates of rainfall from radar low-elevation scans (mapped onto a 4x4 km^2 grid) with estimates from automated ALERT-type (event driven response) rain gauges, and computes mean areal precipitation over each sub-catchment. An adaptive Kalman Filter is used to estimate the values of the bias adjustment factor using intervals of 50 'wet' hours. The variance of the error in the merged estimates of mean areal precipitation for each sub-catchment is produced in real time.

Prior to the merging of radar and rain gauge data, spatial interpolation of the rain gauge data onto the 4x4 Km^2 analysis grid is done using kriging.

The precipitation forecast component is based on *(a)* potential theory air-flow models (*e.g.,* Tateya *et al.,* 1991) for determining the areas of significant updrafts generated by the three-dimensional interaction of the mountainous topography with the approaching 850 mbar wind, and *(b)* stochastic-dynamical cloud microphysical models (*e.g.,* Lee and Georgakakos 1996). The model developed is forced by operational *Eta* forecasts of upper-air boundary conditions on scales of 80 km on the side, and it is used effectively to generate and distribute rainfall in space and time on the basis of *Eta* operational forecasts. It is coupled to a state estimator to allow real-time updates of cloud- and rain-water from hourly mean areal precipitation observations (merged product of radar and rain gauge data) and to produce estimates of rainfall forecast variance in real time. Surface meteorological data are used to determine rapidly changing surface moisture conditions between *Eta* forecasts and twice-daily radiosonde launches are used to facilitate the production of important short-term rainfall forecasts of 1- to 6-hr duration. The components included in the parsimonious model formulation are:

(a) orographic updraft enhancement,

(b) convective updraft development,

(c) advection of storm cloud- and rain-water, and

(d) state estimation (error variance propagation and state updating from observed mean areal rainfall).

As implemented, *PANMAP* integrates 15-min raw polar data from the 10-cm weather radar located on the Engineers Hill in Panama City, hourly data from approximately 40 automated ALERT rain gages located throughout the Panama Canal Watershed, hourly data from 5 ALERT surface meteorological stations, data from radiosondes for upper air information launched daily or twice daily in Panama, and the operational mesoscale meteorological *Eta* model predictions produced at the US-NWS. Provision was made for varying real-time data availability. The system also integrates information from 1 km digital terrain elevation data for surface wind and rainfall analysis. The products of *PANMAP* are:

(a) detailed information on the current state of the atmosphere over each of the Panama sub-catchments, and

(b) current radar and rain gauge hourly rainfall maps, and forecast advisories for hourly rainfall amounts with a maximum forecast lead time of 12 hours.

Meteorologists and hydrologists of the ACP Meteorology and Hydrology Section use these products for operational diagnosis and prediction of severe

events and day-to-day weather. A user's guide for *PANMAP* is given in Sperfslage *et al.* (1999). *PANMAP* rainfall forecasts and associated variance are fed into the streamflow prediction model, which generates flow forecasts and variances in real time for the outlet of each of the PCW sub-catchments. The streamflow model used is an adaptation of the US-NWS Sacramento soil moisture accounting model complemented with a kinematic routing model and running as part of the *NWS-RFS*. The state-space form of the model is used (called *SS-SAC*) as developed by Georgakakos *et al.* (1988), tested by Georgakakos and Smith (1990) in an official World Meteorological Organization (WMO) model intercomparison project, and implemented for national real-time operational use as part of the *NWS-RFS* by Sperfslage and Georgakakos (1996). The development of the final form of the model and tests with historical data from the PCW is documented in Georgakakos *et al.* (1999).

The integrated hydrometeorological system was tested with limited available historical data prior to operational use and during model development (during the period 1997-1998), and initial model parameter adjustments were made at that time. Since 1998, the system is run operationally without any parameter adjustments. The next section presents early results of the first evaluation of operational system performance performed since the time of system implementation.

3. FORECAST PERFORMANCE EVALUATION

Analysis of the *PANMAP* sub-catchment rainfall forecasts for the July-December 2000 and August-December 2001 periods was performed using criteria that are appropriate for the use of the rainfall forecasts for hydrologic forecasting. The error in forecasting the volume of rainfall of various durations was used as a bulk statistic for validation, but individual sub-catchment forecasts, with lead times from 1 to 12 hrs, were also evaluated during periods with significant observed storm rainfall. The analysis also examined the utility of a variety of input data such as the *Eta* forecasts of surface and upper-air fields (temperature, pressure, humidity, winds), the upper air radiosonde observations and the surface ALERT data. The validation effort was performed in close collaboration with the staff of the Meteorology and Hydrology Section of the ACP.

Figure 3 exemplifies dependence of the residual means on the observations means for three-hourly mean rainfall volume forecasts. Only periods with hourly rainfall observations greater than 6.35 mm/h (0.25 in/h) in at least one sub-catchment of the PCW were considered. Light symbols

correspond to the July-September period and dark symbols correspond to the October-December period. The 50% bounds are also shown for the average residual means. The thick black line at the 0% residual mean value is the line of no bias. It is evident that the operational *PANMAP* forecasts tend to overestimate the light (<3 mm/h) amounts of three-hourly rainfall in all months of record and for all sub-catchments of the PCW. It is also evident that *PANMAP* reproduces most of the higher observed rainfall amounts with a bias less than ±50% and largely independent of season within the wetter half of the year.

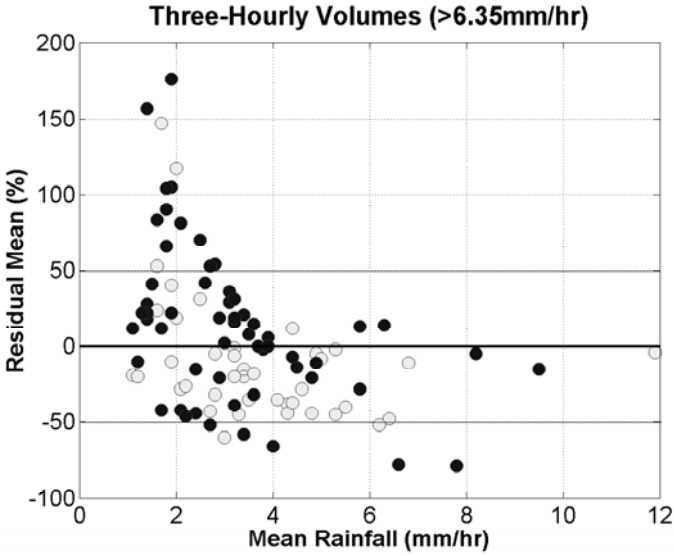

Figure 3. Forecast residual mean as a percent of the observed mean versus the observed mean for three-hourly average volumes of mean areal rainfall over sub-catchments in the Panama Canal Watershed.

The bias of the *PANMAP* 3-hourly mean forecasts for individual sub-catchments of the PCW is indicated in Figure 4. The results shown are for the mountainous northeastern sub-catchments. These sub-catchments typically receive higher mean areal rainfall than the rest of the sub-catchments (maximum observed 3-hourly mean areal rainfall of about 11.5 mm/hr for these sub-catchments compared to a maximum of about 4.5 mm/hr for other sub-catchments). For 3-hourly forecasts, about 70% of the forecast cases are within ±50% of the observed values with more than 95% of the cases being within the ±100% bounds. There are more cases with negative bias than cases with positive bias found for the period of record with significant rainfall (>3 mm/h). This is likely the result of Eta underestimation of the lower-level water-vapor influx into the basin. There

are no significant sub-catchment bias trends across the Panama Canal Watershed.

PANMAP uses a variety of input sources to produce rainfall forecasts. To understand the utility of each data type (*e.g., Eta* model forecasts of wind, temperature, humidity; and upper-air radiosonde and automated surface meteorological observations) for rainfall volume forecasts, a number of sensitivity studies were conducted. The *PANMAP* system was re-run for the test period using a variety of input data configurations. Due to space limitations, detailed results are not shown but the next section contains our significant conclusions from these studies. In this section, we present an example of rainfall and flow hourly forecast performance of the integrated system for an individual significant storm event that occurred in late December 2000 over the PCW, and which caused flash floods in several sub-catchments.

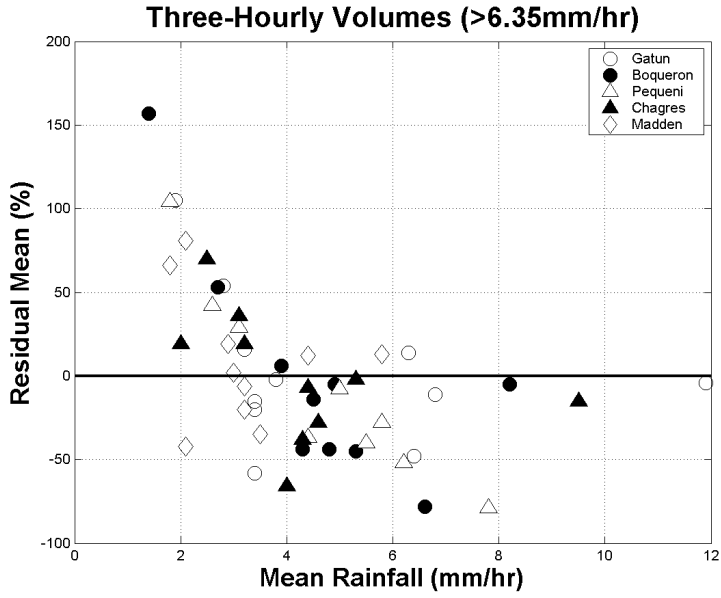

Figure 4. As in *Figure 3* but with results shown for individual northeastern sub-catchments for the wetter half of the years 2000 and 2001.

Figure 5 shows the hourly mean areal rainfall forecasts (dashed) and associated observations (solid) produced by *PANMAP* for each of four northeastern mountainous sub-catchments of the PCW for the period 28-31

December 2000. The results indicate that the short-term hourly-rainfall forecasts possess predictive skill for these sub-catchments with some time shifts present and with overestimation of lower rainfall rates in some instances.

The result of using *PANMAP* mean areal rainfall forecasts as input to the *SS-SAC* hydrologic forecast model for individual sub-catchments is exemplified in Figure 6 for the 154 km^2 Río Pequeni sub-catchment in the northeastern mountainous portion of the PCW (see Fig. 1).

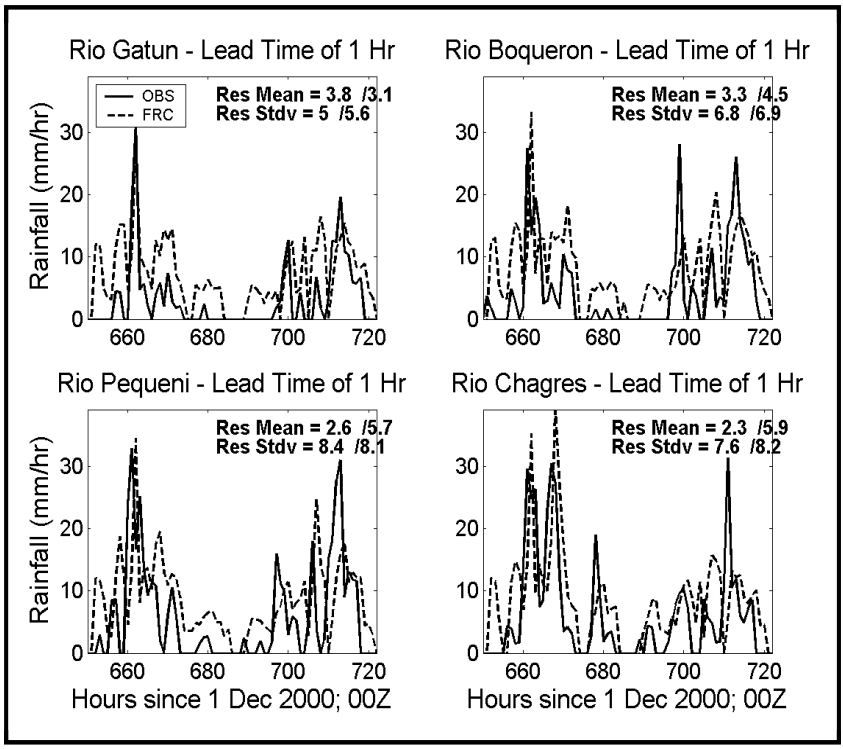

Figure 5. Hourly mean areal rainfall forecasts (dashed) and observations (solid) for the significant storm event of 28-31 December 2000 and for the northeastern mountainous sub-catchments of the PCW. The ratios of residual to observation means and residual to observation standard deviations are shown in each case for the storm period.

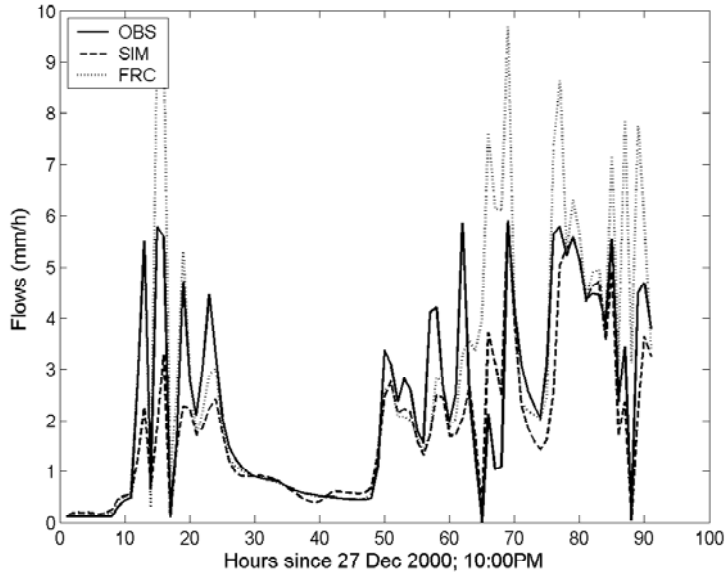

Figure 6. Hourly forecasts (dotted), simulations (dashed) and observations (solid) in mm/h of Río Pequeni flow for the period of 28–31 December 2000. Forecasts are for *PANMAP* forecast input and simulations are for observed rainfall input.

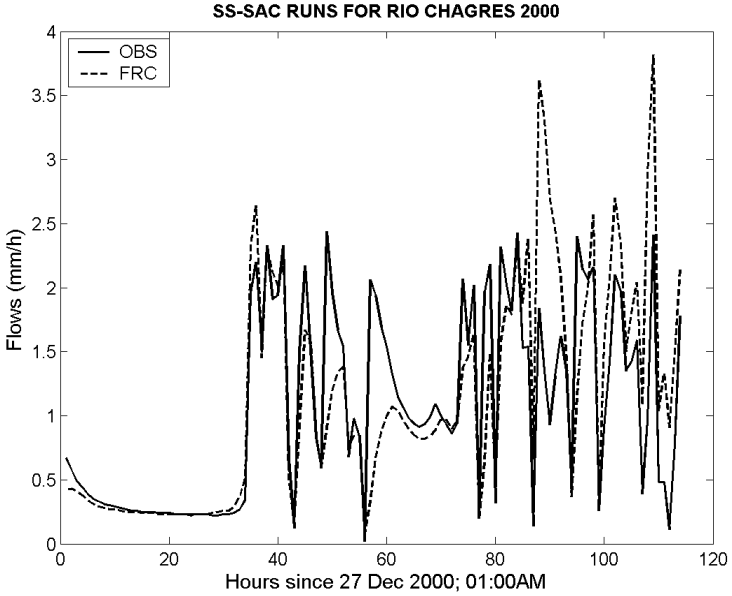

Figure 7. Hourly forecasts (dashed) and observations (solid) in mm/h of Río Chagres flow for the period 28–31 December 2000. *PANMAP* forecast input is used.

For intercomparison, the hydrologic model hourly flow forecast is also shown in Figure 7 when 'observed' mean areal rainfall is used as input. The results in both panels indicate underestimation of the early phases of the flash flood flow with more accurate predictions during the second wave of the event and with overestimation near the end of the storm period. This is likely due to erroneous hydrologic model initial conditions and/or the result of model parameter error. *PANMAP* 'forecast' forcing resulted in underestimation of the flood flows early in the second event compared to 'observed' rainfall forcing, with essentially accurate reproduction of the remainder of the flows. Figure 7 shows analogous 'forecast' results for Río Chagres, with the hourly flows reasonably well reproduced for the entire period.

4. CONCLUDING REMARKS

The primary conclusion from the performance evaluation effort is that the coupled system produced useful forecasts during times of heavy rainfall. The results of the evaluation effort obtained so far indicate that the *PANMAP* forecasts have lowest bias when radiosonde (RAOB) data are used to produce input to the rainfall prediction component for forecast lead-times out to 3 hr, and when new *Eta* forecasts are used to produce input to the rainfall prediction component for forecast lead-times from 6 to 12 hr. The use of surface ALERT data exclusively during storm periods yields reasonable hourly nowcasts, but results in significant underestimation of rainfall volume for longer lead-times. Overestimation of low rainfall amounts is persistent throughout the validation period, with *PANMAP* performing best for the heavier rainfall amounts. Forecast performance is best for the northeastern mountainous catchments of Río Gatun, Río Boqueron, Río Pequeni and Río Chagres and for the Lake Gatun area in the central region of the Panama Canal Watershed. Using the *PANMAP* mean and variance rainfall forecasts as input to the *SS-SAC* hydrologic model produced skilful short-term flow forecasts for several sub-catchments of the PCW.

ACKNOWLEDGEMENTS

The authors acknowledge the contributions of W. Krajewski and A. Kruger of the University of Iowa in the development of radar data quality control procedures, D. Tsintikidis and T. Carpenter of HRC in the development of optimal spatial interpolation estimates of rain gage rainfall,

C. Barrett and R. Jubach of the NOAA International Technology Transfer Office in coordinating the development work, and M. Cane of RTI in implementing the NWSRFS and calibrating the hydrologic model. Also, the many and varied contributions of the Staff of the Meteorology and Hydrology Section of the Autoridad del Canal de Panama, ACP (C. Vargas, M. Chandeck, J. Espinoza, M. Hart, M. Echevers and M. Vilar) are gratefully acknowledged. The comments of an anonymous reviewer helped improve the readability of the paper. The development work was sponsored by a NOAA grant. The performance evaluation work was sponsored by the ACP. The opinions expressed in this paper are those of the authors and do not necessarily reflect those of the sponsoring agencies.

REFERENCES

Georgakakos, KP, Rajaram, H, and Li, SG, 1988, On Improved Operational Hydrologic Forecasting of Streamflows: Iowa Inst. Hydraul. Res., Univ. Iowa, IIHR Report 325.

Georgakakos, KP and Smith, GF, 1990, On improved operational hydrologic forecasting - Results from a WMO real-time forecasting experiment: Jour. Hydrol., 114: 17-45.

Georgakakos, KP, Sperfslage, JA, Tsintikidis, D, Carpenter, TM (with Appendix by Krajewski, WK and Kruger, A), 1999, Design and Tests of an Integrated Hydro-meteorological Forecast System for the Operational Estimation and Forecasting of Rainfall and Streamflow in the Mountainous Panama Canal Watershed: Hydrol. Res. Center, HRC Tech. Rept. 2.

Lee, TH and Georgakakos, KP, 1996, Operational rainfall prediction on meso-γ scales for hydrologic applications: Water Resour. Res., 32: 987-1003.

Sperfslage, JA, and Georgakakos, KP, 1996, Implementation and Testing of the HFS Operation as Part of the National Weather Service River Forecast System (NWSRFS): Hydrol. Res. Center, HRC Tech. Rept. 1.

Sperfslage, JA, Georgakakos, KP, Tsintikidis, D, Kruger, A, and Krajewski, WF, 1999, PANMAP v.1.0.1. A User's Guide: Hydrol. Res. Center, HRC Limited Dist. Rept. 10.

Tateya, K, Nakatsugawa, M, and Yamada, T, 1991, Observations and Simulation of Rainfall in Mountainous Areas: in *Hydrological Applications of Weather Radar* (ID Cluckie and CG Collier, eds.), Ellis Horwood, New York, NY: 279-295.

Chapter 23

PROJECTED LAND-USE CHANGE FOR THE EASTERN PANAMA CANAL WATERSHED AND ITS POTENTIAL IMPACT

Virginia H. Dale[1], Sandra Brown[2], Magnolia O. Calderón[3], Arizmendis S. Montoya[3], and Raúl E. Martínez[3]

[1]Oak Ridge National Laboratory, [2]Winrock International, [3]Panama Canal Authority

Abstract: Human occupation of the Panama Canal Watershed has affected its land cover for the past century. A rule-based model was developed and applied to estimate changes in land use and subsequent carbon emissions over the next twenty years in the Eastern Panama Canal Watershed (EPCW). Projections show that the highest percent change in land use for the 'new-road' scenario compared to the 'business-as-usual' scenario is for urban areas, and the greatest cause of carbon emission is from deforestation. Thus, the most effective way to reduce carbon emissions to the atmosphere in the EPCW is by reducing deforestation. In addition to affecting carbon emissions, reducing deforestation would also protect the soil and water resources of the EPCW, which has important implications for the long-term sustainable operation of the Panama Canal.

Key words: Panama; carbon baselines; carbon benefits; land-cover change; regional analyses; spatial projections; tropical deforestation;

1. INTRODUCTION

Completion of the Panama Canal in 1914 led to recognition of the importance of the Panama Canal Watershed that supplies the millions of gallons of water required for each ship to pass through the Canal, as well as providing potable water to the major urban centers of Panama City and Colón. Today, the watershed is home to some 30% of the people living in Panama. The watershed supports suburban life as well as agriculture, ranching, and forestry (Heckadon-Moreno, 2005, this volume). In addition,

R. S. Harmon (ed.), The Río Chagres, Panama, 337-345.

the Panama Canal Watershed is widely acclaimed for its ecological importance (Condit *et al.,* 2001; Perez *et al.,* 2005, this volume).

At the end of 1999, the United States turned over operation of the Panama Canal to Panama. The Autoridad del Canal de Panama (ACP) (formerly Panama Canal Commission - PCC) is now responsible for permitting land-use changes in the watershed that affect water resources. Portions of the watershed are undergoing rapid changes in land use. There is concern about the compatibility of urban and economic development with hydrological needs and concomitant requirements for conservation of the watershed (Condit *et al.,* 2001). Human activities such as those in the Eastern Panama Canal Watershed (EPCW) can affect future ecological resources, and thus the carbon storage potential. The analysis presented here is designed to project land-cover change through 2020 under 'business-as-usual' and 'new-road development' scenarios. This analysis provides a projected baseline to identify where opportunities exist for implementing potential projects to generate potential carbon benefits.

The storage of carbon has become a newly-recognized value of forests as concern increases over rising levels of atmospheric concentrations of carbon dioxide (Bloomfield *et al.,* 2000; Gitay *et al.,* 2001). To participate in the potential market for carbon credits based on changes in the use and management of the land, a country needs to identify opportunities and implement land-use based emissions reductions or sequestration projects. A key requirement of land-based carbon projects as articulated in the Kyoto Protocol (Article 12, also known as the 'Clean Development Mechanism') is that any activity developed for generating carbon benefits must be additional to business-as-usual baseline. A projection of the business-as-usual scenario of land-use change along with the resulting changes in carbon stocks on the land can be used to demonstrate this baseline requirement (*e.g.,* Brown *et al.,* 2000).

2. BACKGROUND

2.1 The Environment of the EPCW

The Eastern Panama Canal Watershed (EPCW), the focus of this analysis, contains 339,638 ha of largely forested land. This eastern portion of the basin is the historic watershed, but the legal watershed was defined more expansively in 1999. Forests currently cover 158,000 hectares (54%) of the EPCW. Most of the remaining area is pasture, agriculture, or scrubland. Some of the forest has been lost to establish urban areas. In the rural communities, forest land is being converted into agriculture land using fires

to prepare a site for planting. However, because of the poor soil quality, some of these agricultural areas are reconverted to pasture land. Between the 1980's and 1998, satellite imagery shows that 1.7% to 3% of forests per year changed to pasture, agriculture, or scrubby vegetation, and 0.2% per year changed to urban areas (PCWMP, 1999).

There is great concern about the status of the forests in the watershed. LANDSAT Thematic Mapper images have been used to document that forests decreased by 43% between 1974 and 1991, from 275,549 ha to 157,063 ha. Tarté (1999) reports the rate of deforestation in 1999 as 573 ha/yr. Thus, the rate of annual clearing has declined from the 24-year average of 4,937 ha/yr. In 2002, 34% of the 375,000 ha of the EPCW was under some kind of protection, such as being maintained as a national park. Furthermore, the regional land-use plan provided by Panamanian Law 21 in 1997 mandates expansion of the protected area to 40% of the EPCW. Of the forest remaining in the EPCW in 2002, almost 69% were in protected areas, most of which had been established since 1980, when political decisions were made to preserve parts of the watershed by setting them aside in national parks and other protected areas. Most of the protected forests in national parks are primary, while those adjacent to the Panama Canal are secondary.

Commercial timber plantations began to be established in abundance in the watershed in 1998. As early as 1993, a series of Forestry-Incentive Laws were enacted, leading to cultivation of timber-yielding tree species. Tax deductions are allowed during the first five years of forest investments for plantations. The Interoceanic Region Authority (Autoridad de la Región Interoceánica, ARI) donates land-use rights to the private sector for reforestation of degraded lands to reduce erosion and sedimentation. However, in the absence of requirements to monitor these reforestation projects, management of some plantations will likely be abandoned. Anecdotal evidence suggests that some mature secondary forests were cut and replanted as plantations to receive tax deductions under the Forestry Incentives Law.

Historic sediment data suggests that deforestation in the EPCW is likely a source of excess sediment (PCWMP, 1999). However, the increasing protection and recovery of the forests is related to a gradual but constant decrease in soil erosion and rates of sedimentation in the rivers and lakes. Nevertheless, the quality of water is deteriorating (PCWMP, 1999). This decline is largely associated with the 1947 opening of the Trans-Isthmian Highway between the cities of Panama and Colón (Heckadon-Moreno, 2005, this volume). Much agricultural, industrial, and urban development occurs along the highway.

Vegetation regrowth is increasing on cattle farms. This reversion likely results from conservation and reforestation policies of the National Bank of Panama, as required by Panamanian Law 21. The regional land-use plan provided by Law 21 establishes a goal of reduction of cattle farms in the EPCW from 127,000 to 7,000 hectares by the year 2025. This plan will cause a dramatic transformation of land-use in the EPCW. Already tax incentives seem to have curtailed the expansion of cattle pastures that had occurred since the 1950's. Furthermore, the plan discourages population growth in the EPCW, although current policies of the Ministry of Housing do allow construction in two communities (Chilibre and Las Cumbres) within the EPCW.

2.2 Changes in the Human Population

Between 1950 and 1990, the population in the EPCW increased five-fold, from *c.* 22,000 to *c.* 113,000 that undoubtedly contributed to the need for more transportation routes (Tarté, 1999; PCWMP, 1999). By 1998, the estimated population was 142,000 (PCWMP, 1999). In recent decades, the annual population growth rate in the EPCW ranged from a high value of 4.5% for the period 1960 to 1970 to a low of 3.7% for 1970-80 (Prieto *et al.,* 1999). The rate of increase for 1980 to 1990 for the EPCW was 3.8%, compared to a 2.6% population increase for all of Panama (Prieto *et al.,* 1999). Geometric projections from 1990 using a 3.8% rate of growth indicate that population in the EPCW will increase to c. 407,000 people in 2020 with 24% of the growth in Colón and 76% of the growth in the province of Panama (Prieto *et al.,* 1999). There is a growing human population within the protected areas. For example, 2,712 people lived within the borders of Chagres National Park in 1990, with continued population pressure from outside the park likely to induce greater population growth within the park (Prieto *et al.,* 1999). The new Law 21 and Law 19 give the ACP the responsibility to regulate anything that might impact the hydrological resources of the watershed; however, no mechanisms exist for population control.

3. METHODOLOGY

A rule-based model has been developed to project land-cover dynamics in the EPCW that assumes current land-cover trends will continue into the future. The rules are described in detail in Dale *et al.* (2003) and include enforcement of environmental protection in the parks or other protected areas over the next 20 years. The projections map patterns of deforestation

and reforestation based on current land-cover patterns, distance from permanent roads and population centers, population growth, and past land-use trends. Some factors that can exert pressure on the environment are not part of the current model (*e.g.,* economic and technology changes). The new-road scenario includes the establishment of the new bridge across the Panama Canal and completion of the Trans-Isthmian highway between Panama City and Colón. This analysis focused on projecting the effects that land use may have upon land-cover change and carbon storage in the EPCW.

4. RESULTS AND DISCUSSION

4.1 Land-Cover Change Projections

The projections result in major land-cover changes within the EPCW over the next 20 years for the urban areas, plantations, and the lands in pasture, agriculture, or scrub. The forest area gradually declines. Most of the land-cover change occurs where the majority of the roads and communities are located (Heckadon-Moreno, 4004, this volume). Most (80%) of the land that becomes urban derives from the pasture/agriculture/scrub category. At the same time, there is a consistent loss of native forest land that ultimately ends up as plantations.

Under the 'new-road' scenario, the greatest land-cover changes occur near the new highway (see Fig. 1B of Chapter 1), but there are relatively few differences in this case as compared to the 'business-as-usual' case. The greatest difference in land-cover changes for the two projections is the increase in urban lands and decline in plantations and pasture/agriculture/scrub for the new-road scenario (Fig. 1).

These projections of land-cover changes can contribute to an understanding of a variety of environmental issues. The model could provide a basis for estimating carbon stocks (Dale *et al.,* 2003) and for analyzing how different management practices of the land influence changes in carbon stocks. The analysis of different management practices requires spatially-explicit information on the distribution of ownership and better understanding of how different types of agricultural owners clear and farm the land, information that is now being collected. The model could also be used to analyze how management of the protected areas would influence land-cover change and carbon stocks. The effectiveness of various conservation measures and approaches could also be evaluated.

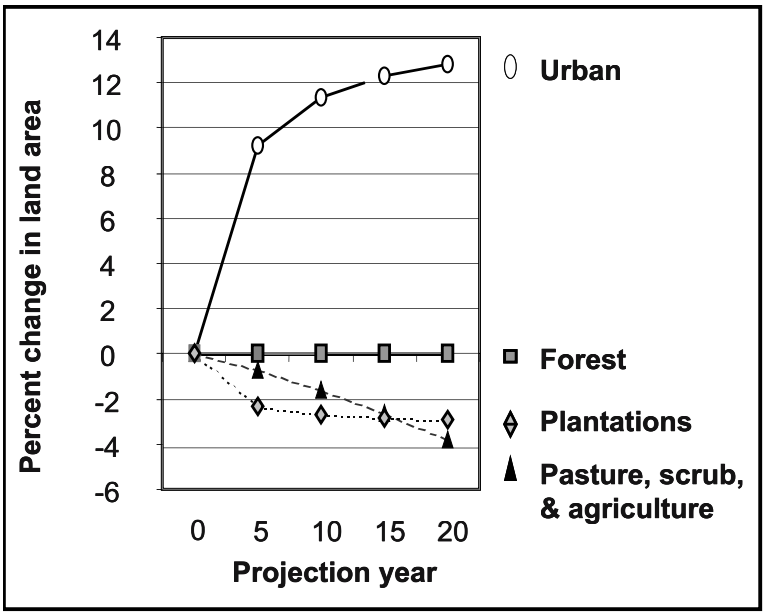

Figure 1. Change in percent land cover for the business-as usual scenario compared to the new-road scenario for the major land cover categories in the EPCW.

4.2 Changes in Carbon Stocks

The projected areas of each land-cover type for the two scenarios were combined with the carbon density data as described in Dale *et al.* (2003) to project the change in carbon stocks—decreases in carbon stocks are counted as emissions and increases in carbon stocks as removals (carbon sequestered). For the 'business-as-usual' scenario, carbon emissions from deforestation gradually decline over the 20-year period, from about 160,000 tons/yr during the first five years to about 130,000 tons/yr during the last five years (Fig. 2). Carbon emissions from deforestation could be lower if secondary forests were preferentially cleared over mature forests because the secondary forests have lower carbon stocks. Clearly, better identification of secondary forests and their land cover and carbon dynamics would decrease the uncertainty of the carbon emissions presented here.

The expansion and growth of plantations removes about 24,000 tons C/yr initially to 205,000 tons C/yr at the end of the 20-yr period (Fig. 2). The carbon balance for the EPCW represents a net source of carbon to the atmosphere, as the emissions from deforestation and conversion to agriculture/pasture/scrub lands exceed the removals by the growing and

expanding plantations. The business-as-usual scenario results in net carbon emissions of 606,000 tons C over the whole 20-yr period.

The 'new-road' scenario and the various assumptions for carbon densities resulted in higher net emissions of carbon (676,000 tons C over the 20-yr period) than the 'business-as-usual' scenarios. The emissions from deforestation for the new-road scenarios were only slightly higher than those for the business-as-usual scenarios; most of the increase in net emissions was caused by a reduction in the area converted to plantations.

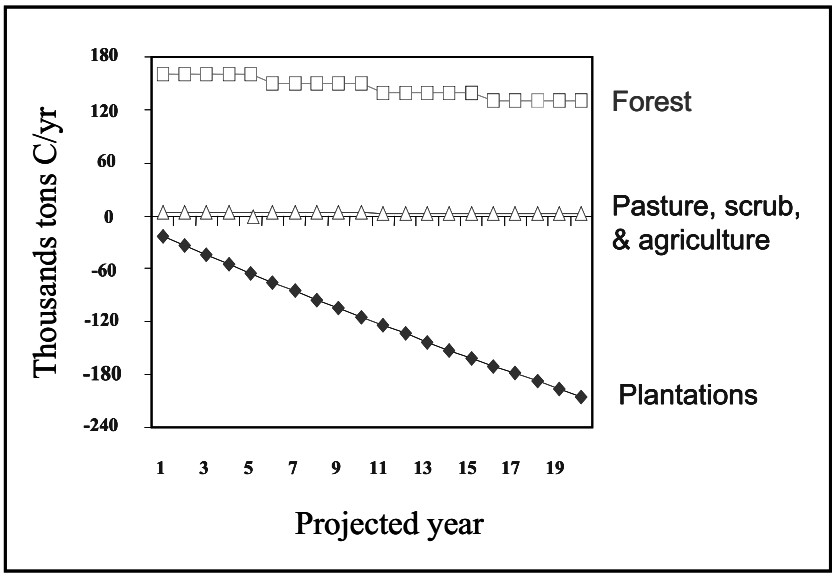

Figure 2. Changes in C emissions over time for three land-cover categories under the 'business-as-usual' scenario for the EPCW.

5. CONCLUSIONS

The small changes on forested land result in the largest source of carbon emissions in the EPCW. Thus, the most effective way to reduce carbon emissions is by reducing deforestation. The effect of forest removal is large because about half of the biomass in trees is carbon. Loss of mature forests contributes more to carbon emissions to the atmosphere than does the loss of secondary forest because mature forests typically contain many large trees and more carbon than trees that are smaller in size and that dominate secondary forests (Brown and Lugo, 1992; Brown *et al.,* 1997). However,

under the current framework of the Clean Development Mechanism (CDM), only carbon benefits arising from reforestation are allowed.

Even after 20 years, carbon gained by reforestation in the EPCW is insufficient to offset the carbon emissions from the ongoing small rate of deforestation. The up-to-20 years of growth and carbon accumulation in the plantations scenario is inadequate to offset the high carbon stocks of established forests that were removed. However, planting larger areas to plantations than occurs in the 'business-as-usual' scenario would cause more carbon to be stored.

ACKNOWLEDGEMENTS

We appreciate the assistance of H. Cardwell, N. de Varela, R. Spadafora, and A. Sanjur. The support of the Autoridad del Canal de Panama was critical. Useful discussions occurred with S. Heckadon-Moreno of the Smithsonian Tropical Research Institute, S. Van der Ende and A. Eke of Futuro Forestal, and A. Sanjur. Data were provided by the Autoridad Nacional de Ambiente de Panama (ANAM), STRI, and the Autoridad del Canal de Panama (ACP). Editorial assistance of F. O'Hara and J. Smith is appreciated. The project was funded by a contract from U.S. Agency for International Development (USAID) with Oak Ridge National Laboratory (ORNL). ORNL is managed by UT-Battelle, LLC, for the U.S. Department of Energy under contract DE-AC05-00OR22725. Support for Sandra Brown was provided by Panama's Institutional Support for Sustainable Environmental Management of the Panama Canal Watershed under USAID's Environmental Policy and Institutional Strengthening Indefinite Quantity Contract (EPIQ) managed by International Resources Group, Ltd. This report does not represent the views of the PCA, the National Environmental Authority (ANAM), or the U.S. Agency for International Development (USAID).

REFERENCES

Bloomfield, J, Ratchford, M and Brown, S (eds.), 2000, Special edition on land-use change and forestry and the Kyoto Protocol: Mitigation and Adaptation Strategies for Climate Change, 5: 1-121.

Brown, S and Lugo, AE, 1992, Aboveground biomass estimates for tropical moist forests of the Brazilian Amazon: Interciencia, 17: 8-18.

Brown, S, Schroeder, P and Birdsey, R, 1997, Aboveground biomass distribution of US Eastern hardwood forests and the use of large trees as an indicator of forest development: Forest Ecol. Mgmt., 96: 37-47.

Brown, S, Masera, O and Sathaye, J, 2000, Project-based activities: in *Land Use, Land-Use Change, and Forestry; Special Report to the Intergovernmental Panel on Climate Change* (R Watson, I Noble, and D Verardo, eds.), Cambridge Univ. Press, Cambridge, UK: 283-338.

Condit, R, Robinson, WD, Ibanez, R, Aguilar, S, Sanjur, A, Martinez, R, Stallard, RF, Garcia, T, Angehr, GR, Petit, L, Wright, SJ, Robinson, TR and Heckadon, S, 2001, The status of the Panama Canal Watershed and its biodiversity at the beginning of the 21st century: BioScience, 51: 389-398.

Dale, VH, Brown, S, Calderón, MO, Montoya, AS, and Martínez, RE, 2003, Estimating baseline carbon emissions for the Eastern Panama Canal Watershed: Mitigation and Adaptation Strategies for Global Change, 8: 323-348.

Gitay, H, Brown, S, Easterling, W, and Jallow, B, 2001, Ecosystems and their Services: in *Climate Change 2001: Impacts, Adaptation, and Vulnerability. Contribution of Working Group II to the Third Assessment Report of the IPCC* (J McCarthy, O Canziani, N Leary, and D Dokken, eds.): Cambridge Univ.Press, Cambridge, UK: 235-342.

Heckadon-Moreno, S, 2005, Light and shadows in the management of the Panama Canal Watershed: in *The Río Chagres: A Multidisciplinary Perspective of a Tropical River Basin* (RS Harmon, ed.), Kluwer Acad./Plenum Pub., New York, NY: 29-44.

Panama Canal Watershed Monitoring Project (STRI – ANAM – USAID), 1999, Panama City, Panama.

Perez, R, Aguilar, S, Somoza, A, Condit, R, Tejada, I, Camargo, C and Lao, S, 2005, Tree species composition and diversity in the upper Chagres River Basin, Panama: in *The Río Chagres: A Multidisciplinary Perspective of a Tropical River Basin* (RS Harmon, ed.), Kluwer Acad./Plenum Pub., New York, NY: 227-235.

Prieto, C, González, B, Ortega, G, Monteza, E, González, F and Sanjur, A, 1999, Canal Watershed Monitoring Project: Human Population component: Panama Canal Watershed Monitoring Project (STRI – ANAM – USAID), Panama City, Panama.

Tarté, R, 1999, Panama Canal Watershed Climate Action/Conservation Project: The Nature Conservancy, Arlington, VA.

Index

Water Science and Technology Library

1. A.S. Eikum and R.W. Seabloom (eds.): *Alternative Wastewater Treatment*. Low-Cost Small Systems, Research and Development. Proceedings of the Conference held in Oslo, Norway (7–10 September 1981). 1982 ISBN 90-277-1430-4
2. W. Brutsaert and G.H. Jirka (eds.): *Gas Transfer at Water Surfaces.* 1984 ISBN 90-277-1697-8
3. D.A. Kraijenhoff and J.R. Moll (eds.): *River Flow Modelling and Forecasting.* 1986 ISBN 90-277-2082-7
4. World Meteorological Organization (ed.): *Microprocessors in Operational Hydrology.* Proceedings of a Conference held in Geneva (4–5 September 1984). 1986 ISBN 90-277-2156-4
5. J. Němec: *Hydrological Forecasting.* Design and Operation of Hydrological Forecasting Systems. 1986 ISBN 90-277-2259-5
6. V.K. Gupta, I. Rodríguez-Iturbe and E.F. Wood (eds.): *Scale Problems in Hydrology.* Runoff Generation and Basin Response. 1986 ISBN 90-277-2258-7
7. D.C. Major and H.E. Schwarz: *Large-Scale Regional Water Resources Planning*. The North Atlantic Regional Study. 1990 ISBN 0-7923-0711-9
8. W.H. Hager: *Energy Dissipators and Hydraulic Jump*. 1992 ISBN 0-7923-1508-1
9. V.P. Singh and M. Fiorentino (eds.): *Entropy and Energy Dissipation in Water Resources*. 1992 ISBN 0-7923-1696-7
10. K.W. Hipel (ed.): *Stochastic and Statistical Methods in Hydrology and Environmental Engineering.* A Four Volume Work Resulting from the International Conference in Honour of Professor T. E. Unny (21–23 June 1993). 1994
    10/1: Extreme values: floods and droughts ISBN 0-7923-2756-X
    10/2: Stochastic and statistical modelling with groundwater and surface water applications ISBN 0-7923-2757-8
    10/3: Time series analysis in hydrology and environmental engineering ISBN 0-7923-2758-6
    10/4: Effective environmental management for sustainable development ISBN 0-7923-2759-4
    Set 10/1–10/4: ISBN 0-7923-2760-8
11. S.N. Rodionov: *Global and Regional Climate Interaction: The Caspian Sea Experience.* 1994 ISBN 0-7923-2784-5
12. A. Peters, G. Wittum, B. Herrling, U. Meissner, C.A. Brebbia, W.G. Gray and G.F. Pinder (eds.): *Computational Methods in Water Resources X*. 1994
    Set 12/1–12/2: ISBN 0-7923-2937-6
13. C.B. Vreugdenhil: *Numerical Methods for Shallow-Water Flow*. 1994 ISBN 0-7923-3164-8
14. E. Cabrera and A.F. Vela (eds.): *Improving Efficiency and Reliability in Water Distribution Systems.* 1995 ISBN 0-7923-3536-8
15. V.P. Singh (ed.): *Environmental Hydrology.* 1995 ISBN 0-7923-3549-X
16. V.P. Singh and B. Kumar (eds.): *Proceedings of the International Conference on Hydrology and Water Resources* (New Delhi, 1993). 1996
    16/1: Surface-water hydrology ISBN 0-7923-3650-X
    16/2: Subsurface-water hydrology ISBN 0-7923-3651-8

16/3: Water-quality hydrology ISBN 0-7923-3652-6
16/4: Water resources planning and management ISBN 0-7923-3653-4
Set 16/1–16/4 ISBN 0-7923-3654-2
17. V.P. Singh: *Dam Breach Modeling Technology.* 1996 ISBN 0-7923-3925-8
18. Z. Kaczmarek, K.M. Strzepek, L. Somlyódy and V. Priazhinskaya (eds.): *Water Resources Management in the Face of Climatic/Hydrologic Uncertainties*. 1996 ISBN 0-7923-3927-4
19. V.P. Singh and W.H. Hager (eds.): *Environmental Hydraulics*. 1996 ISBN 0-7923-3983-5
20. G.B. Engelen and F.H. Kloosterman: *Hydrological Systems Analysis*. Methods and Applications. 1996 ISBN 0-7923-3986-X
21. A.S. Issar and S.D. Resnick (eds.): *Runoff, Infiltration and Subsurface Flow of Water in Arid and Semi-Arid Regions.* 1996 ISBN 0-7923-4034-5
22. M.B. Abbott and J.C. Refsgaard (eds.): *Distributed Hydrological Modelling*. 1996 ISBN 0-7923-4042-6
23. J. Gottlieb and P. DuChateau (eds.): *Parameter Identification and Inverse Problems in Hydrology, Geology and Ecology*. 1996 ISBN 0-7923-4089-2
24. V.P. Singh (ed.): *Hydrology of Disasters.* 1996 ISBN 0-7923-4092-2
25. A. Gianguzza, E. Pelizzetti and S. Sammartano (eds.): *Marine Chemistry.* An Environmental Analytical Chemistry Approach. 1997 ISBN 0-7923-4622-X
26. V.P. Singh and M. Fiorentino (eds.): *Geographical Information Systems in Hydrology.* 1996 ISBN 0-7923-4226-7
27. N.B. Harmancioglu, V.P. Singh and M.N. Alpaslan (eds.): *Environmental Data Management.* 1998 ISBN 0-7923-4857-5
28. G. Gambolati (ed.): *CENAS. Coastline Evolution of the Upper Adriatic Sea Due to Sea Level Rise and Natural and Anthropogenic Land Subsidence*. 1998 ISBN 0-7923-5119-3
29. D. Stephenson: *Water Supply Management*. 1998 ISBN 0-7923-5136-3
30. V.P. Singh: *Entropy-Based Parameter Estimation in Hydrology*. 1998 ISBN 0-7923-5224-6
31. A.S. Issar and N. Brown (eds.): *Water, Environment and Society in Times of Climatic Change*. 1998 ISBN 0-7923-5282-3
32. E. Cabrera and J. García-Serra (eds.): *Drought Management Planning in Water Supply Systems*. 1999 ISBN 0-7923-5294-7
33. N.B. Harmancioglu, O. Fistikoglu, S.D. Ozkul, V.P. Singh and M.N. Alpaslan: *Water Quality Monitoring Network Design*. 1999 ISBN 0-7923-5506-7
34. I. Stober and K. Bucher (eds): *Hydrogeology of Crystalline Rocks*. 2000 ISBN 0-7923-6082-6
35. J.S. Whitmore: *Drought Management on Farmland*. 2000 ISBN 0-7923-5998-4
36. R.S. Govindaraju and A. Ramachandra Rao (eds.): *Artificial Neural Networks in Hydrology*. 2000 ISBN 0-7923-6226-8
37. P. Singh and V.P. Singh: *Snow and Glacier Hydrology*. 2001 ISBN 0-7923-6767-7
38. B.E. Vieux: *Distributed Hydrologic Modeling Using GIS*. 2001 ISBN 0-7923-7002-3

39. I.V. Nagy, K. Asante-Duah and I. Zsuffa: *Hydrological Dimensioning and Operation of Reservoirs*. Practical Design Concepts and Principles. 2002 ISBN 1-4020-0438-9
40. I. Stober and K. Bucher (eds.): *Water-Rock Interaction*. 2002 ISBN 1-4020-0497-4
41. M. Shahin: *Hydrology and Water Resources of Africa*. 2002 ISBN 1-4020-0866-X
42. S.K. Mishra and V.P. Singh: *Soil Conservation Service Curve Number (SCS-CN) Methodology*. 2003 ISBN 1-4020-1132-6
43. C. Ray, G. Melin and R.B. Linsky (eds.): *Riverbank Filtration*. Improving Source-Water Quality. 2003 ISBN 1-4020-1133-4
44. G. Rossi, A. Cancelliere, L.S. Pereira, T. Oweis, M. Shatanawi and A. Zairi (eds.): *Tools for Drought Mitigation in Mediterranean Regions*. 2003 ISBN 1-4020-1140-7
45. A. Ramachandra Rao, K.H. Hamed and H.-L. Chen: *Nonstationarities in Hydrologic and Environmental Time Series*. 2003 ISBN 1-4020-1297-7
46. D.E. Agthe, R.B. Billings and N. Buras (eds.): *Managing Urban Water Supply*. 2003 ISBN 1-4020-1720-0
47. V.P. Singh, N. Sharma and C.S.P. Ojha (eds.): *The Brahmaputra Basin Water Resources*. 2004 ISBN 1-4020-1737-5
48. B.E. Vieux: *Distributed Hydrologic Modeling Using GIS.* Second Edition. 2004 ISBN 1-4020-2459-2
49. M. Monirul Qader Mirza (ed.): *The Ganges Water Diversion: Environmental Effects and Implications*. 2004 ISBN 1-4020-2479-7
50. Y. Rubin and S.S. Hubbard (eds.): *Hydrogeophysics*. 2005 ISBN 1-4020-3101-7
51. K.H. Johannesson (ed.): *Rare Earth Elements in Groundwater Flow Systems*. 2005 ISBN 1-4020-3233-1
52. R.S. Harmon (ed.): *The Río Chagres, Panama*. A Multidisciplinary Profile of a Tropical Watershed. 2005 ISBN 1-4020-3298-6